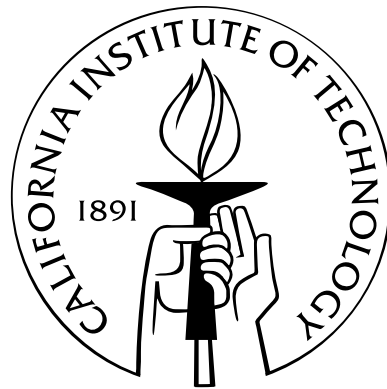


Energy-Minimizing Microstructures in Multiphase Elastic Solids

Thesis by
Isaac Vikram Chenchiah

In Partial Fulfillment of the Requirements
for the Degree of
Doctor of Philosophy



California Institute of Technology
Pasadena, California

2004
(Defended 5th January 2004)

Nos itaque ista quae fecisti videmus, quia sunt, tu autem quia vides ea, sunt.

Acknowledgements

It has been a joy to be a graduate student with Kaushik Bhattacharya. Kaushik epitomizes for me one of the four great virtues in classical Greek thought – *σωφροσύνη*¹. He has guided without hampering initiative, nurtured without ceasing to challenge and related personally without losing professional detachment. Kaushik has also taught me — though I fear I have learnt only little — the value of asking the right questions, distinguishing the essence of a problem from its accidents and focusing on the crucial parts without losing sight of the whole. I wish for many more opportunities to interact with him in the future.

I have greatly enjoyed and have been very instructed by interaction with Johannes Zimmer and especially thank him for his mentorship – I hope it will continue!

For invaluable encouragement and support from September to December 2003, apart from Kaushik, I thank Anne Chen, Meenakshi Dabhade, Jennifer Johnson, Raymond Jones, Prashant Purohit, Denny & Carolyn Repko, Anja Schloemerkerper, Deborah Smith, Ivan Veselic; my parents, Rajkumar & Mercy Chenchiah; my sister, Hephzibah Chenchiah; and especially Thomas Hall, Daniel Katz, Swaminathan Krishnan, Christopher Lee, Judith Mitrani, Robert Nielsen and Winnie “Metafont” Wang. *Ubi caritas et amor, Deus ibi est.*

¹ Sophrosyne: self-possession; harmonious balance in the soul; soundness of mind, self-knowledge. ‘Temperance’ is a common (as in the traditional list of the four cardinal virtues) though weak translation. Impossible to translate into one single English word, it is the spirit behind the two famous Greek sayings: “nothing in excess” and “know thyself”. Sophrosyne is the theme of Plato’s Charmides. For more on sophrosyne see St. Thomas Aquinas, *Summa Theologica*, I-II, 64 and II-II, 141–170.

Abstract

This thesis concerns problems of microstructure and its macroscopic consequences in multiphase elastic solids, both single crystals and polycrystals.

The elastic energy of a two-phase solid is a function of its microstructure. Determining the infimum of the energy of such a solid and characterizing the associated extremal microstructures is an important problem that arises in the modeling of the shape memory effect, microstructure evolution (precipitation, coarsening, etc.), homogenization of composites and optimal design. Mathematically, the problem is to determine the relaxation under fixed volume fraction of a two-well energy.

We compute the relaxation under fixed volume fraction for a two-well linearized elastic energy in two dimensions with no restrictions on the elastic moduli and transformation strains; and show that there always exist rank-I or rank-II laminates that are extremal. By minimizing over the volume fraction we obtain the quasiconvex envelope of the energy. We relate these results to experimental observations on the equilibrium morphology and behavior under external loads of precipitates in Nickel superalloys. We also compute the relaxation under fixed volume fraction for a two-well linearized elastic energy in three dimensions when the elastic moduli are isotropic (with no restrictions on the transformation strains) and show that there always exist rank-I, rank-II or rank-III laminates that are extremal.

Shape memory effect is the ability of a solid to recover on heating apparently plastic deformation sustained below a critical temperature. Since utility of shape memory alloys critically depends on their polycrystalline behavior, understanding and predicting the recoverable strains of shape memory polycrystals is a central open problem in the study of shape memory alloys. Our contributions to the solution of this problem are twofold:

We prove a dual variational characterization of the recoverable strains of shape memory polycrystals and show that dual (stress) fields could be signed Radon measures with finite mass supported on sets with Lebesgue measure zero. We also show that for polycrystals made of materials undergoing cubic-tetragonal transformations the strains fields associated with macroscopic recoverable strains are related to the solutions of hyperbolic partial differential equations.

Contents

Acknowledgements	iv
Abstract	v
List of Figures	ix
List of Tables	xi
1 Introduction	1
1.1 Equilibrium morphology of precipitates	2
1.2 The shape memory effect	6
1.3 Overview of the thesis	11
2 Mathematical framework and statement of results	13
2.1 Equilibrium morphology of precipitates	13
2.2 The shape memory effect	16
2.2.1 The shape memory effect in single crystals	16
2.2.2 The shape memory effect in polycrystals	22
2.3 Statement of results	25
2.3.1 Two-phase solids	25
2.3.2 Polycrystals	26
3 Two-phase solids in two dimensions	28
3.1 An optimal lower bound on the relaxed energy	28
3.1.1 A lower bound by the translation method	28
3.1.2 The determinant as translation	29
3.1.3 Determining the amount of translation	30
3.1.4 Explicit expressions for the optimal strains	32
3.1.5 A lower bound on the relaxed energy	33
3.1.6 Equal elastic moduli	34

3.2	Extremal microstructures	35
3.2.1	Laminates	36
3.2.2	Regime I - rank-I laminates	38
3.2.3	Regime II - rank-I laminates	39
3.2.4	Regime III - rank-II laminates	40
3.3	Related relaxed energy densities	43
3.3.1	The uniform traction problem	43
3.3.2	The quasiconvex envelope	45
3.4	Application to equilibrium morphology of precipitates	45
3.4.1	Explicit expressions for aligned cubic moduli	46
3.4.2	The three regimes	48
3.4.3	Rafting	49
3.4.4	Correlation with experimental results	53
4	Two-phase isotropic solids in three dimensions	55
4.1	Rotated diagonal subdeterminants as translations	55
4.2	Determining the amount of translation	58
4.2.1	Isotropic elastic moduli	60
4.3	Explicit expressions for the optimal strains	70
4.4	An optimal rotation diagonalizes the optimal strain jump	71
4.4.1	Doubly stochastic matrices	71
4.4.2	Proof of theorem 4.10	74
4.5	A lower bound on the relaxed energy	76
4.6	Extremal microstructures	78
4.6.1	Regime I - rank-I laminates	78
4.6.2	Regime II - rank-I laminates	79
4.6.3	Regimes III and IV - rank-II and rank-III laminates	81
4.6.3.1	Regime III - rank-II laminates	82
4.6.3.2	Regime IV - rank-III laminates	85
4.A	Appendix: A family of quasiconvex quadratic functionals on $M_{\text{sym}}^{3 \times 3}$	87
5	Polycrystals	89
5.1	Dual variational characterization of the zero-set of polycrystals	89
5.2	The problem in two dimensions	96
5.2.1	Fields in a grain	97
5.2.2	Polycrystals	101
5.3	Cubic-tetragonal materials	113

6 Conclusions	121
Bibliography	122

List of Figures

1.1	Evolution of microstructure in a nickel silicon alloy.	2
1.2	Evolution of microstructure in a nickel silicon alloy.	3
1.3	Micrographs of solid tin particles embedded in eutectic Pb-Sn matrix.	4
1.4	Directional coarsening in nickel aluminum alloy.	4
1.5	Series of equilibrium shapes for a single particle in a matrix.	6
1.6	A schematic illustration of martensitic phase transformation.	7
1.7	A high-resolution transmission electron micrograph of fine twinning in nickel-aluminum.	7
1.8	Optical micrographs of the microstructure in an alloy of copper, aluminum and nickel.	8
1.9	The shape memory effect.	9
1.10	Schematic of a polycrystal.	10
1.11	Domain patterns in a polycrystalline specimen of BaTiO ₃	11
2.1	The three variants of martensite in a cubic-tetragonal transformation.	17
2.2	The energy density at various temperatures.	18
2.3	The microscopic, mesoscopic and macroscopic energy densities.	20
3.1	Rank-I laminate.	36
3.2	Rank-II laminate.	37
3.3	The three regimes.	49
3.4	Rafting.	52
3.5	Rafting.	53
4.1	The set $B_{i,\text{II}+}$ for $\ell_i = 1$ and $\mu_i = \frac{1}{2}$	63
4.2	The set $B_{i,\text{II}+}$ for $\ell_i = 1$ and $\mu_i = \frac{1}{2}$	64
4.3	The surfaces $B_{i,\text{II}+}^{(1)}$, $B_{i,\text{II}+}^{(2)}$ and $B_{i,\text{II}+}^{(3)}$ for $\ell = 1$ and $\mu = \frac{1}{2}$	65
4.4	The set $B_{i,\text{III}} \cup B_{i,\text{IV}}$ for $\ell = 1$ and $\mu = \frac{1}{2}$	66
4.5	Rank-I laminate.	79
5.1	The mesoscopic energy and the indicator function of its zero-set.	90
5.2	The mesoscopic energy.	97

5.3	The set $\widehat{\mathcal{S}}_\theta$	97
5.4	The ‘space-like’ and ‘time-like’ directions of the wave operator \square_θ^2	98
5.5	A rigid checkerboard.	104
5.6	A dual field for the rigid checkerboard.	106
5.7	A dual field for the rigid checkerboard.	106
5.8	A flexible checkerboard.	107
5.9	A strain field for the flexible checkerboard.	108
5.10	A dual field for the flexible checkerboard.	111
5.11	The same dual field as in Figure 5.10 with more grains shown.	111
5.12	Free body diagrams for dual field shown in Figure 5.10.	112
5.13	A flexible polycrystal.	113
5.14	A polycrystal with 120° symmetry.	114
5.15	A polycrystal with 120° symmetry.	114
5.16	Dual fields for the a polycrystal with 120° symmetry.	115

List of Tables

2.1	Examples of materials undergoing cubic-tetragonal transformation.	18
2.2	Examples of materials undergoing cubic-orthorhombic transformation.	18

Chapter 1

Introduction

A variety of solids are composed of multiple phases. One example is composites, where different materials or phases are brought together artificially. Active materials like shape memory alloys are another. Here the different phases arise as a result of martensitic phase transformation. Alloys used for structural and other purposes are yet another example. Here a second phase is precipitated out as a result of a compositional phase transformation and used to strengthen the solid.

Multi-phase solids often exhibit microstructure, i.e., a distribution of phases at a very fine length scale. As a consequence, the behavior of these solids on macroscopic length scales (length scales much larger than that of the microstructure) is different from the behavior on microscopic length scales (length scales of the microstructure). The microstructure of the solid plays a crucial role in determining macroscopic properties. Therefore engineering the microstructure provides a mechanism for obtaining materials with desirable properties. For these reasons, understanding the link between microstructure and macroscopic properties is of great interest and importance.

The dependence of macroscopic properties on microstructure might be considerably involved in situations when the microstructure itself can change with deformation as, for example, in solids that undergo martensitic phase transformations. The modelling of such solids at macroscopic length scales involves characterization of the microstructures that form in them and how they change as a result of macroscopic deformation. Similar issues arise in the problem of optimal design.

This thesis considers two classes of problems of this genre that arise from solid-solid phase transformations. The first is motivated by nickel superalloys that are used for turbine blades. These alloys are precipitate hardened: an alloy with off-stoichiometric composition is quenched to create numerous small inclusions or precipitates which then increase the hardness and the creep resistance of the alloy. Here the key issue is to understand the equilibrium morphology of the precipitates and its dependence on external loads. The second is motivated by shape memory alloys. The shape memory effect is the temperature induced recovery of apparent plastic deformation. This phenomenon is the

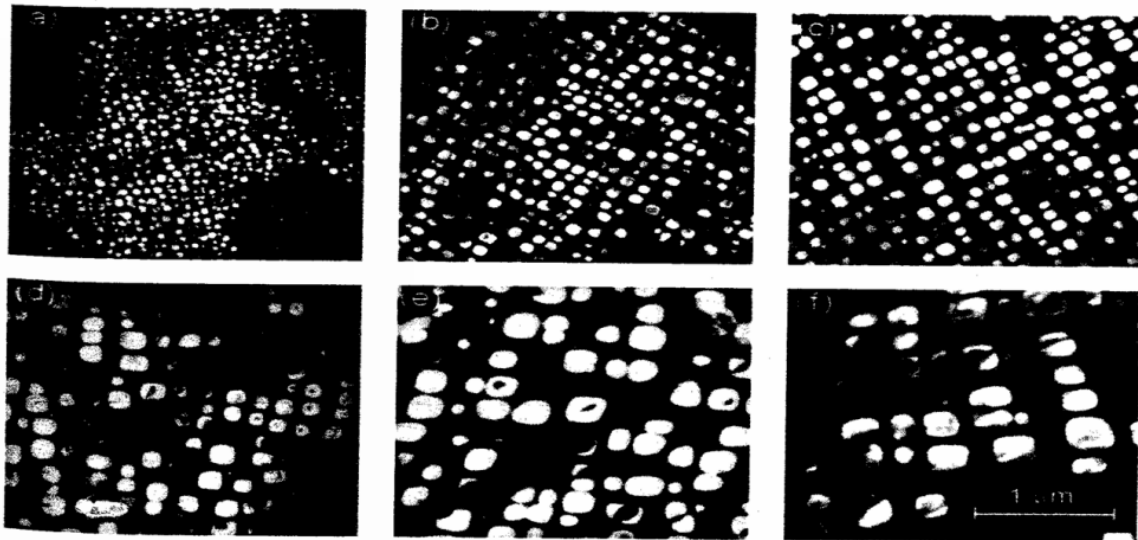


Figure 1.1: Evolution of microstructure in a nickel silicon alloy (22.8% Ni) at aging times (from top left to bottom right) 25, 150, 247, 599, 1446 and 2760 hours [CA97].

result of martensitic phase transformation and the key issue here is to determine the amount of recoverable strain [OW99, Bha03].

1.1 Equilibrium morphology of precipitates

Quenching a multi-component alloy produces a supersaturated metastable solid which under annealing nucleates precipitates [Chr02]. The two-phase system that results at the end of the phase transformation consists of a dispersion of second-phase particles in a matrix. Under further annealing or aging the precipitate morphology evolves by diffusional mass transport as the two-phase mixture tries to minimize its energy. Importantly, during this post phase-transformation morphological evolution, the phase fractions of the matrix and precipitates remain constant; only the morphology changes. Figures 1.1 and 1.2 reproduce the results of Cho and Ardell [CA97, CA98] and show the evolution of Ni_3Si precipitates in a nickel matrix. Understanding the resulting morphology is important since the hardness of the alloy depends on it.

Morphology evolution in coherent solids is driven by two contributions to the energy: interfacial and elastic. The nucleation is local and governed by defects. Therefore, as nucleated the precipitates are small and randomly dispersed. Given their small size, interfacial energy dominates the evolution. The system reduces its energy by diffusional mass transport: smaller particles dissolve into the system transferring their mass to larger particles (smaller particles contribute to a greater proportion of the interfacial area and thus to a greater proportion of the interfacial energy). This process — in

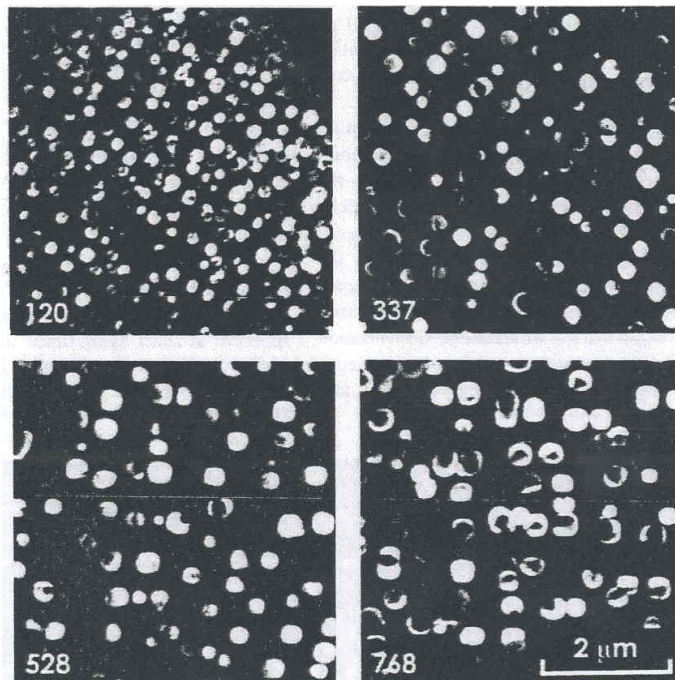
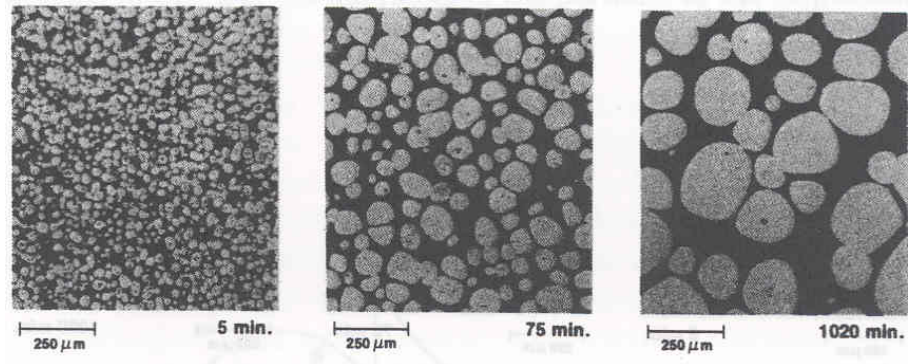


Figure 1.2: Evolution of microstructure in a nickel silicon alloy (6.62% Ni) at aging times (from top left to bottom right) 120, 337, 528 and 768 hours [CA97].

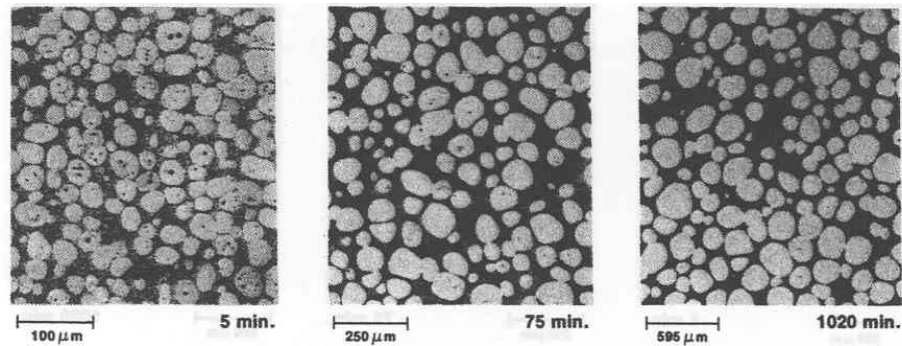
which the larger particles grow at the expense of smaller ones — is known as coarsening or Ostwald ripening. In systems where elastic energy is negligible the growth of the particles is self-similar as shown in Figure 1.3. This phenomenon is well understood [RV02, and references therein].

If interfacial energy alone were to govern coarsening, the lowest energy state would be that of a single particle in a matrix. However as the particle size increases, the evolution of solid systems is increasingly and eventually dominantly influenced by elastic energy arising from the difference in lattice parameters (i.e., difference in stress-free strains) between the phases. Consequently, the rate of growth or coarsening of the particles diminishes and the morphology deviates from the self-similar nature and tends to align along specific crystallographic directions. For example, in Figure 1.1, the particles' shape changes from spherical to cuboidal, the cuboids tend to align themselves along $\langle 100 \rangle$ directions and the length scale changes little in the last two frames. Externally applied stresses also contribute to the energy of the system, in particular by breaking the degeneracy between crystallographically equivalent precipitate shapes. Directional coarsening, also known as rafting, in which precipitates preferentially grow along certain directions has been observed in many systems. Figure 1.4 shows directional coarsening in the presence of tensile and compressive uniaxial loading [MNM79].

Understanding the evolution of microstructures in these systems is of much technological interest

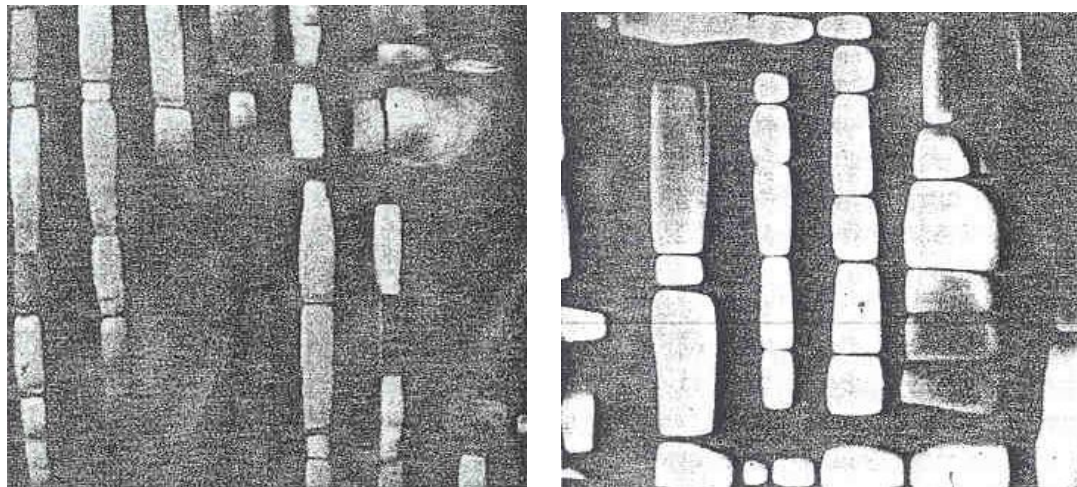


(a) At constant magnification.



(b) The magnification of each picture is scaled by a factor related to constant particle size. All microstructures then look similar.

Figure 1.3: Micrographs of solid tin particles embedded in eutectic Pb-Sn matrix. The alloy was annealed just above the eutectic temperature for different times as shown in the figure [RV02, Fig.6.1,6.2, pg.117,118].



(a) Tensile Stress

(b) Compressive stress

Figure 1.4: Directional coarsening in nickel aluminum alloy annealed at 750°C for 160 hours with tensile/compressive stress of 147 MPa along the $[0\ 0\ 1]$ direction. The $(1\ 0\ 0)$ side plane is shown [MNM79].

since the microstructure of an alloy significantly influences its mechanical behavior. This is however a difficult problem: mathematically it is a free boundary problem coupled to diffusion, interfacial energy and elasticity. Consequently it has been studied extensively through computational means [ATV01, Che02, HC01, JLL97, Kha83, KSM88, LLJ98, LLN00, LLN01, LC97a, LC98a, LC98b, LLN⁺03, LV02a, LV02b, LV03, PC98, SP93, SV96a, SV96b, VC02, VWC02, WCK91, ZCS01]. On the one hand these problems are computationally expensive; on the other hand they are characterized by long-range interactions. Therefore choosing the appropriate computational domain is a critical issue. It is also difficult to distinguish slow evolution close to metastable states from true equilibria. An understanding of the equilibrium microstructures can provide a guidance in these two regards.

The equilibrium microstructure. In the absence of elastic stress, as mentioned earlier, the equilibrium microstructure is that of a single particle in a matrix. The equilibrium morphology of such particle depends solely on the interfacial energy especially through its dependence on crystallographic orientation. This gives rise to the variational problem of minimizing the total interfacial energy of a particle of fixed volume. This problem has been thoroughly explored and placed on a rigorous mathematical footing [Tay78, Fon91].

When the matrix and the precipitate differ in their stress-free strains (i.e., when there is a lattice misfit), a coherent matrix-precipitate interface introduces significant stresses in the crystal. Thus elastic energy could be expected to significantly influence both morphological evolution and the morphology of the equilibrium microstructures. Johnson and Cahn [JC84] studied the equilibrium shape of an isolated precipitate restricting themselves to ellipsoidal shapes. Various groups have built on this by relaxing the restriction to ellipsoidal shape. Figure 1.5 reproduces the results of Thompson et al. [TSV94]. In a system with cubic elastic moduli and cubic mismatch strain (corresponding to Ni alloys), the equilibrium shape of an isolated particle bifurcates away from a cuboidal shape with increasing precipitate size. While this points to the importance of elasticity, Cho and Ardell [CA97] have pointed out that these results are not completely in agreement with experimental observations. This is not surprising given that elasticity acts over long ranges and inter-particle interactions are important as emphasized by Johnson and collaborators [JC84, JV87] through their study of the elastic energy of a small number of precipitates.

Breaking with the tradition of considering a limited number of particles, this thesis examines the optimum morphology of precipitates with no a priori restrictions on their number or morphology. We limit ourselves to elastic energy, i.e., we neglect surface energy, as appropriate for the larger length scales present at the late stages of evolution.

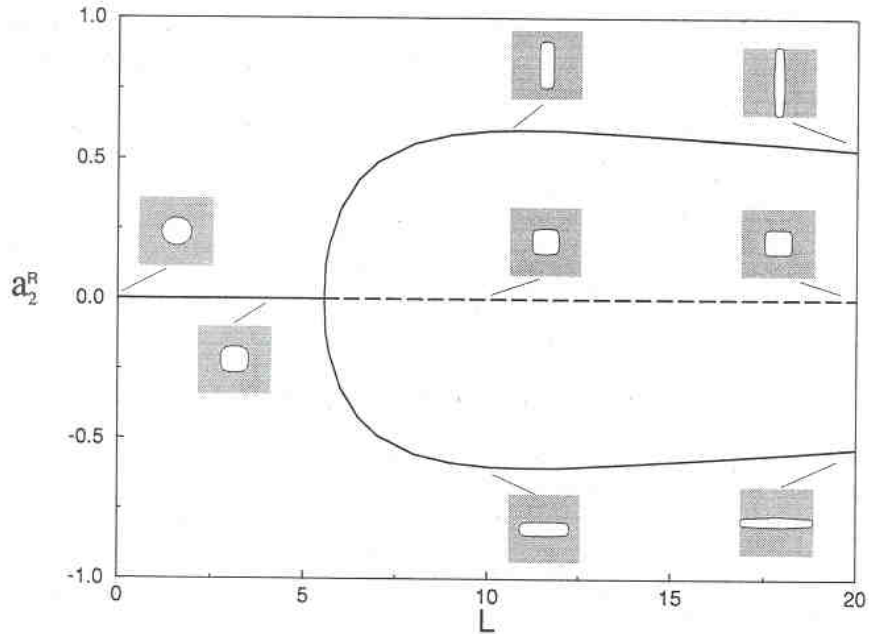


Figure 1.5: Series of equilibrium shapes for a single particle in a matrix. L is a measure of particle size while a_2^R is a measure of deviation from circular shape. The bifurcation from fourfold symmetric shapes to twofold symmetric shapes occurs at $L=5.6$ [TSV94].

1.2 The shape memory effect

Shape memory behavior is the ability of certain materials to recover, on heating, apparently plastic deformation sustained below a critical temperature. The source of the shape memory effect is a martensitic phase transformation. A material which undergoes a martensitic phase transformation has two distinct crystalline structures: the parent or austenite phase which is more symmetric and is preferred at high temperatures; and the product or martensite phase which is less symmetric and is preferred at low temperatures. The transformation is first order (i.e., there is an abrupt change in crystal structure) and displacive (diffusionless). This is illustrated schematically in Figure 1.6 where the transformation takes the square austenite lattice in (a) to a rectangular martensite lattice in (b). Because of the change of symmetry, the martensite phase occurs in several different symmetry related variants which have the same crystalline structure but bear different relations to the austenite lattice. This is illustrated in parts (b) and (c) of the figure. A typical specimen might consist of a mixture of different variants of martensite. Typically the mixture occurs at fine scales and is referred to as martensitic microstructure. Further and importantly, the mixture is coherent so that row of atoms remain unbroken across interfaces. This is illustrated schematically in part (d) of the figure. Figures 1.7 and 1.8 show electron and optical micrographs of microstructure in common shape memory alloys.

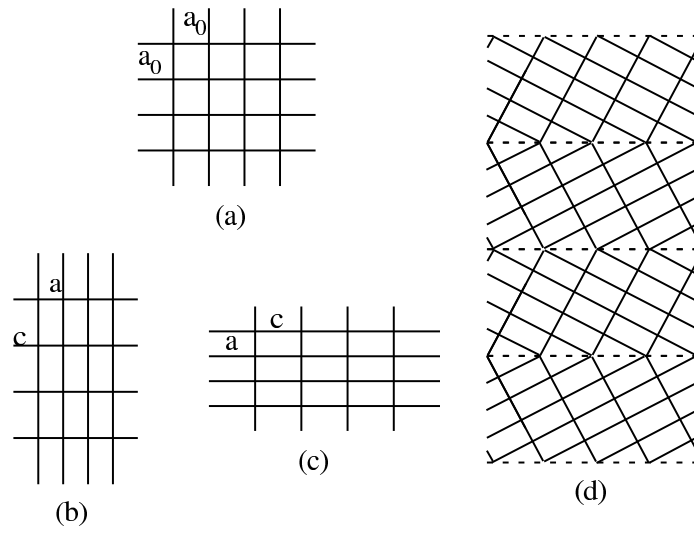


Figure 1.6: A schematic illustration of martensitic phase transformation: (a) Austenite, (b,c) variants of martensite and (d) a coherent arrangement of alternating variants of martensite [Bha03, Fig.1.3, pg.4].

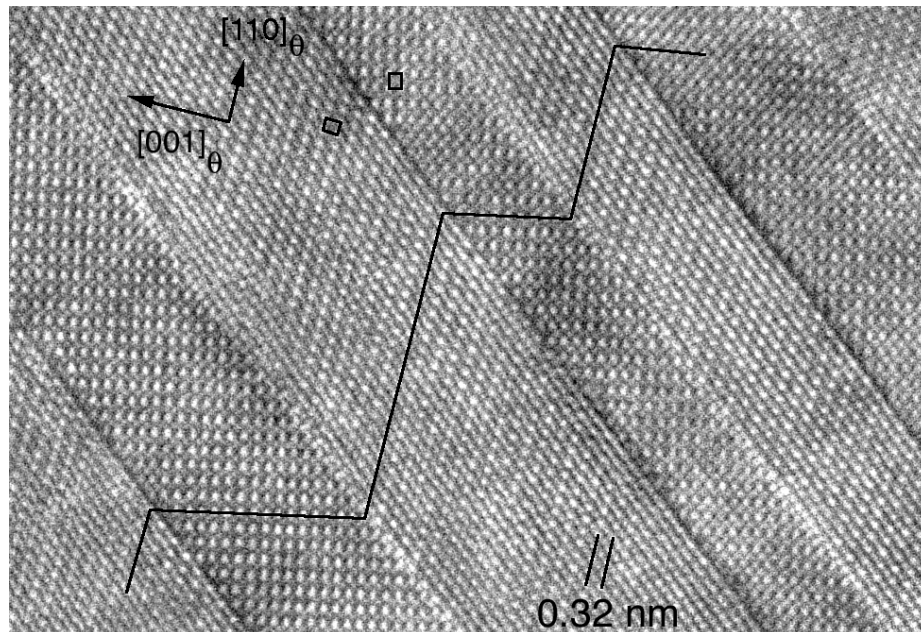
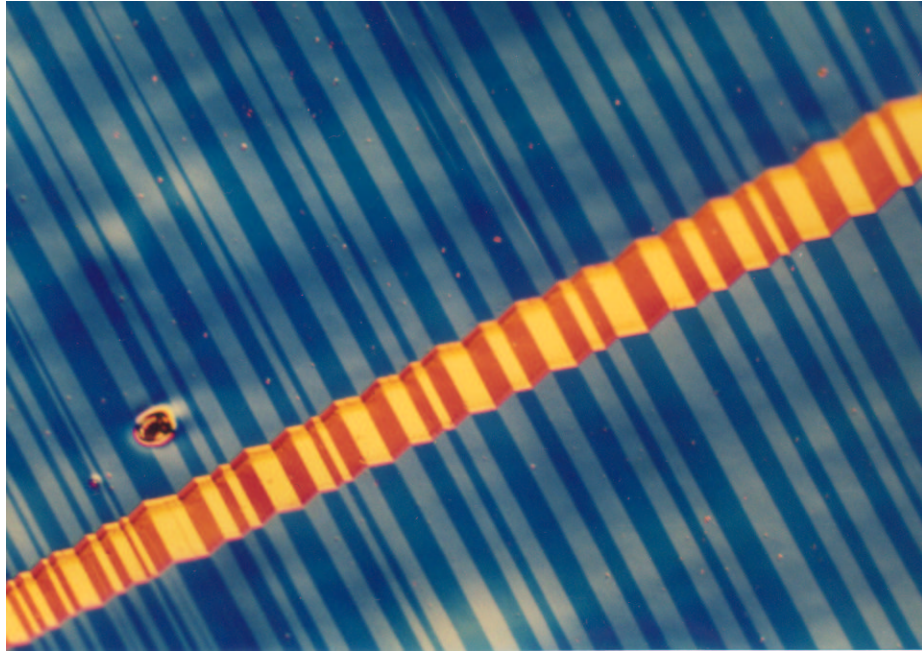
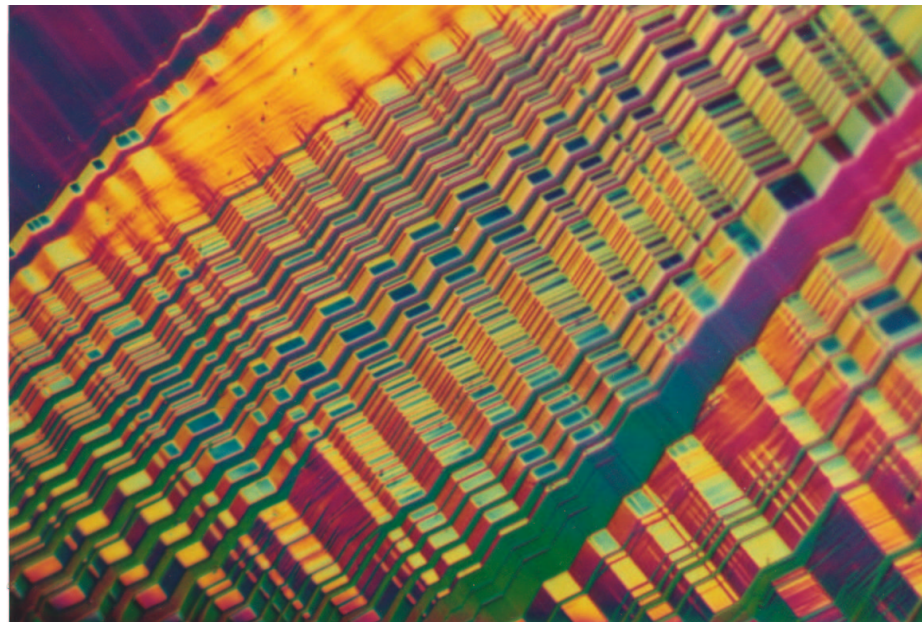


Figure 1.7: A high-resolution transmission electron micrograph of fine twinning in nickel-aluminum. Courtesy of D. Schryvers.



(a) Horizontal field of view is 0.63mm.



(b) Horizontal field of view is 0.75mm.

Figure 1.8: Optical micrographs of the microstructure in an alloy of copper, aluminum and nickel.
Courtesy of C. Chu and R.D. James

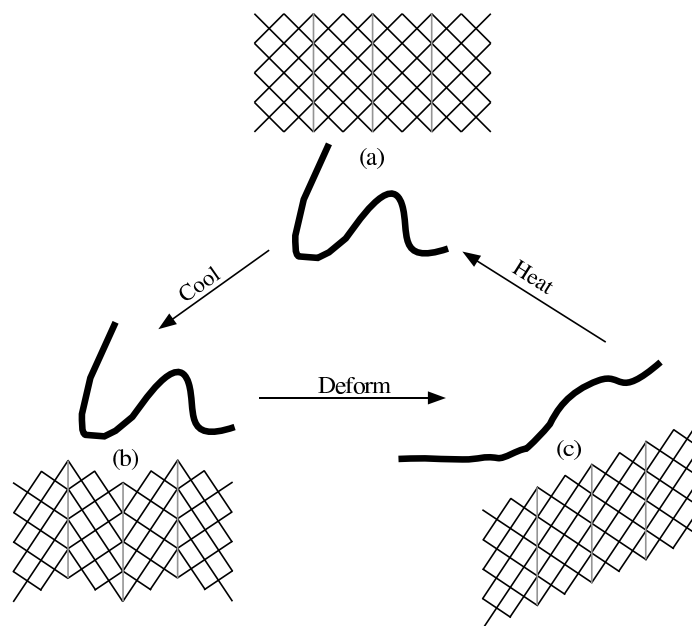


Figure 1.9: The shape memory effect.

The phenomenon and mechanism of the shape memory effect are illustrated schematically in Figure 1.9. As shown in the figure, deformations performed below a critical temperature are recovered on heating. Subsequent cooling does not cause any change in shape. When a specimen in austenite is transformed by cooling to martensite ((a) to (b)), the result is usually not a single variant, but rather a mixture of martensite variants (b). In fact, the different variants of martensite arrange themselves in such a microstructure that there is negligible macroscopic effect (change of shape) during the transformation. This is known as self-accommodation. When the sample is deformed the variants rearrange themselves, if they can, so as to remain stress-free ((b) to (c)). The resulting deformation appears macroscopically plastic: there is no restoring force, since the variants in their new configurations are not stressed. However this deformation is recoverable: heating the crystal above its transformation temperature turns each variant of martensite back to austenite and the crystal returns to its original shape ((c) to (a)). Note however that only those strains can be recovered that can be accommodated by rearrangement of the martensite variants. Subsequent deformation can cause elastic response which gives rise to a restoring force so that the deformation would not appear plastic. The elevated stress during subsequent deformation can lead to true plastic deformation and damage to the crystal and the resulting strains cannot be recovered. The amount of recoverable strain is an important figure of merit in a shape memory alloy.

If the specimen were a single crystal the amount of recoverable strain can readily be determined from the crystallography based on the mechanism described above. The situation is more complex in polycrystals which is the case for most commercial specimens. Here the material is an assemblage

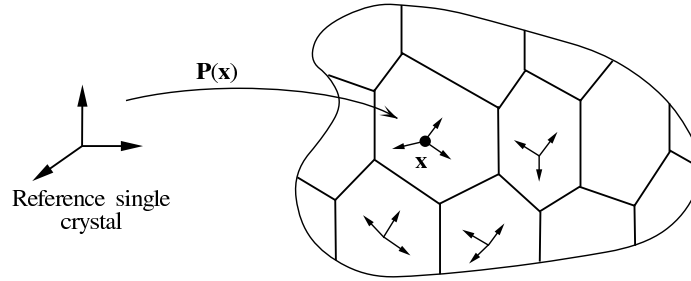


Figure 1.10: Schematic of a polycrystal [Bha03, fig.13.1, pg.227].

of grains, each composed of the same shape memory material in a different orientation as indicated schematically in Figure 1.10. The size, shape and orientation of the grains is collectively referred to as texture. In such a situation, each grain can form a microstructure but this microstructure can vary from grain to grain as shown in Figure 1.11. When a polycrystal in the austenite phase is cooled, each grain transforms to a self-accommodated mixture of martensite variants. Since the grains do not deform due to self-accommodation, this step is essentially the same as in single crystals. As the polycrystal is deformed, each grain tries to accommodate the strain by adjusting its microstructure of stress-free variants. However it faces two constraints in doing so. It is restricted to its own class of microstructures depending on its crystallographic orientation. Moreover, it is not free to deform as it chooses since it is constrained by its neighbors. Therefore, a deformation can be accommodated through rearrangement of variants if and only if the grains collectively and cooperatively succeed. In short, a deformation of the polycrystal is recoverable if and only if the different grains can collectively and cooperatively adjust their microstructure to accommodate it.

Experimental observations show that the amount of recoverable strain in polycrystals can vary widely even amongst materials whose behavior as single crystals is very similar. For example single crystals of Ni-Al can recover 0-13% strain depending on orientation while polycrystals recover hardly any strain. In contrast, single crystals of Ni-Ti can recover 3-10% strain depending on orientation and polycrystals can recover as much as 4-8% strain. Understanding and predicting recoverable strains of shape memory polycrystals is a central open problem in the study of shape memory alloys.

Bhattacharya and Kohn [BK97] argued that the amount of recoverable strain in a polycrystal depends not only on the recoverable strains of single crystals and texture but also critically on the change of symmetry during transformation. In particular, they conjectured that materials that undergo the cubic-tetragonal transformation, as in Ni-Al, have no recoverable strain as polycrystals except for very special textures. They studied model problems and obtained bounds in support of their conjecture. Heuristically, such transformations produced too few martensitic variants to allow cooperative rearrangement. In contrast they showed that materials undergoing cubic-orthorhombic or cubic-monoclinic transformations have significant recoverable strains as in Ni-Ti. This is in good

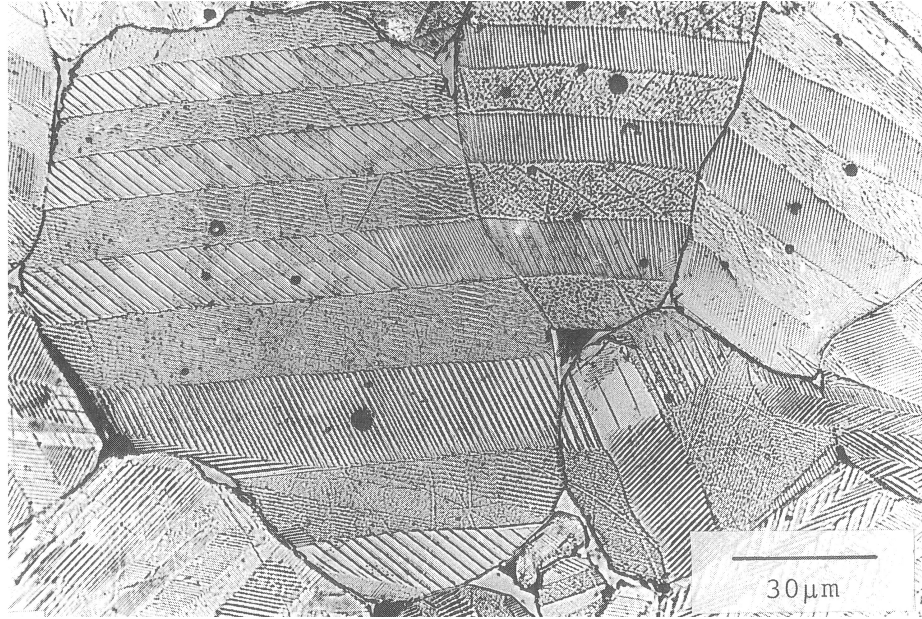


Figure 1.11: Domain patterns in a polycrystalline specimen of the ferroelectric material BaTiO_3 . For our purposes we can think of this as a martensite material undergoing cubic to tetragonal transformation and the domain patterns as fine twins. [Ar190].

agreement with experimental observations.

1.3 Overview of the thesis

This thesis concerns problems of microstructure and its macroscopic consequences in multi-phase solids. There are three pillars to this approach. First, multi-phase solids are characterized by multi-well energy densities where each well corresponds to a phase or variant. Second, we hypothesize that the observed microstructure is obtained as that which minimizes the appropriate potential energy of the system. Developments over the last couple of decades have shown that energy minimization with multi-well energies leads naturally to fine scale microstructure. Third is the notion of effective property. This is introduced through the notion of relaxation in single crystals and homogenization in polycrystals.

We introduce the mathematical framework in Chapter 2. We motivate multi-well energies for both the problem of equilibrium precipitate morphology and the problem of recoverable strains in shape memory alloys. We introduce the notions of relaxation and homogenization and show their relevance to these problems. Having introduced the framework we provide a detailed summary of our main results.

In Chapter 3, we compute the elastic energy at equilibrium for a two-phase system in two dimensions.

We show that the equilibrium microstructures always include laminates. Our results in this chapter are also relevant to the problem of recoverable strains in single crystal shape memory alloys. In Chapter 4 we present results for the problem in three dimensions when the phases are isotropic.

Chapter 5 contains our contributions to the effort to characterize the recoverable strains of shape memory polycrystals in terms of the symmetry change during transformation, recoverable strains for the corresponding single crystals and texture. Specifically our goal is a deeper understanding of this problem. We prove a dual variational principle and show that dual (stress) fields could be signed Radon measures with finite mass. We end with results specific to materials that undergo the cubic-tetragonal transformation.

Chapter 2

Mathematical framework and statement of results

In this chapter we introduce the mathematical framework to model and study the problems in multiphase solids discussed above. We work in the framework of infinitesimal kinematics. We treat the different phases as linear elastic solids, each with its own elastic modulus and stress-free (residual or transformation) strain. We formulate the two problems independently but the connection between them will be clear.

2.1 Equilibrium morphology of precipitates

Consider the Ni-Si system described in §1.1. We have two phases, nickel which forms the matrix and Ni₃Si which forms the precipitate. They have different preferred lattice parameters and elastic moduli. The precipitates are coherent, i.e., the rows of atoms are unbroken at the interfaces. Thus the crystal lattice might be internally stressed. Since the structure is coherent, we refer both lattices to a single reference state and the configuration of the crystal through continuous displacements relative to this reference state. The two phases have distinct stress-free strains reflecting their different preferred lattice parameters. For generality, we present a formulation for N phases.

Consider a material with N phases. Let ϵ_i^T be the stress-free stain of the i^{th} phase relative to the chosen reference configuration and α_i be its elastic modulus. Suppose further that the chemical energy of the i^{th} phase is w_i . We can then say that the energy of this phase subject to a strain ϵ is given by

$$W_i(\epsilon) = \frac{1}{2} \langle \alpha_i(\epsilon - \epsilon_i^T), (\epsilon - \epsilon_i^T) \rangle + w_i. \quad (2.1)$$

The inner product¹ is defined as usual by $\forall A, B \in M^{n \times n}$, $\langle A, B \rangle := \text{Tr}(A^T B)$. Now consider an arrangement of N phases described by the characteristic functions $\chi_i: \Omega \rightarrow \{0, 1\}$, $i = 1, \dots, N$ where Ω is the region occupied by the solid. These functions are chosen such that $\chi_i(x) = 1$ if the point $x \in \Omega$ is occupied by the i^{th} phase and $\chi_i(x) = 0$ otherwise. Consequently

$$\begin{aligned} \chi_i^\epsilon \chi_j^\epsilon &= \delta_{ij}, \\ \sum_{i=1}^N \chi_i^\epsilon &= 1. \end{aligned}$$

The phase fraction of the i^{th} phase is given by

$$\lambda_i := \frac{1}{\text{volume}(\Omega)} \int_{\Omega} \chi_i^\epsilon(x) \, dx.$$

Given some phase arrangement χ_i and a displacement field u , the total energy of the crystal is

$$\int_{\Omega} \sum_{i=1}^N \chi_i^\epsilon(x) W_i(\epsilon(u)) \, dx,$$

where $\epsilon(u) = \frac{1}{2}(\nabla u + (\nabla u)^T)$.

Displacement boundary conditions. In order to find the optimal microstructure we seek to find the χ_i and u that minimize this energy subject to the constraints of volume fractions and displacement boundary conditions, respectively. This problem is specimen specific, i.e., it depends on the domain Ω . It is convenient instead to look at a unit cell of representative volume element, also labelled Ω with abuse of notation, and consider the problem of finding the optimal arrangement of phases and the displacement when the volume fractions and average strain are given. We define the effective energy \widehat{W}_λ through the variational problem

$$\widehat{W}_\lambda(\bar{\epsilon}) := \inf_{\langle \chi_i \rangle = \lambda_i} \inf_{u|_{\partial\Omega} = \bar{\epsilon} \cdot x} \int_{\Omega} \sum_{i=1}^N \chi_i(x) W_i(\epsilon(x)) \, dx \quad (2.2)$$

(as convenient shorthands we use $\int_{\Omega} \cdot \, dx$ and $\langle \cdot \rangle$ to mean $\frac{1}{\text{volume}(\Omega)} \int_{\Omega} \cdot \, dx$). The problem we study is to characterize \widehat{W}_λ and the optimal or energy minimizing microstructures χ_i . The passage from the specimen specific problem to the unit cell problem is justified by the mathematical theory of relaxation which we shall describe in the context of shape memory alloys in the next section. Finally note that it is possible to define \widehat{W}_λ using periodic boundary conditions instead of affine boundary

¹ We use $\langle \cdot, \cdot \rangle$ to denote the inner product in $M^{n \times n}$ and \cdot to denote the inner product in \mathbb{R}^n .

conditions:

$$\widehat{W}_\lambda(\bar{\epsilon}) = \inf_{\langle \chi_i \rangle = \lambda_i} \inf_{\substack{\epsilon: \text{periodic} \\ \langle \epsilon(x) \rangle = \bar{\epsilon}}} \int_\Omega \sum_{i=1}^N \chi_i(x) W_i(\epsilon(x)) \, dx \quad (2.3)$$

Traction boundary conditions. When the specimen is subjected to tractions at the boundary the relevant potential energy is not (2.2) but

$$\int_\Omega \sum_{i=1}^N \chi_i^\epsilon(x) W_i(\epsilon(x)) \, dx - \int_{\partial\Omega} t(x) \cdot u(x) \, dS.$$

If it is further supposed that the applied traction corresponds to a uniform stress, i.e., $t(x) = \sigma \cdot \hat{n}(x)$ where \hat{n} is the unit normal to $\partial\Omega$ this reduces to

$$\int_\Omega \sum_{i=1}^N \chi_i^\epsilon(x) W_i(\epsilon(x)) - \langle \sigma, \epsilon(x) \rangle \, dx.$$

As before, in order to find the optimal microstructure we seek to find the χ_i and u that minimize this energy subject to the constraint on volume fractions. Again, since this problem is specimen specific we look instead at a unit cell of representative volume element also labelled Ω . We define the effective energy $\widehat{W}_\lambda^\sigma$ through the variational problem

$$\widehat{W}_\lambda^\sigma(\sigma) := \inf_{\langle \chi_i \rangle = \lambda_i} \inf_{u|_{\partial\Omega} = \bar{\epsilon} \cdot x} \int_\Omega \sum_{i=1}^N \chi_i(x) W_i(\epsilon(x)) - \langle \sigma, \epsilon(x) \rangle \, dx. \quad (2.4)$$

It is easy to show that $\widehat{W}_\lambda^\sigma$ is the negative of the conjugate (Legendre-Fenchel transform) of \widehat{W}_λ :

$$\begin{aligned} -(\overline{W}_\lambda)^\star(\sigma) &:= -\max_{\bar{\epsilon}} \langle \sigma, \bar{\epsilon} \rangle - \widehat{W}(\bar{\epsilon}) \\ &= \min_{\bar{\epsilon}} \widehat{W}(\bar{\epsilon}) - \langle \sigma, \bar{\epsilon} \rangle \\ &= \min_{\bar{\epsilon}} \left(\inf_{\langle \chi_i \rangle = \lambda_i} \inf_{u|_{\partial\Omega} = \bar{\epsilon} \cdot x} \int_\Omega \sum_{i=1}^N \chi_i(x) W_i(\epsilon(x)) \, dx - \langle \sigma, \bar{\epsilon} \rangle \right) \\ &= \inf_{\langle \chi_i \rangle = \lambda_i} \inf_{u|_{\partial\Omega} = \bar{\epsilon} \cdot x} \int_\Omega \sum_{i=1}^N \chi_i(x) W_i(\epsilon(x)) - \langle \sigma, \epsilon \rangle \, dx \\ &= \widehat{W}_\lambda^\sigma. \end{aligned}$$

2.2 The shape memory effect

2.2.1 The shape memory effect in single crystals

Martensitic transformation in shape memory alloys is coherent, i.e., it does not damage the crystalline lattice. It may therefore be modelled in the framework of elasticity following a long tradition c.f., e.g., Eshelby [Esh61], Wayman [Way64, WW71, Way92], Roytburd [Roy78, Roy93], Khachaturlan [Kha83], Ericksen [Eri84], Ball and James [BJ87, BJ92] and Kohn [Koh90, Koh91]. Here the states of the crystal are identified with strains relative to a fixed reference configuration. We confine ourselves to infinitesimal kinematics² and neglect ordinary thermal expansion.³ It is convenient to use the austenite phase at the transition temperature as our reference state. Thus the stress-free strain of austenite is $\epsilon_0^T = 0$. The transformation from austenite to the i^{th} variant of martensite can be described as a deformation whose strain is ϵ_i^T relative to the reference austenite. Thus ϵ_i^T is the transformation or stress-free strain of the i^{th} variant of martensite and can be determined from lattice parameters. We illustrate this with the example of cubic-tetragonal, cubic-trigonal and cubic-orthorhombic transformations:

Cubic-tetragonal, cubic-trigonal and cubic-orthorhombic transformations. The unit cell of austenite is a cube of side, say, a_o . For the cubic-tetragonal transformation the unit cell of each variant of martensite is a cuboid of sides, say, a , a and c (see Figure 2.1). Then the transformation strains for a cubic-tetragonal transformation are

$$\epsilon_1^T = \begin{pmatrix} \beta & 0 & 0 \\ 0 & \alpha & 0 \\ 0 & 0 & \alpha \end{pmatrix} \quad \epsilon_2^T = \begin{pmatrix} \alpha & 0 & 0 \\ 0 & \beta & 0 \\ 0 & 0 & \alpha \end{pmatrix} \quad \epsilon_3^T = \begin{pmatrix} \alpha & 0 & 0 \\ 0 & \alpha & 0 \\ 0 & 0 & \beta \end{pmatrix},$$

where $\alpha = \frac{a}{a_o} - 1$ and $\beta = \frac{c}{a_o} - 1$. Examples of materials that undergo this transformation are listed in Table 2.1. For a cubic-trigonal transformation, the transformation strains are of the form

$$\epsilon_1^T = \begin{pmatrix} \beta & \alpha & \alpha \\ \alpha & \beta & \alpha \\ \alpha & \alpha & \beta \end{pmatrix} \quad \epsilon_2^T = \begin{pmatrix} \beta & -\alpha & -\alpha \\ -\alpha & \beta & \alpha \\ -\alpha & \alpha & \beta \end{pmatrix} \quad \epsilon_3^T = \begin{pmatrix} \beta & \alpha & -\alpha \\ \alpha & \beta & -\alpha \\ -\alpha & -\alpha & \beta \end{pmatrix} \quad \epsilon_4^T = \begin{pmatrix} \beta & -\alpha & \alpha \\ -\alpha & \beta & -\alpha \\ \alpha & -\alpha & \beta \end{pmatrix}.$$

The transformation in Ni-Ti from austenite to R-phase is of this kind; the parameters strongly depend on temperature. For a cubic-orthorhombic transformation, the transformation strains are of

² See [Bha93] for a detailed discussion of this assumption

³ This is reasonable since we are interested in fixed temperatures, and is easy to generalize.

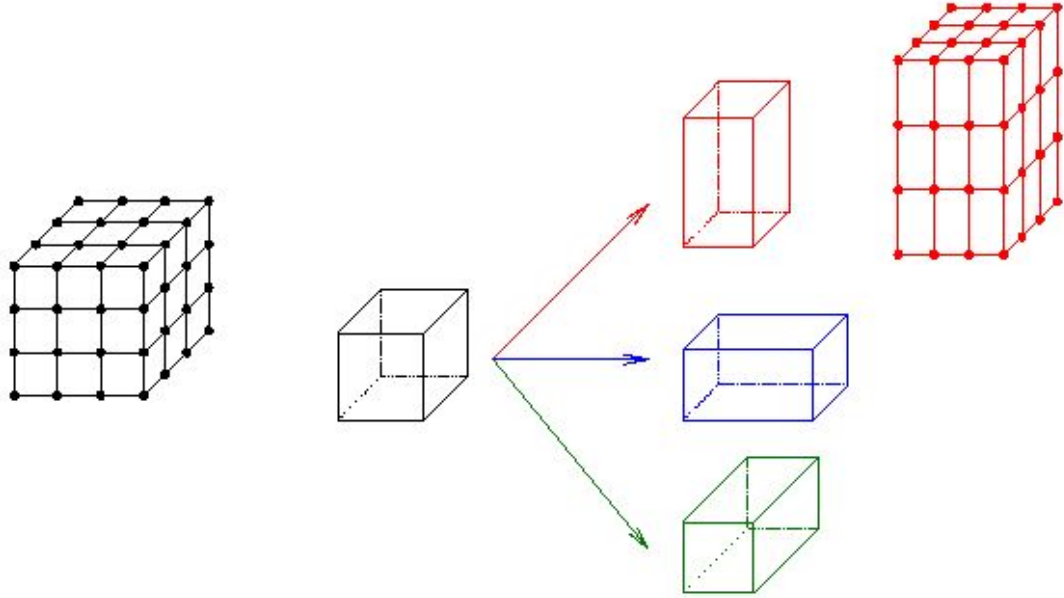


Figure 2.1: The three variants of martensite in a cubic-tetragonal transformation.

the form

$$\begin{aligned} \epsilon_1^T &= \frac{1}{2} \begin{pmatrix} \alpha+\gamma & 0 & \alpha-\gamma \\ 0 & \beta & 0 \\ \alpha-\gamma & 0 & \alpha+\gamma \end{pmatrix} & \epsilon_2^T &= \frac{1}{2} \begin{pmatrix} \alpha+\gamma & 0 & \gamma-\alpha \\ 0 & \beta & 0 \\ \gamma-\alpha & 0 & \alpha+\gamma \end{pmatrix} & \epsilon_3^T &= \frac{1}{2} \begin{pmatrix} \alpha+\gamma & \alpha-\gamma & 0 \\ \alpha-\gamma & \alpha+\alpha & 0 \\ 0 & 0 & \beta \end{pmatrix} \\ \epsilon_4^T &= \frac{1}{2} \begin{pmatrix} \alpha+\gamma & \gamma-\alpha & 0 \\ \gamma-\alpha & \alpha+\gamma & 0 \\ 0 & 0 & \beta \end{pmatrix} & \epsilon_5^T &= \frac{1}{2} \begin{pmatrix} \beta & 0 & 0 \\ 0 & \alpha+\gamma & \alpha-\gamma \\ 0 & \alpha-\gamma & \alpha+\gamma \end{pmatrix} & \epsilon_6^T &= \frac{1}{2} \begin{pmatrix} \beta & 0 & 0 \\ 0 & \alpha+\gamma & \gamma-\alpha \\ 0 & \gamma-\alpha & \alpha+\gamma \end{pmatrix}. \end{aligned}$$

Examples of materials that undergo this transformation are listed in Table 2.2.

Multi-well energy densities. The energy density of the crystal depends on the strain and the temperature. This energy has a multi-well structure as shown in Figure 2.2 reflecting the many stress-free states of the material. At high temperatures, austenite is the stable state and at low temperatures martensite is the stable state. Further, by symmetry, each variant of martensite has the same energy. Therefore the behavior of the energy density is as shown schematically in Figure 2.2.

In this thesis we are interested only in behavior of martensite at a fixed temperature below the transformation temperature. Further, we pursue energy minimization. Therefore it is natural to confine ourselves to regions close to the bottoms of the energy wells. Consequently, we neglect the austenite well and assume that the martensite wells are quadratic about their minima. Finally,

Material	Lattice parameters
In-23at.%Tl	$\alpha = -0.0111, \beta = 0.0212$
In-32at.%Pb	$\alpha = 0.0208, \beta = -0.0312$
Ni-36at.%Al	$\alpha = -0.0608, \beta = 0.1302$
Ni-49.4at.%Mn	$\alpha = -0.088, \beta = 0.1940$
Fe-24at.%Pt	$\alpha = 0.0868, \beta = -0.1497$
Fe-7.9at.%Cr-1.1at.%C	$\alpha = 0.1176, \beta = -0.1757$
Fe-22at.%Ni-0.8at.%C	$\alpha = 0.1083, \beta = -0.181$
Fe-31at.%Ni-0.3at.%C	$\alpha = 0.1241, \beta = -0.1941$
Fe-7at.%Al-1.5at.%C	$\alpha = 0.0946, \beta = -0.1454$
Fe-7at.%Al-2at.%C	$\alpha = 0.0833, \beta = -0.1273$

Table 2.1: Examples of materials undergoing cubic-tetragonal transformation [Bha03, Table 4.1, pg.50].

Material	Lattice parameters
Cu-14.2wt%Al-4.3wt.%Ni	$\alpha = 0.0619, \beta = -0.0822, \gamma = 0.0230$
Au-47.5at.%Cd	$\alpha = 0.0138, \beta = -0.0509, \gamma = 0.0350$
Au-20.7wt.%Cu-30.9wt.%Zn	$\alpha = 0.0649, \beta = -0.0752, \gamma = 0.0371$
Cu-15.3%Sn	$\alpha = 0.0820, \beta = -0.094, \gamma = 0.0350$
Zr-19.5%Th	$\alpha = 0.0690, \beta = -0.098, \gamma = 0.0140$

Table 2.2: Examples of materials undergoing cubic-orthorhombic transformation [Bha03, Table 4.2, pg.52].

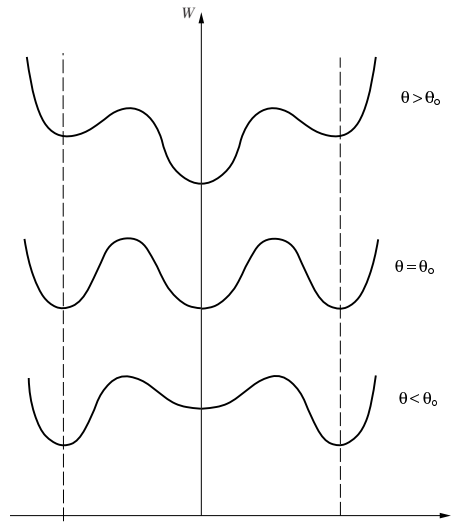


Figure 2.2: The energy density at various temperatures θ . θ_o is the transformation temperature [Bha03, Fig.4.4, pg.60].

with no loss of generality, we assume that the minimum is zero. Putting these together, we write the energy density of the material with N variants of martensite as the minimum over N quadratic energy wells:

$$W(\epsilon) := \min_{i=1,\dots,N} W_i(\epsilon). \quad (2.5a)$$

Here, ϵ is the linearized strain and the energy density of the i^{th} phase is given by

$$W_i(\epsilon) = \frac{1}{2} \langle \alpha_i(\epsilon - \epsilon_i^T), (\epsilon - \epsilon_i^T) \rangle, \quad (2.5b)$$

where α_i is the elastic modulus of the i^{th} phase. We postulate that the state of the single crystal is described by the displacement field that minimizes the total energy:

$$\int_{\Omega} W(\epsilon(u)) \, dx, \quad (2.6)$$

where Ω is the region occupied by the crystal. Since W has a multi-well structure, the problem of minimizing the total energy might not have any solution; instead minimizing sequences develop oscillations and do not converge in any classical sense [Dac89]. In other words, we find ourselves in a situation where we can reduce the energy with strain fields that have finer and finer oscillations but can never attain the minimum. We interpret this as the emergence of microstructure [BJ87] (also [CK88]). For an accessible introduction we refer the reader to [Bha03].

The relaxed energy density. Thus, once a material forms microstructure, its effective behavior is not described by W but by a energy density \widehat{W} that describes its overall effective energy after the formation of microstructure. The theory of relaxation [AF84, Dac89, KP91, DM93] provides a convenient framework for defining such an energy. Let \widehat{W} be defined as

$$\widehat{W}(\bar{\epsilon}) := \inf_{u|_{\partial\Omega}=\bar{\epsilon}\cdot x} \int_{\Omega} W(\epsilon(u)) \, dx. \quad (2.7)$$

\widehat{W} is the energy density of a material with overall strain $\bar{\epsilon}$ after it has formed microstructure. Therefore we call W the microscopic energy density and \widehat{W} the mesoscopic density energy. This is shown schematically in Figure 2.3.

The relaxed energy density can be thought of as the average energy density of the solid accounting for microstructures and describes the behavior of the solid on macroscopic length scales. The theory justifies this since minimizing $\int_{\Omega} W(\epsilon) \, dx$ with specified boundary conditions is equivalent to

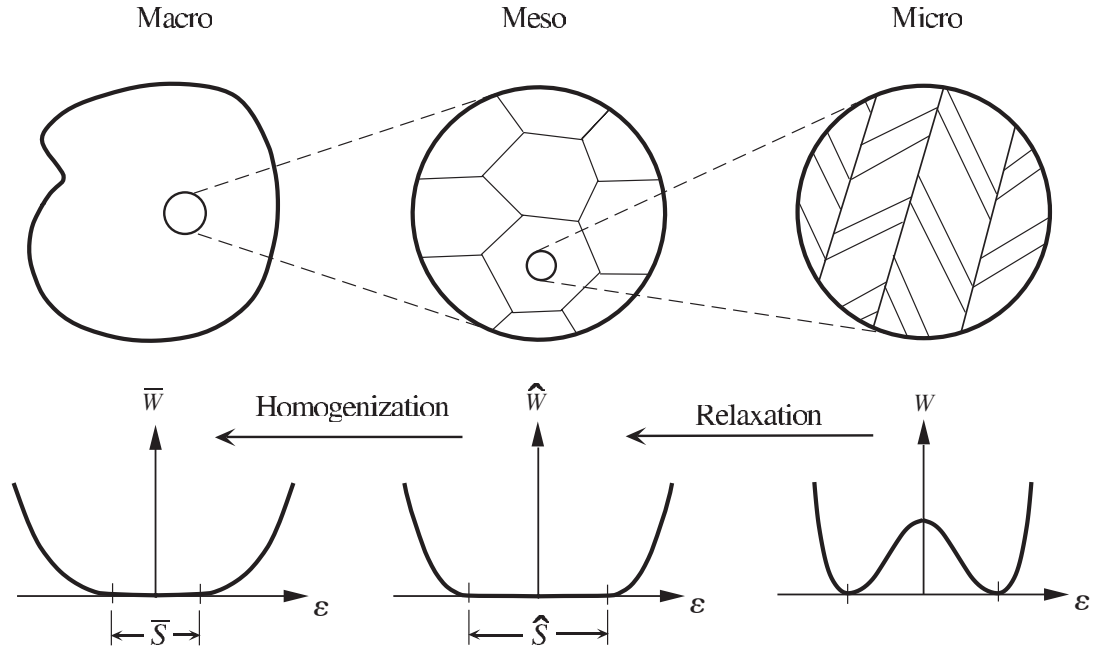


Figure 2.3: The microscopic, mesoscopic and macroscopic length scales and the energy densities associated with each of them [Bha03, Fig.13.10, pg.262].

minimizing the relaxed problem $\int_{\Omega} \widehat{W}(\epsilon) \, dx$ with the same boundary conditions:

$$\inf_{\epsilon \in \mathcal{E}} \int_{\Omega} W(\epsilon) \, dx = \min_{\epsilon \in \mathcal{E}} \int_{\Omega} \widehat{W}(\epsilon) \, dx$$

where \mathcal{E} is the set of all strain fields that satisfy the specified boundary conditions. Further \widehat{W} is independent of Ω ([Dac89, pg.101] or [Mil01, §31.2]). Note that the minimum value of \widehat{W} is the same as that of W , i.e., is 0. An equivalent definition using periodic rather than affine boundary conditions [Mil01, §31.3] is

$$\widehat{W}(\bar{\epsilon}) := \inf_{\substack{\epsilon: \text{periodic} \\ \langle \epsilon(x) \rangle = \bar{\epsilon}}} \int_{\Omega} W(\epsilon(u)) \, dx.$$

A brief and accessible treatment of relaxation can be found in [KV87, §2]; more details can be found, for example, in [AF84, Dac82, Dac89]. Finally we remark that this approach can be extended to the case when variants or phases differ in the chemical energy of the stress-free state as in (2.1).

We now in a position to provide a mathematical formulation of recoverable strains. Recall that we identified the recoverable deformations with precisely those that can be obtained with stress-free mixtures of martensite variants. In other words these are exactly the displacements that the crystal can undergo or the microstructures that the crystal can form with zero energy. Thus the recoverable

deformations are in one-to-one correspondence with the minimizers of (2.6). In light of the discussion above we define the recoverable strains to be the zero-set of the mesoscale energy \widehat{W} :

$$\widehat{S} := \{\epsilon \mid \widehat{W}(\epsilon) = 0\}.$$

To summarize: to predict the recoverable strains of a shape-memory single crystal, we start from the stress-free strains of its martensite variants, $\epsilon_1^T, \dots, \epsilon_N^T$. We first form the microscopic elastic energy W , defined by (2.5). Then we pass to its relaxation, the mesoscopic energy \widehat{W} defined by (2.7). Finally we look at the set \widehat{S} where \widehat{W} achieves its minimum value. According to our model, the elements of \widehat{S} are the overall strains which are recoverable for this crystal. \widehat{S} is compact; non-empty when the austenite is cubic and the martensite is tetragonal, trigonal, orthorhombic or monoclinic [BK97, (2.7), pg.108]; and convex when the martensite is tetragonal, trigonal or orthorhombic [BK97, §3].

Relationship between \widehat{W}_λ and \widehat{W} . The problem of computing \widehat{W} is related to the problem of computing \widehat{W}_λ described in §1.1. For our W , we can write the problem of computing \widehat{W} as (c.f. (2.5) and (2.7))

$$\widehat{W}(\bar{\epsilon}) = \inf_{u \mid \partial\Omega = \bar{\epsilon} \cdot x} \int_{\Omega} \min_{i=1, \dots, N} W_i(\epsilon) \, dx.$$

Note that the minimization over i is to be carried out pointwise. We can rewrite this using the characteristic functions χ_i introduced earlier.

$$\begin{aligned} \widehat{W}(\bar{\epsilon}) &= \inf_{u \mid \partial\Omega = \bar{\epsilon} \cdot x} \int_{\Omega} \min_{\chi_i} \sum_{i=1}^N \chi_i(x) W_i(\epsilon(x)) \, dx \\ &= \inf_{u \mid \partial\Omega = \bar{\epsilon} \cdot x} \min_{\chi_i} \int_{\Omega} \sum_{i=1}^N \chi_i(x) W_i(\epsilon(x)) \, dx \\ &= \inf_{\chi_i} \inf_{u \mid \partial\Omega = \bar{\epsilon} \cdot x} \int_{\Omega} \sum_{i=1}^N \chi_i(x) W_i(\epsilon(x)) \, dx \\ &= \min_{\lambda_i} \inf_{\langle \chi_i \rangle = \lambda_i} \inf_{u \mid \partial\Omega = \bar{\epsilon} \cdot x} \int_{\Omega} \sum_{i=1}^N \chi_i(x) W_i(\epsilon(x)) \, dx \\ &= \min_{\lambda_i} \widehat{W}_\lambda(\bar{\epsilon}). \end{aligned} \tag{2.8}$$

Note that the last problem is a simple algebraic problem if we were given \widehat{W}_λ . Thus the central problem of computing \widehat{W} is that of computing \widehat{W}_λ .

Previous results. We close this section with a description of known results for \widehat{W} . Pipkin [Pip91] and Kohn [Koh91] considered the above problem in arbitrary dimension for the special case of a two-phase material with equal elastic moduli ($\alpha_1 = \alpha_2$). Pipkin’s approach was to determine the rank-I lamination envelope of the energy and then show that it coincided with the quasicconvex hull. This approach fails when the elastic moduli are unequal since then rank-I laminates are no longer necessarily extremal [Lu93, Gra96]. Kohn’s approach was to compute a lower bound using Fourier analysis and then show its optimality by constructing microstructures whose energies attain this bound. Fourier analysis is not an useful approach when $\alpha_1 \neq \alpha_2$. Kohn also used the translation method, and it remains viable even when $\alpha_1 \neq \alpha_2$. Our work here develops on it though the translation we use is different from that used by Kohn.

Allaire and Kohn in a series of papers considered this and related problems for the case of two well ordered materials in arbitrary dimension [AK93b], two isotropic materials in two dimensions [AK93a] and two non-well ordered materials in arbitrary dimension [AK94]. In these papers, the transformation strain of both phases was taken to be equal.

Jiangbo Lu [Lu93] solved this problem in two dimensions using the translation method under the simplifying assumption of two isotropic phases with different elastic moduli. The same approach was used by Grabovsky [Gra96], again in two dimensions, for two materials with arbitrary elastic moduli but equal transformation strains. Our work completes this by studying a general two-phase material in two dimensions with no restrictions on the elastic moduli or transformation strains.

For a material with more than two phases, \widehat{W} is the convexification of the W when the elastic moduli are equal and the transformation strains are pair-wise compatible [Bha03, result 12.1, pg.215]. The problem remains open, even for equal moduli, when the transformation strains are not compatible. For a discussion of difficulties see [Koh91]; for recent progress see [SW99, GMH02].

2.2.2 The shape memory effect in polycrystals

A polycrystal is an assemblage of grains, each composed of the same shape memory material in a different orientation. To describe a polycrystal we must specify its texture, i.e., the shapes of the grains and their orientations. The texture can be represented by a rotation valued function $R: \Omega \rightarrow SO(n)$, constant on each grain, giving the crystalline orientation relative to a fixed, reference crystal. The function R is discontinuous at grain boundaries, so it implicitly determines the shape of each grain as well as its orientation. If $\epsilon_1^T, \dots, \epsilon_N^T$ are the stress-free strains of the reference crystal, then a grain with orientation R has stress-free strains $R\epsilon_1^T R^T, \dots, R\epsilon_N^T R^T$.

The total energy of a polycrystal for a given texture $R(x)$ undergoing a displacement u is given by

$$\int_{\Omega} W(R^T(x)\epsilon(u)R(x)) \, dx. \quad (2.9)$$

We seek to minimize this over all possible displacement fields but as before we expect the formation of microstructure. Therefore we consider the mesoscopic analogue of (2.9):

$$\int_{\Omega} \widehat{W}(R^T(x)\epsilon(u)R(x)) \, dx \quad (2.10)$$

In doing so we are inherently assuming that the microstructure is much smaller than the grain and hence each grain sees only the mesoscale energy averaged over the microstructure. The theory of relaxation supports this [AF84].

The essential difference between (2.9) and (2.10) is the interpretation of the strain field. In (2.9), ϵ represents the microscopic strain, which must take values $R(x)\epsilon_1^T R^T(x), \dots, R(x)\epsilon_N^T R^T(x)$ to describe a stress-free configuration of the polycrystal. In (2.10), by contrast, ϵ represents the mesoscopic strain, i.e., the average of a spatially oscillatory strain field associated with a mixture of martensite variants. Because the mesoscopic strain is an average quantity, it has more freedom than its microscopic analogue — the integrand of (2.10) is minimized whenever $R^T(x)\epsilon R(x) \in \widehat{\mathcal{S}}$, i.e., whenever within each grain ϵ remains in the set of recoverable strains for that grain: $\epsilon(x) \in \widehat{\mathcal{S}}_{R(x)}$ where $\widehat{\mathcal{S}}_R := R\widehat{\mathcal{S}}R^T$. Note that though R is piecewise constant, ϵ need not be; it has only to remain in the set $\widehat{\mathcal{S}}_R$. In other words we do not require the microstructure of each grain to be uniform; the mixture of martensite variants may differ from point to point, due to the influence of neighboring grains.

The homogenized energy density. The new problem is still awkward since the integrand depends explicitly on x . If the grain size is small compared to the specimen size, we seek to introduce an effective energy density that averages over multiple grains. This is a problem in nonlinear homogenization. The functional (2.10) can be viewed as describing a nonlinear polycrystal with reference energy \widehat{W} . Our question concerns its behavior on a length scale much larger than the grain size. The answer therefore involves the macroscopic energy density \overline{W} given by

$$\overline{W}(\bar{\epsilon}) = \inf_{\substack{\epsilon: \text{periodic} \\ \langle \epsilon \rangle = \bar{\epsilon}}} \int_{\Omega} \widehat{W}(R^T(x)\epsilon(u)R(x)) \, dx \quad (2.11)$$

in which the averages are over the periodic cell, and the minimization is over spatially periodic strain fields [Mar78, Sab92, DM93, JKO94]. \overline{W} , like \widehat{W} , is independent of Ω .

This is valid when the texture R is spatially periodic and \widehat{W} is convex. When R is random rather than

periodic, there is an analogous definition using ensemble averaging. For a more general approach based on Γ -convergence c.f., e.g., [DM93, JKO94]. For the relationship between these definitions c.f., e.g., [Mar78, GP83].

$\overline{W}(\bar{\epsilon})$ can be viewed as the average stored energy when the average strain is $\bar{\epsilon}$. The passage from \widehat{W} to \overline{W} is formally similar to that from W to \widehat{W} , except that (i) the averaging is done on a different length scale and (ii) the passage from W to \widehat{W} is associated with the multiwell character of W , and it involves averaging over mixtures of martensite variants on a subgrain length scale; the passage from \widehat{W} to \overline{W} , in contrast, is associated with the polycrystalline texture, and it involves averaging over many grains.

We are now in a position to describe the set of recoverable strains in a polycrystal. When a polycrystal in the austenite state is cooled, each grain transforms to a self-accommodated mixture of martensite variants. As the polycrystal is deformed, say to an average strain $\bar{\epsilon}$, each grain tries to accommodate the strain by adjusting its microstructure of stress-free variants. The deformation is recoverable if and only if they succeed, i.e., if and only if the strain field $\epsilon(x)$ satisfies $\epsilon(x) \in \widehat{\mathcal{S}}_{R(x)}(x)$ and $\bar{\epsilon} = \langle \epsilon(x) \rangle$. Thus the set of recoverable strains of the polycrystal is given by

$$\overline{\mathcal{S}} := \{\bar{\epsilon} \mid \exists \epsilon: \Omega \rightarrow M_{\text{Sym}}^{n \times n} \text{ periodic, such that } \epsilon(x) \in \widehat{\mathcal{S}}_{R(x)} \text{ a.e. and } \langle \epsilon(x) \rangle = \bar{\epsilon}\}. \quad (2.12)$$

Notice from (2.11) that these are precisely the strains $\bar{\epsilon}$ that minimize the mesoscopic energy:

$$\overline{\mathcal{S}} = \{\bar{\epsilon} \mid \overline{W}(\bar{\epsilon}) = 0\}. \quad (2.13)$$

Put differently, they are the macroscopic strains which can be produced by microscopic mixtures of stress-free variants. According to our model, these are the recoverable strains for the polycrystal.

In summary: to predict the recoverable strains for a shape-memory polycrystal, we start from the mesoscopic energy of the reference crystal, \widehat{W} . It has minimum value 0, and this minimum is degenerate since $\widehat{W} = 0$ on $\widehat{\mathcal{S}}$. To incorporate the effects of texture, we use nonlinear homogenization to pass to the macroscopic energy. The recoverable strains of the polycrystal are those contained in the zero-set of \overline{W} .

The Taylor bound. Notice that [BK97, Prop.2.2, pg.112]

$$\mathcal{T} := \bigcap_{x \in \Omega} \mathcal{S}_{R(x)} \subseteq \overline{\mathcal{S}}. \quad (2.14)$$

For, if every grain in a polycrystal can recover a certain strain, then the polycrystal too can recover that same strain. Indeed it can do so with no need for cooperation between the grains. \mathcal{T} is known

as the Taylor bound. \mathcal{T} is nonempty when the martensite is tetragonal, trigonal, orthorhombic or monoclinic [BK97, pg.112]. For materials that undergo cubic-tetragonal or cubic-trigonal transformations, except when the polycrystal has a very special texture, \mathcal{T} contains precisely one point. In this case we say that the Taylor bound is trivial. In contrast the Taylor bound is non-trivial for any cubic-orthorhombic polycrystal.

Previous results. Bhattachary and Kohn [BK97] have conjectured that the Taylor bound is in fact an estimate: in general only polycrystals with non-trivial Taylor bounds will be able to recover any strain. This is in excellent agreement with experimental observations. Consider three examples cited in [BK96, BK97]:

Ni-37at%Al undergoes a cubic-tetragonal transformation. Single crystals recover tensile strains ranging from 0 to 13% depending on orientation [EMT⁺81]. Polycrystals are very poor shape memory materials, recovering only about 0.2% strain in compression [KW92].

Fe-27Ni-0.8C (wt%) also undergoes a cubic-tetragonal transformation. Polycrystalline cold-rolled plates do not fully recover their strains on heating. However they do recover about 50% of a 5–7% tensile strain [KK90].

Cu-14Al-4Ni (wt.%) undergoes both cubic-orthorhombic and cubic-monoclinic transformations, depending on experimental conditions. Single crystals recover tensile strains ranging from 2 to 9% depending on orientation. Polycrystalline ribbons with uncontrolled texture recover only about 2.5% tensile strain, but specially textured polycrystalline ribbons fully recover about 6.5% tensile strain [EH90].

2.3 Statement of results

2.3.1 Two-phase solids

In Chapter 3, we compute \widehat{W}_λ defined in (2.2) or (2.3) for $W: M_{\text{sym}}^{2 \times 2} \rightarrow \mathbb{R}$ given by

$$W(\epsilon) = \min \{W_1(\epsilon), W_2(\epsilon)\}, \quad (2.15a)$$

$$W_i(\epsilon) = \frac{1}{2} \langle \alpha_i(\epsilon - \epsilon_i^T), (\epsilon - \epsilon_i^T) \rangle + w_i \quad (2.15b)$$

and show that there always exist rank-I or rank-II laminates that are extremal. We summarize the results here. Let $T: M_{\text{sym}}^{2 \times 2} \rightarrow M_{\text{sym}}^{2 \times 2}$ be the linear operator defined by $T\epsilon = \epsilon - \text{Tr}(\epsilon)I$. Let $\gamma_i, \gamma_\star > 0$

be defined by

$$\gamma_i := - \max_{\substack{\epsilon \\ \det(\epsilon) < 0}} \frac{\langle \alpha_i \epsilon, \epsilon \rangle}{2 \det(\epsilon)},$$

$$\gamma_\star := \min_{i=1,2} \gamma_i.$$

Then

$$\widehat{W}_\lambda(\epsilon) = \lambda_1 W_1(\epsilon_1^\star) + \lambda_2 W_2(\epsilon_2^\star) + \beta \lambda_1 \lambda_2 \det(\epsilon_2^\star - \epsilon_1^\star) \quad (2.16)$$

where

$$\epsilon_1^\star = (\lambda_2 \alpha_1 + \lambda_1 \alpha_2 - \beta^\star T)^{-1} ((\alpha_2 - \beta^\star T) \bar{\epsilon} - \lambda_2 (\alpha_2 \epsilon_2^\top - \alpha_1 \epsilon_1^\top))$$

$$\epsilon_2^\star = (\lambda_2 \alpha_1 + \lambda_1 \alpha_2 - \beta^\star T)^{-1} ((\alpha_1 - \beta^\star T) \bar{\epsilon} + \lambda_1 (\alpha_2 \epsilon_2^\top - \alpha_1 \epsilon_1^\top))$$

and β^\star is chosen as follows. For $\beta \in [0, \gamma_\star]$, let

$$f(\beta) := \det \left((\lambda_2 \alpha_1 + \lambda_1 \alpha_2 - \beta T)^{-1} (\alpha_2 (\epsilon_2^\top - \bar{\epsilon}) - \alpha_1 (\epsilon_1^\top - \bar{\epsilon})) \right)$$

be a quadratic in β . When $f(0) > 0$ and $f(\gamma_\star) < 0$, $f(\beta) = 0$ has a unique root, β_{II} . Let

$$\beta^\star = \begin{cases} 0 & \text{if } f(0) < 0 & \text{(Regime I)} \\ \beta_{\text{II}} & \text{if } f(0) > 0 \text{ and } f(\gamma_\star) < 0 & \text{(Regime II)} \\ \gamma_\star & \text{if } f(\gamma_\star) > 0. & \text{(Regime III)} \end{cases}$$

We prove this by first using the translation method to show that the right-hand side of (2.16) is a lower bound for \overline{W}_λ , and then constructing microstructures whose effective energy equals this bound: In regime I, there exists two rank-I laminates that are extremal; other extremal microstructures might also exist. In regime II, the unique extremal microstructure is a rank-I laminate. In regime III, there exists two rank-II laminates that are extremal; other extremal microstructures might also exist but no rank-I laminate is extremal.

In Chapter 4 we solve the problem in three dimensions when the elastic moduli are isotropic.

2.3.2 Polycrystals

In Chapter 5, we begin by proving a dual variational characterization of the zero-set of polycrystals. This characterization suggests that dual (stress) fields could be signed Radon measures with finite

mass. For a two-dimensional material whose microscopic energy is of the form (2.15), we exhibit examples where this is indeed the case. These examples also illustrate discontinuous dependence of the zero-set (of polycrystals) on microstructure and effects of symmetry. They also enable us to comment on connections to percolation theory observed earlier [BK97]. For the two-dimensional material and for materials that undergo cubic-tetragonal transformations, we show that strain fields associated with macroscopically recoverable strains are related to solutions of hyperbolic partial differential equations.

Chapter 3

Two-phase solids in two dimensions

3.1 An optimal lower bound on the relaxed energy

We use the translation method to obtain a lower bound on the relaxed energy. Good introductions and overviews of the translation method can be found in [Che00, Chs.8,15,16] and [Mil01, Chs.4,24,25]. For development of the method and applications to a wide range of problems see, for example, Tartar [Tar79a, Tar85, Tar79b]; Murat [Mur87]; Murat and Tartar [MT85]; Lurie and Cherkaev [LC81, LC82a, LC82b, LC86a]; Cherkaev and Gibiansky [CG92]; Gibiansky and Cherkaev [GC84, GC87]; Kohn and Strang [KS82, KS83, KS86a, KS86b, KS86c]; Strang and Kohn [SK88]; Avellaneda, Cherkaev, Lurie and Milton [ACLM88]; Firoozye [Fir91] and Milton [Mil90a, Mil90b].

3.1.1 A lower bound by the translation method

Proposition 3.1 (Translation lower bound). Let W , W_1 and W_2 be as in (2.5), $f: M_{\text{sym}}^{n \times n} \rightarrow \mathbb{R}$ be quasiconvex and $\beta \in \mathbb{R}$. Then

$$\widehat{W}_\lambda(\bar{\epsilon}) \geq \max_{\substack{\beta \geq 0 \\ W_i - \beta f: \text{convex}}} \min_{\substack{\epsilon_1, \epsilon_2 \in M_{\text{sym}}^{n \times n} \\ \lambda_1 \epsilon_1 + \lambda_2 \epsilon_2 = \bar{\epsilon}}} \lambda_1 (W_1 - \beta f)(\epsilon_1) + \lambda_2 (W_2 - \beta f)(\epsilon_2) + \beta f(\bar{\epsilon}). \quad (3.1)$$

Proof. From (2.2),

$$\widehat{W}_\lambda(\bar{\epsilon}) := \inf_{\langle \chi_i \rangle = \lambda_i} \inf_{u|_{\partial\Omega} = \bar{\epsilon} \cdot x} \int_{\Omega} \chi_1 W_1(\epsilon) + \chi_2 W_2(\epsilon) \, dx.$$

From the definition of quasiconvexity,

$$f(\bar{\epsilon}) \leq \inf_{u|_{\partial\Omega} = \bar{\epsilon} \cdot x} \int_{\Omega} f(\epsilon) \, dx.$$

Thus we have the lower bound

$$\widehat{W}_\lambda(\bar{\epsilon}) \geq \inf_{\langle \chi_i \rangle = \lambda_i} \inf_{u|_{\partial\Omega} = \bar{\epsilon} \cdot x} \int_{\Omega} \chi_1(W_1(\epsilon) - \beta f(\epsilon)) + \chi_2(W_2(\epsilon) - \beta f(\epsilon)) \, dx + \beta f(\bar{\epsilon})$$

for each $\beta \geq 0$. Restricting ourselves to β such that the function $W_i - \beta f$ is convex (the reason for this will become clear in the next step), we have

$$\widehat{W}_\lambda(\bar{\epsilon}) \geq \max_{\substack{\beta \geq 0 \\ W_i - \beta f: \text{convex}}} \min_{\langle \chi_i \rangle = \lambda_i} \inf_{u|_{\partial\Omega} = \bar{\epsilon} \cdot x} \int_{\Omega} \chi_1(W_1(\epsilon) - \beta f(\epsilon)) + \chi_2(W_2(\epsilon) - \beta f(\epsilon)) \, dx + \beta f(\bar{\epsilon}).$$

Since $W_i - \beta f$ is convex, using Jensen's inequality,

$$\begin{aligned} \widehat{W}_\lambda(\bar{\epsilon}) \geq \max_{\substack{\beta \geq 0 \\ W_i - \beta f: \text{convex}}} \min_{\langle \chi_i \rangle = \lambda_i} \inf_{u|_{\partial\Omega} = \bar{\epsilon} \cdot x} \lambda_1(W_1 - \beta f) \left(\frac{\int_{\Omega} \chi_1 \epsilon \, dx}{\int_{\Omega} \chi_1 \, dx} \right) \\ + \lambda_2(W_2 - \beta f) \left(\frac{\int_{\Omega} \chi_2 \epsilon \, dx}{\int_{\Omega} \chi_2 \, dx} \right) + \beta f(\bar{\epsilon}). \end{aligned}$$

Setting $\epsilon_i = \frac{\langle \chi_i \epsilon \rangle}{\langle \chi_i \rangle}$ and noting that $\lambda_1 \epsilon_1 + \lambda_2 \epsilon_2 = \bar{\epsilon}$, we obtain the desired result (3.1). \square

3.1.2 The determinant as translation

The lower bound presented above is valid for any translation $f: M_{\text{sym}}^{n \times n} \rightarrow \mathbb{R}$ which is quasiconvex. This is the mathematics of the translation method; the art of the translation method lies in choosing the right translation. In two dimensions we pick the translation to be the negative of the determinant:

$$f(\epsilon) \equiv \phi(\epsilon) := -\det(\epsilon) = \epsilon_{12}^2 - \epsilon_{11}\epsilon_{22}.$$

This choice of the translation might appear to be arbitrary, but in fact is a posteriori natural. ϕ is quasiconvex on the space of all symmetrized gradients since it is quadratic and rank-I convex [Dac89, pg.126]: $\forall m, n \in \mathbb{R}^2$, $\phi(m \otimes_s n) \geq 0$. Here $\hat{m} \otimes_s \hat{n} := \frac{1}{2}(\hat{n} \otimes \hat{m} + \hat{m} \otimes \hat{n})$; $\hat{m} \otimes \hat{n}$ is defined as usual by $(\hat{m} \otimes \hat{n})_{ij} = m_i n_j$.

Since ϕ is quadratic there exists a (unique) linear operator $T: M_{\text{sym}}^{2 \times 2} \rightarrow M_{\text{sym}}^{2 \times 2}$ such that

$$\phi(\epsilon) = \frac{1}{2} \langle T\epsilon, \epsilon \rangle.$$

It is easy to verify that T is self-adjoint and is given by $T\epsilon = \epsilon - \text{Tr}(\epsilon)I$ (i.e., $-T\epsilon$ is the adjoint of ϵ). T has eigenvalues -1 and 1 , repeated once and twice, respectively: $TI = -I$ and $T\epsilon = \epsilon$ for all $\epsilon \in M_{\text{sym}}^{2 \times 2}$ such that $\text{Tr}(\epsilon) = 0$ (a two-dimensional subspace of $M_{\text{sym}}^{2 \times 2}$). It follows that T is invertible and is neither positive nor negative definite.

To further understand T and for future use, note that $\left\{ \begin{pmatrix} 1 & 0 \\ 0 & 1 \end{pmatrix}, \begin{pmatrix} 1 & 0 \\ 0 & -1 \end{pmatrix}, \begin{pmatrix} 0 & 1 \\ 1 & 0 \end{pmatrix} \right\}$ form an orthogonal basis for $M_{\text{sym}}^{2 \times 2}$ and let $\mathbf{\Lambda}_h, \mathbf{\Lambda}_d$ and $\mathbf{\Lambda}_o: M_{\text{sym}}^{2 \times 2} \rightarrow M_{\text{sym}}^{2 \times 2}$ be orthogonal projection operators defined by

$$\text{Range}(\mathbf{\Lambda}_h) = \text{Span} \left\{ \begin{pmatrix} 1 & 0 \\ 0 & 1 \end{pmatrix} \right\}, \quad (3.2a)$$

$$\text{Range}(\mathbf{\Lambda}_d) = \text{Span} \left\{ \begin{pmatrix} 1 & 0 \\ 0 & -1 \end{pmatrix} \right\}, \quad (3.2b)$$

$$\text{Range}(\mathbf{\Lambda}_o) = \text{Span} \left\{ \begin{pmatrix} 0 & 1 \\ 1 & 0 \end{pmatrix} \right\}. \quad (3.2c)$$

It is easy to see that $T \equiv -\mathbf{\Lambda}_h + \mathbf{\Lambda}_d + \mathbf{\Lambda}_o$. Thus T is a reflection about the plane of deviatoric (i.e., trace-free) strains.

With this choice for the translation, exploiting the quadraticity of W_i and ϕ , (3.1) may be rewritten as

$$\widehat{W}_\lambda(\bar{\epsilon}) \geq \max_{\substack{\beta \geq 0 \\ W_i - \beta\phi: \text{convex}}} W_\lambda(\beta, \bar{\epsilon}) \quad (3.3a)$$

where

$$W_\lambda(\beta, \bar{\epsilon}) := \min_{\substack{\epsilon_1, \epsilon_2 \in M_{\text{sym}}^{2 \times 2} \\ \lambda_1 \epsilon_1 + \lambda_2 \epsilon_2 = \bar{\epsilon}}} \lambda_1 W_1(\epsilon_1) + \lambda_2 W_2(\epsilon_2) - \beta \lambda_1 \lambda_2 \phi(\epsilon_2 - \epsilon_1). \quad (3.3b)$$

3.1.3 Determining the amount of translation

Our next step is to characterize the set $\{\beta \mid \beta \geq 0, W_i - \beta\phi: \text{convex}\}$.

Lemma 3.2 (Convexity of translated energies). Let $\gamma_i, \gamma_\star > 0$ be defined by

$$\gamma_i := \min_{\substack{\epsilon \\ \phi(\epsilon) > 0}} \frac{\langle \alpha_i \epsilon, \epsilon \rangle}{2\phi(\epsilon)},$$

$$\gamma_\star := \min_{i=1,2} \gamma_i.$$

Then

$$[0, \gamma_\star] = \{\beta \mid \beta \geq 0, W_i - \beta\phi: \text{convex}\},$$

$$[0, \gamma_\star) = \{\beta \mid \beta \geq 0, W_i - \beta\phi: \text{strictly convex}\}.$$

Proof. By quadraticity, the convexity of $W_i - \beta\phi$ is equivalent to the nonnegativity of $\epsilon \mapsto \langle (\alpha_i -$

$\beta T)\epsilon, \epsilon\rangle$. Thus

$$\begin{aligned} \langle (\alpha_i - \beta T)\epsilon, \epsilon \rangle \geq 0 &\Leftrightarrow \langle \alpha_i \epsilon, \epsilon \rangle - 2\beta\phi(\epsilon) \geq 0 \\ &\Leftrightarrow \max_{\substack{\epsilon \\ \phi(\epsilon) < 0}} \frac{\langle \alpha_i \epsilon, \epsilon \rangle}{2\phi(\epsilon)} \leq \beta \leq \min_{\substack{\epsilon \\ \phi(\epsilon) > 0}} \frac{\langle \alpha_i \epsilon, \epsilon \rangle}{2\phi(\epsilon)} \\ &\Leftrightarrow \beta \leq \gamma_i \end{aligned}$$

where the last step follows since $\alpha_i > 0$ and $\beta \geq 0$. Thus for $W_i - \beta\phi$ to be convex we need $\beta < \gamma_i$.

This shows that $[0, \gamma_i] = \{\beta \mid \beta \geq 0, W_i - \beta\phi: \text{convex}\}$.

Alternatively,

$$\langle (\alpha_i - \beta T)\epsilon, \epsilon \rangle = \left\langle \sqrt{\alpha_i} \left(I - \beta \alpha_i^{-\frac{1}{2}} T \alpha_i^{-\frac{1}{2}} \right) \sqrt{\alpha_i} \epsilon, \epsilon \right\rangle = \|\tilde{\epsilon}\|^2 - \beta \left\langle \alpha_i^{-\frac{1}{2}} T \alpha_i^{-\frac{1}{2}} \tilde{\epsilon}, \tilde{\epsilon} \right\rangle$$

where $\tilde{\epsilon} = \sqrt{\alpha_i} \epsilon$ and $\sqrt{\alpha_i}$ is the unique positive-definite self-adjoint square root of α_i . Thus

$$\begin{aligned} W_i - \beta\phi: \text{strictly convex} &\Leftrightarrow \forall \epsilon \neq 0, \|\epsilon\|^2 - \beta \left\langle \left(\alpha_i^{-\frac{1}{2}} T \alpha_i^{-\frac{1}{2}} \right) \epsilon, \epsilon \right\rangle > 0 \\ &\Leftrightarrow \forall \epsilon \neq 0, \frac{1}{\beta} > \frac{\left\langle \left(\alpha_i^{-\frac{1}{2}} T \alpha_i^{-\frac{1}{2}} \right) \epsilon, \epsilon \right\rangle}{\|\epsilon\|^2} \end{aligned}$$

where we have used the invertibility of $\sqrt{\alpha_i}$. Note that in this case an equivalent definition for γ_i is

$$\frac{1}{\gamma_i} = \max_{\|\epsilon\|=1} \left\langle \left(\alpha_i^{-\frac{1}{2}} T \alpha_i^{-\frac{1}{2}} \right) \epsilon, \epsilon \right\rangle.$$

γ_i is non-negative since T has a positive eigenvalue and all eigenvalues of α_i are non-negative. The result follows. \square

Remark 3.3. When α_i is cubic, aligning our axis with the principal axis of α_i (which might be different for each phase), we have

$$\alpha_i = 2\kappa_i \mathbf{\Lambda}_h + 2\mu_i \mathbf{\Lambda}_d + 2\eta_i \mathbf{\Lambda}_o,$$

where κ_i , μ_i and η_i are, respectively, the bulk, diagonal shear and off-diagonal shear moduli of the i^{th} phase. ($\mathbf{\Lambda}_h$, $\mathbf{\Lambda}_d$ and $\mathbf{\Lambda}_o: M_{\text{sym}}^{2 \times 2} \rightarrow M_{\text{sym}}^{2 \times 2}$ are orthogonal projection operators defined by (3.2).)

Since $T \equiv -\mathbf{\Lambda}_h + \mathbf{\Lambda}_d + \mathbf{\Lambda}_o$,

$$\alpha_i^{-\frac{1}{2}} T \alpha_i^{-\frac{1}{2}} = \frac{-1}{2\kappa_i} \mathbf{\Lambda}_h + \frac{1}{2\mu_i} \mathbf{\Lambda}_d + \frac{1}{2\eta_i} \mathbf{\Lambda}_o \quad \Rightarrow \quad \frac{1}{\gamma_i} = \max \left(\frac{1}{2\mu_i}, \frac{1}{2\eta_i} \right)$$

Thus when α_i is cubic, $\gamma_i = 2 \min\{\mu_i, \eta_i\}$. When α_i is isotropic, setting $\mu_i = \eta_i$, $\gamma_i = 2\mu_i$.

3.1.4 Explicit expressions for the optimal strains

Let us return to the minimization problem (3.3b) and find the minimizers $\epsilon_1^*(\beta, \bar{\epsilon})$ and $\epsilon_2^*(\beta, \bar{\epsilon})$. By differentiating the argument on the right-hand side of (3.3b),

$$\alpha_1(\epsilon_1^* - \epsilon_1^T) - \alpha_2(\epsilon_2^* - \epsilon_2^T) + \beta T(\epsilon_2^* - \epsilon_1^*) = 0. \quad (3.4)$$

In other words,

$$\Delta\sigma^* = \beta T \Delta\epsilon^* \quad (3.5)$$

where $\Delta\epsilon^* := \epsilon_2^* - \epsilon_1^*$, $\Delta\sigma^* := \sigma_2^* - \sigma_1^*$ and $\sigma_i^* = \alpha_i(\epsilon_i^* - \epsilon_i^T)$. Using $\lambda_1\epsilon_1 + \lambda_2\epsilon_2 = \bar{\epsilon}$, (3.4) gives

$$\begin{aligned} (\lambda_2\alpha_1 + \lambda_1\alpha_2 - \beta T)\epsilon_1^* &= (\alpha_2 - \beta T)\bar{\epsilon} + \lambda_2(\alpha_1\epsilon_1^T - \alpha_2\epsilon_2^T) \\ (\lambda_2\alpha_1 + \lambda_1\alpha_2 - \beta T)\epsilon_2^* &= (\alpha_1 - \beta T)\bar{\epsilon} - \lambda_1(\alpha_1\epsilon_1^T - \alpha_2\epsilon_2^T) \\ (\lambda_2\alpha_1 + \lambda_1\alpha_2 - \beta T)\Delta\epsilon^* &= (\alpha_2\epsilon_2^T - \alpha_1\epsilon_1^T) - (\Delta\alpha)\bar{\epsilon}. \end{aligned}$$

where $\Delta\alpha := \alpha_2 - \alpha_1$. Thus

$$(\lambda_2\alpha_1 + \lambda_1\alpha_2 - \beta T) \frac{\partial \Delta\epsilon^*}{\partial \beta} - T \Delta\epsilon^* - \beta T \frac{\partial \Delta\epsilon^*}{\partial \beta} = 0.$$

To get explicit expressions we need the invertibility of $\lambda_2\alpha_1 + \lambda_1\alpha_2 - \beta T$. Note that $\lambda_2\alpha_1 + \lambda_1\alpha_2 - \beta T = \lambda_2(\alpha_1 - \beta T) + \lambda_1(\alpha_2 - \beta T)$. Hence, for $\beta \in [0, \gamma_*)$, it is the sum of two positive definite linear operators and consequently positive definite and thus invertible. In fact even when $\beta = \gamma_*$, $\lambda_2\alpha_1 + \lambda_1\alpha_2 - \beta T$ is invertible as long as $\ker(\alpha_1 - \gamma_*T) \cap \ker(\alpha_2 - \gamma_*T) = \{0\}$. In either case,

$$\epsilon_1^* = (\lambda_2\alpha_1 + \lambda_1\alpha_2 - \beta T)^{-1} ((\alpha_2 - \beta T)\bar{\epsilon} - \lambda_2(\alpha_2\epsilon_2^T - \alpha_1\epsilon_1^T)), \quad (3.6a)$$

$$\epsilon_2^* = (\lambda_2\alpha_1 + \lambda_1\alpha_2 - \beta T)^{-1} ((\alpha_1 - \beta T)\bar{\epsilon} + \lambda_1(\alpha_2\epsilon_2^T - \alpha_1\epsilon_1^T)), \quad (3.6b)$$

$$\Delta\epsilon^* = (\lambda_2\alpha_1 + \lambda_1\alpha_2 - \beta T)^{-1} ((\alpha_2\epsilon_2^T - \alpha_1\epsilon_1^T) - (\Delta\alpha)\bar{\epsilon}), \quad (3.6c)$$

and

$$\frac{\partial \Delta\epsilon^*}{\partial \beta} = (\lambda_2\alpha_1 + \lambda_1\alpha_2 - \beta T)^{-1} T \Delta\epsilon^*. \quad (3.7)$$

3.1.5 A lower bound on the relaxed energy

Applying lemma 3.2 to the lower bound (3.3a), we have

$$\widehat{W}_\lambda(\bar{\epsilon}) \geq \max_{\beta \in [0, \gamma_\star]} W_\lambda(\beta, \bar{\epsilon}). \quad (3.8)$$

Determining this maximum is easy since we have the following lemma:

Lemma 3.4. When $\gamma_\star > 0$, $\beta \mapsto W_\lambda(\beta, \bar{\epsilon})$ is either constant or strictly concave for $\beta \in (0, \gamma_\star)$.

Proof. From (3.3b) and (3.7),

$$\begin{aligned} \frac{\partial}{\partial \beta} W_\lambda(\beta, \bar{\epsilon}) &= -\lambda_1 \lambda_2 \phi(\Delta \epsilon^\star(\beta, \bar{\epsilon})) \\ \frac{\partial^2}{\partial \beta^2} W_\lambda(\beta, \bar{\epsilon}) &= -\lambda_1 \lambda_2 \left\langle T \Delta \epsilon^\star, \frac{\partial \Delta \epsilon^\star}{\partial \beta} \right\rangle \\ &= -\lambda_1 \lambda_2 \left\langle T \Delta \epsilon^\star, (\lambda_2 \alpha_1 + \lambda_1 \alpha_2 - \beta T)^{-1} T \Delta \epsilon^\star \right\rangle \\ &< 0 \end{aligned} \quad (3.9)$$

except when $\Delta \epsilon^\star(\beta, \bar{\epsilon}) = 0$. Note, from (3.6), that $\Delta \epsilon^\star(\beta, \bar{\epsilon}) = 0$ for some β implies that $\Delta \epsilon^\star(\beta, \bar{\epsilon}) = 0$ for all β . However when $\Delta \epsilon^\star \equiv 0$, from (3.9), $W_\lambda(\beta, \bar{\epsilon})$ is independent of β . \square

Theorem 3.5. Let β_{II} be the unique solution of $\phi(\Delta \epsilon^\star(\beta_{\text{II}}, \bar{\epsilon})) = 0$. Then

$$\widehat{W}_\lambda(\bar{\epsilon}) \geq \widehat{W}_\lambda^l(\bar{\epsilon})$$

where

$$\widehat{W}_\lambda^l(\bar{\epsilon}) = \begin{cases} W_\lambda(0, \bar{\epsilon}) & \text{if } \phi(\Delta \epsilon^\star(0, \bar{\epsilon})) > 0 & \text{(Regime I)} \\ W_\lambda(\beta_{\text{II}}, \bar{\epsilon}) & \text{otherwise} & \text{(Regime II)} \\ W_\lambda(\gamma_\star, \bar{\epsilon}) & \text{if } \phi(\Delta \epsilon^\star(\gamma_\star, \bar{\epsilon})) < 0. & \text{(Regime III)} \end{cases} \quad (3.10)$$

Note from (3.6) that

$$\phi(\Delta \epsilon^\star(\beta, \bar{\epsilon})) \equiv \phi\left((\lambda_2 \alpha_1 + \lambda_1 \alpha_2 - \beta T)^{-1} ((\alpha_2 \epsilon_2^T - \alpha_1 \epsilon_1^T) - \Delta \alpha \bar{\epsilon})\right).$$

Proof. From (3.6), $\Delta \epsilon^\star(\beta, \bar{\epsilon}) \equiv 0$ precisely when $\alpha_2(\bar{\epsilon} - \epsilon_2^T) = \alpha_1(\bar{\epsilon} - \epsilon_1^T)$. Then, from lemma 3.4, $\beta \mapsto W_\lambda(\beta, \bar{\epsilon})$ is constant and thus (3.10) is the same as (3.8). Consider the case when $\beta \mapsto W_\lambda(\beta, \bar{\epsilon})$ is strictly concave.

Using (3.9), from the concavity of $\beta \mapsto W_\lambda(\beta, \bar{\epsilon})$, the maximum occurs at $\beta = 0$ whenever $\phi(\Delta\epsilon^*(0, \bar{\epsilon})) > 0$ and at $\beta = \gamma_\star$ whenever $\phi(\Delta\epsilon^*(\gamma_\star, \bar{\epsilon}))$ exists and is less than zero.

Since $\beta \mapsto W_\lambda(\beta, \bar{\epsilon})$ is strictly concave, from (3.9), $\beta \mapsto \phi(\Delta\epsilon^*(\beta, \bar{\epsilon}))$ is strictly increasing. Thus when $\phi(\Delta\epsilon^*(\gamma_\star, \bar{\epsilon}))$ does not exist, $\phi(\Delta\epsilon^*(\beta, \bar{\epsilon})) \rightarrow \infty$ as $\beta \rightarrow \gamma_\star$. If in addition $\phi(\Delta\epsilon^*(0, \bar{\epsilon})) \leq 0$, it follows that for some unique $\beta_{\text{II}} \in [0, \gamma_\star)$, $\phi(\Delta\epsilon^*(\beta_{\text{II}}, \bar{\epsilon})) = 0$.

The remaining possibility is that $\phi(\Delta\epsilon^*(0, \bar{\epsilon})) \leq 0$ and $\phi(\Delta\epsilon^*(\gamma_\star, \bar{\epsilon})) \geq 0$. Then again from the strict convexity of $\beta \mapsto W_\lambda(\beta, \bar{\epsilon})$, there exists a unique β_{II} such that $\phi(\Delta\epsilon^*(\beta_{\text{II}}, \bar{\epsilon})) = 0$ and the maximum occurs at $\beta = \beta_{\text{II}}$. Note that it is possible that $\beta_{\text{II}} \in \{0, \gamma_\star\}$. \square

Remark 3.6. Regime III does not occur whenever $\phi(\Delta\epsilon^*(\gamma_\star, \bar{\epsilon}))$ does not exist. From §3.1.4 this happens when $\ker(\alpha_1 - \gamma_\star T) \cap \ker(\alpha_2 - \gamma_\star T) \neq \{0\}$. This includes, in particular, the cases (i) $\alpha_1 = \alpha_2$ and (ii) both phases being isotropic with equal shear moduli. We will show below that in this case there exists a rank-I laminate that is extremal. This is consistent with the results in [Koh91, Pip91].

3.1.6 Equal elastic moduli

In this section we consider the special case of equal elastic moduli. From (3.6), $\Delta\epsilon^*(0, \bar{\epsilon}) = \epsilon_2^T - \epsilon_1^T$. From remark 3.6, regime III does not occur in this case. Thus, from (3.10), \widehat{W}_λ^l , the lower bound for \widehat{W}_λ reduces to

$$\widehat{W}_\lambda^l(\bar{\epsilon}) = \begin{cases} W_\lambda(0, \bar{\epsilon}) & \text{if } \phi(\epsilon_2^T - \epsilon_1^T) > 0 \\ W_\lambda(\beta_{\text{II}}, \bar{\epsilon}) & \text{otherwise, i.e., if } \phi(\epsilon_2^T - \epsilon_1^T) \leq 0, \end{cases}$$

where β_{II} is the unique solution of

$$\phi\left((\alpha - \beta T)^{-1} \alpha (\epsilon_2^T - \epsilon_1^T)\right) = 0.$$

A moment's thought reveals that this is infact equivalent to

$$\widehat{W}_\lambda^l(\bar{\epsilon}) = \begin{cases} W_\lambda(0, \bar{\epsilon}) & \text{if } \phi(\epsilon_2^T - \epsilon_1^T) \geq 0 \\ W_\lambda(\beta_{\text{II}}, \bar{\epsilon}) & \text{otherwise, i.e., if } \phi(\epsilon_2^T - \epsilon_1^T) < 0. \end{cases}$$

That is (c.f. §3.2.1),

$$\widehat{W}_\lambda^l(\bar{\epsilon}) = \begin{cases} W_\lambda(0, \bar{\epsilon}) & \text{if } \epsilon_1^T \text{ and } \epsilon_2^T \text{ are compatible} \\ W_\lambda(\beta_{\text{II}}, \bar{\epsilon}) & \text{otherwise, i.e., if } \epsilon_1^T \text{ and } \epsilon_2^T \text{ are incompatible.} \end{cases} \quad (3.11)$$

Explicit expressions for the optimal strains when the elastic moduli are equal. (3.6)

simplifies to

$$\epsilon_1^* = \bar{\epsilon} - \lambda_2(\alpha - \beta T)^{-1}\alpha(\epsilon_2^T - \epsilon_1^T), \quad (3.12a)$$

$$\epsilon_2^* = \bar{\epsilon} + \lambda_1(\alpha - \beta T)^{-1}\alpha(\epsilon_2^T - \epsilon_1^T), \quad (3.12b)$$

$$\Delta\epsilon^* = (\alpha - \beta T)^{-1}\alpha(\epsilon_2^T - \epsilon_1^T). \quad (3.12c)$$

If, in addition, $\beta = 0$, then,

$$\epsilon_1^* = \bar{\epsilon} - \lambda_2(\epsilon_2^T - \epsilon_1^T), \quad (3.12d)$$

$$\epsilon_2^* = \bar{\epsilon} + \lambda_1(\epsilon_2^T - \epsilon_1^T), \quad (3.12e)$$

$$\Delta\epsilon^* = \epsilon_2^T - \epsilon_1^T. \quad (3.12f)$$

From (3.11) and (3.12), we obtain,

$$\widehat{W}_\lambda^l(\bar{\epsilon}) = \begin{cases} \lambda_1 W_1(\bar{\epsilon} - \lambda_2(\epsilon_2^T - \epsilon_1^T)) + \lambda_2 W_2(\bar{\epsilon} + \lambda_1(\epsilon_2^T - \epsilon_1^T)) & \text{if } \epsilon_1^T \text{ and } \epsilon_2^T \text{ are compatible} \\ \lambda_1 W_1\left(\bar{\epsilon} - \lambda_2(\alpha - \beta T)^{-1}\alpha(\epsilon_2^T - \epsilon_1^T)\right) \\ \quad + \lambda_2 W_2\left(\bar{\epsilon} + \lambda_1(\alpha - \beta T)^{-1}\alpha(\epsilon_2^T - \epsilon_1^T)\right) \\ \quad - \beta\lambda_1\lambda_2\phi\left((\alpha - \beta T)^{-1}\alpha(\epsilon_2^T - \epsilon_1^T)\right) & \text{if } \epsilon_1^T \text{ and } \epsilon_2^T \text{ are incompatible.} \end{cases}$$

3.2 Extremal microstructures

In this section we prove that the lower bound presented in theorem 3.5 is optimal,

$$\widehat{W}_\lambda(\bar{\epsilon}) = \widehat{W}_\lambda^l(\bar{\epsilon}) \quad (3.13)$$

Our strategy of proof is determining upper bounds by explicitly constructing microstructures. Given any (sequence of) microstructures χ_i that satisfy $\langle \chi_i \rangle = \lambda_i$, it follows from the definition of \widehat{W}_λ in (2.2) that

$$\widehat{W}_\lambda(\bar{\epsilon}) \leq \inf_{u|_{\partial\Omega}=\bar{\epsilon}.x} \int_{\Omega} \chi_1 W_1(\epsilon) + \chi_2 W_2(\epsilon) \, dx =: \widehat{W}_\lambda^x(\bar{\epsilon}). \quad (3.14)$$

So we have

$$\widehat{W}_\lambda^x(\bar{\epsilon}) \geq \widehat{W}_\lambda(\bar{\epsilon}) \geq \widehat{W}_\lambda^l(\bar{\epsilon}). \quad (3.15)$$

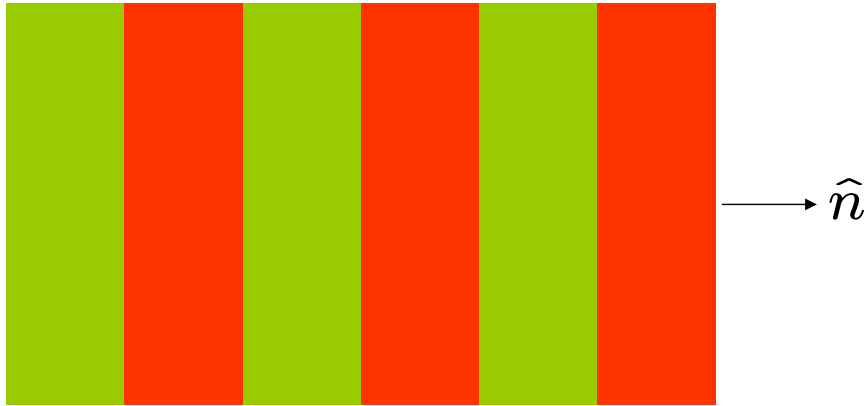


Figure 3.1: A two-phase rank-I laminate in two dimensions. \hat{n} is the lamination direction. The strains are constant in the shaded and unshaded regions.

If we are able to pick the microstructure χ_i such that $\widehat{W}_\lambda^\chi(\bar{\epsilon}) = \widehat{W}_\lambda^l(\bar{\epsilon})$ it follows that the inequalities in (3.15) are in fact an equality, and the lower bound of theorem 3.5 is in fact the expression for \widehat{W}_λ . We construct microstructures whose effective energy is equal to that of the lower bound. We call such microstructures extremal microstructures. The results are presented in lemmas 3.8, 3.10 and 3.12 corresponding to regime I, II and III, respectively.

Given χ_i , the variational problem in (3.14) is the classical problem in linear elasticity. Further $\chi_1 W_1 + \chi_2 W_2$ is pointwise convex. Therefore $u : \Omega \rightarrow \mathbb{R}^2$ that satisfies the boundary condition $u|_{\partial\Omega} = \bar{\epsilon} \cdot x$, is a solution of (3.14) if and only if it satisfies the Euler-Lagrange equation

$$\operatorname{div}(\alpha_i \epsilon(u)) = \operatorname{div}(\alpha_i \epsilon_i^T). \quad (3.16)$$

3.2.1 Laminates

The extremal microstructures we construct are laminates. Good introductions and overviews can be found in [Che00, Ch.7] and [Mil01, Ch.9]. Laminates arise in a variety of contexts; see, for example, [Tar79b, Tar85, FM86, Tar00], [Che00, Ch.7], [Mil01, Ch.9] and references therein. We say that a strain field is a rank-I laminate if it is periodic and piecewise constant in one direction (referred to as the lamination direction) and constant in all other directions. Figure 3.1 shows a rank-I laminate in two dimensions. We say a strain field is a rank-II laminate if it is a rank-I laminate of rank-I laminates at a smaller length scale. Figure 3.2 shows a rank-II laminate in two dimensions

The strains in a laminate are piecewise constant, say, ϵ_1 and $\epsilon_2 \in M_{\text{sym}}^{n \times n}$. ϵ_1 and ϵ_2 are compatible — i.e., $\exists \hat{m}, \hat{n} \in \mathbb{R}^2$ such that $\epsilon_2 - \epsilon_1 \parallel \hat{m} \otimes_s \hat{n}$ — if and only if $\det(\epsilon_2 - \epsilon_1) \leq 0$, that is, by definition, if and

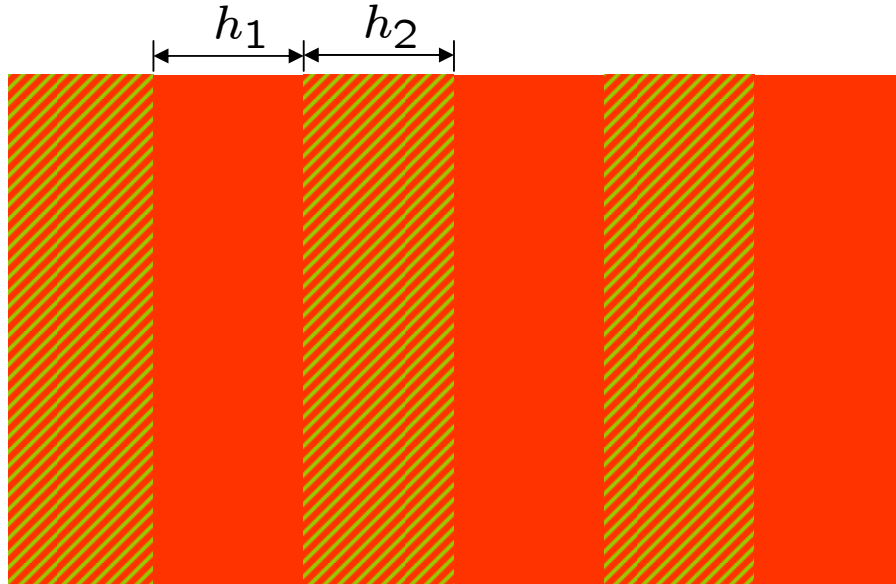


Figure 3.2: A two-phase rank-II laminate in two dimensions. The widths h_1 and h_2 of the slabs should be much larger than the thicknesses of the layers within each slab.

only if $\phi(\epsilon_2 - \epsilon_1) \geq 0$. Further $\exists \hat{n} \in \mathbb{R}^2$ such that $\epsilon_2 - \epsilon_1 \parallel \hat{n} \otimes \hat{n}$ if and only if $\det(\epsilon_2 - \epsilon_1) = 0$, that is, by definition, if and only if $\phi(\epsilon_2 - \epsilon_1) = 0$. Though these results are well known [Roy78, Kha83, Koh91], a proof is presented in lemma 3.7 below. Finally the strains have to satisfy (3.16) in weak form,

$$\llbracket \alpha_i(\epsilon - \epsilon_i^T) \rrbracket \hat{n} = 0;$$

i.e.,

$$\llbracket \sigma \rrbracket \hat{n} = 0. \tag{3.17}$$

Our strategy is to find laminated strain fields consistent with the lower bound, and arrange χ_i accordingly so that we satisfy $\widehat{W}_\lambda^x(\bar{\epsilon}) = \widehat{W}_\lambda^l(\bar{\epsilon})$ (c.f. (3.15)).

Lemma 3.7. Let $\Delta\epsilon \in M_{\text{sym}}^{n \times n}$ with eigenvalues $\lambda_1 \leq \lambda_2 \leq \dots \leq \lambda_n$. Then, when $n = 2$

$$\begin{aligned} \Delta\epsilon \parallel \hat{m} \otimes_s \hat{n} &\Leftrightarrow \lambda_1 \leq 0 \leq \lambda_2, \\ \Delta\epsilon \parallel \hat{n} \otimes \hat{n} &\Leftrightarrow \lambda_1 \lambda_2 = 0; \end{aligned}$$

and when $n > 2$,

$$\begin{aligned}\Delta\epsilon \parallel \hat{m} \otimes_s \hat{n} &\Leftrightarrow \lambda_1 \leq 0 = \lambda_2, \dots, \lambda_{n-1} = 0 \leq \lambda_n \\ \Delta\epsilon \parallel \hat{n} \otimes \hat{n} &\Leftrightarrow \lambda_2 = \lambda_3 = \dots = \lambda_{n-1} = 0 \text{ and } \lambda_1 \lambda_n = 0\end{aligned}$$

\hat{m} and \hat{n} are unique to a choice of sign.

Proof. Necessity: Assume $\Delta\epsilon = |m|(\hat{m} \otimes_s \hat{n}) = \frac{|m|}{2}(\hat{m} \otimes \hat{n} + \hat{n} \otimes \hat{m})$. We consider the case $\hat{m} \not\parallel \hat{n}$; a similar proof holds otherwise. $\Delta\epsilon$ has $n - 2$ zero eigenvalues since $\forall \vec{v} \in \text{Span}\{\hat{m}, \hat{n}\}^\perp$, $\Delta\epsilon \vec{v} = 0$. $\Delta\epsilon \hat{n} = \frac{|m|}{2}(\hat{m} + (m \cdot \hat{n})\hat{n})$ and $\Delta\epsilon \hat{m} = \frac{|m|}{2}((\hat{m} \cdot \hat{n})\hat{m} + \hat{n})$. Thus

$$\begin{aligned}\Delta\epsilon(\hat{n} + \hat{m}) &= \frac{|m|}{2}(\hat{m} \cdot \hat{n} + 1)(\hat{n} + \hat{m}) &\Rightarrow \frac{|m|}{2}(\hat{m} \cdot \hat{n} + 1) \text{ is an eigenvalue} \\ \Delta\epsilon(\hat{n} - \hat{m}) &= \frac{|m|}{2}(\hat{m} \cdot \hat{n} - 1)(\hat{n} - \hat{m}) &\Rightarrow \frac{|m|}{2}(\hat{m} \cdot \hat{n} - 1) \text{ is an eigenvalue}\end{aligned}$$

Clearly one of these is nonnegative and the other is nonpositive. Further one of these is zero if and only if $\hat{m} \parallel \hat{n}$. Note also that $\lambda_n - \lambda_1 = |m|$.

Sufficiency: Assume that the eigenvalues of $\Delta\epsilon$ satisfy $\lambda_1 \leq 0 = \lambda_2, \dots, \lambda_{n-1} = 0 \leq \lambda_n$. Let

$$\Delta\epsilon' = \left(\sqrt{\lambda_n}\hat{v}_n + \sqrt{-\lambda_1}\hat{v}_1\right) \otimes_s \left(\sqrt{\lambda_n}\hat{v}_n - \sqrt{-\lambda_1}\hat{v}_1\right)$$

where \hat{v}_1 and \hat{v}_n are orthonormal eigenvectors of $\Delta\epsilon$ corresponding to λ_1 and λ_n , respectively. We will show that $\Delta\epsilon = \Delta\epsilon'$ by showing that they have the same eigenvalues and corresponding eigenspaces. Clearly $\Delta\epsilon'$ has $n - 2$ zero eigenvalues. Further

$$\begin{aligned}\Delta\epsilon' \hat{v}_1 &= \frac{-\sqrt{-\lambda_1}}{2} \left(\sqrt{\lambda_n}\hat{v}_n + \sqrt{-\lambda_1}\hat{v}_1\right) + \frac{\sqrt{-\lambda_1}}{2} \left(\sqrt{\lambda_n}\hat{v}_n - \sqrt{-\lambda_1}\hat{v}_1\right) = \lambda_1 \hat{v}_1 \\ \Delta\epsilon' \hat{v}_n &= \frac{\sqrt{\lambda_n}}{2} \left(\sqrt{\lambda_n}\hat{v}_n + \sqrt{-\lambda_1}\hat{v}_1\right) + \frac{\sqrt{\lambda_n}}{2} \left(\sqrt{\lambda_n}\hat{v}_n - \sqrt{-\lambda_1}\hat{v}_1\right) = \lambda_n \hat{v}_n\end{aligned}$$

which completes the proof. □

3.2.2 Regime I - rank-I laminates

We show that the lower bound $\widehat{W}_\lambda(\bar{\epsilon}) \geq W_\lambda(0, \bar{\epsilon})$ is optimal:

Lemma 3.8. In regime I there exist a pair of extremal rank-I laminates.

Proof. From (3.10), $\phi(\Delta\epsilon^*) > 0$: the strains ϵ_1^* and ϵ_2^* are compatible. Since from (3.5), $\Delta\sigma^* = 0$, the stress jump condition is satisfied across any interface between regions with strain ϵ_1^* and ϵ_2^* . It

follows that there exist precisely two rank-I laminates (that differ only in lamination direction) in which the strain of phase i is ϵ_i^* . \square

These rank-I laminates show that in regime I,

$$\widehat{W}_\lambda(\bar{\epsilon}) = W_\lambda(0, \bar{\epsilon}) = \lambda_1 W_1(\epsilon_1^*) + \lambda_2 W_2(\epsilon_2^*).$$

The average values of the optimal strain fields are obtained by substituting $\beta = 0$ in (3.6):

$$\begin{aligned} \epsilon_1^* &= (\lambda_2 \alpha_1 + \lambda_1 \alpha_2)^{-1} (\alpha_2 \bar{\epsilon} - \lambda_2 (\alpha_2 \epsilon_2^{\text{T}} - \alpha_1 \epsilon_1^{\text{T}})) \\ \epsilon_2^* &= (\lambda_2 \alpha_1 + \lambda_1 \alpha_2)^{-1} (\alpha_1 \bar{\epsilon} + \lambda_1 (\alpha_2 \epsilon_2^{\text{T}} - \alpha_1 \epsilon_1^{\text{T}})) \end{aligned}$$

and

$$\sigma_1^* = \sigma_2^* = \alpha_1 (\lambda_2 \alpha_1 + \lambda_1 \alpha_2)^{-1} \alpha_2 (\bar{\epsilon} - (\lambda_1 \epsilon_1^{\text{T}} + \lambda_2 \epsilon_2^{\text{T}})) = \alpha_2 (\lambda_2 \alpha_1 + \lambda_1 \alpha_2)^{-1} \alpha_1 (\bar{\epsilon} - (\lambda_1 \epsilon_1^{\text{T}} + \lambda_2 \epsilon_2^{\text{T}})).$$

Since $\Delta \sigma^* = 0$ in this regime, the stress is constant in any extremal microstructure.

From the strict convexity of W_1 and W_2 it follows that ϵ_i^* is the unique constant strain in phase i . However it does not follow that rank-I laminates are unique extremal microstructures: for example, as is easy to see, an extremal rank-II laminate can be formed by laminating the two extremal rank-I laminates.

3.2.3 Regime II - rank-I laminates

We need the following result which says that when the jump in stress is parallel to the adjoint of the jump in strain, both strain compatibility and equilibrium (i.e., (3.17)) are satisfied precisely when the strain jump is rank-I.

Lemma 3.9. Let $\Delta \epsilon, \Delta \sigma \in M_{\text{sym}}^{2 \times 2}$ be such that $\Delta \sigma \parallel T \Delta \epsilon$. Then the following are equivalent:

1. $\exists \hat{m}, \hat{n} \in \mathbb{R}^2$ such that $\Delta \epsilon \parallel \hat{m} \otimes_s \hat{n}$ and either $\Delta \sigma \hat{m} = 0$ or $\Delta \sigma \hat{n} = 0$.
2. $\exists \hat{n} \in \mathbb{R}^2$ such that $\Delta \epsilon \parallel \hat{n} \otimes \hat{n}$ and $\Delta \sigma \hat{n} = 0$.
3. $\phi(\Delta \epsilon) = 0$.

Proof. (1) \Rightarrow (3): From (3.5), $\Delta \sigma \hat{n} \parallel (T \Delta \epsilon) \hat{n} \parallel T(\hat{m} \otimes_s \hat{n}) \hat{n} = (\hat{m} \otimes_s \hat{n} - (\hat{m} \cdot \hat{n})I) \hat{n} = \frac{1}{2}(\hat{m} - (\hat{m} \cdot \hat{n})\hat{n})$. Similarly $\Delta \sigma \hat{m} \parallel \frac{1}{2}(\hat{n} - (\hat{n} \cdot \hat{m})\hat{m})$. Thus $\Delta \sigma \hat{m} = 0$ or $\Delta \sigma \hat{n} = 0 \Rightarrow \hat{m} \parallel \hat{n} \Rightarrow \phi(\Delta \epsilon) = 0$.

(3) \Rightarrow (2): Assume $\phi(\Delta\epsilon) = 0$; that is, $\exists n \in \mathbb{R}^2$, $\Delta\epsilon \parallel \hat{n} \otimes \hat{n}$. It is easy to check that $T(\hat{n} \otimes \hat{n}) = \hat{n} \otimes \hat{n} - I$. Thus, $\Delta\sigma \hat{n} \parallel (T\Delta\epsilon) \hat{n} \parallel (T\hat{n} \otimes \hat{n}) \hat{n} = (\hat{n} \otimes \hat{n} - I) \hat{n} = 0$.

Finally (2) \Rightarrow (1) trivially. \square

We are now ready to show that the lower bound $\widehat{W}_\lambda(\bar{\epsilon}) \geq W_\lambda(\beta_{\text{II}}, \bar{\epsilon})$ is optimal:

Lemma 3.10. In regime II the unique extremal microstructure is a rank-I laminate.

Proof. From (3.10), $\phi(\Delta\epsilon^*) = 0$ and from (3.5), $\Delta\sigma^* = \beta_{\text{II}} T \Delta\epsilon^*$. Thus from lemma 3.9, $\exists \hat{n} \ni \Delta\epsilon^* \parallel \hat{n} \otimes \hat{n}$ and $\Delta\sigma^* \hat{n} = 0$. It follows that there exists a rank-I laminate in which the strain of phase i is ϵ_i^* . This shows that in regime II,

$$\widehat{W}_\lambda(\bar{\epsilon}) = W_\lambda(\beta_{\text{II}}, \bar{\epsilon}) = \lambda_1 W_1(\epsilon_1^*) + \lambda_2 W_2(\epsilon_2^*).$$

From the strict convexity of W_1 and W_2 it follows that ϵ_i^* is the unique constant strain in phase i . Further since $\Delta\epsilon^* \parallel \hat{n} \otimes \hat{n}$, the strains are compatible only across a plane with normal \hat{n} . Thus the microstructure is uniquely a rank-I laminate. \square

3.2.4 Regime III - rank-II laminates

In regime III, since $\phi(\Delta\epsilon^*) < 0$, ϵ_1^* and ϵ_2^* cannot form a rank-I laminate. We show the existence of extremal rank-II laminates.

Let $\mathcal{N}_i := \ker(\alpha_i - \gamma_i T)$. Note that

$$\epsilon \in \mathcal{N}_i \Rightarrow \alpha_i \epsilon = \gamma_i T \epsilon \tag{3.18a}$$

and $\epsilon \in \mathcal{N}_i$ implies that $\phi(\epsilon) \equiv \frac{1}{2} \langle T \epsilon, \epsilon \rangle = \frac{1}{2\gamma_i} \langle \alpha_i \epsilon, \epsilon \rangle \geq 0$, giving

$$\phi(\epsilon) < 0 \Rightarrow \epsilon \notin \mathcal{N}_i. \tag{3.18b}$$

Since (c.f. lemma 3.2) $\gamma_\star = \gamma_i$ for $i = 1$ or 2 , $\mathcal{N}_i \neq \{0\}$ for $i = 1$ or 2 . Thus either $W_i - \gamma_\star \phi$ or $W_i - \gamma_\star \phi$ is convex but not strictly convex. By the convexity of $W_i - \gamma_\star \phi$ on \mathcal{N}_i^\perp and its affinity on \mathcal{N}_i , the strain field $\epsilon_i(x)$ in phase i of any extremal microstructure must satisfy:

$$\mathbf{\Lambda}_{\mathcal{N}_i^\perp} \epsilon_i(x) = \mathbf{\Lambda}_{\mathcal{N}_i^\perp} \epsilon_i^* \tag{3.19a}$$

$$\int_{\Omega} \chi_i \mathbf{\Lambda}_{\mathcal{N}_i} \epsilon_i(x) dx = \lambda_i \mathbf{\Lambda}_{\mathcal{N}_i} \epsilon_i^* \tag{3.19b}$$

Where $\mathbf{\Lambda}_{\mathcal{N}_i}$ and $\mathbf{\Lambda}_{\mathcal{N}_i^\perp}$ are projection operators on \mathcal{N}_i and \mathcal{N}_i^\perp , respectively. (When $\mathcal{N}_i = \{0\}$, from (3.19a), $\epsilon_i(x) = \epsilon_i^*$ and (3.19b) is trivially satisfied.)

We first present a necessary and sufficient condition for the existence of an extremal rank-II laminate in regime III. As a convenient shorthand we denote by $\mathcal{R}(\rho, \epsilon_1, \epsilon_2)$ the rank-I laminate in which phase 1 has phase fraction $\rho \in (0, \lambda_1)$ and strain ϵ_1 and phase 2 has phase fraction $1 - \rho$ and strain ϵ_2 .

Lemma 3.11. Let $\dim(\mathcal{N}_1) \neq 0$. There exists a rank-II laminate $\mathcal{R}\left(\frac{\lambda_1 - \rho}{1 - \rho}, \epsilon_1^{II}, \mathcal{R}(\rho, \epsilon_1^I, \epsilon_2^*)\right)$ with $\rho \in (0, \lambda_1)$ and $\epsilon_1^I, \epsilon_1^{II} \in \epsilon_1^* + \mathcal{N}_1$ if and only if there exists $\epsilon_n \in \mathcal{N}_1$ such that

$$\phi(\Delta\epsilon^* - \epsilon_n) = 0 \quad \text{and} \quad \phi\left(\Delta\epsilon^* + \frac{\rho}{\lambda_1 - \rho}\epsilon_n\right) = 0$$

Proof. Since $\epsilon_1^I \in \epsilon_1^* + \mathcal{N}_1$, $\exists \epsilon_n \in \mathcal{N}_1$ such that $\epsilon_1^I = \epsilon_1^* + \epsilon_n$. The average strain in phase 1 is ϵ_1^* :

$$\epsilon_1^* = \frac{1}{\lambda_1} \left(\rho \frac{\lambda_2}{1 - \rho} \epsilon_1^I + \frac{\lambda_1 - \rho}{1 - \rho} \epsilon_1^{II} \right) \Rightarrow \epsilon_1^{II} = \epsilon_1^* - \frac{\rho \lambda_2}{\lambda_1 - \rho} \epsilon_n$$

For the rank-I laminate $\mathcal{R}(\rho, \epsilon_1^* + \epsilon_n, \epsilon_2^*)$, the jump in strain across the interface is $\epsilon_2^* - (\epsilon_1^* + \epsilon_n) = \Delta\epsilon^* - \epsilon_n$. The jump in stress is

$$\alpha_2(\epsilon_2^* - \epsilon_2^T) - \alpha_1(\epsilon_1^I - \epsilon_1^T) = \alpha_2(\epsilon_2^* - \epsilon_2^T) - \alpha_1(\epsilon_1^* - \epsilon_1^T) - \alpha_1\epsilon_n = \Delta\sigma^* - \gamma_1 T \epsilon_n \parallel T(\Delta\epsilon^* - \epsilon_n)$$

where we have used (3.5) and (3.18). Thus from lemma 3.9, $\phi(\Delta\epsilon^* - \epsilon_n) = 0$ is necessary and sufficient for strain and stress compatibility for this rank-I laminate $\mathcal{R}(\rho, \epsilon_1^* + \epsilon_n, \epsilon_2^*)$.

For the rank-II laminate $\mathcal{R}\left(\frac{\lambda_1 - \rho}{1 - \rho}, \epsilon_1^{II}, \mathcal{R}(\rho, \epsilon_1^I, \epsilon_2^*)\right)$ the jump in strain across the interface is

$$\epsilon_1^{II} - \left(\rho \epsilon_1^I + (1 - \rho)\epsilon_2^*\right) \parallel \Delta\epsilon^* + \frac{\rho}{\lambda_1 - \rho}\epsilon_n.$$

The jump in stress, again using (3.5) and (3.18) is

$$\begin{aligned} & \rho \alpha_1(\epsilon_1^I - \epsilon_1^T) + (1 - \rho)\alpha_2(\epsilon_2^* - \epsilon_2^T) - \alpha_1(\epsilon_1^{II} - \epsilon_1^T) \\ &= \rho \alpha_1(\epsilon_1^* - \epsilon_1^T + \epsilon_n) + (1 - \rho)\alpha_2\epsilon_2^* - \alpha_1\left(\epsilon_1^* - \epsilon_1^T - \frac{\rho \lambda_2}{\lambda_1 - \rho}\epsilon_n\right) \\ &= (1 - \rho)\Delta\sigma^* + \frac{\rho(1 - \rho)}{\lambda_1 - \rho}\alpha_1\epsilon_n \\ &\parallel \Delta\sigma^* + \gamma_1 \frac{\rho}{\lambda_1 - \rho} T \epsilon_n \\ &\parallel T\left(\Delta\epsilon^* + \frac{\rho}{\lambda_1 - \rho}\epsilon_n\right) \end{aligned}$$

Thus from lemma 3.9, $\phi(\Delta\epsilon^* + \frac{\rho}{\lambda_1 - \rho}\epsilon_n) = 0$ is necessary and sufficient for strain and stress compatibility for the rank-II laminate.

It remains to be shown that the layering direction in $\mathcal{R}(\rho, \epsilon_1^* + \epsilon_n, \epsilon_2^*)$ and $\mathcal{R}\left(\frac{\lambda_1 - \rho}{1 - \rho}, \epsilon_1^{II}, \mathcal{R}(\rho, \epsilon_1^I, \epsilon_2^*)\right)$ are not parallel. Assume on the contrary that they are. Then from lemma 3.9 we have¹ $\Delta\epsilon^* - \epsilon_n \parallel \Delta\epsilon^* + \frac{\rho}{\lambda_1 - \rho}\epsilon_n$. Therefore either $\frac{\rho}{\lambda_1 - \rho} = -1$, i.e., $\lambda_1 = 0$ — which is not possible — or $\Delta\epsilon^* \in \mathcal{N}_1$, which contradicts (3.18). \square

We are now ready to prove that the lower bound $\widehat{W}_\lambda(\bar{\epsilon}) \geq W_\lambda(\gamma_\star, \bar{\epsilon})$ is optimal:

Lemma 3.12. When $\dim(\mathcal{N}_1) = 1$ there exist precisely two extremal rank-II laminates. When $\dim(\mathcal{N}_1) = 2$ there exist uncountable extremal rank-II laminates.² ($\dim(\mathcal{N}_i) \leq 2$ since T has eigenvalues -1 and 1 repeated once and twice, respectively.)

Proof. Let $\epsilon_n \in \mathcal{N}_1$. Note that the quadratic polynomial $z \mapsto \phi(\Delta\epsilon^* + z\epsilon_n)$ has two real roots of opposite sign:

$$\phi(\Delta\epsilon^* + z\epsilon_n) = 0 \Leftrightarrow \phi(\Delta\epsilon^*) + z\langle T\Delta\epsilon^*, \epsilon_n \rangle + z^2\phi(\epsilon_n) = 0. \quad (3.20)$$

In this regime $\phi(\Delta\epsilon^*) < 0$ and from (3.18), $\phi(\epsilon_n) > 0$. Thus the discriminant of the quadratic equation (3.20), $\langle T\Delta\epsilon^*, \epsilon_n \rangle^2 - 4\phi(\epsilon_n)\phi(\Delta\epsilon^*)$, is positive and the product of the roots, $\frac{\phi(\Delta\epsilon^*)}{\phi(\epsilon_n)}$ is negative: the polynomial $z \mapsto \phi(\Delta\epsilon^* + z\epsilon_n)$ has two real roots of opposite sign.

Let $-r$, $r > 0$ be the ratio of the roots. From the comments above r can take precisely two values whose product is 1. If we set $-\frac{\rho}{\lambda_1 - \rho} = -r$ then $\rho = \frac{r}{r+1}\lambda_1 \in (0, \lambda_1)$. Thus from the previous lemma, associated with \mathcal{N}_1 are precisely two rank-II laminates $\mathcal{R}\left(\frac{\lambda_1 - \rho}{1 - \rho}, \epsilon_1^{II}, \mathcal{R}(\rho, \epsilon_1^I, \epsilon_2^*)\right)$. When $\dim(\mathcal{N}_1) = 1$ there exists only one 1-D subspace of \mathcal{N}_1 . Else there exist uncountable 1-D subspaces of \mathcal{N}_1 . The result follows. \square

By a similar argument, when $\dim(\mathcal{N}_2) \neq 0$, rank-II laminates $\mathcal{R}\left(\frac{\lambda_1}{\rho}, \mathcal{R}(\rho, \epsilon_1^*, \epsilon_2^I), \epsilon_2^{II}\right)$, $\rho \in (\lambda_1, 1)$ which satisfy (3.19) exist and are extremal. These rank-II laminates show that in regime III,

$$\widehat{W}_\lambda(\bar{\epsilon}) = W_\lambda(\gamma_\star, \bar{\epsilon}) = \lambda_1 W_1(\epsilon_1^*) + \lambda_2 W_2(\epsilon_2^*) - \lambda_1 \lambda_2 \gamma_\star \phi(\Delta\epsilon^*).$$

When $\dim(\mathcal{N}_i) = 2$ for $i = 1$ or 2 extremal microstructures that are not laminates — for example, ‘confocal ellipses’ or ‘Vigredgauz microstructures’ — also exist. The reader is referred to [Lu93, Vig94, GK95a, GK95b, GK95c, Gra96] for a discussion of these microstructures.

Remark 3.13. Let $\alpha_i > 0$ and $\dim(\mathcal{N}_i) = 1$ for $i = 1$ or 2 . Then in any (classical) extremal microstructure $\epsilon_i(x)$ must be piecewise constant.

¹ $\forall \hat{m}, \hat{n} \in \mathbb{R}^2, \hat{m} \parallel \hat{n} \Rightarrow \hat{n} \otimes n \parallel \hat{m} \otimes \hat{m}$

² For example, when α_1 is isotropic, \mathcal{N}_1 is precisely the set of all deviatoric strains and $\dim(\mathcal{N}_1) = 2$.

Proof. Let $\epsilon_n \in \mathcal{N}_i$, $\epsilon_n \neq 0$. Viewed as linear operators on \mathbb{R}^2 , ϵ_n and $\alpha_i \epsilon_n$ are invertible:

$$\begin{aligned} \det(\epsilon_n) &= -\frac{1}{2} \langle T \epsilon_n, \epsilon_n \rangle = -\frac{1}{2\gamma_i} \langle \alpha_i \epsilon_n, \epsilon_n \rangle < 0 \\ \det(\alpha_i \epsilon_n) &= -\frac{1}{2} \langle T \alpha_i \epsilon_n, \alpha_i \epsilon_n \rangle = -\frac{\gamma_i}{2} \langle \alpha_i \epsilon_n, \epsilon_n \rangle < 0 \end{aligned}$$

Where we have used (3.18) and $T^2 = I$. Let $\dim(\mathcal{N}_i) = 1$. Then from (3.19) there exists $0 \neq \epsilon_n \in \mathcal{N}_i$ and $c : \Omega \rightarrow \mathbb{R}$ such that $\epsilon_i(x) = \epsilon_i^* + c(x)\epsilon_n$ and $\int_{\Omega} \chi_i c(x) dx = 0$. Thus

$$\operatorname{div} \sigma_i(x) = 0 \Rightarrow \operatorname{div}(\alpha_i(\epsilon_i^* - \epsilon_i^T)) + \operatorname{div}(c(x)\alpha_i \epsilon_n) \Rightarrow \alpha_i \epsilon_n \nabla c(x) = 0 \Rightarrow \nabla c(x) = 0$$

Where the last step follows because $\alpha_i \epsilon_n$ is invertible. Thus $c : \Omega \rightarrow \mathbb{R}$ is piecewise constant. \square

3.3 Related relaxed energy densities

3.3.1 The uniform traction problem

We now turn to the uniform traction problem (2.4) for W given by (2.5). Note first that $W_{\lambda}(\beta, \bar{\epsilon})$ is strictly convex in $\bar{\epsilon}$:

$$\begin{aligned} \frac{\partial^2 W_{\lambda}}{\partial \bar{\epsilon}^2} &= \lambda_1 \frac{\partial^2}{\partial \bar{\epsilon}^2} (W_1 - \beta \phi)(\epsilon_1^*(\beta, \bar{\epsilon})) + \lambda_2 \frac{\partial^2}{\partial \bar{\epsilon}^2} (W_2 - \beta \phi)(\epsilon_2^*(\beta, \bar{\epsilon})) + \beta \frac{\partial^2}{\partial \bar{\epsilon}^2} \phi(\bar{\epsilon}) \\ &= \lambda_1(\alpha_1 - \beta T) + \lambda_2(\alpha_2 - \beta T) + \beta T \\ &= \lambda_1 \alpha_1 + \lambda_2 \alpha_2 \\ &> 0 \end{aligned}$$

where ϵ_1^* and ϵ_2^* are as defined in (3.6). Since $W_{\lambda}(\beta, \bar{\epsilon})$ is convex in $\bar{\epsilon}$ and concave in β (lemma 3.4), from a saddle point theorem [ET76, Proposition II.2.4, pg176],

$$\min_{\bar{\epsilon}} \max_{\beta \in [0, \gamma_{\star}]} W_{\lambda}(\beta, \bar{\epsilon}) = \max_{\beta \in [0, \gamma_{\star}]} \min_{\bar{\epsilon}} W_{\lambda}(\beta, \bar{\epsilon}). \quad (3.21)$$

From (2.4)

$$\begin{aligned}
\widehat{W}_\lambda^\sigma(\sigma) &= \inf_{\langle \chi_i \rangle = \lambda_i} \inf_{\bar{\epsilon}} \inf_{u|_{\partial\Omega} = \bar{\epsilon} \cdot x} \int_{\Omega} \chi_1(x) W_1(\epsilon(x)) + \chi_2(x) W_2(\epsilon(x)) - \langle \sigma, \bar{\epsilon} \rangle \, dx \\
&= \inf_{\bar{\epsilon}} \inf_{\langle \chi_i \rangle = \lambda_i} \inf_{u|_{\partial\Omega} = \bar{\epsilon} \cdot x} \int_{\Omega} \chi_1(x) W_1(\epsilon(x)) + \chi_2(x) W_2(\epsilon(x)) \, dx - \langle \sigma, \bar{\epsilon} \rangle \\
&= \inf_{\bar{\epsilon}} \left(\max_{\beta \in [0, \gamma_\star]} W_\lambda(\beta, \bar{\epsilon}) - \langle \sigma, \bar{\epsilon} \rangle \right) \\
&= \max_{\beta \in [0, \gamma_\star]} \left(\min_{\bar{\epsilon}} W_\lambda(\beta, \bar{\epsilon}) - \langle \sigma, \bar{\epsilon} \rangle \right)
\end{aligned}$$

where we have used (3.21). Note that

$$\begin{aligned}
W_i(\epsilon) - \langle \sigma, \epsilon \rangle &= \frac{1}{2} \langle \alpha_i(\epsilon - \epsilon_i^T), (\epsilon - \epsilon_i^T) \rangle + w_i - \langle \sigma, \epsilon \rangle \\
&= \frac{1}{2} \langle \alpha_i \epsilon, \epsilon \rangle - \langle \alpha_i(\epsilon_i^T + \alpha_i^{-1} \sigma), \epsilon \rangle + \frac{1}{2} \langle \alpha_i(\epsilon_i^T - \alpha_i^{-1} \sigma), (\epsilon_i^T - \alpha_i^{-1} \sigma) \rangle \\
&\quad + w_i + \langle \alpha_i \epsilon_i^T, \sigma \rangle + \frac{1}{2} \langle \alpha_i^{-1} \sigma, \sigma \rangle.
\end{aligned}$$

Thus substituting $\epsilon_i^T + \alpha_i^{-1} \sigma$ for ϵ_i^T and $w_i + \langle \alpha_i \epsilon_i^T, \sigma \rangle + \frac{1}{2} \langle \alpha_i^{-1} \sigma, \sigma \rangle$ for w_i , $\widehat{W}_\lambda(\beta, \bar{\epsilon}) - \langle \sigma, \bar{\epsilon} \rangle$ can be put in the same form as $\widehat{W}_\lambda(\beta, \bar{\epsilon})$. Further let $\epsilon_1^\star(\beta)$ and $\epsilon_2^\star(\beta)$ minimize $W_\lambda(\beta, \bar{\epsilon})$. Explicitly performing the minimization in (3.3b) without the constraint $\lambda_1 \epsilon_1 + \lambda_2 \epsilon_2 = \bar{\epsilon}$, we obtain

$$\begin{aligned}
\alpha_1(\epsilon_1^\star - \epsilon_i^T) + \beta \lambda_2 T(\epsilon_2^\star - \epsilon_1^\star) &= \sigma \\
\alpha_2(\epsilon_2^\star - \epsilon_i^T) - \beta \lambda_1 T(\epsilon_2^\star - \epsilon_1^\star) &= \sigma.
\end{aligned}$$

Thus as in (3.5), $\Delta \sigma^\star = \beta T \Delta \epsilon^\star$. In explicit form,

$$\epsilon_1^\star = (\alpha_2 T \alpha_1 - \beta(\lambda_1 \alpha_1 + \lambda_2 \alpha_2))^{-1} (\alpha_2 T \alpha_1 \epsilon_1^T + \alpha_2 T \sigma - \beta(\lambda_1 \alpha_1 \epsilon_1^T + \lambda_2 \alpha_2 \epsilon_2^T) - \beta \sigma) \quad (3.22a)$$

$$\epsilon_2^\star = (\alpha_1 T \alpha_2 - \beta(\lambda_1 \alpha_1 + \lambda_2 \alpha_2))^{-1} (\alpha_1 T \alpha_2 \epsilon_2^T + \alpha_1 T \sigma - \beta(\lambda_1 \alpha_1 \epsilon_1^T + \lambda_2 \alpha_2 \epsilon_2^T) - \beta \sigma). \quad (3.22b)$$

Recall that $\bar{\epsilon}$ is given by

$$\bar{\epsilon} = \lambda_1 \epsilon_1^\star + \lambda_2 \epsilon_2^\star. \quad (3.22c)$$

We conclude that the uniform traction problem reduces to an affine displacement problem and the results in §3.1.5 and §3.2 remain valid with the appropriate substitutions from (3.22).

Remark 3.14. If $\alpha_1 T \alpha_2 = \alpha_2 T \alpha_1$, which occurs, for example, (i) when $\alpha_1 = \alpha_2$, (ii) for cubic

materials with aligned moduli³ and (iii) for isotropic materials,

$$\Delta\epsilon^*(\beta, \sigma) = (\alpha_1 T \alpha_2 - \beta(\lambda_1 \alpha_1 + \lambda_2 \alpha_2))^{-1} (\alpha_1 T \alpha_2 (\epsilon_2^T - \epsilon_1^T) - (\Delta\alpha) T \sigma) \quad (3.23)$$

3.3.2 The quasiconvex envelope

For the case of equal elastic moduli with compatible transformation strains, from (2.8), (3.13), (3.11) and (3.3b),

$$\widehat{W}(\epsilon) = \min_{\substack{\lambda_1, \lambda_2 \in [0,1] \\ \lambda_1 + \lambda_2 = 1}} \min_{\substack{\epsilon_1, \epsilon_2 \in M_{\text{sym}}^{2 \times 2} \\ \lambda_1 \epsilon_1 + \lambda_2 \epsilon_2 = \bar{\epsilon}}} \lambda_1 W_1(\epsilon_1) + \lambda_2 W_2(\epsilon_2).$$

Thus, in this case, the quasiconvex hull coincides with the convex hull. This is a special case of a more general result [Bha03, result 12.1, pg.215].

3.4 Application to equilibrium morphology of precipitates

Remark 3.15 (Matrix and inclusions). From remark 3.3, for cubic elastic moduli

$$\gamma_\star = \min_{i=1,2} \min\{\mu_i, \eta_i\}.$$

In conjunction with lemmas 3.11 and 3.12 this implies that when the microstructure consists of inclusions in a matrix (i.e., in regime III) always the material with the smaller shear modulus forms the matrix and the material with the larger shear modulus forms the inclusion. This has been observed before [AK93a, pg.697, remark 2.8]. Thus Cho and Ardell [CA97, pg.1399] were right in speculating that it is more than coincidental that aligned Ni₃Al precipitates, which are elastically softer than the matrix, coalesce relatively readily into plates while Ni₃Al precipitates, which are harder than the matrix, do not. For materials with arbitrary elastic moduli, that material forms the inclusion, for which the largest eigenvalue of $\alpha^{-\frac{1}{2}} T \alpha^{-\frac{1}{2}}$ is larger. This follows from lemma 3.2.

Morphological transitions and rafting. As the applied load (strain or stress) changes, the optimal regime might change and consequently the morphology of the extremal microstructure might also change. For example, along a certain loading path the optimal regime could change from regime III to regime II and consequently the extremal microstructure would change from a rank-II laminate to a rank-I laminate. We call such transitions morphological transitions. Further, even within the

³ We explain what we mean by ‘cubic materials with aligned moduli’ in §3.4.

same regime, as the applied load changes, the orientation of the rank-I or rank-II laminate might change. This is an example of rafting.

In this section we explore morphological transitions and rafting and their dependence on the elastic moduli and transformation strains of the phases. Since the relevant expressions are difficult to analyze analytically for arbitrary elastic moduli — c.f. (3.6) and (3.23) — we focus on two special cases: (i) equal moduli and (ii) aligned cubic moduli.

Equal moduli. When the elastic moduli are equal, regime III does not occur (c.f. remark 3.6). Further, from (3.6) and (3.23), $\Delta\epsilon^*(\beta, \bar{\epsilon})$ and $\Delta\epsilon^*(\beta, \sigma)$ are independent of $\bar{\epsilon}$ and σ , respectively. This implies that neither morphological transitions nor rafting occur when the elastic moduli are equal.

Aligned cubic moduli. Let the orthogonal projection operators $\mathbf{\Lambda}_h, \mathbf{\Lambda}_d, \mathbf{\Lambda}_o: M_{\text{sym}}^{2 \times 2} \rightarrow M_{\text{sym}}^{2 \times 2}$ be defined by (3.2). Let α_1 and α_2 be cubic elastic moduli. We say that α_1 and α_2 are aligned, if for a suitable choice of coordinate axis,

$$\alpha_i = 2\kappa_i \mathbf{\Lambda}_h + 2\mu_i \mathbf{\Lambda}_d + 2\eta_i \mathbf{\Lambda}_o. \quad (3.24)$$

where κ_i, μ_i and η_i are, respectively, the bulk, diagonal shear and off-diagonal shear moduli of the i^{th} phase. For the rest of this chapter, unless otherwise stated, we assume that the elastic moduli are of the form (3.24).

3.4.1 Explicit expressions for aligned cubic moduli

Any $\epsilon \in M_{\text{sym}}^{2 \times 2}$ can be written as

$$\epsilon = \epsilon_h \begin{pmatrix} 1 & 0 \\ 0 & 1 \end{pmatrix} + \epsilon_d \begin{pmatrix} 1 & 0 \\ 0 & -1 \end{pmatrix} + \epsilon_o \begin{pmatrix} 0 & 1 \\ 1 & 0 \end{pmatrix},$$

where ϵ_h, ϵ_d and ϵ_o are the hydrostatic, diagonal shear and off diagonal shear components of ϵ , respectively. Note that $\phi(\epsilon) \equiv -\det(\epsilon) = -\epsilon_h^2 + \epsilon_d^2 + \epsilon_o^2$.

The affine displacement problem. Using $T \equiv -\mathbf{\Lambda}_h + \mathbf{\Lambda}_d + \mathbf{\Lambda}_o$, from (3.6),

$$\begin{aligned} \Delta\epsilon^*(\beta, \bar{\epsilon}) &= 2 \frac{(\kappa_2 \epsilon_{2h}^T - \kappa_1 \epsilon_{1h}^T) - (\kappa_2 - \kappa_1) \bar{\epsilon}_h}{2(\lambda_2 \kappa_1 + \lambda_1 \kappa_2) + \beta} \begin{pmatrix} 1 & 0 \\ 0 & 1 \end{pmatrix} + 2 \frac{(\mu_2 \epsilon_{2d}^T - \mu_1 \epsilon_{1d}^T) - (\mu_2 - \mu_1) \bar{\epsilon}_d}{2(\lambda_2 \mu_1 + \lambda_1 \mu_2) - \beta} \begin{pmatrix} 1 & 0 \\ 0 & -1 \end{pmatrix} \\ &+ 2 \frac{(\eta_2 \epsilon_{2o}^T - \eta_1 \epsilon_{1o}^T) - (\eta_2 - \eta_1) \bar{\epsilon}_o}{2(\lambda_2 \eta_1 + \lambda_1 \eta_2) - \beta} \begin{pmatrix} 0 & 1 \\ 1 & 0 \end{pmatrix}. \end{aligned}$$

Let

$$\Gamma_h := \frac{(\kappa_2 \epsilon_{2h}^T - \kappa_1 \epsilon_{1h}^T) - (\kappa_2 - \kappa_1) \bar{\epsilon}_h}{\lambda_2 \kappa_1 + \lambda_1 \kappa_2} \quad (3.25a)$$

$$\Gamma_d := \frac{(\mu_2 \epsilon_{2d}^T - \mu_1 \epsilon_{1d}^T) - (\mu_2 - \mu_1) \bar{\epsilon}_d}{\lambda_2 \mu_1 + \lambda_1 \mu_2} \quad (3.25b)$$

$$\Gamma_o := \frac{(\eta_2 \epsilon_{2o}^T - \eta_1 \epsilon_{1o}^T) - (\eta_2 - \eta_1) \bar{\epsilon}_o}{\lambda_2 \eta_1 + \lambda_1 \eta_2}. \quad (3.25c)$$

Note that the Γ s are independent of β . Then

$$\Delta \epsilon^*(\beta, \bar{\epsilon}) = \frac{\Gamma_h}{1 + \frac{\beta}{2(\lambda_2 \kappa_1 + \lambda_1 \kappa_2)}} \begin{pmatrix} 1 & 0 \\ 0 & 1 \end{pmatrix} + \frac{\Gamma_d}{1 - \frac{\beta}{2(\lambda_2 \mu_1 + \lambda_1 \mu_2)}} \begin{pmatrix} 1 & 0 \\ 0 & -1 \end{pmatrix} + \frac{\Gamma_o}{1 - \frac{\beta}{2(\lambda_2 \eta_1 + \lambda_1 \eta_2)}} \begin{pmatrix} 0 & 1 \\ 1 & 0 \end{pmatrix}. \quad (3.26)$$

Recall, from remark 3.3, that for cubic moduli $\gamma_i = 2 \min(\mu_i, \eta_i)$. This implies that for $\beta \in [0, \gamma_\star]$,

$$0 \leq \frac{\beta}{2(\lambda_2 \mu_1 + \lambda_1 \mu_2)}, \frac{\beta}{2(\lambda_2 \eta_1 + \lambda_1 \eta_2)} \leq 1.$$

Thus the coefficients of the Γ s in (3.26) are always positive.

The uniform traction problem. Using $T \equiv -\mathbf{\Lambda}_h + \mathbf{\Lambda}_d + \mathbf{\Lambda}_o$, from (3.23),

$$\Delta \epsilon^*(\beta, \sigma) = \frac{4\kappa_1 \kappa_2 (\epsilon_{2h}^T - \epsilon_{1h}^T) - (\kappa_2 - \kappa_1) \sigma_h}{4\kappa_1 \kappa_2 + \beta(\lambda_1 \kappa_1 + \lambda_2 \kappa_2)} \begin{pmatrix} 1 & 0 \\ 0 & 1 \end{pmatrix} + \frac{4\mu_1 \mu_2 (\epsilon_{2d}^T - \epsilon_{1d}^T) - (\mu_2 - \mu_1) \sigma_d}{4\mu_1 \mu_2 - \beta(\lambda_1 \mu_1 + \lambda_2 \mu_2)} \begin{pmatrix} 1 & 0 \\ 0 & -1 \end{pmatrix} \\ + \frac{4\eta_1 \eta_2 (\epsilon_{2o}^T - \eta_1 \epsilon_{1o}^T) - (\eta_2 - \eta_1) \sigma_o}{4\eta_1 \eta_2} \begin{pmatrix} 0 & 1 \\ 1 & 0 \end{pmatrix}.$$

Let

$$\Upsilon_h := \frac{4\kappa_1 \kappa_2 (\epsilon_{2h}^T - \epsilon_{1h}^T) - (\kappa_2 - \kappa_1) \sigma_h}{4\kappa_1 \kappa_2} \quad (3.27a)$$

$$\Upsilon_d := \frac{4\mu_1 \mu_2 (\epsilon_{2d}^T - \epsilon_{1d}^T) - (\mu_2 - \mu_1) \sigma_d}{4\mu_1 \mu_2} \quad (3.27b)$$

$$\Upsilon_o := \frac{4\eta_1 \eta_2 (\epsilon_{2o}^T - \eta_1 \epsilon_{1o}^T) - (\eta_2 - \eta_1) \sigma_o}{4\eta_1 \eta_2 - \beta(\lambda_1 \eta_1 + \lambda_2 \eta_2)}. \quad (3.27c)$$

As before, the Υ s are independent of β . Then

$$\Delta \epsilon^*(\beta, \sigma) = \frac{\Upsilon_h}{1 + \frac{\lambda_1 \kappa_1 + \lambda_2 \kappa_2}{4\kappa_1 \kappa_2} \beta} \begin{pmatrix} 1 & 0 \\ 0 & 1 \end{pmatrix} + \frac{\Upsilon_d}{1 - \frac{\lambda_1 \mu_1 + \lambda_2 \mu_2}{4\mu_1 \mu_2} \beta} \begin{pmatrix} 1 & 0 \\ 0 & -1 \end{pmatrix} + \frac{\Upsilon_o}{1 - \frac{\lambda_1 \eta_1 + \lambda_2 \eta_2}{4\eta_1 \eta_2} \beta} \begin{pmatrix} 0 & 1 \\ 1 & 0 \end{pmatrix}. \quad (3.28)$$

The coefficients of the Υ s in (3.26) are always positive since for $\beta \in [0, \gamma_\star]$,

$$0 \leq \frac{\lambda_1 \mu_1 + \lambda_2 \mu_2}{4\mu_1 \mu_2} \beta, \frac{\lambda_1 \eta_1 + \lambda_2 \eta_2}{4\eta_1 \eta_2} \beta \leq \frac{1}{4}.$$

Note that the Γ s and Υ s depend linearly on the appropriate component of $\bar{\epsilon}$ and σ , respectively.

3.4.2 The three regimes

The affine displacement problem. From theorem 3.5, regime I occurs precisely when $\phi(\Delta^*(0, \bar{\epsilon})) > 0$. From (3.26) this is

$$-\Gamma_h^2 + \Gamma_d^2 + \Gamma_o^2 > 0 \quad (3.29a)$$

This is the exterior of a cone (of circular cross section) in Γ -space. Equivalently, when $\Gamma_h \neq 0$,

$$\left(\frac{\Gamma_d}{\Gamma_h}\right)^2 + \left(\frac{\Gamma_o}{\Gamma_h}\right)^2 > 1 \quad (3.29b)$$

which is the exterior of the unit circle in the $\frac{\Gamma_d}{\Gamma_h} - \frac{\Gamma_o}{\Gamma_h}$ plane. Regime III occurs precisely when $\phi(\Delta^*(\gamma_*, \bar{\epsilon})) < 0$. From (3.26) this is

$$-\frac{1}{\left(1 + \frac{\gamma_*}{2(\lambda_2\kappa_1 + \lambda_1\kappa_2)}\right)^2} \Gamma_h^2 + \frac{1}{\left(1 - \frac{\gamma_*}{2(\lambda_2\mu_1 + \lambda_1\mu_2)}\right)^2} \Gamma_d^2 + \frac{1}{\left(1 - \frac{\gamma_*}{2(\lambda_2\eta_1 + \lambda_1\eta_2)}\right)^2} \Gamma_o^2 < 0. \quad (3.30a)$$

This is the interior of a cone of elliptic cross section (circular cross section when the moduli are isotropic) in Γ -space. Equivalently, when $\Gamma_h \neq 0$,

$$\left(\frac{1 + \frac{\gamma_*}{2(\lambda_2\kappa_1 + \lambda_1\kappa_2)}}{1 - \frac{\gamma_*}{2(\lambda_2\mu_1 + \lambda_1\mu_2)}}\right)^2 \left(\frac{\Gamma_d}{\Gamma_h}\right)^2 + \left(\frac{1 + \frac{\gamma_*}{2(\lambda_2\kappa_1 + \lambda_1\kappa_2)}}{1 - \frac{\gamma_*}{2(\lambda_2\eta_1 + \lambda_1\eta_2)}}\right)^2 \left(\frac{\Gamma_o}{\Gamma_h}\right)^2 < 1 \quad (3.30b)$$

which is the interior of an ellipse (circle when the moduli are isotropic) in the $\frac{\Gamma_d}{\Gamma_h} - \frac{\Gamma_o}{\Gamma_h}$ plane.

The uniform traction problem. Analogously, regime I occurs precisely when

$$-\Upsilon_h^2 + \Upsilon_d^2 + \Upsilon_o^2 > 0. \quad (3.31a)$$

Equivalently, when $\Upsilon_h \neq 0$,

$$\left(\frac{\Upsilon_d}{\Upsilon_h}\right)^2 + \left(\frac{\Upsilon_o}{\Upsilon_h}\right)^2 > 1. \quad (3.31b)$$

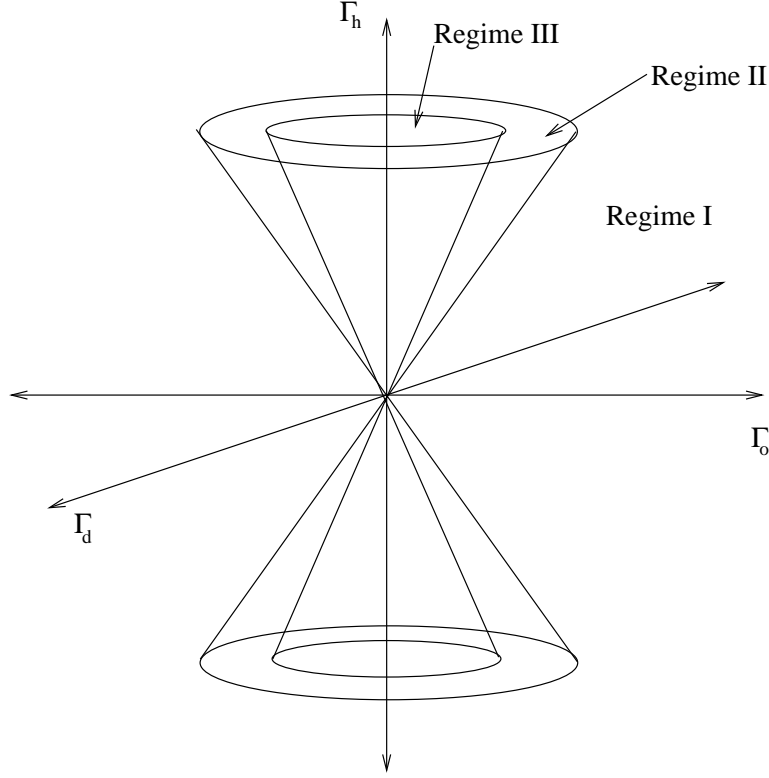


Figure 3.3: The three regimes.

Regime III occurs precisely when

$$-\frac{1}{\left(1 + \frac{\lambda_1 \kappa_1 + \lambda_2 \kappa_2}{4\kappa_1 \kappa_2} \gamma_\star\right)^2} \Upsilon_h^2 + \frac{1}{\left(1 - \frac{\lambda_1 \mu_1 + \lambda_2 \mu_2}{4\mu_1 \mu_2} \gamma_\star\right)^2} \Upsilon_d^2 + \frac{1}{\left(1 - \frac{\lambda_1 \eta_1 + \lambda_2 \eta_2}{4\eta_1 \eta_2} \gamma_\star\right)^2} \Upsilon_o^2 < 0. \quad (3.32a)$$

Equivalently, when $\Upsilon_h \neq 0$,

$$\left(\frac{1 + \frac{\lambda_1 \kappa_1 + \lambda_2 \kappa_2}{4\kappa_1 \kappa_2} \gamma_\star}{1 - \frac{\lambda_1 \mu_1 + \lambda_2 \mu_2}{4\mu_1 \mu_2} \gamma_\star}\right)^2 \left(\frac{\Upsilon_d}{\Upsilon_h}\right)^2 + \left(\frac{1 + \frac{\lambda_1 \kappa_1 + \lambda_2 \kappa_2}{4\kappa_1 \kappa_2} \gamma_\star}{1 - \frac{\lambda_1 \eta_1 + \lambda_2 \eta_2}{4\eta_1 \eta_2} \gamma_\star}\right)^2 \left(\frac{\Upsilon_o}{\Upsilon_h}\right)^2 < 1 \quad (3.32b)$$

Figure 3.3 shows the three regimes. Note in particular that for any initial conditions other than $\Gamma_d, \Gamma_o = 0$ or $\Upsilon_d, \Upsilon_o = 0$, morphological transitions can be induced by appropriately changing the hydrostatic stress.

3.4.3 Rafting

From (3.25), (3.26), (3.27) and (3.28) we observe that the dependence of $\Delta\epsilon^\star(\beta, \sigma)$ on σ is analogous to the dependence of $\Delta\epsilon^\star(\beta, \bar{\epsilon})$ on $\bar{\epsilon}$. Thus henceforth we present explicit expressions for the affine

displacement problem only. All our results can be trivially extended to the uniform traction problem.

We begin by presenting explicit expressions for the lamination directions for the rank-I laminates in regime I and regime II. Let \hat{n} be an unit vector perpendicular to the interface. From lemma 3.8 there are two possible choices (up to sign) of \hat{n} in regime I, say \hat{n}_1 and \hat{n}_2 . Let $\hat{n}_1 = (\cos \theta_1, \sin \theta_1)^T$ and $\hat{n}_2 = (\cos \theta_2, \sin \theta_2)^T$. Since $\Delta\epsilon^* \parallel \hat{n}_1 \otimes_s \hat{n}_2$,

$$\Delta\epsilon^* \parallel \begin{pmatrix} 2 \cos \theta_1 \cos \theta_2 & \cos \theta_1 \sin \theta_2 + \sin \theta_1 \cos \theta_2 \\ \cos \theta_1 \sin \theta_2 + \sin \theta_1 \cos \theta_2 & 2 \sin \theta_1 \sin \theta_2 \end{pmatrix}. \quad (3.33)$$

Notice that θ is the angle between the normal to the rank-I laminate and $(1, 0)^T$. For example, if the applied load were in the $\begin{pmatrix} 1 & 0 \\ 0 & 0 \end{pmatrix}$ direction, θ would be the angle between this direction and the normal to the rank-I laminate. From equation (3.33), for some κ ,

$$\begin{aligned} \cos(\theta_1 - \theta_2) &= \kappa \Delta\epsilon_h^* \\ \cos(\theta_1 + \theta_2) &= \kappa \Delta\epsilon_d^* \\ \sin(\theta_1 + \theta_2) &= \kappa \Delta\epsilon_o^*. \end{aligned}$$

Further (recall that $-\det(\Delta\epsilon^*) \equiv \phi(\Delta\epsilon^*) \geq 0$)

$$\sin(\theta_1 - \theta_2) = \kappa \sqrt{\phi(\Delta\epsilon^*)}.$$

This gives

$$\begin{aligned} \tan(\theta_1 - \theta_2) &= \frac{\sqrt{\phi(\Delta\epsilon^*)}}{\Delta\epsilon_h^*} \\ \tan(\theta_1 + \theta_2) &= \frac{\Delta\epsilon_{12}^*}{\Delta\epsilon_d^*}. \end{aligned}$$

Thus we obtain

$$\theta_1 = \frac{1}{2} \tan^{-1} \frac{\Delta\epsilon_o^*}{\Delta\epsilon_d^*} + \frac{1}{2} \tan^{-1} \frac{\sqrt{\phi(\Delta\epsilon^*)}}{\Delta\epsilon_h^*} \quad (3.34a)$$

$$\theta_2 = \frac{1}{2} \tan^{-1} \frac{\Delta\epsilon_o^*}{\Delta\epsilon_d^*} - \frac{1}{2} \tan^{-1} \frac{\sqrt{\phi(\Delta\epsilon^*)}}{\Delta\epsilon_h^*}. \quad (3.34b)$$

From lemma 3.10, \hat{n} is unique (up to sign) in regime II. Let $\hat{n} = (\cos \theta, \sin \theta)^T$. Setting $\phi(\Delta\epsilon^*) = 0$ in the expressions above we obtain

$$\theta = \frac{1}{2} \tan^{-1} \frac{\Delta\epsilon_o^*}{\Delta\epsilon_d^*} \quad (3.35)$$

Regime I. Recall from (3.26) that in this regime

$$\Delta\epsilon^*(\beta, \bar{\epsilon}) = \Gamma_h \begin{pmatrix} 1 & 0 \\ 0 & 1 \end{pmatrix} + \Gamma_d \begin{pmatrix} 1 & 0 \\ 0 & -1 \end{pmatrix} + \Gamma_o \begin{pmatrix} 0 & 1 \\ 1 & 0 \end{pmatrix}.$$

Thus the expressions in (3.34) can be rewritten as

$$\begin{aligned} \theta_1 &= \frac{1}{2} \tan^{-1} \frac{\Gamma_o/\Gamma_h}{\Gamma_d/\Gamma_h} + \frac{1}{2} \tan^{-1} \sqrt{-1 + \left(\frac{\Gamma_d}{\Gamma_h}\right)^2 + \left(\frac{\Gamma_o}{\Gamma_h}\right)^2} \\ \theta_2 &= \frac{1}{2} \tan^{-1} \frac{\Gamma_o/\Gamma_h}{\Gamma_d/\Gamma_h} - \frac{1}{2} \tan^{-1} \sqrt{-1 + \left(\frac{\Gamma_d}{\Gamma_h}\right)^2 + \left(\frac{\Gamma_o}{\Gamma_h}\right)^2}. \end{aligned}$$

Regime II. Recall from (3.26) that in this regime

$$\Delta\epsilon^* = \frac{\Gamma_h}{1 + \frac{\beta_{II}}{2(\lambda_2\kappa_1 + \lambda_1\kappa_2)}} \begin{pmatrix} 1 & 0 \\ 0 & 1 \end{pmatrix} + \frac{\Gamma_d}{1 - \frac{\beta_{II}}{2(\lambda_2\mu_1 + \lambda_1\mu_2)}} \begin{pmatrix} 1 & 0 \\ 0 & -1 \end{pmatrix} + \frac{\Gamma_o}{1 - \frac{\beta_{II}}{2(\lambda_2\eta_1 + \lambda_1\eta_2)}} \begin{pmatrix} 0 & 1 \\ 1 & 0 \end{pmatrix}$$

and thus from (3.35),

$$\theta = \frac{1}{2} \tan^{-1} \left(\frac{1 - \frac{\beta_{II}}{2(\lambda_2\mu_1 + \lambda_1\mu_2)} \frac{\Gamma_o}{\Gamma_d}}{1 - \frac{\beta_{II}}{2(\lambda_2\eta_1 + \lambda_1\eta_2)} \frac{\Gamma_d}{\Gamma_o}} \right)$$

where β_{II} is the unique solution of

$$-\frac{\Gamma_h^2}{\left(1 + \frac{\beta_{II}}{2(\lambda_2\kappa_1 + \lambda_1\kappa_2)}\right)^2} + \frac{\Gamma_d^2}{\left(1 - \frac{\beta_{II}}{2(\lambda_2\mu_1 + \lambda_1\mu_2)}\right)^2} + \frac{\Gamma_o^2}{\left(1 - \frac{\beta_{II}}{2(\lambda_2\eta_1 + \lambda_1\eta_2)}\right)^2} = 0.$$

In general this cannot be solved analytically, but when the moduli are isotropic, we obtain

$$\theta = \frac{1}{2} \tan^{-1} \frac{\Gamma_o/\Gamma_h}{\Gamma_d/\Gamma_h}.$$

Note that this is independent of Γ_h . Thus for isotropic moduli in regime II, the hydrostatic component of the applied load does not play any role in rafting.

Figures 3.4 and 3.5 show two views of θ plotted as a function of $\frac{\Gamma_d}{\Gamma_h}$ and $\frac{\Gamma_o}{\Gamma_h}$. The bifurcation at $\left(\frac{\Gamma_d}{\Gamma_h}\right)^2 + \left(\frac{\Gamma_o}{\Gamma_h}\right)^2 = 1$ is clearly visible. The bifurcated part of the figure is valid for aligned cubic moduli but the non-bifurcated part is valid for isotropic moduli only. The discontinuity at $\Gamma_o = 0$ is an artifact of the fact that \tan^{-1} is multi-valued.

Remark 3.16 (Change in effective modulus). The effective elastic modulus of a rank-n laminate depends on its lamination directions [Che00, Mil01]. We have shown that these change with applied stress. Consequently the effective elastic modulus can change with applied stress.

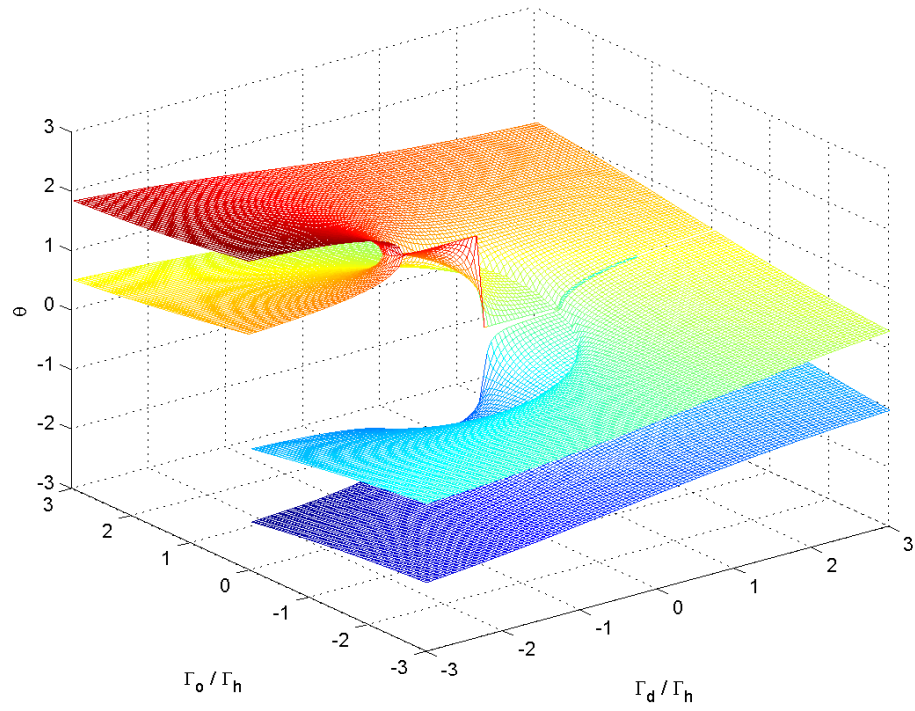


Figure 3.4: Angle between the normal to the rank-I laminates and $(1,0)^T$. Note the bifurcation at $\left(\frac{\Gamma_d}{\Gamma_h}\right)^2 + \left(\frac{\Gamma_o}{\Gamma_h}\right)^2 = 1$.

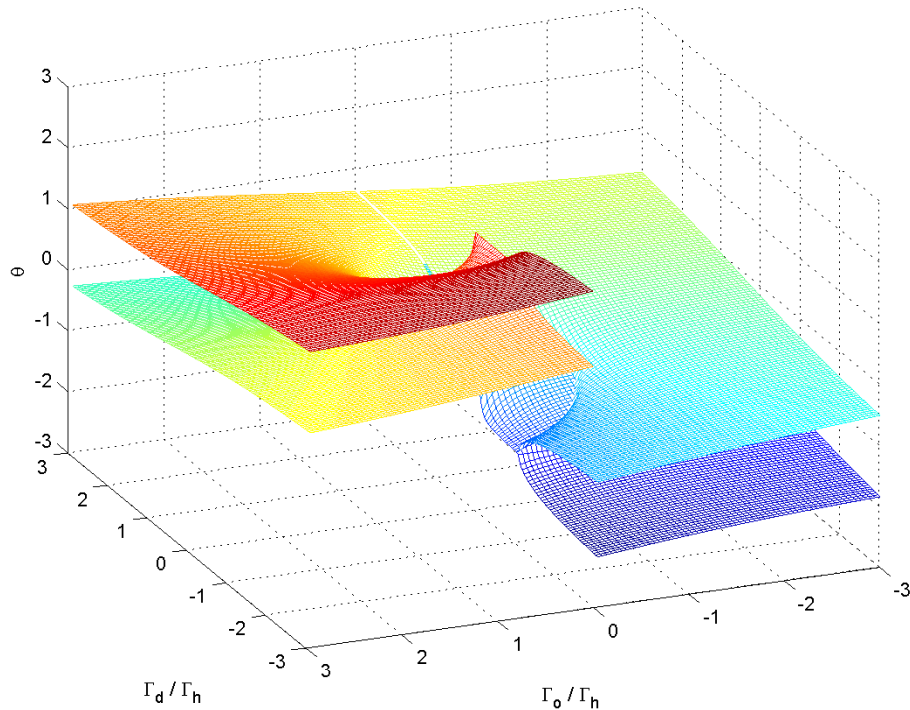


Figure 3.5: Figure 3.4 seen from a different angle.

3.4.4 Correlation with experimental results

The calculation above sheds light on several experimental observations reported by Cho and Ardell [CA97]. They studied the coarsening of Ni_3Si precipitates in binary Ni-Si alloys. For γ' precipitates in Ni-based alloys such as these the difference in transformation strain between the precipitate and the matrix is purely dilatational. Further, the system under consideration was allowed to coarsen under zero stress. Thus, from (3.27), $\Upsilon_d = \Upsilon_o = 0$: from (3.32) the system is in regime III. Recall that in regime III rank-II laminates are extremal but no rank-I laminate is.

This is consistent with the experimental observation⁴ that — contra [TSV94] — the precipitates are extremely resistant to coalescence or rafting and no splitting of cuboidal precipitates into platelets was observed.

As noted above $\Upsilon_d = \Upsilon_o = 0$ here; from (3.28), $\Delta\epsilon^* \parallel \begin{pmatrix} 1 & 0 \\ 0 & 1 \end{pmatrix}$. From remark 3.15, $\min\{\mu_{\text{matrix}}, \eta_{\text{matrix}}\} \leq \min\{\mu_{\text{ppt}}, \eta_{\text{ppt}}\}$. For the system under consideration $\eta_{\text{ppt}} < \mu_{\text{ppt}}$. Thus from remark 3.3,

$$\mathcal{N}_{\text{matrix}} = \text{Span} \left\{ \begin{pmatrix} 1 & 0 \\ 0 & -1 \end{pmatrix} \right\}.$$

⁴ We stop short of saying that our analysis explains the observations since we have neglected interfacial energy.

It follows that ϵ_n in lemmas 3.11 and 3.12 should be picked to be parallel to $\begin{pmatrix} 1 & 0 \\ 0 & -1 \end{pmatrix}$. Thus, from lemma 3.11, the strain jump in the two layers of the extremal rank-II laminate is parallel to

$$\begin{pmatrix} 1 & 0 \\ 0 & 1 \end{pmatrix} + \begin{pmatrix} 1 & 0 \\ 0 & -1 \end{pmatrix}, \quad \text{i.e.,} \quad \begin{pmatrix} 1 & 0 \\ 0 & 0 \end{pmatrix}$$

and

$$\begin{pmatrix} 1 & 0 \\ 0 & 1 \end{pmatrix} - \begin{pmatrix} 1 & 0 \\ 0 & -1 \end{pmatrix}, \quad \text{i.e.,} \quad \begin{pmatrix} 0 & 0 \\ 0 & 1 \end{pmatrix}$$

for it is precisely these two linear combinations of $\begin{pmatrix} 1 & 0 \\ 0 & 1 \end{pmatrix}$ and $\begin{pmatrix} 1 & 0 \\ 0 & -1 \end{pmatrix}$ that have determinant zero. It follows that the layering directions are $\begin{pmatrix} 1 \\ 0 \end{pmatrix}$ and $\begin{pmatrix} 0 \\ 1 \end{pmatrix}$. This is consistent with observations [CA97, pg.1399] that the precipitates are aligned along $\langle 100 \rangle$.

Let us explore the other alternative: $\eta_{\text{ppt}} < \mu_{\text{ppt}}$. Then, from remark 3.3,

$$\mathcal{N}_{\text{matrix}} = \text{Span} \left\{ \begin{pmatrix} 0 & 1 \\ 1 & 0 \end{pmatrix} \right\}.$$

It follows that ϵ_n in lemmas 3.11 and 3.12 should be picked to be parallel to $\begin{pmatrix} 0 & 1 \\ 1 & 0 \end{pmatrix}$. Thus, from lemma 3.11, the strain jump in the two layers of the extremal rank-II laminate is parallel to

$$\begin{pmatrix} 1 & 0 \\ 0 & 1 \end{pmatrix} + \begin{pmatrix} 0 & 1 \\ 1 & 0 \end{pmatrix}, \quad \text{i.e.,} \quad \begin{pmatrix} 1 & 1 \\ 1 & 1 \end{pmatrix}$$

and

$$\begin{pmatrix} 1 & 0 \\ 0 & 1 \end{pmatrix} - \begin{pmatrix} 0 & 1 \\ 1 & 0 \end{pmatrix}, \quad \text{i.e.,} \quad \begin{pmatrix} 1 & -1 \\ -1 & 1 \end{pmatrix}$$

for it is precisely these two linear combinations of $\begin{pmatrix} 1 & 0 \\ 0 & 1 \end{pmatrix}$ and $\begin{pmatrix} 0 & 1 \\ 1 & 0 \end{pmatrix}$ that have determinant zero. It follows that the layering directions are $\begin{pmatrix} 1 \\ 1 \end{pmatrix}$ and $\begin{pmatrix} 1 \\ -1 \end{pmatrix}$.

Finally note that since the system is in regime III regardless of the phase fraction of the precipitates, the particle morphology should be independent of the precipitate phase fraction, exactly as reported [CA97, pg.1395 and ref.31 therein].

Chapter 4

Two-phase isotropic solids in three dimensions

We generalize the preceding approach to solve the problem in three dimensions when the elastic moduli are isotropic. The determinant is a useful translation in two dimensions because it captures information on strain compatibility: $\epsilon_1, \epsilon_2 \in M_{\text{sym}}^{2 \times 2}$ are compatible if and only if $\det(\epsilon_2 - \epsilon_1) \leq 0$. The three-dimensional analogue is that $\epsilon_1, \epsilon_2 \in M_{\text{sym}}^{3 \times 3}$ are compatible if and only if of the three eigenvalues of $\epsilon_2 - \epsilon_1$, one is non-negative, another is zero and the third is non-positive (c.f. lemma 3.7).

4.1 Rotated diagonal subdeterminants as translations

Choice of translations. Motivated by this we choose *three* translations

$$\phi_j^M(\epsilon) := \phi_j(M^T \epsilon M) \tag{4.1a}$$

where $M \in M^{3 \times 3}$ is yet to be determined and $\phi_j: M_{\text{sym}}^{3 \times 3} \rightarrow \mathbb{R}$ are the diagonal subdeterminants:

$$\phi_1(\epsilon) := \epsilon_{23}^2 - \epsilon_{22}\epsilon_{33} \tag{4.1b}$$

$$\phi_2(\epsilon) := \epsilon_{31}^2 - \epsilon_{33}\epsilon_{11} \tag{4.1c}$$

$$\phi_3(\epsilon) := \epsilon_{12}^2 - \epsilon_{11}\epsilon_{22}. \tag{4.1d}$$

For notational convenience we define $\Phi: M_{\text{sym}}^{3 \times 3} \rightarrow \mathbb{R}^3$ and $\Phi^M: M_{\text{sym}}^{3 \times 3} \rightarrow \mathbb{R}^3$ by

$$\Phi(\epsilon) := \begin{pmatrix} \phi_1(\epsilon) \\ \phi_2(\epsilon) \\ \phi_3(\epsilon) \end{pmatrix},$$

$$\Phi^M(\epsilon) := \begin{pmatrix} \phi_1^M(\epsilon) \\ \phi_2^M(\epsilon) \\ \phi_3^M(\epsilon) \end{pmatrix}.$$

Note that $\phi_j^I = \phi_j$ and $\Phi^I = \Phi$.

Quasiconvexity of the translations. ϕ_j^M is quasiconvex since it is quadratic and rank-I convex:
 $\forall m', n' \in \mathbb{R}^3$,

$$\phi_j^M(m' \otimes_s n') = \phi_j(M^T(m' \otimes_s n')M) = \phi_j((M^T m') \otimes_s (M^T n')) = \phi_j(m \otimes_s n)$$

where $m = M^T m'$, $n = M^T n'$ and

$$\phi_1(m \otimes_s n) = \frac{1}{4}(m_2 n_3 + m_3 n_2)^2 - m_2 n_2 m_3 n_3 = \frac{1}{4}(m_2 n_3 - m_3 n_2)^2 \geq 0$$

with similar results for ϕ_2^M and ϕ_3^M . It follows that $\forall \beta \in (\mathbb{R}_+)^3$, $M_{\text{sym}}^{3 \times 3} \ni \epsilon \mapsto \langle \beta, \Phi(\epsilon) \rangle \in \mathbb{R}$ is quasiconvex ($\mathbb{R}_+ := \{x \in \mathbb{R} \mid x \geq 0\}$).

Quadraticity of the translations. Since ϕ_j is quadratic there exists a (unique) linear operator $T_j: M_{\text{sym}}^{3 \times 3} \rightarrow M_{\text{sym}}^{3 \times 3}$ such that

$$\phi_j(\epsilon) = \frac{1}{2} \langle T_j \epsilon, \epsilon \rangle.$$

Similarly there exists a (unique) linear operator $T_j^M: M_{\text{sym}}^{3 \times 3} \rightarrow M_{\text{sym}}^{3 \times 3}$ such that

$$\phi_j^M(\epsilon) = \frac{1}{2} \langle T_j^M \epsilon, \epsilon \rangle.$$

It is easy to verify that T_j is given by

$$T_1\epsilon = \begin{pmatrix} 0 & 0 & 0 \\ 0 & -\epsilon_{33} & \epsilon_{23} \\ 0 & \epsilon_{23} & -\epsilon_{22} \end{pmatrix}, \quad (4.2a)$$

$$T_2\epsilon = \begin{pmatrix} -\epsilon_{33} & 0 & \epsilon_{31} \\ 0 & 0 & 0 \\ \epsilon_{31} & 0 & -\epsilon_{11} \end{pmatrix}, \quad (4.2b)$$

$$T_3\epsilon = \begin{pmatrix} -\epsilon_{22} & \epsilon_{12} & 0 \\ \epsilon_{12} & -\epsilon_{11} & 0 \\ 0 & 0 & 0 \end{pmatrix}. \quad (4.2c)$$

and T_j^M by

$$T_j^M\epsilon = M \left(T_j(M^T\epsilon M) \right) M^T. \quad (4.2d)$$

Note that $(T_1 + T_2 + T_3)\epsilon = \epsilon - \text{Tr}(\epsilon)I$. For $\beta \in \mathbb{R}^3$, let $\beta \cdot T: M_{\text{sym}}^{3 \times 3} \rightarrow M_{\text{sym}}^{3 \times 3}$ and $\beta \cdot T^M: M_{\text{sym}}^{3 \times 3} \rightarrow M_{\text{sym}}^{3 \times 3}$ to be the linear operators defined by

$$\beta \cdot T\epsilon = \sum_{j=1}^3 \beta_j T_j\epsilon, \quad (4.3a)$$

$$\beta \cdot T^M\epsilon = \sum_{j=1}^3 \beta_j T_j^M\epsilon = M \left(\sum_{j=1}^3 \beta_j T_j(M^T\epsilon M) \right) M^T = M \left(\beta \cdot T(M^T\epsilon M) \right) M^T. \quad (4.3b)$$

Thus

$$\begin{aligned} \langle \beta, \Phi(\epsilon) \rangle &= \frac{1}{2} \langle (\beta \cdot T)\epsilon, \epsilon \rangle, \\ \langle \beta, \Phi^M(\epsilon) \rangle &= \frac{1}{2} \langle (\beta \cdot T^M)\epsilon, \epsilon \rangle. \end{aligned}$$

Restrictions on the choice of translations. For reasons that will become clear later we restrict M to be in $SO(3)$. For $R \in SO(3)$, let

$$\begin{aligned} B_i(R) &:= \{\beta \in (\mathbb{R}_+)^3 \mid W_i - \beta \cdot \Phi^R: \text{convex}\}, \\ B(R) &:= \bigcap_{i=1}^2 B_i(R). \end{aligned}$$

By quadraticity, the convexity of $W_i - \beta \cdot \Phi^R$ is equivalent to the nonnegativity of

$$\epsilon \mapsto \frac{1}{2} \langle \alpha_i \epsilon, \epsilon \rangle - \beta \cdot \Phi^R(\epsilon).$$

Thus

$$\begin{aligned} B_i(R) &= \left\{ \beta \in (\mathbb{R}_+)^3 \mid W_i - \beta \cdot \Phi^R: \text{convex} \right\} \\ &= \left\{ \beta \in (\mathbb{R}_+)^3 \mid \forall \epsilon \in M_{\text{sym}}^{3 \times 3}, \frac{1}{2} \langle \alpha_i \epsilon, \epsilon \rangle - \beta \cdot \Phi(R^T \epsilon R) \geq 0 \right\} \end{aligned} \quad (4.4a)$$

$$= \left\{ \beta \in (\mathbb{R}_+)^3 \mid \forall \epsilon \in M_{\text{sym}}^{3 \times 3}, \frac{1}{2} \langle \alpha_i R \epsilon R^T, R \epsilon R^T \rangle - \beta \cdot \Phi(\epsilon) \geq 0 \right\}. \quad (4.4b)$$

A lower bound on the relaxed energy. From the preceding remarks and the results in §3.1.1 and §3.1.2 we immediately obtain the following analogue of (3.3a) and (3.3b):

$$\widehat{W}_\lambda(\bar{\epsilon}) \geq \max_{R \in SO(3)} \max_{\beta \in B(R)} W_\lambda(R, \beta, \bar{\epsilon}), \quad (4.5a)$$

where

$$W_\lambda(R, \beta, \bar{\epsilon}) := \min_{\substack{\epsilon_1, \epsilon_2 \in M_{\text{sym}}^{3 \times 3} \\ \lambda_1 \epsilon_1 + \lambda_2 \epsilon_2 = \bar{\epsilon}}} \lambda_1 W_1(\epsilon_1) + \lambda_2 W_2(\epsilon_2) - \lambda_1 \lambda_2 \beta \cdot \Phi^R(\epsilon_2 - \epsilon_1). \quad (4.5b)$$

4.2 Determining the amount of translation

Our next step is to characterize the sets $B_i(R)$ and $B(R)$.

Lemma 4.1. $B_i(R)$ is compact and convex.

Proof. Let

$$B_{i,\epsilon}(R) := \left\{ \beta \in (\mathbb{R}_+)^3 \mid \frac{1}{2} \langle \alpha_i R \epsilon R^T, R \epsilon R^T \rangle - \beta \cdot \Phi(\epsilon) \geq 0 \right\}.$$

From (4.4),

$$B_i(R) = \bigcap_{\epsilon} B_{i,\epsilon}(R).$$

For fixed ϵ , the map $\beta \mapsto \frac{1}{2} \langle \alpha_i R \epsilon R^T, R \epsilon R^T \rangle - \beta \cdot \Phi(\epsilon)$ is continuous. Thus the pre-image under this map of the closed set \mathbb{R}_+ is closed. It follows that $B_{i,\epsilon}(R)$ is closed. Since $\frac{1}{2} \langle \alpha_i R \epsilon R^T, R \epsilon R^T \rangle - \beta \cdot \Phi(\epsilon)$ is linear in β , $B_{i,\epsilon}(R)$ is convex. Thus $B_i(R)$, the intersection of all these closed, convex sets is closed and convex.

Let $\epsilon_1 = \begin{pmatrix} 0 & 0 & 0 \\ 0 & 0 & 1 \\ 0 & 1 & 0 \end{pmatrix}$; note that $\phi_1(\epsilon_1) = 1$, $\phi_2(\epsilon_1) = \phi_3(\epsilon_1) = 0$. Thus

$$\frac{1}{2} \langle \alpha_i R \epsilon_1 R^T, R \epsilon_1 R^T \rangle - \beta \cdot \Phi(\epsilon_1) \geq 0 \Leftrightarrow \beta_1 \leq \frac{1}{2} \langle \alpha_i R \epsilon_1 R^T, R \epsilon_1 R^T \rangle \Rightarrow \beta_1 \leq \frac{1}{2} \|\alpha_i\| \|R \epsilon_1 R^T\|^2 = \|\alpha_i\|,$$

where we have used $\|\epsilon_1\|^2 = 2$ and $\|\alpha_i\| := \max_{\epsilon \in M_{\text{sym}}^{3 \times 3}} \frac{\langle \alpha_i \epsilon, \epsilon \rangle}{\|\epsilon\|^2}$. Similarly, by considering $\epsilon_2 = \begin{pmatrix} 0 & 0 & 1 \\ 0 & 0 & 0 \\ 1 & 0 & 0 \end{pmatrix}$ and $\epsilon_3 = \begin{pmatrix} 0 & 1 & 0 \\ 1 & 0 & 0 \\ 0 & 0 & 0 \end{pmatrix}$ we obtain

$$B_i(R) \subset B_{i,\epsilon_1}(R) \cap B_{i,\epsilon_2}(R) \cap B_{i,\epsilon_3}(R) \subset [0, \|\alpha_i\|]^3.$$

Thus $B_i(R)$ is bounded. □

By an argument similar to that in lemma 3.2, $\forall \beta \in (\mathbb{R}_+)^3$,

$$B_i(R) \cap \mathbb{R} \times \{0\} \times \{0\} = \gamma_{i,1},$$

$$B_i(R) \cap \{0\} \times \mathbb{R} \times \{0\} = \gamma_{i,2},$$

$$B_i(R) \cap \{0\} \times \{0\} \times \mathbb{R} = \gamma_{i,3},$$

where

$$\gamma_{i,j} := \min_{\substack{\epsilon \\ \phi_j^R(\epsilon) > 0}} \frac{\langle \alpha_i \epsilon, \epsilon \rangle}{2\phi_j^R(\epsilon)}.$$

When $\alpha_i > 0$, equivalently

$$\frac{1}{\gamma_{i,j}} = \max_{\|\epsilon\|=1} \left\langle \left(\alpha_i^{-\frac{1}{2}} T_j^R \alpha_i^{-\frac{1}{2}} \right) \epsilon, \epsilon \right\rangle,$$

$$\frac{1}{\gamma_{i,j}} = \max_{\epsilon \neq 0} \frac{2\phi_j^R(\epsilon)}{\langle \alpha_i \epsilon, \epsilon \rangle}.$$

Let

$$B_{i,\text{II}^+}(R) := \overline{\partial B_i(R) \cap \text{Int}((\mathbb{R}_+)^3)},$$

$$B_{\text{II}^+}(R) := \overline{\partial B(R) \cap \text{Int}((\mathbb{R}_+)^3)}.$$

In other words $B_{i,\text{II}^+}(R)$ is the closure of that part of the boundary of $B_i(R)$ that does not intersect the coordinate planes $\{0\} \times \mathbb{R} \times \mathbb{R}$, $\mathbb{R} \times \{0\} \times \mathbb{R}$ and $\mathbb{R} \times \mathbb{R} \times \{0\}$. The significance of these sets and the reason for this terminology will become clear later. From the definition of $B_i(R)$ and $B(R)$ it is easy to see that

$$\left\{ \beta \in (\mathbb{R}_+)^3 \mid W_i - \beta \cdot \Phi^R: \text{strictly convex} \right\} = B_i(R) \setminus B_{i,\text{II}^+}(R), \quad (4.6a)$$

$$\left\{ \beta \in (\mathbb{R}_+)^3 \mid \forall i = 1, 2, W_i - \beta \cdot \Phi^R: \text{strictly convex} \right\} = B(R) \setminus B_{\text{II}^+}(R), \quad (4.6b)$$

$$\left\{ \beta \in (\mathbb{R}_+)^3 \mid W_i - \beta \cdot \Phi^R: \text{convex but not strictly convex} \right\} = B_{i, \text{II}^+}(R), \quad (4.6c)$$

$$\left\{ \beta \in (\mathbb{R}_+)^3 \mid \forall i = 1, 2, W_i - \beta \cdot \Phi^R: \text{convex but not strictly convex} \right\} = B_{\text{II}^+}(R). \quad (4.6d)$$

Remark 4.2. From (4.6), $\alpha_i - \beta \cdot T^R$ is invertible on $B_i(R) \setminus B_{i, \text{II}^+}(R)$ but not on $B_{i, \text{II}^+}(R)$. Both $\alpha_1 - \beta \cdot T^R$ and $\alpha_2 - \beta \cdot T^R$ are invertible on $B(R) \setminus B_{\text{II}^+}(R)$ and at least one of them is not invertible on $B_{\text{II}^+}(R)$.

4.2.1 Isotropic elastic moduli

An isotropic elastic modulus is of the form

$$\alpha = 3\kappa \mathbf{\Lambda}_h + 2\mu \mathbf{\Lambda}_s$$

where κ is the bulk modulus, μ the shear modulus and

$$\mathbf{\Lambda}_h \epsilon = \frac{1}{3} \text{Tr}(\epsilon) I,$$

$$\mathbf{\Lambda}_s := I - \mathbf{\Lambda}_h.$$

Lemma 4.3 (For isotropic elastic moduli, B_i and B are independent of R). For isotropic α_i ,

$$B_i(R) = B_i := \{ \beta \in (\mathbb{R}_+)^3 \mid W_i - \beta \cdot \Phi: \text{convex} \}. \quad (4.7)$$

Proof. Using (4.4) and the isotropy of α ,

$$\begin{aligned} B_i(R) &= \left\{ \beta \in (\mathbb{R}_+)^3 \mid \forall \epsilon \in M_{\text{sym}}^{3 \times 3}, \frac{1}{2} \langle \alpha_i R \epsilon R^T, R \epsilon R^T \rangle - \beta \cdot \Phi(\epsilon) \geq 0 \right\} \\ &= \left\{ \beta \in (\mathbb{R}_+)^3 \mid \forall \epsilon \in M_{\text{sym}}^{3 \times 3}, \frac{1}{2} \langle \alpha_i \epsilon, \epsilon \rangle - \beta \cdot \Phi(\epsilon) \geq 0 \right\} \\ &= \left\{ \beta \in (\mathbb{R}_+)^3 \mid W_i - \beta \cdot \Phi: \text{convex} \right\} \\ &= B_i. \end{aligned}$$

Since B_1 and B_2 are independent of R , so is B . □

Lemma 4.4. When α_i is isotropic,

$$B_{i,\Pi^+} = \left\{ \beta \in [0, 2\mu_i]^3 \left| \begin{array}{l} 2\beta_1\beta_2\beta_3 - (\ell_i + 2\mu_i)(\beta_1^2 + \beta_2^2 + \beta_3^2) + 2\ell_i(\beta_1\beta_2 + \beta_2\beta_3 + \beta_3\beta_1) \\ -4\ell_i\mu_i(\beta_1 + \beta_2 + \beta_3) + 12\ell_i\mu_i^2 + 8\mu_i^3 = 0 \end{array} \right. \right\}, \quad (4.8a)$$

$$B_i = \left\{ \beta \in [0, 2\mu_i]^3 \left| \begin{array}{l} 2\beta_1\beta_2\beta_3 - (\ell_i + 2\mu_i)(\beta_1^2 + \beta_2^2 + \beta_3^2) + 2\ell_i(\beta_1\beta_2 + \beta_2\beta_3 + \beta_3\beta_1) \\ -4\ell_i\mu_i(\beta_1 + \beta_2 + \beta_3) + 12\ell_i\mu_i^2 + 8\mu_i^3 \geq 0 \end{array} \right. \right\} \quad (4.8b)$$

$$= \text{Conv}(\{0\} \cup B_{i,\Pi^+}).$$

where $\ell_i := \kappa_i - \frac{2}{3}\mu_i > 0$ is the Lamé modulus of the material.

Proof. From the proof of lemma 4.3,

$$B_i = \left\{ \beta \in (\mathbb{R}_+)^3 \mid \forall \epsilon \in M_{\text{sym}}^{3 \times 3}, \langle \alpha_i \epsilon, \epsilon \rangle - 2(\beta_1 \phi_1(\epsilon) + \beta_2 \phi_2(\epsilon) + \beta_3 \phi_3(\epsilon)) \geq 0 \right\}.$$

Since $\alpha_i = 3\kappa_i \mathbf{\Lambda}_h + 2\mu_i \mathbf{\Lambda}_s$,

$$\begin{aligned} \langle \alpha_i \epsilon, \epsilon \rangle &= \left\langle (\kappa_i \text{Tr}(\epsilon)I + 2\mu_i \left(\epsilon - \frac{1}{3} \text{Tr}(\epsilon)I \right)), \epsilon \right\rangle \\ &= \langle \ell_i \text{Tr}(\epsilon)I + 2\mu_i \epsilon, \epsilon \rangle \\ &= \ell_i (\text{Tr}(\epsilon))^2 + 2\mu_i \|\epsilon\|^2 \\ &= (\ell_i + 2\mu_i)(\epsilon_{11}^2 + \epsilon_{22}^2 + \epsilon_{33}^2) + 2\ell_i(\epsilon_{11}\epsilon_{22} + \epsilon_{22}\epsilon_{33} + \epsilon_{33}\epsilon_{11}) + 4\mu_i(\epsilon_{12}^2 + \epsilon_{23}^2 + \epsilon_{31}^2), \end{aligned}$$

and

$$\begin{aligned} &\langle \alpha_i \epsilon, \epsilon \rangle - 2(\beta_1 \phi_1(\epsilon) + \beta_2 \phi_2(\epsilon) + \beta_3 \phi_3(\epsilon)) \\ &= (\ell_i + 2\mu_i)(\epsilon_{11}^2 + \epsilon_{22}^2 + \epsilon_{33}^2) + 2(\ell_i + \beta_3)\epsilon_{11}\epsilon_{22} + 2(\ell_i + \beta_1)\epsilon_{22}\epsilon_{33} + 2(\ell_i + \beta_2)\epsilon_{33}\epsilon_{11} \\ &\quad + 2(2\mu_i - \beta_3)\epsilon_{12}^2 + 2(2\mu_i - \beta_1)\epsilon_{23}^2 + 2(2\mu_i - \beta_2)\epsilon_{31}^2. \end{aligned} \quad (4.9)$$

We want the function on the left above to be non-negative, or equivalently since it is quadratic, to be convex. This requires $\beta_1, \beta_2, \beta_3 \leq 2\mu_i$ (that is, $\beta_1, \beta_2, \beta_3 \in [0, 2\mu_i]$) and the non-negativity of all the eigenvalues of the Hessian

$$H_i = 2 \begin{pmatrix} \ell_i + 2\mu_i & \ell_i + \beta_3 & \ell_i + \beta_2 \\ \ell_i + \beta_3 & \ell_i + 2\mu_i & \ell_i + \beta_1 \\ \ell_i + \beta_2 & \ell_i + \beta_1 & \ell_i + 2\mu_i \end{pmatrix}$$

of $\epsilon \mapsto (\ell_i + 2\mu_i)(\epsilon_{11}^2 + \epsilon_{22}^2 + \epsilon_{33}^2) + 2(\ell_i + \beta_3)\epsilon_{11}\epsilon_{22} + 2(\ell_i + \beta_1)\epsilon_{22}\epsilon_{33} + 2(\ell_i + \beta_2)\epsilon_{33}\epsilon_{11}$. A calculation

reveals that $\det(H_i) = 0$ is the equation

$$2\beta_1\beta_2\beta_3 - (\ell_i + 2\mu_i)(\beta_1^2 + \beta_2^2 + \beta_3^2) + 2\ell_i(\beta_1\beta_2 + \beta_2\beta_3 + \beta_3\beta_1) - 4\ell_i\mu_i(\beta_1 + \beta_2 + \beta_3) + 12\ell_i\mu_i^2 + 8\mu_i^3 = 0. \quad (4.10)$$

Further

$$\text{Tr}(H_i) = 3(\ell_i + 2\mu_i) > 0$$

and another calculation shows that

$$\text{Tr}(H_i^2) = 3(\ell_i + 2\mu_i)^2 + 2(\ell_i + \beta_1)^2 + 2(\ell_i + \beta_2)^2 + 2(\ell_i + \beta_3)^2.$$

Thus the sum of the pairwise products of the eigenvalues of H_i is

$$\begin{aligned} \frac{1}{2} \left((\text{Tr}(H_i))^2 - \text{Tr}(H_i^2) \right) &= \frac{1}{2} \left(9(\ell_i + 2\mu_i)^2 - 3(\ell_i + 2\mu_i)^2 - 2(\ell_i + \beta_1)^2 - 2(\ell_i + \beta_2)^2 - 2(\ell_i + \beta_3)^2 \right) \\ &= 3(\ell_i + 2\mu_i)^2 - (\ell_i + \beta_1)^2 - (\ell_i + \beta_2)^2 - (\ell_i + \beta_3)^2 \\ &= \underbrace{(\ell_i + 2\mu_i)^2 - (\ell_i + \beta_1)^2}_{\geq 0} + \underbrace{(\ell_i + 2\mu_i)^2 - (\ell_i + \beta_2)^2}_{\geq 0} + \underbrace{(\ell_i + 2\mu_i)^2 - (\ell_i + \beta_3)^2}_{\geq 0} \\ &\geq 0 \end{aligned} \quad (4.11)$$

where we have used $\beta_1, \beta_2, \beta_3 \in [0, \mu_i]$. Thus on the surface $\{\beta \in (\mathbb{R}_+)^3 \mid \det(H_i) = 0\}$ one eigenvalue of H_i is zero, and the other two are both positive (they cannot both be negative since $\text{Tr}(H_i) > 0$). It follows that

$$\begin{aligned} B_{i, \text{II}^+} &= \{\beta \in [0, 2\mu_i]^3 \mid \det(H_i) = 0\} \\ &= \left\{ \beta \in [0, 2\mu_i]^3 \left| \begin{array}{l} 2\beta_1\beta_2\beta_3 - (\ell_i + 2\mu_i)(\beta_1^2 + \beta_2^2 + \beta_3^2) + 2\ell_i(\beta_1\beta_2 + \beta_2\beta_3 + \beta_3\beta_1) \\ -4\ell_i\mu_i(\beta_1 + \beta_2 + \beta_3) + 12\ell_i\mu_i^2 + 8\mu_i^3 = 0 \end{array} \right. \right\} \end{aligned}$$

which is (4.8a). Since $0 \in B_i$ and from lemma 4.1 B_i is convex it follows that

$$B_i = \left\{ \beta \in [0, 2\mu_i]^3 \left| \begin{array}{l} 2\beta_1\beta_2\beta_3 - (\ell_i + 2\mu_i)(\beta_1^2 + \beta_2^2 + \beta_3^2) + 2\ell_i(\beta_1\beta_2 + \beta_2\beta_3 + \beta_3\beta_1) \\ -4\ell_i\mu_i(\beta_1 + \beta_2 + \beta_3) + 12\ell_i\mu_i^2 + 8\mu_i^3 \geq 0 \end{array} \right. \right\}$$

which is (4.8b). Finally it is easy to see that in fact

$$B_i = \text{Conv}(\{0\} \cup B_{i, \text{II}^+}).$$

□

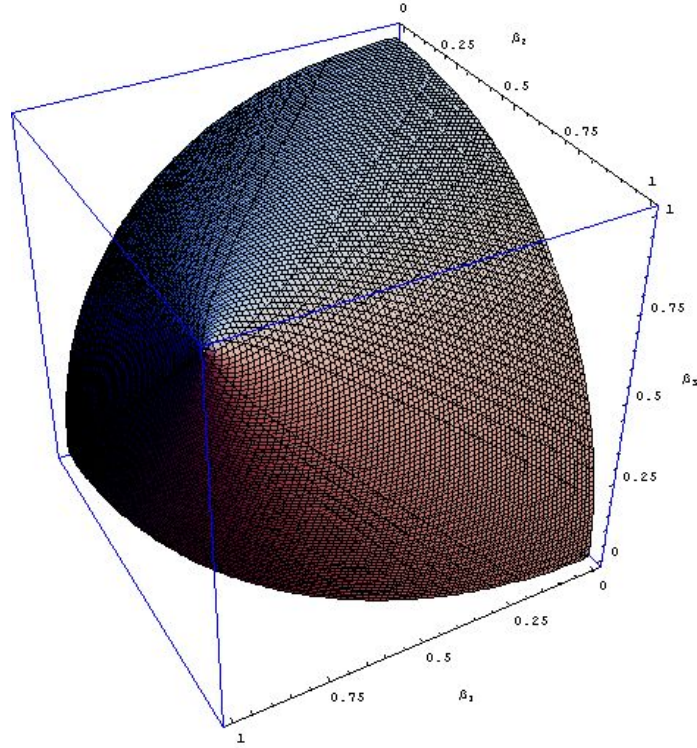


Figure 4.1: The set $B_{i,II+}$ for $\ell_i = 1$ and $\mu_i = \frac{1}{2}$. (View 1 of 2.)

B_i and $B_{i,II+}$ are illustrated in Figures 4.1 and 4.2. Notice that

1. $\gamma_{i,1} = \gamma_{i,2} = \gamma_{i,3} = 2\mu_i$: When $\beta_2 = \beta_3 = 0$, (4.10) reduces to $(\ell_i + 2\mu_i)\beta_1^2 + 4\ell_i\mu_i\beta_1 - (12\ell_i\mu_i^2 + 8\mu_i^3) = 0$. It is easy to verify that $2\mu_i$ is a root of this equation. The other root is negative since the product of the roots is negative. The same is true when $\beta_3 = \beta_1 = 0$ and $\beta_1 = \beta_2 = 0$.¹
2. *The intersection of B_i with the coordinate planes is a segment of an ellipse*: When $\beta_3 = 0$, (4.10) reduces to $-(\ell_i + 2\mu_i)(\beta_1^2 + \beta_2^2) + 2\ell_i\beta_1\beta_2 - 4\ell_i\mu_i(\beta_1 + \beta_2) + 12\ell_i\mu_i^2 + 8\mu_i^3 = 0$, which is the equation of an ellipse. The same is true when $\beta_3 = \beta_1 = 0$ and $\beta_1 = \beta_2 = 0$.¹
3. *The intersection of B_i with the plane $\beta_3 = 2\mu_i$ is the straight line segment $\beta_1 = \beta_2 \in [0, 2\mu_i]$* . This is easy to verify by substituting $\beta_3 = 2\mu_i$ in (4.10). The same is true when $\beta_2 = 2\mu_i$ and $\beta_3 = 2\mu_i$.¹

¹ This follows from symmetry too.

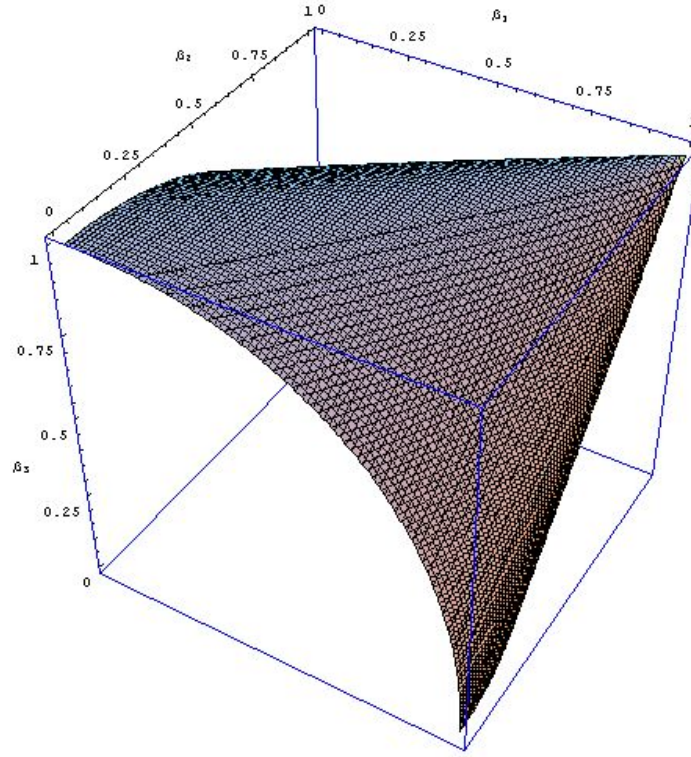


Figure 4.2: The set $B_{i,\Pi+}$ for $\ell_i = 1$ and $\mu_i = \frac{1}{2}$. (View 2 of 2.)

Let

$$B_{i,\Pi+}^{(1)} := B_{i,\Pi+} \cap \left\{ \beta \in (\mathbb{R}_+)^3 \mid \beta_2 > \beta_1, \beta_3 > \beta_1 \right\},$$

$$B_{i,\Pi+}^{(2)} := B_{i,\Pi+} \cap \left\{ \beta \in (\mathbb{R}_+)^3 \mid \beta_1 > \beta_2, \beta_3 > \beta_2 \right\},$$

$$B_{i,\Pi+}^{(3)} := B_{i,\Pi+} \cap \left\{ \beta \in (\mathbb{R}_+)^3 \mid \beta_1 > \beta_3, \beta_2 > \beta_3 \right\}.$$

$B_{i,\Pi+}^{(1)}$, $B_{i,\Pi+}^{(2)}$ and $B_{i,\Pi+}^{(3)}$ are shown in Figure 4.3. Let

$$B_{i,\text{III}}^{(1)} := \left\{ \beta \in (\mathbb{R}_+)^3 \mid \beta_2 = \beta_3 \in [0, 2\mu_i), \beta_1 = 2\mu_i \right\},$$

$$B_{i,\text{III}}^{(2)} := \left\{ \beta \in (\mathbb{R}_+)^3 \mid \beta_3 = \beta_1 \in [0, 2\mu_i), \beta_2 = 2\mu_i \right\},$$

$$B_{i,\text{III}}^{(3)} := \left\{ \beta \in (\mathbb{R}_+)^3 \mid \beta_1 = \beta_2 \in [0, 2\mu_i), \beta_3 = 2\mu_i \right\};$$

and

$$B_{i,\text{III}} := \cup_{i=1}^3 B_{i,\text{III}}^{(i)},$$

$$B_{i,\text{IV}} := \{2\mu_i(1, 1, 1)^T\}.$$

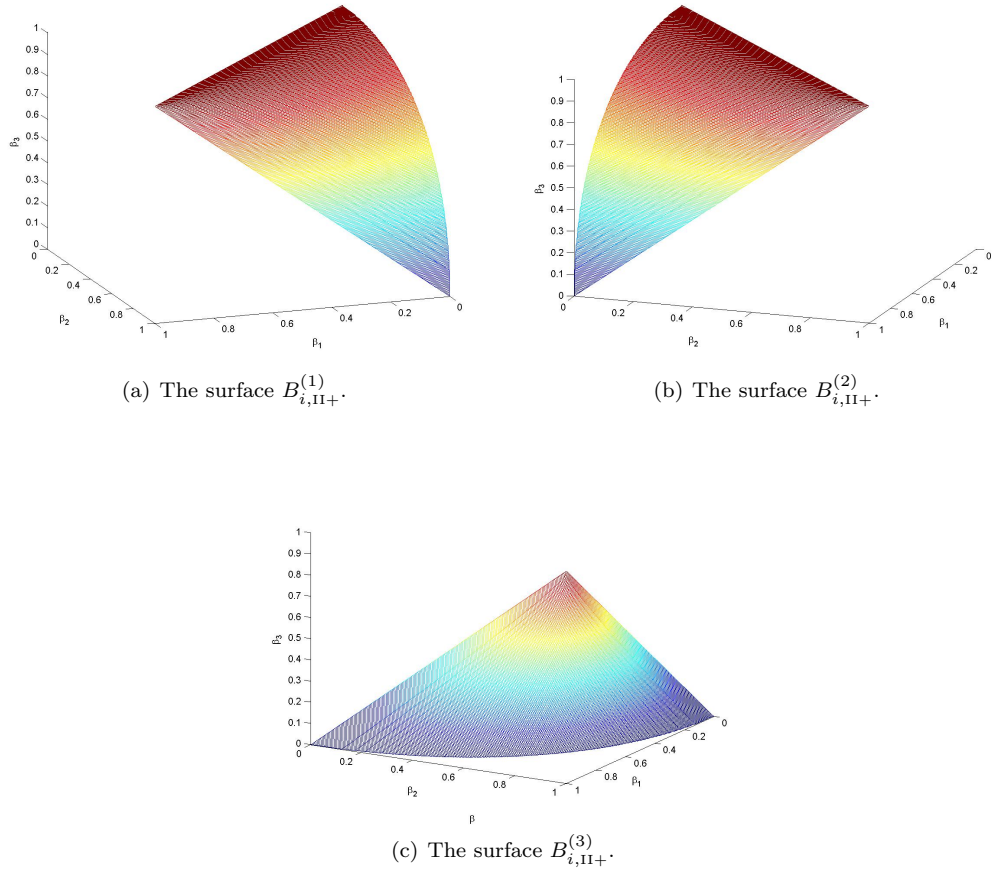


Figure 4.3: The surfaces $B_{i,II+}^{(1)}$, $B_{i,II+}^{(2)}$ and $B_{i,II+}^{(3)}$ for $\ell = 1$ and $\mu = \frac{1}{2}$.

$B_{i,III} \cup B_{i,IV}$ is shown in Figure 4.4. Note that the seven sets $B_{i,II+}^{(1)}$, $B_{i,II+}^{(2)}$, $B_{i,II+}^{(3)}$, $B_{i,III}^{(1)}$, $B_{i,III}^{(2)}$, $B_{i,III}^{(3)}$ and $B_{i,IV}$ are disjoint and their union is $B_{i,II+}$.

The sets $B_{III}^{(1)}$, $B_{III}^{(2)}$, $B_{III}^{(3)}$, B_{III} and B_{IV} are defined in an analogous manner. Let $j \in \{1, 2\}$ such that $\mu_j = \min\{\mu_1, \mu_2\}$. From the preceding it should be clear that $B_{III}^{(1)} = B_{j,III}^{(1)}$, $B_{III}^{(2)} = B_{j,III}^{(2)}$, $B_{III}^{(3)} = B_{j,III}^{(3)}$, $B_{III} = B_{j,III}$ and $B_{IV} = B_{j,IV}$.

Remark 4.5. From (4.11) note that $(\text{Tr}(H_i))^2 - \text{Tr}(H_i^2) > 0$ except when $\beta_1 = \beta_2 = \beta_3 = 2\mu_i$. Thus, when $\beta \in B_{i,II+}$, precisely one eigenvalue of H_i is zero, except when $\beta_1 = \beta_2 = \beta_3 = 2\mu_i$ (in which case two eigenvalues are zero). In conjunction with (4.9) this implies that

$$\dim(\ker(\alpha - \beta \cdot T)) = \begin{cases} 1 & \text{when } \beta \in B_{i,II+} \setminus (B_{i,III} \cup B_{i,IV}) \\ 2 & \text{when } \beta \in B_{i,III} \\ 5 & \text{when } \beta \in B_{i,IV}. \end{cases}$$

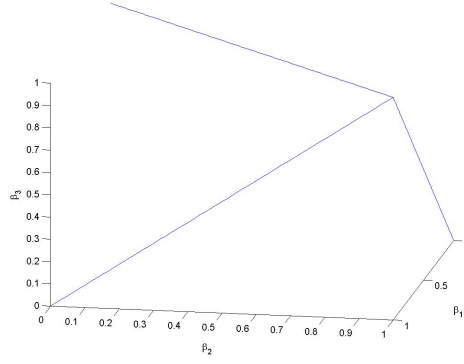


Figure 4.4: The set $B_{i,\text{III}} \cup B_{i,\text{IV}}$ for $\ell = 1$ and $\mu = \frac{1}{2}$.

We shall use this fact later.

As can be observed in Figures 4.1 and 4.2, $B_{i,\text{II}+}$ is smooth except at $2\mu_i(1, 1, 1)^T$ (c.f. remark 4.9).

Thus, except at $2\mu_i(1, 1, 1)^T$, the normal to the surface $B_{i,\text{II}+}$ exists and from (4.8a) is parallel to

$$N(\beta) = - \begin{pmatrix} \frac{\partial}{\partial \beta_1} \det(H_i) \\ \frac{\partial}{\partial \beta_2} \det(H_i) \\ \frac{\partial}{\partial \beta_3} \det(H_i) \end{pmatrix} = \begin{pmatrix} -2\beta_2\beta_3 + 2(\ell_i + 2\mu_i)\beta_1 - 2\ell_i(\beta_2 + \beta_3) + 4\ell_i\mu_i \\ -2\beta_3\beta_1 + 2(\ell_i + 2\mu_i)\beta_2 - 2\ell_i(\beta_3 + \beta_1) + 4\ell_i\mu_i \\ -2\beta_1\beta_2 + 2(\ell_i + 2\mu_i)\beta_3 - 2\ell_i(\beta_1 + \beta_2) + 4\ell_i\mu_i \end{pmatrix}. \quad (4.12)$$

Remark 4.6. Note that for $\beta \in B_{i,\text{II}+}$,

1. $\beta \cdot N(\beta) \geq 0$,
2. $\begin{pmatrix} 1 \\ 1 \\ 1 \end{pmatrix} \cdot N(\beta) \geq 0$,
3. N is in fact in the direction of the outward normal (this follows from (1) and (2)).

Proof. Using (4.8a),

$$\begin{aligned} \beta \cdot N(\beta) &= -6\beta_1\beta_2\beta_3 + 2(\ell_i + 2\mu_i)(\beta_1^2 + \beta_2^2 + \beta_3^2) - 4\ell_i(\beta_1\beta_2 + \beta_2\beta_3 + \beta_3\beta_1) + 4\ell_i\mu_i(\beta_1 + \beta_2 + \beta_3) \\ &= -2\beta_1\beta_2\beta_3 - 4\ell_i\mu_i(\beta_1 + \beta_2 + \beta_3) + 24\ell_i\mu_i^2 + 16\mu_i^3 \\ &\quad - 2 \left(2\beta_1\beta_2\beta_3 - (\ell_i + 2\mu_i)(\beta_1^2 + \beta_2^2 + \beta_3^2) + 2\ell_i(\beta_1\beta_2 + \beta_2\beta_3 + \beta_3\beta_1) \right. \\ &\quad \left. - 4\ell_i\mu_i(\beta_1 + \beta_2 + \beta_3) + 12\ell_i\mu_i^2 + 8\mu_i^3 \right) \\ &= 2(8\mu_i^3 - \beta_1\beta_2\beta_3) + 4\ell_i\mu_i(6\mu_i - (\beta_1 + \beta_2 + \beta_3)) \\ &\geq 0, \end{aligned}$$

and

$$\begin{aligned} \begin{pmatrix} 1 \\ 1 \\ 1 \end{pmatrix} \cdot N(\beta) &= -2(\beta_1\beta_2 + \beta_2\beta_3 + \beta_3\beta_1) + 4\mu_i(\beta_1 + \beta_2 + \beta_3) - 2\ell_i(\beta_1 + \beta_2 + \beta_3) + 12\ell_i\mu_i \\ &= 2(2\mu_i(\beta_1 + \beta_2 + \beta_3) - (\beta_1\beta_2 + \beta_2\beta_3 + \beta_3\beta_1)) + 2\ell_i(6\mu_i - (\beta_1 + \beta_2 + \beta_3)) \\ &\geq 0 \end{aligned}$$

(the first term is non-negative since $\beta_j \in [0, 2\mu_i] \Rightarrow \beta_j\beta_k \in [0, 2\mu_i\beta_k]$). □

We end this section with an important lemma.

Lemma 4.7 (sign(N) on $B_{i,\text{II}+}$).

1. On $B_{i,\text{II}+}^{(1)}$, $\text{sign}(N) = \begin{pmatrix} - \\ + \\ + \end{pmatrix}$.
2. On $B_{i,\text{II}+}^{(2)}$, $\text{sign}(N) = \begin{pmatrix} + \\ + \\ + \end{pmatrix}$.
3. On $B_{i,\text{II}+}^{(3)}$, $\text{sign}(N) = \begin{pmatrix} + \\ + \\ - \end{pmatrix}$.
4. On $B_{i,\text{III}}^{(1)}$, $\text{sign}(N) = \begin{pmatrix} + \\ 0 \\ 0 \end{pmatrix}$.
5. On $B_{i,\text{III}}^{(2)}$, $\text{sign}(N) = \begin{pmatrix} 0 \\ + \\ 0 \end{pmatrix}$.
6. On $B_{i,\text{III}}^{(3)}$, $\text{sign}(N) = \begin{pmatrix} 0 \\ 0 \\ + \end{pmatrix}$.

Remark 4.8. Let $c_i := \frac{\ell_i}{\ell_i + 2\mu_i} \in (0, 1)$. With the transformation $\beta'_j := \frac{\ell_i + \beta_j}{\ell_i + 2\mu_i} \in [c_i, 1]$, in the proof of lemma 4.4

$$H_i \parallel H'_i := \begin{pmatrix} 1 & \beta'_3 & \beta'_2 \\ \beta'_3 & 1 & \beta'_1 \\ \beta'_2 & \beta'_1 & 1 \end{pmatrix}.$$

Thus (4.10) is equivalent to

$$2 \prod_{j=1}^3 \beta'_j - \|\beta'\|^2 + 1 = 0$$

and (4.8a) and (4.8b) can be written as

$$B_{i,\text{II}+} = \left\{ \beta \in [c_i, 1]^3 \mid 2 \prod_{j=1}^3 \beta'_j - \|\beta'\|^2 + 1 = 0 \right\} \quad (4.13)$$

and

$$B_i = \left\{ \beta \in [c_i, 1]^3 \mid 2 \prod_{j=1}^3 \beta'_j - \|\beta'\|^2 + 1 \geq 0 \right\}$$

respectively. Finally from (4.12),

$$N(\beta') \parallel \begin{pmatrix} \beta'_1 - \beta'_2 \beta'_3 \\ \beta'_2 - \beta'_3 \beta'_1 \\ \beta'_3 - \beta_1 \beta_2 \end{pmatrix}.$$

Proof of lemma 4.7. We prove the first statement; the next two follow from symmetry. The last three statements follow from the first three statements and in any case are easy to verify. It might be helpful to refer to Figures 4.3(a) and 4.4.

It will be convenient to work in the coordinates β' (c.f. remark 4.8). Now

$$\nabla_{\beta'} N_1(\beta') \parallel \begin{pmatrix} 1 \\ -\beta'_3 \\ -\beta'_2 \end{pmatrix}.$$

Clearly, $\nabla_{\beta'} N_1(\beta') \neq 0$. Further, $\nabla_{\beta'} N_1(\beta') \nparallel N(\beta')$ on $B_{i,II+} \setminus B_{i,IV}$ as can be easily verified by a simple calculation. Thus the maximum and minimum of N_1 on $B_{i,II+}$ is attained at its boundary, i.e., on $B_{i,III}^{(2)} \cup B_{i,III}^{(3)} \cup B_{i,IV} \cup (B_{i,II+}^{(1)} \cap \{\beta \mid \beta - 1 = 0\})$. A simple calculation shows that $N_1 = 0$ on $B_{i,III}^{(2)}$, $B_{i,III}^{(3)}$ and $B_{i,IV}$.² In the next paragraph we show that $N_1 < 0$ on $B_{i,II+}^{(1)} \cap \{\beta \mid \beta - 1 = 0\}$. It follows that $N_1(\beta) < 0$ on $B_{i,III}^{(1)}$.

Proof that $N_1 < 0$ on $B_{i,II+}^{(1)} \cap \{\beta \mid \beta - 1 = 0\}$: Note from remark 4.8 (in particular (4.13)) that $B_{i,II+}^{(1)} \cap \{\beta \mid \beta - 1 = 0\}$ is the curve

$$(\beta'_3)^2 - 2c\beta'_2\beta'_3 + c^2 + (\beta'_2)^2 - 1 = 0, \quad \beta'_2, \beta'_3 \in (c, 1).$$

solving for β'_3 , we obtain, $\beta'_3 = c\beta'_2 \pm \sqrt{(1-c^2)(1-(\beta'_2)^2)}$. However,

$$c\beta'_2 - \sqrt{(1-c^2)(1-(\beta'_2)^2)} < c\beta'_2 - (1-(\beta'_2)^2)^2 = c\beta'_2 + (\beta'_2)^2 - 1 < c\beta'_2 < c.$$

² This also proves part of (5) and (6).

Thus the solution we seek is $\beta'_3 = c\beta'_2 + \sqrt{(1-c^2)(1-(\beta'_2)^2)}$. Thus on $B_{i,II+}^{(1)} \cap \{\beta \mid \beta - 1 = 0\}$,

$$\begin{aligned} N_1(\beta') &= c - c(\beta'_2)^2 - (\beta'_2)\sqrt{(1-c^2)(1-(\beta'_2)^2)} \\ &< c - c(\beta'_2)^2 - c\sqrt{(1-c^2)(1-(\beta'_2)^2)} \\ &< c - c(\beta'_2)^2 - c(1 - (\beta'_2)^2) \\ &= 0. \end{aligned}$$

This completes the proof that $\text{sign}(N_1) < 0$ on $\beta \in B_{i,II+}^{(1)}$.

Now $\beta \in B_{i,II+}^{(1)}$ implies that $\beta_2 > \beta_1$ and $\beta_3 > \beta_1$. Thus,

$$\begin{aligned} N_2 &= -2\beta_3\beta_1 + 2(\ell_i + 2\mu_i)\beta_2 - 2\ell_i(\beta_3 + \beta_1) + 4\ell_i\mu_i \\ &> -2\beta_3\beta_1 + 2(\ell_i + 2\mu_i)\beta_1 - 2\ell_i(\beta_3 + \beta_1) + 4\ell_i\mu_i \\ &= -2\beta_3\beta_1 + 4\mu_i\beta_1 - 2\ell_i\beta_3 + 4\ell_i\mu_i \\ &= 2(\ell_i + \beta_1)(2\mu_i - \beta_3) \\ &> 0 \end{aligned}$$

and

$$\begin{aligned} N_3 &= -2\beta_1\beta_2 + 2(\ell_i + 2\mu_i)\beta_3 - 2\ell_i(\beta_1 + \beta_2) + 4\ell_i\mu_i \\ &> -2\beta_1\beta_2 + 2(\ell_i + 2\mu_i)\beta_1 - 2\ell_i(\beta_1 + \beta_2) + 4\ell_i\mu_i \\ &= -2\beta_1\beta_2 + 4\mu_i\beta_1 - 2\ell_i\beta_2 + 4\ell_i\mu_i \\ &= 2(\ell_i + \beta_1)(2\mu_i - \beta_2) \\ &> 0. \end{aligned}$$

□

Remark 4.9. From (4), (5) and (6) in lemma 4.7 it follows that the surface is not smooth at $2\mu(1, 1, 1)^T$ (i.e., on $B_{i,IV}$) for,

$$\lim_{\substack{\beta \rightarrow 2\mu_i(1,1,1)^T \\ \beta \in B_{i,III}^{(1)}}} N(\beta) \neq \lim_{\substack{\beta \rightarrow 2\mu_i(1,1,1)^T \\ \beta \in B_{i,III}^{(2)}}} N(\beta) \neq \lim_{\substack{\beta \rightarrow 2\mu_i(1,1,1)^T \\ \beta \in B_{i,III}^{(3)}}} N(\beta).$$

4.3 Explicit expressions for the optimal strains³

Let us return to the minimization problem (4.5b) and find the minimizers $\epsilon_1^*(R, \beta, \bar{\epsilon})$ and $\epsilon_2^*(R, \beta, \bar{\epsilon})$. By differentiating the argument on the right-hand side of (4.5b),

$$\alpha_1(\epsilon_1^* - \epsilon_1^T) - \alpha_2(\epsilon_2^* - \epsilon_2^T) + (\beta \cdot T^R)(\epsilon_2^* - \epsilon_1^*) = 0 \quad (4.14)$$

In other words,

$$\Delta\sigma^* = (\beta \cdot T^R)\Delta\epsilon^* \quad (4.15)$$

where $\Delta\epsilon^* = \epsilon_2^* - \epsilon_1^*$, $\Delta\sigma^* := \sigma_2^* - \sigma_1^*$ and $\sigma_i^* = \alpha_i(\epsilon_i^* - \epsilon_i^T)$. Using $\lambda_1\epsilon_1 + \lambda_2\epsilon_2 = \bar{\epsilon}$, (4.14) gives

$$\begin{aligned} (\lambda_2\alpha_1 + \lambda_1\alpha_2 - \beta \cdot T^R)\epsilon_1^* &= (\alpha_2 - \beta \cdot T^R)\bar{\epsilon} + \lambda_2(\alpha_1\epsilon_1^T - \alpha_2\epsilon_2^T), \\ (\lambda_2\alpha_1 + \lambda_1\alpha_2 - \beta \cdot T^R)\epsilon_2^* &= (\alpha_1 - \beta \cdot T^R)\bar{\epsilon} - \lambda_1(\alpha_1\epsilon_1^T - \alpha_2\epsilon_2^T), \\ (\lambda_2\alpha_1 + \lambda_1\alpha_2 - \beta \cdot T^R)\Delta\epsilon^* &= (\alpha_2\epsilon_2^T - \alpha_1\epsilon_1^T) - (\Delta\alpha)\bar{\epsilon}. \end{aligned}$$

where $\Delta\alpha := \alpha_2 - \alpha_1$. To get explicit expressions we need the invertibility of $\lambda_2\alpha_1 + \lambda_1\alpha_2 - \beta \cdot T^R$. Note that $\lambda_2\alpha_1 + \lambda_1\alpha_2 - \beta \cdot T^R = \lambda_2(\alpha_1 - \beta \cdot T^R) + \lambda_1(\alpha_2 - \beta \cdot T^R)$. Hence, for $\beta \in B(R) \setminus B_{\text{II}+}$, it is the sum of two positive definite linear operators and consequently positive definite and thus invertible. In fact even when $\beta \in B_{\text{II}+}$, $\lambda_2\alpha_1 + \lambda_1\alpha_2 - \beta \cdot T^R$ is invertible as long as $\ker(\alpha_1 - \beta \cdot T^R) \cap \ker(\alpha_2 - \beta \cdot T^R) = \{0\}$. In either case,

$$\epsilon_1^* = \left(\lambda_2\alpha_1 + \lambda_1\alpha_2 - \beta \cdot T^R\right)^{-1} \left((\alpha_2 - \beta \cdot T^R)\bar{\epsilon} - \lambda_2(\alpha_2\epsilon_2^T - \alpha_1\epsilon_1^T)\right), \quad (4.16a)$$

$$\epsilon_2^* = \left(\lambda_2\alpha_1 + \lambda_1\alpha_2 - \beta \cdot T^R\right)^{-1} \left((\alpha_1 - \beta \cdot T^R)\bar{\epsilon} + \lambda_1(\alpha_2\epsilon_2^T - \alpha_1\epsilon_1^T)\right), \quad (4.16b)$$

$$\Delta\epsilon^* = \left(\lambda_2\alpha_1 + \lambda_1\alpha_2 - \beta \cdot T^R\right)^{-1} \left((\alpha_2\epsilon_2^T - \alpha_1\epsilon_1^T) - (\Delta\alpha)\bar{\epsilon}\right). \quad (4.16c)$$

and

$$\frac{\partial \Delta\epsilon^*}{\partial \beta_i} = (\lambda_2\alpha_1 + \lambda_1\alpha_2 - \beta \cdot T^R)^{-1} T_i^R \Delta\epsilon^* \quad (4.17)$$

³The expressions in this section can be obtained from those in section 3.1.4 by the formal substitution of $\beta \cdot T^R$ for βT , $\beta \in B(R) \setminus B_{\text{II}+}(R)$ for $\beta \in [0, \gamma_*)$ and $\beta \in B_{\text{II}+}(R)$ for $\beta = \gamma_*$.

4.4 An optimal rotation diagonalizes the optimal strain jump

Henceforth we assume that the elastic moduli are isotropic. From lemma 4.3, for isotropic moduli B is independent of R . Thus from (4.5a), we have the lower bound

$$\widehat{W}_\lambda(\bar{\epsilon}) \geq \max_{\beta \in B} W_\lambda(\beta, \bar{\epsilon}) \quad (4.18a)$$

where

$$W_\lambda(\beta, \bar{\epsilon}) := \max_{R \in SO(3)} \min_{\substack{\epsilon_1, \epsilon_2 \in M_{\text{sym}}^{3 \times 3} \\ \lambda_1 \epsilon_1 + \lambda_2 \epsilon_2 = \bar{\epsilon}}} \lambda_1 W_1(\epsilon_1) + \lambda_2 W_2(\epsilon_2) - \lambda_1 \lambda_2 \beta \cdot \Phi^R(\epsilon_2 - \epsilon_1). \quad (4.18b)$$

Theorem 4.10 (An optimal rotation diagonalizes the optimal strain jump). There exist $R_\star(\beta, \bar{\epsilon}) \in SO(3)$, $\epsilon_1^\star(R_\star, \beta, \bar{\epsilon})$, $\epsilon_2^\star(R_\star, \beta, \bar{\epsilon}) \in M_{\text{sym}}^{3 \times 3}$ that extremize (4.18b) such that $R_\star^T \Delta \epsilon^\star R_\star$ is diagonal.

Our proof of theorem 4.10 uses doubly stochastic matrices and is presented at the end of this section.

4.4.1 Doubly stochastic matrices

A doubly stochastic matrix is a square matrix, all of whose entries are positive and each of whose rows and columns add up to one. Let Ω_3 be the set of all doubly stochastic matrices in $M^{3 \times 3}$. Ω_3 is a four-dimensional convex set the set of whose extreme points is \mathbb{P}_3 , the set of permutation matrices in $M^{3 \times 3}$ [Bir46] (or, e.g., [MI79, pg.19,34]). $\mathbb{P}_3 = \{P_j \mid j = 1, 2 \dots 6\}$, where

$$\begin{aligned} P_1 &:= \begin{pmatrix} 1 & 0 & 0 \\ 0 & 1 & 0 \\ 0 & 0 & 1 \end{pmatrix}, & P_2 &:= \begin{pmatrix} 0 & 1 & 0 \\ 0 & 0 & 1 \\ 1 & 0 & 0 \end{pmatrix}, & P_3 &:= \begin{pmatrix} 0 & 0 & 1 \\ 1 & 0 & 0 \\ 0 & 1 & 0 \end{pmatrix}, \\ P_4 &:= \begin{pmatrix} 1 & 0 & 0 \\ 0 & 0 & 1 \\ 0 & 1 & 0 \end{pmatrix}, & P_5 &:= \begin{pmatrix} 0 & 1 & 0 \\ 1 & 0 & 0 \\ 0 & 0 & 1 \end{pmatrix}, & P_6 &:= \begin{pmatrix} 0 & 0 & 1 \\ 0 & 1 & 0 \\ 1 & 0 & 0 \end{pmatrix}. \end{aligned}$$

Note that the first three of these belong to $SO(3)$ and the next three to $O(3) \setminus SO(3)$.

Remark 4.11.

1. $\forall P \in \mathbb{P}_3$, $\Phi(P^T \epsilon P) = P^T \Phi(\epsilon)$.
2. $\forall P \in \mathbb{P}_3$ there exists $R(P) \in SO(3)$ such that $\Phi(P^T \epsilon P) = \Phi(R(P)^T \epsilon R(P))$.

Proof. The first statement is easily verified. Each $P \in \mathbb{P}$ is a matrix precisely three of whose components is 1. For each $P \in \mathbb{P} \cap SO(3)$ replacing none or two 1s by -1 generates a matrix

$R(P) \in SO(3)$. For each $P \in \mathbb{P} \setminus SO(3)$ replacing one or three 1 by -1 generates a matrix $R(P) \in SO(3)$. It is easily verified that for every such choice of $R(P)$, $\Phi(P^T \epsilon P) = \Phi(R(P)^T \epsilon R(P))$. \square

A map from $SO(3)$ to Ω_3 . Define $S: SO(3) \rightarrow \Omega_3$ by

$$SO(3) \ni \begin{pmatrix} R_{11} & R_{12} & R_{13} \\ R_{21} & R_{22} & R_{23} \\ R_{31} & R_{32} & R_{33} \end{pmatrix} \xrightarrow{S} \begin{pmatrix} R_{11}^2 & R_{12}^2 & R_{13}^2 \\ R_{21}^2 & R_{22}^2 & R_{23}^2 \\ R_{31}^2 & R_{32}^2 & R_{33}^2 \end{pmatrix} \in \Omega_3. \quad (4.19)$$

For $R(P)$ defined as in remark 4.11, $S(R(P)) = P$. Thus $\mathbb{P}_3 \subset \text{Range}(S)$. The following remark and lemma will shed light on some subsequent comments.

Remark 4.12. Since the only fixed points of $\mathbb{R} \ni x \mapsto x^2 \in \mathbb{R}$ are 0 and 1, it follows that

1. The fixed points of S are precisely $\mathbb{P}_3 \cap SO(3)$.
2. S can be extended to a map from $O(3)$ to Ω_3 , in which case its fixed points are precisely \mathbb{P}_3 .

Lemma 4.13 ([Kat03]). S is not onto.

Proof. Assume on the contrary that $\exists R \in SO(3)$ such that

$$S(R) = \frac{1}{3} \begin{pmatrix} 1 & 1 & 1 \\ 1 & 1 & 1 \\ 1 & 1 & 1 \end{pmatrix} \in \Omega_3.$$

Then, from (4.19), for some choice of signs

$$R = \frac{1}{\sqrt{3}} \begin{pmatrix} \pm 1 & \pm 1 & \pm 1 \\ \pm 1 & \pm 1 & \pm 1 \\ \pm 1 & \pm 1 & \pm 1 \end{pmatrix}.$$

However the rows and columns of this R cannot be orthogonal: $R \notin SO(3)$, which is a contradiction. \square

Let $\sigma: \{1, 2, 3\} \rightarrow \{1, 2, 3\}$ be a permutation (i.e., invertible function). For $\epsilon \in M_{\text{sym}}^{3 \times 3}$ let $v_1(\epsilon)$, $v_2(\epsilon)$ and $v_3(\epsilon)$ be the eigenvalues of ϵ . By $\text{diag}(\epsilon)$ we denote an arbitrary (but fixed) matrix of the form

$$\begin{pmatrix} v_{\sigma(1)}(\epsilon) & 0 & 0 \\ 0 & v_{\sigma(2)}(\epsilon) & 0 \\ 0 & 0 & v_{\sigma(3)}(\epsilon) \end{pmatrix}.$$

In other words, $\text{diag}(\epsilon)$ is a diagonal matrix whose diagonal elements are the eigenvalues of ϵ in some arbitrary (but fixed) order. Similarly, let

$$\Upsilon(\epsilon) := \begin{pmatrix} v_{\sigma(2)}(\epsilon) & v_{\sigma(3)}(\epsilon) \\ v_{\sigma(3)}(\epsilon) & v_{\sigma(1)}(\epsilon) \\ v_{\sigma(1)}(\epsilon) & v_{\sigma(2)}(\epsilon) \end{pmatrix}.$$

Lemma 4.14. $\forall R \in SO(3), \forall \epsilon \in M_{\text{sym}}^{3 \times 3}, \exists D \in \Omega_3$ such that $\beta \cdot \Phi^R(\epsilon) = -D\beta \cdot \Upsilon(\epsilon)$.

Proof. There exist $R_d(\epsilon) \in SO(3)$ such that

$$\epsilon = (R_d(\epsilon))^T \text{diag}(\epsilon) R_d(\epsilon).$$

Thus

$$\begin{aligned} R^T \epsilon R &= (R_d(\epsilon) R)^T \text{diag}(\epsilon) R_d(\epsilon) R \\ &= (R')^T \text{diag}(\epsilon) R' \end{aligned}$$

where $R' := R_d(\epsilon) R$. An easy exercise reveals that

$$\begin{aligned} -\phi_1(R^T \epsilon R) &= (R'_{22} R'_{33} - R'_{32} R'_{23})^2 v_{\sigma(2)}(\epsilon) v_{\sigma(3)}(\epsilon) + (R'_{23} R'_{31} - R'_{33} R'_{21})^2 v_{\sigma(3)}(\epsilon) v_{\sigma(1)}(\epsilon) \\ &\quad + (R'_{21} R'_{32} - R'_{31} R'_{22})^2 v_{\sigma(1)}(\epsilon) v_{\sigma(2)}(\epsilon) \\ -\phi_2(R^T \epsilon R) &= (R'_{32} R'_{13} - R'_{12} R'_{33})^2 v_{\sigma(2)}(\epsilon) v_{\sigma(3)}(\epsilon) + (R'_{33} R'_{11} - R'_{13} R'_{31})^2 v_{\sigma(3)}(\epsilon) v_{\sigma(1)}(\epsilon) \\ &\quad + (R'_{31} R'_{12} - R'_{11} R'_{32})^2 v_{\sigma(1)}(\epsilon) v_{\sigma(2)}(\epsilon) \\ -\phi_3(R^T \epsilon R) &= (R'_{12} R'_{23} - R'_{22} R'_{13})^2 v_{\sigma(2)}(\epsilon) v_{\sigma(3)}(\epsilon) + (R'_{13} R'_{21} - R'_{23} R'_{11})^2 v_{\sigma(3)}(\epsilon) v_{\sigma(1)}(\epsilon) \\ &\quad + (R'_{11} R'_{22} - R'_{21} R'_{12})^2 v_{\sigma(1)}(\epsilon) v_{\sigma(2)}(\epsilon). \end{aligned}$$

We obtain

$$\beta \cdot \Phi(R^T \epsilon R) = -\beta \cdot \begin{pmatrix} (R'_{22} R'_{33} - R'_{32} R'_{23})^2 & (R'_{23} R'_{31} - R'_{33} R'_{21})^2 & (R'_{21} R'_{32} - R'_{31} R'_{22})^2 \\ (R'_{32} R'_{13} - R'_{12} R'_{33})^2 & (R'_{33} R'_{11} - R'_{13} R'_{31})^2 & (R'_{31} R'_{12} - R'_{11} R'_{32})^2 \\ (R'_{12} R'_{23} - R'_{22} R'_{13})^2 & (R'_{13} R'_{21} - R'_{23} R'_{11})^2 & (R'_{11} R'_{22} - R'_{21} R'_{12})^2 \end{pmatrix} \Upsilon(\epsilon)$$

Note that the ij^{th} element of the matrix above is the square of the ij^{th} sub-determinant of R' . Since $R' \in SO(3)$, its rows and columns are orthonormal: $R'_{22} R'_{33} - R'_{32} R'_{23} = R'_{11}$, $R'_{23} R'_{31} - R'_{33} R'_{21} =$

$R'_{12} \dots$. This gives

$$\begin{aligned}
\beta \cdot \Phi^R(\epsilon) &= -\beta \cdot \begin{pmatrix} (R'_{11})^2 & (R'_{12})^2 & (R'_{13})^2 \\ (R'_{21})^2 & (R'_{22})^2 & (R'_{23})^2 \\ (R'_{31})^2 & (R'_{13})^2 & (R'_{11})^2 \end{pmatrix} \Upsilon(\epsilon) \\
&= -\beta \cdot S(R') \Upsilon(\epsilon) \\
&= -(S(R_d(\epsilon)R))^T \beta \cdot \Upsilon(\epsilon) \\
&= D\beta \cdot \Upsilon(\epsilon).
\end{aligned} \tag{4.20}$$

where $D := -(S(R_d(\epsilon)R))^T$. □

Corollary 4.15 ($\sum_{j=1}^3 \phi_j^R$ is independent of R). With $\beta = (1, 1, 1)^T$ in (4.20), since any doubly stochastic matrix has $(1, 1, 1)^T$ as eigenvector with eigenvalue 1, we obtain

$$\sum_{j=1}^3 \phi_j(R^T \epsilon R) = -D \begin{pmatrix} 1 \\ 1 \\ 1 \end{pmatrix} \cdot \Upsilon(\epsilon) = - \begin{pmatrix} 1 \\ 1 \\ 1 \end{pmatrix} \cdot \Upsilon(\epsilon) = -(v_2(\epsilon)v_3(\epsilon) + v_3(\epsilon)v_1(\epsilon) + v_1(\epsilon)v_2(\epsilon))$$

which is independent of R .

We are now ready to prove theorem 4.10.

4.4.2 Proof of theorem 4.10

The existence of R_\star and ϵ_i^\star follows from the convexity for each $R \in SO(3)$ of $W_i - \beta \cdot \Phi^R$, the continuity for each $\epsilon \in M_{\text{sym}}^{3 \times 3}$ of $R \mapsto \Phi^R(\epsilon)$ and the compactness of $SO(3)$. It remains to show that $R_\star^T \Delta \epsilon^\star R_\star$ is diagonal. From (4.18b) and (4.20),

$$W_\lambda(\beta, \bar{\epsilon}) = \max_{R \in SO(3)} \min_{\substack{\epsilon_1, \epsilon_2 \in M_{\text{sym}}^{3 \times 3} \\ \lambda_1 \epsilon_1 + \lambda_2 \epsilon_2 = \bar{\epsilon}}} \lambda_1 W_1(\epsilon_1) + \lambda_2 W_2(\epsilon_2) + \lambda_1 \lambda_2 S^T(R_d(\epsilon_2 - \epsilon_1)R) \beta \cdot \Upsilon(\epsilon_2 - \epsilon_1).$$

Thus

$$W_\lambda(\beta, \bar{\epsilon}) \leq \max_{S \in \Omega_3} \min_{\substack{\epsilon_1, \epsilon_2 \in M_{\text{sym}}^{3 \times 3} \\ \lambda_1 \epsilon_1 + \lambda_2 \epsilon_2 = \bar{\epsilon}}} \lambda_1 W_1(\epsilon_1) + \lambda_2 W_2(\epsilon_2) + \lambda_1 \lambda_2 S \beta \cdot \Upsilon(\epsilon_2 - \epsilon_1), \tag{4.21}$$

where the inequality arises since (a) we are replacing $S^T(R_d(\epsilon_2 - \epsilon_1)R)$ with an arbitrary $S \in \Omega_3$ and (b) the maximization is performed over $S \in \Omega_3$ and not just $\text{Range}(S) \subsetneq \Omega_3$. Now

$$\Omega_3 \ni S \mapsto \min_{\substack{\epsilon_1, \epsilon_2 \in M_{\text{sym}}^{3 \times 3} \\ \lambda_1 \epsilon_1 + \lambda_2 \epsilon_2 = \bar{\epsilon}}} \lambda_1 W_1(\epsilon_1) + \lambda_2 W_2(\epsilon_2) + \lambda_1 \lambda_2 S \beta \cdot \Upsilon(\epsilon_2 - \epsilon_1)$$

is convex: $\forall \theta \in (0, 1)$,

$$\begin{aligned} \min_{\substack{\epsilon_1, \epsilon_2 \in M_{\text{sym}}^{3 \times 3} \\ \lambda_1 \epsilon_1 + \lambda_2 \epsilon_2 = \bar{\epsilon}}} \lambda_1 W_1(\epsilon_1) + \lambda_2 W_2(\epsilon_2) + \lambda_1 \lambda_2 (\theta S + (1 - \theta) S') \beta \cdot \Upsilon(\epsilon_2 - \epsilon_1) \\ \geq \min_{\substack{\epsilon_1, \epsilon_2 \in M_{\text{sym}}^{3 \times 3} \\ \lambda_1 \epsilon_1 + \lambda_2 \epsilon_2 = \bar{\epsilon}}} \theta \lambda_1 W_1(\epsilon_1) + \theta \lambda_2 W_2(\epsilon_2) + \theta \lambda_1 \lambda_2 S \beta \cdot \Upsilon(\epsilon_2 - \epsilon_1) \\ + \min_{\substack{\epsilon_1, \epsilon_2 \in M_{\text{sym}}^{3 \times 3} \\ \lambda_1 \epsilon_1 + \lambda_2 \epsilon_2 = \bar{\epsilon}}} (1 - \theta) \lambda_1 W_1(\epsilon_1) + (1 - \theta) \lambda_2 W_2(\epsilon_2) + (1 - \theta) \lambda_1 \lambda_2 S' \beta \cdot \Upsilon(\epsilon_2 - \epsilon_1), \end{aligned}$$

where we have used $\min_x (f(x) + g(x)) \geq \min_x f(x) + \min_x g(x)$. Since convex functions attain their maximum on the extreme points of convex sets, there exists $S_\star \in \mathbb{P}_3$ that maximizes the left-hand side of (4.21). Since $\mathbb{P}_3 \subset \text{Range}(S)$, this implies the existence of $R_\star \in SO(3)$ such that $S(R_d R_\star) = S_\star$ which maximizes the left-hand side of (4.18b). Thus the inequality in (4.21) is actually an equality. Further

$$\begin{aligned} S(R_d R_\star) \in \mathbb{P}_3 &\Rightarrow R_d R_\star \text{ is a signed permutation matrix} \\ &\Rightarrow (R_d R_\star)^T \text{diag}(\Delta \epsilon^\star)(R_d R_\star) \text{ is diagonal} \\ &\Rightarrow R_\star^T \Delta \epsilon^\star R_\star \text{ is diagonal} \end{aligned}$$

which completes the proof. \square

Note that, since $R_\star^T \Delta \epsilon^\star R_\star$ is diagonal,

$$R_\star^T \Delta \epsilon^\star R_\star = \begin{pmatrix} v_{\sigma(1)}(\Delta \epsilon^\star) & 0 & 0 \\ 0 & v_{\sigma(2)}(\Delta \epsilon^\star) & 0 \\ 0 & 0 & v_{\sigma(3)}(\Delta \epsilon^\star) \end{pmatrix}$$

and thus

$$\phi_1(R_\star^T \Delta \epsilon^\star R_\star) = -v_{\sigma(2)}(\Delta \epsilon^\star) v_{\sigma(3)}(\Delta \epsilon^\star), \quad (4.22a)$$

$$\phi_2(R_\star^T \Delta \epsilon^\star R_\star) = -v_{\sigma(3)}(\Delta \epsilon^\star) v_{\sigma(1)}(\Delta \epsilon^\star), \quad (4.22b)$$

$$\phi_3(R_\star^T \Delta \epsilon^\star R_\star) = -v_{\sigma(1)}(\Delta \epsilon^\star) v_{\sigma(2)}(\Delta \epsilon^\star). \quad (4.22c)$$

4.5 A lower bound on the relaxed energy

Recall from (4.18a) and (4.18b) that we have the lower bound

$$\widehat{W}_\lambda(\bar{\epsilon}) \geq \max_{\beta \in B} W_\lambda(\beta, \bar{\epsilon}) \quad (4.18a)$$

where

$$W_\lambda(\beta, \bar{\epsilon}) := \max_{R \in SO(3)} \min_{\substack{\epsilon_1, \epsilon_2 \in M_{\text{sym}}^{3 \times 3} \\ \lambda_1 \epsilon_1 + \lambda_2 \epsilon_2 = \bar{\epsilon}}} \lambda_1 W_1(\epsilon_1) + \lambda_2 W_2(\epsilon_2) - \lambda_1 \lambda_2 \beta \cdot \Phi^R(\epsilon_2 - \epsilon_1). \quad (4.18b)$$

Determining $\max_{\beta \in B} W_\lambda(\beta, \bar{\epsilon})$ is easy since we have the following lemma.

Lemma 4.16. $\beta \mapsto W_\lambda(\beta, \bar{\epsilon})$ is concave for $\beta \in B \setminus B_{\text{II}+}$.

Proof. Let $\theta \in (0, 1)$. Using $\min_x f(x) + \min_x g(x) \leq \min_x (f(x) + g(x))$,

$$\begin{aligned} & \theta W_\lambda(\beta, \bar{\epsilon}) + (1 - \theta) W_\lambda(\beta', \bar{\epsilon}) \\ &= \min_{\lambda_1 \epsilon_1 + \lambda_2 \epsilon_2 = \bar{\epsilon}} \theta \lambda_1 W_1(\epsilon_1) + \theta \lambda_2 W_2(\epsilon_2) - \theta \lambda_1 \lambda_2 \beta \cdot \Phi^R(\epsilon_2 - \epsilon_1) \\ & \quad + \min_{\lambda_1 \epsilon_1 + \lambda_2 \epsilon_2 = \bar{\epsilon}} (1 - \theta) \lambda_1 W_1(\epsilon_1) + (1 - \theta) \lambda_2 W_2(\epsilon_2) - (1 - \theta) \lambda_1 \lambda_2 \beta' \cdot \Phi(\epsilon_2 - \epsilon_1). \\ & \leq W_\lambda((\theta \beta + (1 - \theta) \beta'), \bar{\epsilon}). \end{aligned}$$

□

From (4.18b),

$$\frac{\partial}{\partial \beta_i} W_\lambda(\beta, \bar{\epsilon}) = -\lambda_1 \lambda_2 \phi_i^{R_\star(\beta, \bar{\epsilon})}(\Delta \epsilon^\star(R_\star(\beta, \bar{\epsilon}), \beta, \bar{\epsilon})); \quad (4.23a)$$

in other words,

$$\nabla_\beta W_\lambda(\beta, \bar{\epsilon}) = -\lambda_1 \lambda_2 \Phi^{R_\star(\beta, \bar{\epsilon})}(\Delta \epsilon^\star(R_\star(\beta, \bar{\epsilon}), \beta, \bar{\epsilon})). \quad (4.23b)$$

From lemma 4.16, $\beta_1 \mapsto W_\lambda(\beta, \bar{\epsilon})$ is concave for $\beta \in B \setminus B_{\text{II}+}$. Fix $\beta_2, \beta_3 \in \mathbb{R}$ such that $B \cap (\mathbb{R} \times \{\beta_2\} \times \{\beta_3\})$ is nonempty. Then $\exists \beta_{1\star} \in \mathbb{R}$ such that

$$\{(\beta_{1\star}, \beta_2, \beta_3)^T\} = B_{\text{II}+} \cap (\mathbb{R} \times \{\beta_2\} \times \{\beta_3\}).$$

By an argument similar to that in theorem 3.5 we obtain the following lower envelope for $\widehat{W}_\lambda(\bar{\epsilon})$:

$$\begin{aligned} & \widehat{W}_\lambda(\bar{\epsilon}) \\ & \geq \max_{\beta_1 \in [0, \beta_{1\star}]} W_\lambda((\beta_1, \beta_2, \beta_3)^T, \bar{\epsilon}) \\ & = \begin{cases} W_\lambda((0, \beta_2, \beta_3)^T, \bar{\epsilon}) & \text{if } \phi_1^{R_\star((0, \beta_2, \beta_3)^T, \bar{\epsilon})}(\Delta\epsilon^\star(R_\star((0, \beta_2, \beta_3)^T, \bar{\epsilon}), (0, \beta_2, \beta_3)^T, \bar{\epsilon})) \geq 0 \\ W_\lambda((\beta_{1\text{II}}, \beta_2, \beta_3)^T, \bar{\epsilon}) & \text{otherwise} \\ W_\lambda((\beta_{1\star}, \beta_2, \beta_3)^T, \bar{\epsilon}) & \text{if } \phi_1^{R_\star((\beta_{1\star}, \beta_2, \beta_3)^T, \bar{\epsilon})}(\Delta\epsilon^\star(R_\star((\beta_{1\star}, \beta_2, \beta_3)^T, \bar{\epsilon}), (\beta_{1\star}, \beta_2, \beta_3)^T, \bar{\epsilon})) \\ & \text{exists and is less than zero} \end{cases} \end{aligned}$$

where $\beta_{1\text{II}}$ satisfies $\phi_1^{R_\star((\beta_{1\text{II}}, \beta_2, \beta_3)^T, \bar{\epsilon})}(\Delta\epsilon^\star(R_\star((\beta_{1\text{II}}, \beta_2, \beta_3)^T, \bar{\epsilon}), (\beta_{1\text{II}}, \beta_2, \beta_3)^T, \bar{\epsilon})) = 0$. Note that it is possible that $\beta_{1\text{II}} = \beta_{1\star}$.

Similarly by considering $\beta_2 \mapsto W_\lambda(\beta, \bar{\epsilon})$ and $\beta_3 \mapsto W_\lambda(\beta, \bar{\epsilon})$ we obtain two other lower bounds for $\widehat{W}_\lambda(\bar{\epsilon})$. Together they give

$$\widehat{W}_\lambda(\bar{\epsilon}) \geq \begin{cases} W_\lambda(\beta_I, \bar{\epsilon}) & \text{if } \exists \beta_I \in B \cap \partial(\mathbb{R}_+)^3 \text{ such that} \\ & \forall j = 1, 2, 3, \phi_j^{R_\star(\beta_I, \bar{\epsilon})}(\Delta\epsilon^\star(R_\star(\beta_I, \bar{\epsilon}), \beta_I, \bar{\epsilon})) \geq 0 \\ & \text{and } \exists j \in \{1, 2, 3\}, \phi_j^{R_\star(\beta_I, \bar{\epsilon})}(\Delta\epsilon^\star(R_\star(\beta_I, \bar{\epsilon}), \beta_I, \bar{\epsilon})) > 0 \quad (\text{Regime I}) \\ W_\lambda(\beta_{\text{II}}, \bar{\epsilon}) & \text{otherwise} \quad (\text{Regime II}) \\ W_\lambda(\beta_{\text{II}+}, \bar{\epsilon}) & \text{if } \exists \beta_{\text{II}+} \in B_{\text{II}+}, \exists j \in \{1, 2, 3\} \text{ such that} \\ & \phi_j^{R_\star(\beta_{\text{II}+}, \bar{\epsilon})}(\Delta\epsilon^\star(R_\star(\beta_{\text{II}+}, \bar{\epsilon}), \beta_{\text{II}+}, \bar{\epsilon})) > 0 \quad (\text{Regimes III} \\ & \text{and IV}) \\ & \text{exists and is less than 0} \end{cases} \quad (4.24)$$

where β_{II} satisfies $\Phi^{R_\star(\beta_{\text{II}}, \bar{\epsilon})}(\Delta\epsilon^\star(R_\star(\beta_{\text{II}}, \bar{\epsilon}), \beta_{\text{II}}, \bar{\epsilon})) = 0$. Further, for $j = 1, 2, 3$, if $(\beta_I)_j \neq 0$, then β_I satisfies $\phi_j^{R_\star(\beta_I, \bar{\epsilon})}(\Delta\epsilon^\star(R_\star(\beta_I, \bar{\epsilon}), \beta_I, \bar{\epsilon})) = 0$. Note that it is possible that $\beta_I, \beta_{\text{II}} \in B_{\text{II}+}$.

Remark 4.17. As in the two-dimensional case, whenever $\phi_j^{R_\star(\beta_{\text{II}+}, \bar{\epsilon})}(\Delta\epsilon^\star(R_\star(\beta_{\text{II}+}, \bar{\epsilon}), \beta_{\text{II}+}, \bar{\epsilon}))$ does not exist, regimes III and IV do not occur. From §4.3 this happens when $\ker(\alpha_1 - \beta_{\text{II}+} \cdot T^{R_\star(\beta_{\text{II}+}, \bar{\epsilon})}) \cap \ker(\alpha_2 - \beta_{\text{II}+} \cdot T^{R_\star(\beta_{\text{II}+}, \bar{\epsilon})}) \neq \{0\}$ which occurs, for example, when $\alpha_1 = \alpha_2$ or when both phases are isotopic and the shear moduli are equal. We will show below that in this case there exists a rank-I laminate that is extremal. This is consistent with the results in [Koh91, Pip91].

4.6 Extremal microstructures

In this section we prove that the lower bound presented in (4.24) is optimal. Our strategy is the same as in §3.2.

Lemma 4.18. Let $\epsilon \in M_{\text{sym}}^{3 \times 3}$. Then $\exists \hat{n} \in \mathbb{R}^3$ such that $\epsilon \parallel \hat{n} \otimes \hat{n}$ if and only if $\Phi(\epsilon) = 0$.

Proof. It is easy to verify that $\Phi(\hat{n} \otimes \hat{n}) = 0$. We need to show that $\Phi(\epsilon) = 0$ implies that ϵ is rank-I. From (4.1),

$$\begin{aligned} \phi_1(\epsilon) = 0 &\Rightarrow \exists \kappa_1 \in \mathbb{R} \text{ such that } \epsilon_{23} = \kappa_1 \epsilon_{22} \text{ and } \epsilon_{33} = \kappa_1 \epsilon_{23} = \kappa_1^2 \epsilon_{22}; \\ \phi_2(\epsilon) = 0 &\Rightarrow \exists \kappa_2 \in \mathbb{R} \text{ such that } \epsilon_{31} = \kappa_2 \epsilon_{33} = \kappa_2 \kappa_1^2 \epsilon_{22} \text{ and } \epsilon_{11} = \kappa_2 \epsilon_{31} = \kappa_2^2 \kappa_1^2 \epsilon_{22}; \\ \phi_3(\epsilon) = 0 &\Rightarrow \exists \kappa_3 \in \mathbb{R} \text{ such that } \epsilon_{12} = \kappa_3 \epsilon_{11} = \kappa_3 \kappa_2^2 \kappa_1^2 \epsilon_{22} \text{ and } \epsilon_{22} = \kappa_3 \epsilon_{12} = \kappa_3^2 \kappa_2^2 \kappa_1^2 \epsilon_{22}. \end{aligned}$$

The last equation implies that $\kappa_1^2 \kappa_2^2 \kappa_3^2 = 1$. Thus

$$\Phi(\epsilon) = 0 \Rightarrow \exists \kappa_1, \kappa_2, \kappa_3 \in \mathbb{R}, \epsilon \parallel \begin{pmatrix} \kappa_1^2 \kappa_2^2 & \kappa_1^2 \kappa_2^2 \kappa_3 & \kappa_1^2 \kappa_2 \\ \kappa_1^2 \kappa_2^2 \kappa_3 & 1 & \kappa_1 \\ \kappa_1^2 \kappa_2 & \kappa_1 & \kappa_1^2 \end{pmatrix} =: K$$

Let η_1, η_2, η_3 be the eigenvalues of K . An easy calculation shows that

$$\begin{aligned} \eta_1 \eta_2 \eta_3 &= \det(K) = 0, \\ \eta_1 \eta_2 + \eta_2 \eta_3 + \eta_3 \eta_1 &= (\text{Tr}(K))^2 - \text{Tr}(K^2) = 0. \end{aligned}$$

Thus two of the three eigenvalues of K are zero. This implies that K , and thus ϵ , is rank-I. \square

4.6.1 Regime I - rank-I laminates

We show that the lower bound $\widehat{W}_\lambda(\bar{\epsilon}) \geq W_\lambda(\beta_1, \bar{\epsilon})$ is optimal:

Lemma 4.19 (Extremal microstructures in Regime I). In regime I there exist a pair of extremal rank-I laminates. A rank-I laminate in three dimensions is shown in Figure 4.5.

Proof. From (4.24), $\forall j = 1, 2, 3$, $\phi_j^{R^*}(\Delta \epsilon^*) \geq 0$. From (4.22),

$$\begin{aligned} v_2(\Delta \epsilon^*) v_3(\Delta \epsilon^*) &\leq 0, \\ v_3(\Delta \epsilon^*) v_1(\Delta \epsilon^*) &\leq 0, \\ v_1(\Delta \epsilon^*) v_2(\Delta \epsilon^*) &\leq 0. \end{aligned}$$

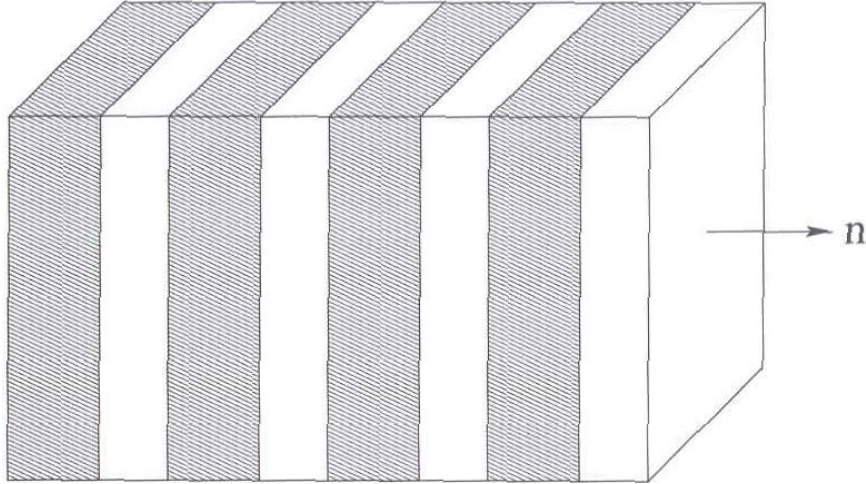


Figure 4.5: A two-phase rank-I laminate in three dimensions. n is the lamination direction. The strains are constant in the shaded and unshaded regions. Figure taken from [Mil01, Fig.9.1, pg.160].

This implies that one of the v s is non-negative, another is zero and the third is non-positive: from lemma 3.7 the strains ϵ_1^* and ϵ_2^* are compatible: $\exists \hat{m}, \hat{n} \in \mathbb{R}^3, \epsilon_2^* - \epsilon_1^* \parallel \hat{m} \otimes_s \hat{n}$. A calculation using (4.15) shows that $\Delta \sigma^* \hat{m} = \Delta \sigma^* \hat{n} = 0$: the stress jump condition is satisfied across any interface between regions with strain ϵ_1^* and ϵ_2^* . It follows that there exist precisely two rank-I laminates⁴ (that differ only in lamination direction) in which the strain of phase i is ϵ_i^* . \square

These rank-I laminates show that $\widehat{W}_\lambda(\bar{\epsilon}) = W_\lambda(\beta_i, \bar{\epsilon})$ in regime I:

$$\widehat{W}_\lambda(\bar{\epsilon}) = \lambda_1 W_1(\epsilon_1^*) + \lambda_2 W_2(\epsilon_2^*) - \lambda_1 \lambda_2 \beta_i \cdot \Phi^{R_\star(\beta_i, \bar{\epsilon})}(\Delta \epsilon^*).$$

From the strict convexity of $W_1 - \beta_1 \cdot \Phi$ and $W_2 - \beta_1 \cdot \Phi$ it follows that ϵ_i^* is the unique constant strain in phase i . However it does not follow that rank-I laminates are unique extremal microstructures: for example, as is easy to see, an extremal rank-II laminate can be formed by laminating the two extremal rank-I laminates.

4.6.2 Regime II - rank-I laminates

We need the following analogue of lemma 3.9.

Lemma 4.20. Let $\beta_j \neq 0$ for $j = 1, 2, 3$. Let $\Delta \epsilon, \Delta \sigma \in M_{\text{sym}}^{3 \times 3}$ be such that $\Delta \sigma \parallel (\beta \cdot T^R) \Delta \epsilon$. Then the following are equivalent

1. $\exists \hat{m}, \hat{n} \in \mathbb{R}^3$ such that $\Delta \epsilon \parallel \hat{m} \otimes_s \hat{n}$ and either $\Delta \sigma \hat{m} = 0$ or $\Delta \sigma \hat{n} = 0$.

⁴ Precisely two because not all $\phi_j^{R_\star}(\Delta \epsilon^*)$ are zero and thus two v s are non zero

2. $\exists \hat{n} \in \mathbb{R}^3$ such that $\Delta\epsilon \parallel \hat{n} \otimes \hat{n}$ and $\Delta\sigma\hat{n} = 0$.
3. $\Phi(\Delta\epsilon) = 0$.

Proof. We begin with some preliminary calculations:

$$T_1(\hat{m} \otimes_s \hat{n}) = \begin{pmatrix} 0 & 0 & 0 \\ 0 & -2m_3n_3 & m_3n_2+m_2n_3 \\ 0 & m_3n_2+m_2n_3 & -2m_2n_2 \end{pmatrix} \text{ and } (T_1(\hat{m} \otimes_s \hat{n}))\hat{n} = (\hat{m} \times \hat{n})_1 \begin{pmatrix} 0 \\ n_3 \\ -n_2 \end{pmatrix}$$

$$T_2(\hat{m} \otimes_s \hat{n}) = \begin{pmatrix} -2n_3m_3 & 0 & m_3n_1+m_1n_3 \\ 0 & 0 & 0 \\ m_3n_1+m_1n_3 & 0 & -2m_1n_1 \end{pmatrix} \text{ and } (T_2(\hat{m} \otimes_s \hat{n}))\hat{n} = (\hat{m} \times \hat{n})_2 \begin{pmatrix} -n_3 \\ 0 \\ n_1 \end{pmatrix}$$

$$T_3(\hat{m} \otimes_s \hat{n}) = \begin{pmatrix} -2m_2n_2 & m_2n_1+m_1n_2 & 0 \\ m_2n_1+m_1n_2 & -2m_1n_1 & 0 \\ 0 & 0 & 0 \end{pmatrix} \text{ and } (T_3(\hat{m} \otimes_s \hat{n}))\hat{n} = (\hat{m} \times \hat{n})_3 \begin{pmatrix} n_2 \\ -n_1 \\ 0 \end{pmatrix}$$

These give

$$((\beta \cdot T)(\hat{m} \otimes_s \hat{n}))\hat{n} = \begin{pmatrix} \beta_3(\hat{m} \times \hat{n})_3n_2 - \beta_2(\hat{m} \times \hat{n})_2n_3 \\ \beta_1(\hat{m} \times \hat{n})_1n_3 - \beta_3(\hat{m} \times \hat{n})_3n_1 \\ \beta_2(\hat{m} \times \hat{n})_2n_1 - \beta_1(\hat{m} \times \hat{n})_1n_2 \end{pmatrix} = \hat{n} \times \begin{pmatrix} \beta_1 & 0 & 0 \\ 0 & \beta_2 & 0 \\ 0 & 0 & \beta_3 \end{pmatrix} (\hat{m} \times \hat{n}).$$

Thus

$$\begin{aligned} ((\beta \cdot T)(\hat{m} \otimes_s \hat{n}))\hat{n} = 0 &\Rightarrow \begin{pmatrix} \beta_1 & 0 & 0 \\ 0 & \beta_2 & 0 \\ 0 & 0 & \beta_3 \end{pmatrix} (\hat{m} \times \hat{n}) \parallel \hat{n} \\ &\Rightarrow \begin{pmatrix} \beta_1 & 0 & 0 \\ 0 & \beta_2 & 0 \\ 0 & 0 & \beta_3 \end{pmatrix} (\hat{m} \times \hat{n}) \cdot (\hat{m} \times \hat{n}) = 0 \\ &\Rightarrow \hat{m} \times \hat{n} = 0 \\ &\Rightarrow \hat{m} \parallel \hat{n}. \end{aligned}$$

By a similar calculation the same conclusion follows from $((\beta \cdot T)(\hat{m} \otimes_s \hat{n}))\hat{m} = 0$. We are now ready to prove the lemma:

(1) \Rightarrow (3): $\Delta\sigma \parallel (\beta \cdot T^R)\Delta\epsilon \parallel (\beta \cdot T^R)(\hat{m} \otimes_s \hat{n})$. Thus from the calculation above $\Delta\sigma\hat{m} = 0$ or $\Delta\sigma\hat{n} = 0 \Rightarrow \hat{m} \parallel \hat{n} \Rightarrow \phi(\Delta\epsilon) = 0$.

(3) \Rightarrow (2): Assume $\Phi(\Delta\epsilon) = 0$; that is, $\exists \hat{n} \in \mathbb{R}^3$, $\Delta\epsilon \parallel \hat{n} \otimes \hat{n}$. From the calculation above, $\forall \hat{m} \in \mathbb{R}^3$, $(T_j\hat{m} \otimes \hat{m})\hat{m} = 0$. Thus, $\Delta\sigma\hat{n} \parallel ((\beta \cdot T^R)\Delta\epsilon)\hat{n} \parallel R((\beta \cdot T)R^T(\hat{n} \otimes \hat{n})R)R^T\hat{n} = R(\beta \cdot T)(R^T\hat{n} \otimes R^T\hat{n})(R^T\hat{n}) = 0$. \square

We are now ready to show that $\widehat{W}_\lambda(\bar{\epsilon}) \geq W_\lambda(\beta_{II}, \bar{\epsilon})$ is optimal:

Lemma 4.21 (Extremal microstructures in Regime II). In regime II there exists a rank-I laminate that is extremal.

Proof. From (4.24), $\Phi^{R_\star}(\Delta\epsilon^\star) = 0$ and from (4.15) $\Delta\sigma^\star = (\beta_{\text{II}} \cdot T^{R_\star})\Delta\epsilon^\star$. Thus from lemma 4.20, $\exists \hat{n} \ni \Delta\epsilon^\star \parallel \hat{n} \otimes \hat{n}$ and $\Delta\sigma^\star \hat{n} = 0$. It follows that there exists a rank-I laminate in which the strain of phase i is ϵ_i^\star . This shows that in regime II,

$$\widehat{W}_\lambda(\bar{\epsilon}) = W_\lambda(\beta_{\text{II}}, \bar{\epsilon}) = \lambda W_1(\epsilon_1^\star) + (1 - \lambda)W_2(\epsilon_2^\star).$$

□

4.6.3 Regimes III and IV - rank-II and rank-III laminates

In regimes III and IV, since $\phi_j^{R_\star}(\Delta\epsilon^\star) < 0$ for some $j \in \{1, 2, 3\}$, from (4.22) atleast two eigenvalues are non-zero and have the same sign. Thus, from lemma 3.7, the phases cannot form a rank-I laminate. We show the existence of extremal rank-II and rank-III laminates.

From (4.24), in this regime $\beta_{\text{II}+}$ (the optimal value of β) is contained in $B_{\text{II}+}$. In fact this statement can be greatly strengthened:

Lemma 4.22. $\beta_{\text{II}+} \in B_{\text{III}} \cup B_{\text{IV}}$.

Proof. Using (4.23) and (4.22),

$$\nabla_\beta W_\lambda(\beta, \bar{\epsilon}) = -\lambda_1 \lambda_2 \begin{pmatrix} \phi_1^{R_\star(\beta, \bar{\epsilon})}(\Delta\epsilon^\star(R_\star(\beta, \bar{\epsilon}), \beta, \bar{\epsilon})) \\ \phi_1^{R_\star(\beta, \bar{\epsilon})}(\Delta\epsilon^\star(R_\star(\beta, \bar{\epsilon}), \beta, \bar{\epsilon})) \\ \phi_1^{R_\star(\beta, \bar{\epsilon})}(\Delta\epsilon^\star(R_\star(\beta, \bar{\epsilon}), \beta, \bar{\epsilon})) \end{pmatrix} = \lambda_1 \lambda_2 \begin{pmatrix} v_{\sigma(2)}(\Delta\epsilon^\star) & v_{\sigma(3)}(\Delta\epsilon^\star) \\ v_{\sigma(3)}(\Delta\epsilon^\star) & v_{\sigma(1)}(\Delta\epsilon^\star) \\ v_{\sigma(1)}(\Delta\epsilon^\star) & v_{\sigma(2)}(\Delta\epsilon^\star) \end{pmatrix}.$$

Since $B \ni \beta \mapsto W_\lambda(\beta, \bar{\epsilon})$ attains its maximum at $\beta_{\text{II}} \in B_{\text{II}+}$, $\nabla_\beta W_\lambda(\beta, \bar{\epsilon})$ must point along the outward normal to $B_{\text{II}+}$ at β_{II} . If $\beta_{\text{II}} \in B_{\text{III}} \setminus (B_{\text{III}} \cup B_{\text{IV}})$, then from lemma 4.7,

$$\text{sign} \left(\begin{pmatrix} v_{\sigma(2)}(\Delta\epsilon^\star) & v_{\sigma(3)}(\Delta\epsilon^\star) \\ v_{\sigma(3)}(\Delta\epsilon^\star) & v_{\sigma(1)}(\Delta\epsilon^\star) \\ v_{\sigma(1)}(\Delta\epsilon^\star) & v_{\sigma(2)}(\Delta\epsilon^\star) \end{pmatrix} \right) \in \left\{ \begin{pmatrix} - \\ + \\ + \end{pmatrix}, \begin{pmatrix} + \\ - \\ + \end{pmatrix}, \begin{pmatrix} + \\ + \\ - \end{pmatrix} \right\}.$$

But of the pairwise products of three numbers it is impossible for precisely one to be negative and precisely two to be positive. □

We shall consider the case $\beta_{\text{II}+} \in B_{\text{III}}$ (regime III) and the case $\beta_{\text{II}+} \in B_{\text{IV}}$ (regime IV) separately.

4.6.3.1 Regime III - rank-II laminates

By the same argument as in the proof of lemma 4.22,

$$\beta_{\text{II}+} \in B_{\text{III}}^{(1)} \Rightarrow \text{sign} \left(\begin{pmatrix} v_{\sigma(2)}(\Delta\epsilon^*) & v_{\sigma(3)}(\Delta\epsilon^*) \\ v_{\sigma(3)}(\Delta\epsilon^*) & v_{\sigma(1)}(\Delta\epsilon^*) \\ v_{\sigma(1)}(\Delta\epsilon^*) & v_{\sigma(2)}(\Delta\epsilon^*) \end{pmatrix} \right) = \begin{pmatrix} + \\ 0 \\ 0 \end{pmatrix}; \quad (4.25a)$$

$$\beta_{\text{II}+} \in B_{\text{III}}^{(2)} \Rightarrow \text{sign} \left(\begin{pmatrix} v_{\sigma(2)}(\Delta\epsilon^*) & v_{\sigma(3)}(\Delta\epsilon^*) \\ v_{\sigma(3)}(\Delta\epsilon^*) & v_{\sigma(1)}(\Delta\epsilon^*) \\ v_{\sigma(1)}(\Delta\epsilon^*) & v_{\sigma(2)}(\Delta\epsilon^*) \end{pmatrix} \right) = \begin{pmatrix} 0 \\ + \\ 0 \end{pmatrix}; \quad (4.25b)$$

$$\beta_{\text{II}+} \in B_{\text{III}}^{(3)} \Rightarrow \text{sign} \left(\begin{pmatrix} v_{\sigma(2)}(\Delta\epsilon^*) & v_{\sigma(3)}(\Delta\epsilon^*) \\ v_{\sigma(3)}(\Delta\epsilon^*) & v_{\sigma(1)}(\Delta\epsilon^*) \\ v_{\sigma(1)}(\Delta\epsilon^*) & v_{\sigma(2)}(\Delta\epsilon^*) \end{pmatrix} \right) = \begin{pmatrix} 0 \\ 0 \\ + \end{pmatrix}. \quad (4.25c)$$

When $\beta_{\text{II}+} \in B_{\text{III}}$, three cases arise: (i) $\beta_{\text{II}+} \in B_{\text{III}}^{(1)}$, (ii) $\beta_{\text{II}+} \in B_{\text{III}}^{(2)}$ and (iii) $\beta_{\text{II}+} \in B_{\text{III}}^{(3)}$. When $\beta_{\text{II}+} \in B_{\text{III}}^{(1)}$, from (4.25),

$$\text{sign} \left(\begin{pmatrix} v_{\sigma(2)}(\Delta\epsilon^*) & v_{\sigma(3)}(\Delta\epsilon^*) \\ v_{\sigma(3)}(\Delta\epsilon^*) & v_{\sigma(1)}(\Delta\epsilon^*) \\ v_{\sigma(1)}(\Delta\epsilon^*) & v_{\sigma(2)}(\Delta\epsilon^*) \end{pmatrix} \right) = \begin{pmatrix} + \\ 0 \\ 0 \end{pmatrix}.$$

This implies that $\text{sign}(v_{\sigma(2)}(\Delta\epsilon^*)) = \text{sign}(v_{\sigma(3)}(\Delta\epsilon^*))$ and $v_{\sigma(1)}(\Delta\epsilon^*) = 0$. Since, by theorem 4.10, $R_{\star}^T \Delta\epsilon^* R_{\star}$ is diagonal:

$$R_{\star}^T \Delta\epsilon^* R_{\star} = \begin{pmatrix} 0 & 0 & 0 \\ 0 & v_{\sigma(2)}(\Delta\epsilon^*) & 0 \\ 0 & 0 & v_{\sigma(3)}(\Delta\epsilon^*) \end{pmatrix};$$

$$\Delta\epsilon^* = R_{\star} \begin{pmatrix} 0 & 0 & 0 \\ 0 & v_{\sigma(2)}(\Delta\epsilon^*) & 0 \\ 0 & 0 & v_{\sigma(3)}(\Delta\epsilon^*) \end{pmatrix} R_{\star}^T$$

and $v_{\sigma(2)}$ and $v_{\sigma(3)}$ have the same sign. Likewise, when $\beta_{\text{II}+} \in B_{\text{III}}^{(2)}$,

$$\Delta\epsilon^* = R_{\star} \begin{pmatrix} v_{\sigma(1)}(\Delta\epsilon^*) & 0 & 0 \\ 0 & 0 & 0 \\ 0 & 0 & v_{\sigma(3)}(\Delta\epsilon^*) \end{pmatrix} R_{\star}^T,$$

$v_{\sigma(1)}$ and $v_{\sigma(3)}$ have the same sign; and when $\beta_{\text{II}+} \in B_{\text{III}}^{(3)}$,

$$\Delta\epsilon^* = R_{\star} \begin{pmatrix} v_{\sigma(1)}(\Delta\epsilon^*) & 0 & 0 \\ 0 & v_{\sigma(2)}(\Delta\epsilon^*) & 0 \\ 0 & 0 & 0 \end{pmatrix} R_{\star}^T,$$

$v_{\sigma(1)}$ and $v_{\sigma(2)}$ have the same sign.

From remark 4.2 and lemma 4.3, $\alpha_i - \beta \cdot T^R$ and $\alpha_i - \beta \cdot T$ are not invertible on B_{i,III^+} . The kernels of these operators are related as follows:

Lemma 4.23. $\epsilon \in \ker(\alpha - \beta \cdot T) \Leftrightarrow R\epsilon R^T \in \ker(\alpha - \beta \cdot T^R)$.

Proof. Using (4.3) and isotropy of α ,

$$\begin{aligned}
\epsilon \in \ker(\alpha - \beta \cdot T) &\Leftrightarrow \alpha\epsilon - \beta \cdot T\epsilon = 0 \\
&\Leftrightarrow \alpha\epsilon - R^T(\beta \cdot T^R(R\epsilon R^T))R = 0 \\
&\Leftrightarrow R^T(\alpha(R\epsilon R^T))R - R^T(\beta \cdot T^R(R\epsilon R^T))R = 0 \\
&\Leftrightarrow \alpha(R\epsilon R^T) - (\beta \cdot T^R(R\epsilon R^T)) = 0 \\
&\Leftrightarrow \ker(\alpha - \beta \cdot T^R) \ni 0.
\end{aligned}$$

□

From remark 4.5, $\dim(\ker(\alpha_i - \beta \cdot T)) = 2$ on $B_{i,III}$. These kernels are easy to characterize:

Lemma 4.24.

1. On $B_{i,III}^{(1)}$, $\ker(\alpha_i - \beta \cdot T) = \text{Span} \left\{ \begin{pmatrix} 0 & 0 & 0 \\ 0 & 1 & 0 \\ 0 & 0 & -1 \end{pmatrix}, \begin{pmatrix} 0 & 0 & 0 \\ 0 & 0 & 1 \\ 0 & 1 & 0 \end{pmatrix} \right\}$.
2. On $B_{i,III}^{(2)}$, $\ker(\alpha_i - \beta \cdot T) = \text{Span} \left\{ \begin{pmatrix} 1 & 0 & 0 \\ 0 & 0 & 0 \\ 0 & 0 & -1 \end{pmatrix}, \begin{pmatrix} 0 & 0 & 1 \\ 0 & 0 & 0 \\ 1 & 0 & 0 \end{pmatrix} \right\}$.
3. On $B_{i,III}^{(3)}$, $\ker(\alpha_i - \beta \cdot T) = \text{Span} \left\{ \begin{pmatrix} 1 & 0 & 0 \\ 0 & -1 & 0 \\ 0 & 0 & 0 \end{pmatrix}, \begin{pmatrix} 0 & 1 & 0 \\ 1 & 0 & 0 \\ 0 & 0 & 0 \end{pmatrix} \right\}$.

Proof. We prove the first statement; the other two follow similarly. When $\beta \in B_{i,III}^{(1)}$, $\beta_1 = 2\mu_i$ and $\beta_2 = \beta_3 \in [0, 2\mu_i]$. Thus

$$\begin{aligned}
(\alpha_i - \beta \cdot T)\epsilon &= \alpha_i\epsilon - (2\mu_i T_1 + \beta_2 T_2 + \beta_2 T_3)\epsilon \\
&= \kappa_i(\epsilon_{11} + \epsilon_{22} + \epsilon_{33}) + 2\mu_i \left\| \begin{pmatrix} \epsilon_{11} - \frac{\epsilon_{11} + \epsilon_{22} + \epsilon_{33}}{3} & \epsilon_{12} & \epsilon_{31} \\ \epsilon_{12} & \epsilon_{22} - \frac{\epsilon_{11} + \epsilon_{22} + \epsilon_{33}}{3} & \epsilon_{23} \\ \epsilon_{31} & \epsilon_{23} & \epsilon_{33} - \frac{\epsilon_{11} + \epsilon_{22} + \epsilon_{33}}{3} \end{pmatrix} \right\| \\
&\quad - 2\mu_i \begin{pmatrix} 0 & 0 & 0 \\ 0 & -\epsilon_{33} & \epsilon_{23} \\ 0 & \epsilon_{23} & -\epsilon_{22} \end{pmatrix} - \beta_2 \begin{pmatrix} -\epsilon_{33} & 0 & \epsilon_{31} \\ 0 & 0 & 0 \\ \epsilon_{31} & 0 & -\epsilon_{11} \end{pmatrix} - \beta_2 \begin{pmatrix} -\epsilon_{22} & \epsilon_{12} & 0 \\ \epsilon_{12} & -\epsilon_{11} & 0 \\ 0 & 0 & 0 \end{pmatrix} \\
&= \begin{pmatrix} (\kappa_i - \frac{2}{3}\mu_i)(\epsilon_{11} + \epsilon_{22} + \epsilon_{33}) + 2\mu_i\epsilon_{11} + \beta_2\epsilon_{22} + \beta_2\epsilon_{33} & (2\mu_i - \beta_2)\epsilon_{12} & (2\mu_i - \beta_2)\epsilon_{31} \\ (2\mu_i - \beta_2)\epsilon_{12} & (\kappa_i - \frac{2}{3}\mu_i)(\epsilon_{11} + \epsilon_{22} + \epsilon_{33}) + \beta_2\epsilon_{11} + 2\mu_i\epsilon_{22} + 2\mu_i\epsilon_{33} & 0 \\ (2\mu_i - \beta_2)\epsilon_{31} & 0 & (\kappa_i - \frac{2}{3}\mu_i)(\epsilon_{11} + \epsilon_{22} + \epsilon_{33}) + \beta_2\epsilon_{11} + 2\mu_i\epsilon_{22} + 2\mu_i\epsilon_{33} \end{pmatrix}
\end{aligned}$$

Thus $(\alpha_i - \beta \cdot T)\epsilon = 0$ if and only if

$$\epsilon_{12} = 0$$

$$\epsilon_{31} = 0$$

and

$$\left(\kappa_i - \frac{2}{3}\mu_i\right)(\epsilon_{11} + \epsilon_{22} + \epsilon_{33}) + 2\mu_i\epsilon_{11} + \beta_2\epsilon_{22} + \beta_2\epsilon_{33} = 0$$

$$\left(\kappa_i - \frac{2}{3}\mu_i\right)(\epsilon_{11} + \epsilon_{22} + \epsilon_{33}) + \beta_2\epsilon_{11} + 2\mu_i\epsilon_{22} + 2\mu_i\epsilon_{33} = 0$$

Since $\beta_2 \neq 2\mu_i$ these four equations are independent: $\dim(\ker(\alpha_i - \beta \cdot T)) = 2$. Indeed, from (4.2),

$$\alpha_i \begin{pmatrix} 0 & 0 & 0 \\ 0 & 1 & 0 \\ 0 & 0 & -1 \end{pmatrix} = 2\mu_i \begin{pmatrix} 0 & 0 & 0 \\ 0 & 1 & 0 \\ 0 & 0 & -1 \end{pmatrix},$$

$$T_1 \begin{pmatrix} 0 & 0 & 0 \\ 0 & 1 & 0 \\ 0 & 0 & -1 \end{pmatrix} = \begin{pmatrix} 0 & 0 & 0 \\ 0 & 1 & 0 \\ 0 & 0 & -1 \end{pmatrix},$$

$$T_2 \begin{pmatrix} 0 & 0 & 0 \\ 0 & 1 & 0 \\ 0 & 0 & -1 \end{pmatrix} = \begin{pmatrix} 1 & 0 & 0 \\ 0 & 0 & 0 \\ 0 & 0 & 0 \end{pmatrix},$$

$$T_3 \begin{pmatrix} 0 & 0 & 0 \\ 0 & 1 & 0 \\ 0 & 0 & -1 \end{pmatrix} = \begin{pmatrix} -1 & 0 & 0 \\ 0 & 1 & 0 \\ 0 & 0 & 0 \end{pmatrix}$$

and hence

$$\begin{pmatrix} 0 & 0 & 0 \\ 0 & 1 & 0 \\ 0 & 0 & -1 \end{pmatrix} \in \ker(\alpha_i - \beta \cdot T).$$

Likewise,

$$\alpha_i \begin{pmatrix} 0 & 0 & 0 \\ 0 & 0 & 1 \\ 0 & 1 & 0 \end{pmatrix} = 2\mu_i \begin{pmatrix} 0 & 0 & 0 \\ 0 & 0 & 1 \\ 0 & 1 & 0 \end{pmatrix},$$

$$T_1 \begin{pmatrix} 0 & 0 & 0 \\ 0 & 0 & 1 \\ 0 & 1 & 0 \end{pmatrix} = \begin{pmatrix} 0 & 0 & 0 \\ 0 & 0 & 1 \\ 0 & 1 & 0 \end{pmatrix},$$

$$T_2 \begin{pmatrix} 0 & 0 & 0 \\ 0 & 0 & 1 \\ 0 & 1 & 0 \end{pmatrix} = \begin{pmatrix} 0 & 0 & 0 \\ 0 & 0 & 0 \\ 0 & 0 & 0 \end{pmatrix},$$

$$T_3 \begin{pmatrix} 0 & 0 & 0 \\ 0 & 0 & 1 \\ 0 & 1 & 0 \end{pmatrix} = \begin{pmatrix} 0 & 0 & 0 \\ 0 & 0 & 0 \\ 0 & 0 & 0 \end{pmatrix}$$

and hence

$$\begin{pmatrix} 0 & 0 & 0 \\ 0 & 0 & 1 \\ 0 & 1 & 0 \end{pmatrix} \in \ker(\alpha_i - \beta \cdot T).$$

□

Summarizing these results we have

1. When $\beta_{\text{II}+} \in B_{i,\text{III}}^{(1)}$:

$$\Delta\epsilon^* = R_\star \begin{pmatrix} 0 & 0 & 0 \\ 0 & v_{\sigma(2)}(\Delta\epsilon^*) & 0 \\ 0 & 0 & v_{\sigma(3)}(\Delta\epsilon^*) \end{pmatrix} R_\star^T,$$

$$\ker(\alpha_i - \beta_{\beta_{\text{II}+}} \cdot T^{R_\star}) = \text{Span} \left\{ R_\star \begin{pmatrix} 0 & 0 & 0 \\ 0 & 1 & 0 \\ 0 & 0 & -1 \end{pmatrix} R_\star^T, R_\star \begin{pmatrix} 0 & 0 & 0 \\ 0 & 0 & 1 \\ 0 & 1 & 0 \end{pmatrix} R_\star^T \right\}.$$

2. When $\beta_{\text{II}+} \in B_{i,\text{III}}^{(2)}$:

$$\Delta\epsilon^* = R_\star \begin{pmatrix} v_{\sigma(1)}(\Delta\epsilon^*) & 0 & 0 \\ 0 & 0 & 0 \\ 0 & 0 & v_{\sigma(3)}(\Delta\epsilon^*) \end{pmatrix} R_\star^T,$$

$$\ker(\alpha_i - \beta_{\beta_{\text{II}+}} \cdot T^{R_\star}) = \text{Span} \left\{ R_\star \begin{pmatrix} 1 & 0 & 0 \\ 0 & 0 & 0 \\ 0 & 0 & -1 \end{pmatrix} R_\star^T, R_\star \begin{pmatrix} 0 & 0 & 1 \\ 0 & 0 & 0 \\ 1 & 0 & 0 \end{pmatrix} R_\star^T \right\}.$$

3. When $\beta_{\text{II}+} \in B_{i,\text{III}}^{(3)}$:

$$\Delta\epsilon^* = R_\star \begin{pmatrix} v_{\sigma(1)}(\Delta\epsilon^*) & 0 & 0 \\ 0 & v_{\sigma(2)}(\Delta\epsilon^*) & 0 \\ 0 & 0 & 0 \end{pmatrix} R_\star^T,$$

$$\ker(\alpha_i - \beta_{\beta_{\text{II}+}} \cdot T^{R_\star}) = \text{Span} \left\{ R_\star \begin{pmatrix} 1 & 0 & 0 \\ 0 & -1 & 0 \\ 0 & 0 & 0 \end{pmatrix} R_\star^T, R_\star \begin{pmatrix} 0 & 1 & 0 \\ 1 & 0 & 0 \\ 0 & 0 & 0 \end{pmatrix} R_\star^T \right\}.$$

Note that these expressions show that the problem of constructing an extremal microstructure in this regime is essentially a two-dimensional problem. Comparing these expressions with the results in §3.2.4 we conclude that there exist uncountably many extremal rank-II laminates. These rank-II laminates show that $\widehat{W}_\lambda(\bar{\epsilon}) = W_\lambda(\beta_{\text{II}+}, \bar{\epsilon})$ in regime II:

$$\widehat{W}_\lambda(\bar{\epsilon}) = \lambda_1 W_1(\epsilon_1^*) + \lambda_2 W_2(\epsilon_2^*) - \lambda_1 \lambda_2 \beta_{\text{II}+} \cdot \Phi^{R_\star(\beta_{\text{II}+}, \bar{\epsilon})}(\Delta\epsilon^*).$$

4.6.3.2 Regime IV - rank-III laminates

In regime IV,

$$\Delta\epsilon^* = R_\star \begin{pmatrix} v_{\sigma(1)}(\Delta\epsilon^*) & 0 & 0 \\ 0 & v_{\sigma(2)}(\Delta\epsilon^*) & 0 \\ 0 & 0 & v_{\sigma(3)}(\Delta\epsilon^*) \end{pmatrix} R_\star^T,$$

and $\text{sign}(v_{\sigma(1)}(\Delta\epsilon^*)) = \text{sign}(v_{\sigma(2)}(\Delta\epsilon^*)) = \text{sign}(v_{\sigma(3)}(\Delta\epsilon^*))$.

From remark 4.5, on B_{IV} , $\dim(\ker(\alpha_i - \beta \cdot T)) = 5$. Again, these kernels are easy to characterize:

Lemma 4.25. When $\beta_{II+} \in B_{i,IV}$,

$$\begin{aligned} \ker(\alpha_i - \beta \cdot T) &= \text{Span} \left\{ \begin{pmatrix} 1 & 0 & 0 \\ 0 & -1 & 0 \\ 0 & 0 & 0 \end{pmatrix}, \begin{pmatrix} 0 & 0 & 0 \\ 0 & 1 & 0 \\ 0 & 0 & -1 \end{pmatrix}, \begin{pmatrix} -1 & 0 & 0 \\ 0 & 0 & 0 \\ 0 & 0 & 1 \end{pmatrix}, \begin{pmatrix} 0 & 1 & 0 \\ 1 & 0 & 0 \\ 0 & 0 & 0 \end{pmatrix}, \begin{pmatrix} 0 & 0 & 0 \\ 0 & 0 & 1 \\ 0 & 1 & 0 \end{pmatrix}, \begin{pmatrix} 0 & 0 & 1 \\ 0 & 0 & 0 \\ 1 & 0 & 0 \end{pmatrix} \right\}; \\ \ker(\alpha_i - \beta \cdot T^{R_\star}) &= \text{Span} \left\{ R_\star \begin{pmatrix} 1 & 0 & 0 \\ 0 & -1 & 0 \\ 0 & 0 & 0 \end{pmatrix} R_\star^T, R_\star \begin{pmatrix} 0 & 0 & 0 \\ 0 & 1 & 0 \\ 0 & 0 & -1 \end{pmatrix} R_\star^T, R_\star \begin{pmatrix} -1 & 0 & 0 \\ 0 & 0 & 0 \\ 0 & 0 & 1 \end{pmatrix} R_\star^T, \right. \\ &\quad \left. R_\star \begin{pmatrix} 0 & 1 & 0 \\ 1 & 0 & 0 \\ 0 & 0 & 0 \end{pmatrix} R_\star^T, R_\star \begin{pmatrix} 0 & 0 & 0 \\ 0 & 0 & 1 \\ 0 & 1 & 0 \end{pmatrix} R_\star^T, R_\star \begin{pmatrix} 0 & 0 & 1 \\ 0 & 0 & 0 \\ 1 & 0 & 0 \end{pmatrix} R_\star^T \right\}. \end{aligned}$$

Proof. When $\beta \in B_{i,IV}$, $\beta_1 = \beta_2 = \beta_3 = 2\mu_i$. Thus

$$\begin{aligned} (\alpha_i - \beta \cdot T)\epsilon &= \alpha_i\epsilon - 2\mu_i(T_1 + T_2 + T_3)\epsilon \\ &= \kappa_i(\epsilon_{11} + \epsilon_{22} + \epsilon_{33}) + 2\mu_i \left\| \begin{pmatrix} \epsilon_{11} - \frac{\epsilon_{11} + \epsilon_{22} + \epsilon_{33}}{3} & \epsilon_{12} & \epsilon_{31} \\ \epsilon_{12} & \epsilon_{22} - \frac{\epsilon_{11} + \epsilon_{22} + \epsilon_{33}}{3} & \epsilon_{23} \\ \epsilon_{31} & \epsilon_{23} & \epsilon_{33} - \frac{\epsilon_{11} + \epsilon_{22} + \epsilon_{33}}{3} \end{pmatrix} \right\| \\ &\quad - 2\mu_i \begin{pmatrix} 0 & 0 & 0 \\ 0 & -\epsilon_{33} & \epsilon_{23} \\ 0 & \epsilon_{23} & -\epsilon_{22} \end{pmatrix} - 2\mu_i \begin{pmatrix} -\epsilon_{33} & 0 & \epsilon_{31} \\ 0 & 0 & 0 \\ \epsilon_{31} & 0 & -\epsilon_{11} \end{pmatrix} - 2\mu_i \begin{pmatrix} -\epsilon_{22} & \epsilon_{12} & 0 \\ \epsilon_{12} & -\epsilon_{11} & 0 \\ 0 & 0 & 0 \end{pmatrix} \\ &= \begin{pmatrix} (\kappa_i + \frac{4}{3}\mu_i)(\epsilon_{11} + \epsilon_{22} + \epsilon_{33}) & 0 & 0 \\ 0 & (\kappa_i + \frac{4}{3}\mu_i)(\epsilon_{11} + \epsilon_{22} + \epsilon_{33}) & 0 \\ 0 & 0 & (\kappa_i + \frac{4}{3}\mu_i)(\epsilon_{11} + \epsilon_{22} + \epsilon_{33}) \end{pmatrix} \end{aligned}$$

Thus $(\alpha_i - \beta \cdot T)\epsilon = 0$ precisely when $\text{Tr}(\epsilon) = 0$. The result follows. \square

We outline the construction of an extremal rank-III laminate. It is easy to see that a linear combination of any two strains from the set

$$\left\{ R_\star \begin{pmatrix} 1 & 0 & 0 \\ 0 & -1 & 0 \\ 0 & 0 & 0 \end{pmatrix} R_\star^T, R_\star \begin{pmatrix} 0 & 0 & 0 \\ 0 & 1 & 0 \\ 0 & 0 & -1 \end{pmatrix} R_\star^T, R_\star \begin{pmatrix} -1 & 0 & 0 \\ 0 & 0 & 0 \\ 0 & 0 & 1 \end{pmatrix} R_\star^T \right\}$$

is rank-I connected to

$$\Delta\epsilon^* = R_\star \begin{pmatrix} v_{\sigma(1)}(\Delta\epsilon^*) & 0 & 0 \\ 0 & v_{\sigma(2)}(\Delta\epsilon^*) & 0 \\ 0 & 0 & v_{\sigma(3)}(\Delta\epsilon^*) \end{pmatrix} R_\star^T.$$

Indeed the lamination direction can be chosen to be along the rotated coordinate directions. A laminate of rank-III would suffice to enforce in addition the restrictions on volume fraction. These rank-III laminates show that $\widehat{W}_\lambda(\bar{\epsilon}) = W_\lambda(\beta_{II+}, \bar{\epsilon})$ in regime IV:

$$\widehat{W}_\lambda(\bar{\epsilon}) = \lambda_1 W_1(\epsilon_1^*) + \lambda_2 W_2(\epsilon_2^*) - \lambda_1 \lambda_2 \beta_{II+} \cdot \Phi^{R_\star(\beta_{II+}, \bar{\epsilon})}(\Delta\epsilon^*).$$

4.A Appendix: A family of quasiconvex quadratic functionals on $M_{\text{sym}}^{3 \times 3}$

The translations introduced in §4.1 were related to the diagonal subdeterminants — c.f. (4.1) — of the elements of $M_{\text{sym}}^{3 \times 3}$. As shown in that section, these diagonal subdeterminants are quasiconvex. The three other subdeterminants of $\epsilon \in M_{\text{sym}}^{3 \times 3}$,

$$\phi_{12}(\epsilon) := \epsilon_{12}\epsilon_{33} - \epsilon_{23}\epsilon_{31},$$

$$\phi_{23}(\epsilon) := \epsilon_{11}\epsilon_{23} - \epsilon_{31}\epsilon_{12},$$

$$\phi_{31}(\epsilon) := \epsilon_{12}\epsilon_{23} - \epsilon_{22}\epsilon_{31},$$

are neither quasiconvex nor quasiconcave⁵.

It is of interest to ask which linear combinations of these six subdeterminants are quasiconvex. This appendix provides a partial answer to this question by presenting a family of quasiconvex quadratic functionals on $M_{\text{sym}}^{3 \times 3}$. The translations introduced in (4.1) belong to this family.

Lemma 4.26. For $M \in M^{3 \times 3}$, let ϕ_{12}^M , ϕ_{23}^M and ϕ_{31}^M be defined analogous to (4.1). Then $\forall M \in M^{3 \times 3}$ and $\forall p, q, r \in \mathbb{R}$,

$$p^2 \phi_1^M + q^2 \phi_2^M + r^2 \phi_3^M - 2pq\phi_{12}^M - 2qr\phi_{23}^M - 2rp\phi_{31}^M : M_{\text{sym}}^{3 \times 3} \rightarrow \mathbb{R} \quad (4.26)$$

is quasiconvex.

Proof. For $\hat{m}, \hat{n} \in \mathbb{R}^3$, let

$$\omega_1(\hat{m}, \hat{n}) := m_2 n_3 - m_3 n_2,$$

$$\omega_2(\hat{m}, \hat{n}) := m_1 n_3 - m_3 n_1,$$

$$\omega_3(\hat{m}, \hat{n}) := m_1 n_2 - m_2 n_1.$$

Note that

$$\begin{pmatrix} 0 & \omega_3(\hat{m}, \hat{n}) & \omega_2(\hat{m}, \hat{n}) \\ -\omega_3(\hat{m}, \hat{n}) & 0 & \omega_1(\hat{m}, \hat{n}) \\ \omega_2(\hat{m}, \hat{n}) & \omega_1(\hat{m}, \hat{n}) & 0 \end{pmatrix}$$

⁵ Since these subdeterminants are quadratic, it suffices to show that they are neither rank-I convex nor rank-I concave. That is, it suffices to find $\hat{m}, \hat{n}, \hat{m}', \hat{n}' \in \mathbb{R}^3$ such that $\phi_{ij}(\hat{m} \otimes_s \hat{n}) > 0$ and $\phi_{ij}(\hat{m}' \otimes_s \hat{n}') < 0$ for $i, j = 1, 2, 3; i \neq j$. It is easy to find such $\hat{m}, \hat{n}, \hat{m}', \hat{n}'$.

is the anti-symmetric component of $\hat{m} \otimes \hat{n}$. Now

$$\phi_1(\hat{m} \otimes_s \hat{n}) = (m_2 n_3 + m_3 n_2)^2 - 4m_2 n_2 m_3 n_3 = (m_2 n_3 - m_3 n_2)^2 = \omega_1^2(\hat{m}, \hat{n})$$

with similar results for ϕ_2 and ϕ_3 . Likewise

$$\begin{aligned} \phi_{12}(\hat{m} \otimes_s \hat{n}) &= (m_1 n_2 + m_2 n_1)(2m_3 n_3) - (m_2 n_3 + m_3 n_2)(m_1 n_3 + m_3 n_1) \\ &= -(m_1 n_3 - m_3 n_1)(m_2 n_3 - m_3 n_2) \\ &= -\omega_1(\hat{m}, \hat{n}) \omega_2(\hat{m}, \hat{n}) \end{aligned}$$

with similar results for ϕ_{23} and ϕ_{31} . To summarize:

$$\begin{aligned} \phi_1(\hat{m} \otimes_s \hat{n}) &= \omega_1^2(\hat{m}, \hat{n}), \\ \phi_2(\hat{m} \otimes_s \hat{n}) &= \omega_2^2(\hat{m}, \hat{n}), \\ \phi_3(\hat{m} \otimes_s \hat{n}) &= \omega_3^2(\hat{m}, \hat{n}), \\ \phi_{12}(\hat{m} \otimes_s \hat{n}) &= -\omega_1(\hat{m}, \hat{n}) \omega_2(\hat{m}, \hat{n}), \\ \phi_{23}(\hat{m} \otimes_s \hat{n}) &= -\omega_2(\hat{m}, \hat{n}) \omega_3(\hat{m}, \hat{n}), \\ \phi_{31}(\hat{m} \otimes_s \hat{n}) &= -\omega_3(\hat{m}, \hat{n}) \omega_1(\hat{m}, \hat{n}). \end{aligned}$$

We are now ready to prove the lemma. Since any linear combination of the ϕ s is quadratic it suffices to prove rank-I convexity:

$$\begin{aligned} & \left(p^2 \phi_1^M + q^2 \phi_2^M + r^2 \phi_3^M - 2pq\phi_{12}^M - 2qr\phi_{23}^M - 2rp\phi_{31}^M \right) (\hat{m} \otimes_s \hat{n}) \\ &= \left(p^2 \phi_1 + q^2 \phi_2 + r^2 \phi_3 - 2pq\phi_{12} - 2qr\phi_{23} - 2rp\phi_{31} \right) (M^T \hat{m} \otimes_s M^T \hat{n}) \\ &= (p\omega_1(M^T \hat{m}, M^T \hat{n}) + q\omega_2(M^T \hat{m}, M^T \hat{n}) + r\omega_3(M^T \hat{m}, M^T \hat{n}))^2 \\ &\geq 0 \end{aligned}$$

which completes the proof. □

Remark 4.27.

1. There are quasiconvex quadratic functionals not of the form (4.26), for example, $\phi_1 + \phi_2$.
2. Positive linear combinations of functionals of the form (4.26) are quasiconvex (and quadratic).
3. From the proof above, $\exists \hat{n} \in \mathbb{R}^3$ such that $\epsilon \parallel \hat{n} \otimes \hat{n}$ if and only if

$$\phi_1(\epsilon) = \phi_2(\epsilon) = \phi_3(\epsilon) = \phi_{12}(\epsilon) = \phi_{23}(\epsilon) = \phi_{31}(\epsilon) = 0.$$

Chapter 5

Polycrystals

The study of shape-memory polycrystals is an area of active research. Theoretical models include Taylor models [Ono90a, Ono90b, OS88, OSO89, TA01], Sachs models [SN00] and models based on mean-field approximations [BL99a, BL99b, BL99c, BL99d, BL96, Fal89, LW98, LTT⁺00, NBZACP02, PEB88, PEB93, PEB94, SPBE99, SH93a, SH93b]. For computational studies that explicitly compute the microstructure within the grains see [ALS03, AJK02]. Experimental studies include [MNK⁺00, LVB⁺02, SLN⁺02, SNL⁺02]. The energy of the polycrystal plays a central role in most of these approaches.

Our work is a departure from this since we focus on the zero-set of the mesoscopic energy and make explicit use of the compatibility equation. In §5.1 we prove a dual variational characterization of the zero-set of polycrystals. Uses of this characterization are illustrated through examples in §5.2.2. In §5.2.1 and §5.3 we show that for a two-dimensional material and for materials undergoing cubic-tertagonal transformations, compatibility forces the strain fields to be related to solutions of hyperbolic partial differential equations.

We work in the setting of periodic polycrystals. Each grain has a non-empty interior and Lipschitz boundary. Recall the mathematical framework introduced in §2 and in particular in §2.2.2.

5.1 Dual variational characterization of the zero-set of polycrystals

Observe from the discussion in §2.2.2 (in particular (2.12)) that to characterize the recoverable strains of a polycrystal it suffices to characterize strain fields constrained locally (i.e., pointwise in each grain) to lie in the zero-set of the mesoscopic energy. In other words, it is not so much the mesoscopic energy \widehat{W} that is of relevance but its zero-set $\widehat{\mathcal{S}}$. Motivated by this observation we shift

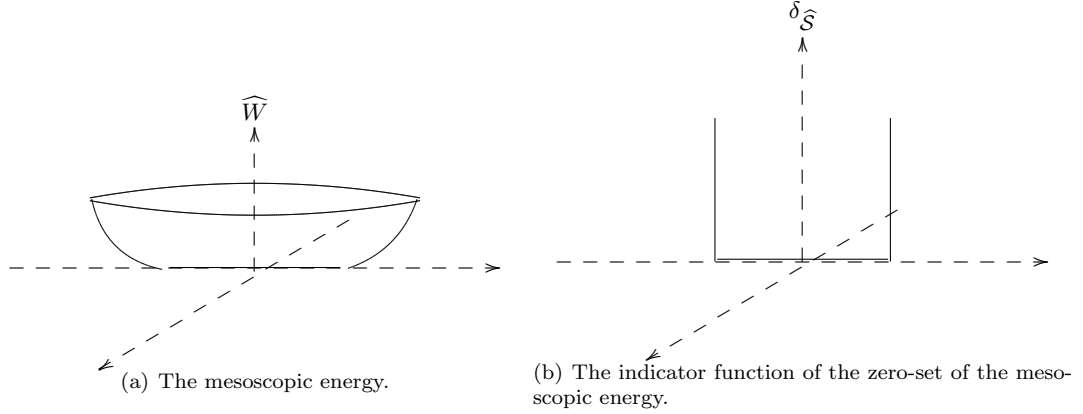


Figure 5.1: The mesoscopic energy and the indicator function of its zero-set.

our focus from \widehat{W} to the indicator function of $\widehat{\mathcal{S}}$, $\delta_{\widehat{\mathcal{S}}}: M_{\text{sym}}^{n \times n} \rightarrow \{0, \infty\}$ defined by

$$\delta_{\widehat{\mathcal{S}}}(\epsilon) := \begin{cases} 0 & \epsilon \in \widehat{\mathcal{S}} \\ \infty & \text{otherwise} \end{cases}$$

(see Figure 5.1). In other words, as is standard in convex analysis, we are exploiting the duality between constraint sets and their indicator functions [RW98, §1A]. Note that $\delta_{\widehat{\mathcal{S}}}$ is a convex function since $\widehat{\mathcal{S}}$ is a convex set.¹ Likewise, associated with $\overline{\mathcal{S}}$ is its indicator function $\delta_{\overline{\mathcal{S}}}: M_{\text{sym}}^{n \times n} \rightarrow \{0, \infty\}$ defined by

$$\delta_{\overline{\mathcal{S}}}(\bar{\epsilon}) := \begin{cases} 0 & \bar{\epsilon} \in \overline{\mathcal{S}} \\ \infty & \text{otherwise.} \end{cases}$$

For a polycrystal with texture R and a strain field $\epsilon: \Omega \rightarrow M_{\text{sym}}^{n \times n}$ notice that $\epsilon(x) \in \widehat{\mathcal{S}}_{R(x)}$ a.e. precisely when $\int_{\Omega} \delta_{\widehat{\mathcal{S}}}(R^T(x)\epsilon(x)R(x)) \, dx = 0$ and $\epsilon(x) \notin \widehat{\mathcal{S}}_{R(x)}$ on a non-negligible set² precisely when $\int_{\Omega} \delta_{\widehat{\mathcal{S}}}(R^T(x)\epsilon(x)R(x)) \, dx = \infty$. Thus $\delta_{\overline{\mathcal{S}}}(\bar{\epsilon}) = 0$ precisely when

$$\text{There exists } \epsilon: \Omega \rightarrow M_{\text{sym}}^{n \times n} \text{ periodic, such that } \langle \epsilon(x) \rangle = \bar{\epsilon} \text{ and } \int_{\Omega} \delta_{\widehat{\mathcal{S}}}(R^T(x)\epsilon(x)R(x)) \, dx = 0;$$

and $\delta_{\overline{\mathcal{S}}}(\bar{\epsilon}) = \infty$ precisely when

$$\text{For every periodic } \epsilon: \Omega \rightarrow M_{\text{sym}}^{n \times n} \text{ such that } \langle \epsilon(x) \rangle = \bar{\epsilon}, \int_{\Omega} \delta_{\widehat{\mathcal{S}}}(R^T(x)\epsilon(x)R(x)) \, dx = \infty.$$

¹ We restrict ourselves to the case when martensite is tetragonal, trigonal or orthorhombic.

² A non-negligible set is a set whose Lebesgue measure is non-zero.

That is to say,

$$\delta_{\widehat{\mathcal{S}}}(\bar{\epsilon}) = \inf_{\substack{\epsilon: \text{periodic} \\ \langle \epsilon(x) \rangle = \bar{\epsilon}}} \int_{\Omega} \delta_{\widehat{\mathcal{S}}}(R^T(x)\epsilon(x)R(x)) \, dx. \quad (5.1)$$

Since $\delta_{\widehat{\mathcal{S}}}$ is infinite outside the bounded set $\widehat{\mathcal{S}}$ the integral in (5.1) is finite only when ϵ is essentially bounded. Thus it suffices to evaluate the infimum in (5.1) over all strain fields $\epsilon \in L_{\text{per}}^{\infty}(\Omega, M_{\text{sym}}^{n \times n})$ (the subscript ‘per’ indicates that the strains are periodic). Since $\delta_{\widehat{\mathcal{S}}}$ vanishes inside $\widehat{\mathcal{S}}$ no further integrability conditions are imposed on ϵ . The corresponding displacements lie in

$$U_{\text{per}}^{\infty} := \left\{ u \in L^{\infty}(\Omega, \mathbb{R}^n) \mid \epsilon(u) \in L_{\text{per}}^{\infty}(\Omega, M_{\text{sym}}^{n \times n}), u(0) = 0 \right\}.$$

Here we have assumed, with no loss of generality, that $0 \in \Omega$ and $u(0) = 0$. For $\bar{\epsilon} \in M_{\text{sym}}^{n \times n}$, let

$$\mathcal{U}_{\text{ad}}(\bar{\epsilon}) := \{ u \in U_{\text{per}}^{\infty} \mid \langle \epsilon(u) \rangle = \bar{\epsilon} \}.$$

(5.1) can now be written as

$$\delta_{\widehat{\mathcal{S}}}(\bar{\epsilon}) = \inf_{\epsilon \in \mathcal{U}_{\text{ad}}(\bar{\epsilon})} \int_{\Omega} \delta_{\widehat{\mathcal{S}}}(R^T(x)\epsilon(x)R(x)) \, dx$$

Remark 5.1. Since \widehat{W} grows quadratically away from the zero-set, the discussion of homogenization in §2.2.2 — c.f. (2.11) — was implicitly in

$$U_{\text{per}}^2 := \left\{ u \in L^2(\Omega, \mathbb{R}^n) \mid \epsilon(u) \in L_{\text{per}}^2(\Omega, M_{\text{sym}}^{n \times n}) \right\}.$$

Let \mathcal{I} be the map that maps a function to the indicator function of its zero-set. The relationship between \widehat{W} , \overline{W} , $\delta_{\widehat{\mathcal{S}}}$ and $\delta_{\overline{\mathcal{S}}}$ can be represented as

$$\begin{array}{ccc} \widehat{W} & \xrightarrow{\text{Homogenization in } U_{\text{per}}^2} & \overline{W} \\ \downarrow \mathcal{I} & & \downarrow \mathcal{I} \\ \delta_{\widehat{\mathcal{S}}} & & \delta_{\overline{\mathcal{S}}} \end{array}$$

For the preceding discussion to be self-consistent and consistent with the discussion in §2.2.2 we need the following commutative diagram to hold:

$$\begin{array}{ccc} \widehat{W} & \xrightarrow{\text{Homogenization in } U_{\text{per}}^2} & \overline{W} \\ \downarrow \mathcal{I} & & \downarrow \mathcal{I} \\ \delta_{\widehat{\mathcal{S}}} & \xrightarrow{\text{Homogenization in } U_{\text{per}}^{\infty}} & \delta_{\overline{\mathcal{S}}} \end{array}$$

Guided by this, work on the modeling of locking materials (remark 5.2), and the work of Carbone, De Arcangelis et al. on the homogenization of unbounded functionals³ [CA01, and references therein] we conjecture that $\delta_{\widehat{\mathcal{S}}}$ is indeed the homogenized limit in U_{per}^∞ of $\delta_{\widehat{\mathcal{S}}}$.

We proceed, on the assumption that this conjecture is true.

Remark 5.2 (Connections to locking materials). The mathematical framework described here is closely connected to that which arises in the analysis of locking materials. These are hyperelastic materials for which the strain tensor is constrained to stay in a convex set (with interior). See [Pra57, Pra58, DS86, Dem85a, Dem85b].

In the sequel we will use the following definitions: Let $\overline{\mathbb{R}} := \mathbb{R} \cup \{\infty\}$. The conjugate of $\delta_{\widehat{\mathcal{S}}}$ is $\delta_{\widehat{\mathcal{S}}}^*: M_{\text{sym}}^{n \times n} \rightarrow \overline{\mathbb{R}}$ defined by

$$\delta_{\widehat{\mathcal{S}}}^*(\sigma) := \sup_{\epsilon \in M_{\text{sym}}^{n \times n}} \epsilon \cdot \sigma - \delta_{\widehat{\mathcal{S}}}(\epsilon).$$

$\delta_{\widehat{\mathcal{S}}}^*$ is the support function of $\widehat{\mathcal{S}}$ [RW98, Eg.11.4(a), pg.477]. Let $\underline{\mathcal{S}} \subset L^\infty(\Omega, M_{\text{sym}}^{n \times n})$ be defined by

$$\underline{\mathcal{S}} := \left\{ \epsilon \mid \exists u \in U_{\text{per}}^\infty, \epsilon = \epsilon(u) \text{ and } \epsilon(x) \in \widehat{\mathcal{S}}_{R(x)} \right\}.$$

Let $\mathcal{M}_{\text{per}}^1(\Omega, M_{\text{sym}}^{n \times n}) \equiv (L_{\text{per}}^\infty(\Omega, M_{\text{sym}}^{n \times n}))^*$ be the space of all periodic signed Radon measures with finite mass and let

$$\mathcal{S}_{\text{ad}} := \left\{ \sigma \in M_{\text{per}}^1(\Omega, M_{\text{sym}}^{n \times n}) \mid \text{div}(\sigma) = 0 \right\}.$$

Theorem 5.3 (Dual variational characterization of polycrystalline zero-sets). The indicator function of the zero-set of a polycrystal has the dual variational characterization:

$$\delta_{\widehat{\mathcal{S}}}(\bar{\epsilon}) = \sup_{\sigma \in \mathcal{S}_{\text{ad}}} \int_{\Omega} \sigma \cdot \bar{\epsilon} - \delta_{\widehat{\mathcal{S}}}^*(R^T(x)\sigma(x)R(x)) \, dx. \quad (5.2)$$

Our proof follows the same strategy used to prove a similar result in [DS86]. The proof is presented after lemma 5.4, lemma 5.5 and proposition 5.6 below.

Lemma 5.4. The following inequality holds:

$$\sup_{\sigma \in \mathcal{S}_{\text{ad}}} \int_{\Omega} \sigma \cdot \bar{\epsilon} - \delta_{\widehat{\mathcal{S}}}^*(R^T(x)\sigma(x)R(x)) \, dx \leq \inf_{u \in \mathcal{U}_{\text{ad}}(\bar{\epsilon})} \int_{\Omega} \delta_{\widehat{\mathcal{S}}}(R^T(x)\epsilon(x)R(x)) \, dx \equiv \delta_{\widehat{\mathcal{S}}}(\bar{\epsilon}).$$

³ Unbounded functionals are functionals taking values in $\overline{\mathbb{R}}$.

Moreover, the variational problem on the left is the dual of the variational problem on the right.

Proof. We shall denote the indicator function of $\mathcal{U}_{\text{ad}}(\bar{\epsilon})$ on U_{per}^∞ by $F_{\bar{\epsilon}}$:

$$F_{\bar{\epsilon}}(u) := \begin{cases} 0 & u \in \mathcal{U}_{\text{ad}}(\bar{\epsilon}) \\ \infty & \text{otherwise;} \end{cases}$$

$F_{\bar{\epsilon}}^*(-\epsilon^*(\sigma)) : (U_{\text{per}}^\infty)^* \rightarrow \bar{\mathbb{R}}$ is given by [ET76]:

$$F_{\bar{\epsilon}}^*(-\epsilon^*(\sigma)) = \begin{cases} \langle \sigma \rangle \cdot \bar{\epsilon} & \text{if } \text{div}(\sigma) = 0 \\ \infty & \text{otherwise.} \end{cases}$$

Let $G : L_{\text{per}}^\infty(\Omega, M_{\text{sym}}^{n \times n}) \rightarrow \bar{\mathbb{R}}$ be defined by

$$G(\epsilon) := \int_{\Omega} \delta_{\mathcal{S}}(R^T(x)\epsilon(x)R(x)) \, dx;$$

it is easy to verify that $G^* : \mathcal{M}_{\text{per}}^1(\Omega, M_{\text{sym}}^{n \times n}) \rightarrow \bar{\mathbb{R}}$ is given by

$$G^*(\sigma) = \int_{\Omega} \delta_{\mathcal{S}}^*(R^T(x)\sigma(x)R(x)) \, dx.$$

$F_{\bar{\epsilon}}$ and G are convex, proper⁴ and lower semi-continuous. Let $\epsilon^* : \mathcal{M}_{\text{per}}^1(\Omega, M_{\text{sym}}^{n \times n}) \rightarrow (U_{\text{per}}^\infty)^*$ be the conjugate of the continuous map $U_{\text{per}}^\infty \ni u \mapsto \epsilon(u) \in L_{\text{per}}^\infty(\Omega, M_{\text{sym}}^{n \times n})$. $\delta_{\mathcal{S}}(\bar{\epsilon})$ is the solution of the problem

$$P : \inf_{u \in U_{\text{per}}^\infty} F_{\bar{\epsilon}}(u) + G(\epsilon(u)).$$

From a theorem in convex analysis [ET76], the dual of P is

$$P^* : \sup_{\sigma \in \mathcal{M}_{\text{per}}^1(\Omega, M_{\text{sym}}^{n \times n})} -F_{\bar{\epsilon}}^*(-\epsilon^*(\sigma)) - G^*(\sigma).$$

In particular, $P^* \leq P$.⁵ The result follows. □

We now show that the inequality in lemma 5.4 above is in fact an equality. We do so by regularizing the problem with a small parameter η and then taking the limit $\eta \rightarrow 0$.

⁴ That is, not everywhere ∞ [ET76, pg.8] [RW98, pg.5].

⁵ Further, if $\exists u \in U_{\text{per}}^\infty$ such that $F_{\bar{\epsilon}}(u) < \infty$ and G is finite and continuous at $\epsilon(u)$, then $P^* = P < \infty$ and P^* possesses at least one solution. We shall use this fact later.

For $\eta \in \mathbb{R}_+$, let $\widehat{W}_\eta: M_{\text{sym}}^{n \times n} \rightarrow \overline{\mathbb{R}}$ be defined by

$$\widehat{W}_\eta(\epsilon) := \begin{cases} 0 & \epsilon \in \widehat{\mathcal{S}} \\ \frac{1}{1 - \frac{1}{\eta}d(\epsilon, \widehat{\mathcal{S}})} - 1 & 0 < d(\epsilon, \widehat{\mathcal{S}}) < \eta \\ \infty & \text{otherwise} \end{cases}$$

where $d(\epsilon, \widehat{\mathcal{S}})$ is the distance in $M_{\text{sym}}^{n \times n}$ between ϵ and $\widehat{\mathcal{S}}$:

$$d(\epsilon, \widehat{\mathcal{S}}) := \max_{1 \leq i, j \leq n} \max_{\epsilon' \in \widehat{\mathcal{S}}} |\epsilon_{ij} - \epsilon'_{ij}|.$$

Note that $d(R^T \epsilon R, \widehat{\mathcal{S}}) = d(\epsilon, \widehat{R\mathcal{S}R^T}) = d(\epsilon, \widehat{\mathcal{S}}_R)$. $\widehat{W}_0 \equiv \delta_{\widehat{\mathcal{S}}}$ and \widehat{W}_η is continuous for $\eta > 0$. Let \widehat{W}_η^* be the conjugate of \widehat{W}_η .

Lemma 5.5. For $\eta > 0$, the following inequality holds:

$$\sup_{\sigma \in \mathcal{S}_{\text{ad}}} \int_{\Omega} \sigma \cdot \bar{\epsilon} - \widehat{W}_\eta^*(R^T(x)\sigma(x)R(x)) \, dx \leq \inf_{u \in \mathcal{U}_{\text{ad}}(\bar{\epsilon})} \int_{\Omega} \widehat{W}_\eta(R^T(x)\epsilon(x)R(x)) \, dx.$$

Moreover, the variational problem on the left is the dual of the variational problem on the right.

Further, if $\mathcal{U}_{\text{ad}}(\bar{\epsilon}) \cap \underline{\mathcal{S}} \neq \{\}$,

$$\sup_{\sigma \in \mathcal{S}_{\text{ad}}} \int_{\Omega} \sigma \cdot \bar{\epsilon} - \widehat{W}_\eta^*(R^T(x)\sigma(x)R(x)) \, dx = \inf_{u \in \mathcal{U}_{\text{ad}}(\bar{\epsilon})} \int_{\Omega} \widehat{W}_\eta(R^T(x)\epsilon(x)R(x)) \, dx = 0.$$

Proof. Let $G_\eta: L_{\text{per}}^\infty(\Omega, M_{\text{sym}}^{n \times n}) \rightarrow \overline{\mathbb{R}}$ be defined by

$$G_\eta(\epsilon) := \int_{\Omega} \widehat{W}_\eta(R^T(x)\epsilon(x)R(x)) \, dx.$$

G_η is convex, proper and lower semi-continuous. It is easy to verify that $G_\eta^*: \mathcal{M}_{\text{per}}^1(\Omega, M_{\text{sym}}^{n \times n}) \rightarrow \overline{\mathbb{R}}$ is given by

$$G_\eta^*(\sigma) = \int_{\Omega} \widehat{W}_\eta^*(R^T(x)\sigma(x)R(x)) \, dx.$$

We introduce the problem

$$P_\eta: \quad \inf_{u \in \mathcal{U}_{\text{ad}}(\bar{\epsilon})} \int_{\Omega} \widehat{W}_\eta(R^T(x)\epsilon(x)R(x)) \, dx,$$

which can also be written as

$$\inf_{u \in U_{\text{per}}^\infty} F_{\bar{\epsilon}}(u) + G_\eta(\epsilon(u)).$$

From the afore mentioned theorem in convex analysis, the dual of P_η is

$$P_\eta^* : \sup_{\sigma \in \mathcal{M}_{\text{per}}^1(\Omega, M_{\text{sym}}^{n \times n})} -F_{\bar{\epsilon}}^*(-\epsilon^*(\sigma)) - G_\eta^*(\sigma)$$

and $P_\eta^* \leq P_\eta$. When $\mathcal{U}_{\text{ad}}(\bar{\epsilon}) \cap \underline{\mathcal{S}} \neq \{\}$, from the same theorem (including footnote (5)): $P_\eta^* = P_\eta = 0$. \square

Proposition 5.6. When $\mathcal{U}_{\text{ad}}(\bar{\epsilon}) \cap \underline{\mathcal{S}} \neq \{\}$, $P = 0$.

Proof. Let $\mathcal{U}_{\text{ad}}(\bar{\epsilon}) \cap \underline{\mathcal{S}} \neq \{\}$. Let u_η be a solution of P_η . Since $P_\eta < \infty$,

$$\begin{aligned} \|\epsilon(u_\eta)\|_{L^\infty(\Omega, M_{\text{sym}}^{n \times n})} &= \text{ess sup}_{x \in \Omega} \|\epsilon(u_\eta)(x)\| \\ &\leq \text{ess sup}_{x \in \Omega} \left\{ \max_{\epsilon' \in \widehat{\mathcal{S}}_{R(x)}} \|\epsilon(u_\eta)(x) - \epsilon'\| + \max_{\epsilon' \in \widehat{\mathcal{S}}_{R(x)}} \|\epsilon'\| \right\} \\ &\leq \eta + \max_{R \in SO(n)} \max_{\epsilon \in \widehat{\mathcal{S}}_R} \|\epsilon\|. \end{aligned}$$

Thus $\epsilon(u_\eta)$ is bounded in $L^\infty(\Omega, M_{\text{sym}}^{n \times n})$. From [Dem85a, Prop.1.1 and Prop.1.2], u_η is bounded in U_{per}^∞ . It follows that $\exists u_o \in U_{\text{per}}^\infty$ such that

$$u_\eta \xrightarrow{*} u_o \text{ in } U_{\text{per}}^\infty.$$

On the other hand, $d(\epsilon(u_\eta)(x), \widehat{\mathcal{S}}_{R(x)}) < \eta$ for a.e. $x \in \Omega$. Let $D(\epsilon, \underline{\mathcal{S}}) := \sup_{\epsilon' \in \underline{\mathcal{S}}} \|\epsilon - \epsilon'\|_{L^\infty(\Omega, M_{\text{sym}}^{n \times n})}$, so $D(\epsilon, \underline{\mathcal{S}}) = \text{ess sup}_{x \in \Omega} d(\epsilon(u_\eta)(x), \widehat{\mathcal{S}}_{R(x)}) < \eta$. Since $D(\cdot, \underline{\mathcal{S}})$ is weak* lower semi-continuous

$$D(\epsilon(u_o), \underline{\mathcal{S}}) \leq \liminf_{\eta \rightarrow 0} d(\epsilon(u_\eta), \underline{\mathcal{S}}) = 0.$$

Thus $\epsilon(u_o) \in \underline{\mathcal{S}}$. In other words u_o is in fact a solution of P : $P = 0$. \square

Proof of theorem 5.3. Note that $\widehat{W}_\eta \leq \delta_{\widehat{\mathcal{S}}}$, i.e., $G_\eta \leq G$. Thus $P_\eta \leq P$. Moreover $G_\eta \leq G$ implies that $G_\eta^* \geq G^*$ [RW98, pg.475]. Thus $P_\eta^* \leq P^*$. From lemma 5.4, $P^* \leq P < \infty$.

When $\mathcal{U}_{\text{ad}}(\bar{\epsilon}) \cap \underline{\mathcal{S}} \neq \{\}$, from lemma 5.5, $P_\eta^* = P_\eta = 0$ and from proposition 5.6 $P = 0$. Thus

$$0 = P_\eta = P_\eta^* \leq P^* \leq P = 0$$

which shows that $P^* = 0 = P$.

When $\mathcal{U}_{\text{ad}}(\bar{\epsilon}) \cap \underline{\mathcal{S}} = \{\}$, $P_\eta^* = \infty$ for some η . Since $P_\eta^* \leq P^*$ this shows that $P^* = \infty = P$. \square

Theorem 5.3 allows for the possibility that the solution (stress-field) of the dual variational problem is a measure and not a regular function. Indeed, in §5.2.2 we present examples where optimal dual fields are signed Radon measures supported on sets of Lebesgue measure zero. The concentration of dual fields on lines was computationally observed for scalar problems by Bhattacharya and Suquet [BS04]. For descriptions of related problems in plasticity theory where stress concentrations occur c.f. [Str79, Tem81, KS83, SK83, Dem89].

On the other hand the theorem does not exclude regular solutions. Indeed, the trivial example of a homogeneous polycrystal (single crystal) would have a regular optimal dual (stress) field.

5.2 The problem in two dimensions⁶

In §3.3 we computed the mesoscopic energy of the two-well microscopic energy in two dimensions:

$$\begin{aligned} W(\epsilon) &= \min \{W_1(\epsilon), W_2(\epsilon)\}, \\ W_i(\epsilon) &= \frac{1}{2} \langle \alpha_i(\epsilon - \epsilon_i^T), (\epsilon - \epsilon_i^T) \rangle + w_i. \end{aligned}$$

When W_1 and W_2 are the microscopic energy densities of two variants of martensite, $w_1 = w_2 = 0$ and the transformation strains have the same hydrostatic component: $\Lambda_h \epsilon_1^T = \Lambda_h \epsilon_2^T$. The later equation implies that ϵ_1^T and ϵ_2^T are compatible. With no loss of generality set

$$\begin{aligned} w_1 &= w_2 = 0, \\ -\epsilon_1^T &= \epsilon_2^T = \begin{pmatrix} 1 & 0 \\ 0 & -1 \end{pmatrix}. \end{aligned}$$

The corresponding mesoscopic energy is shown in Figure 5.2. $\widehat{\mathcal{S}}$, the zero-set of the mesoscopic energy is given by

$$\widehat{\mathcal{S}} = \text{Conv} \{\epsilon_1^T, \epsilon_2^T\} = \left\{ s \begin{pmatrix} 1 & 0 \\ 0 & -1 \end{pmatrix} \mid s \in \mathbb{R}, |s| \leq 1 \right\} \quad (5.3)$$

(see Figure 5.3). Note that $\widehat{\mathcal{S}}$ is balanced: $\bar{\epsilon} \in \widehat{\mathcal{S}} \Rightarrow \forall |\alpha| \leq 1, \alpha \bar{\epsilon} \in \widehat{\mathcal{S}}$ [Rud91, pg.6]. For a grain oriented at an angle θ , the mesoscopic energy is given by

$$\widehat{W}_\theta(\epsilon) = \widehat{W}(R_\theta^T \epsilon R_\theta) \quad (5.4)$$

Consequently, in a grain oriented at an angle θ , the zero set of the energy is given by

$$\widehat{\mathcal{S}}_\theta = R_\theta \widehat{\mathcal{S}} R_\theta^T = \left\{ s \hat{\epsilon}_{2\theta} \mid s \in \mathbb{R}, |s| \leq \sqrt{2} \right\}. \quad (5.5)$$

⁶ The material considered here is called ‘Two-Dimensional Diagonal Trace-Free Elastic Material’ in [BK97].

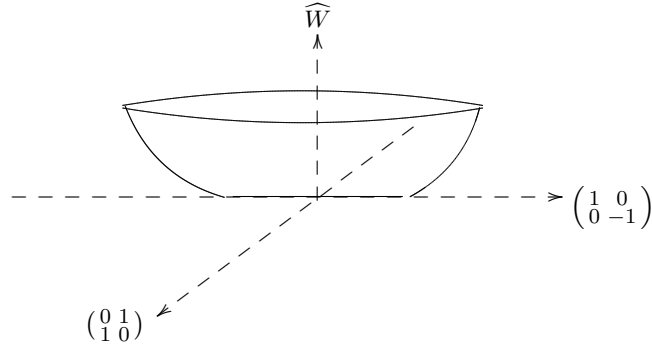


Figure 5.2: The mesoscopic energy.

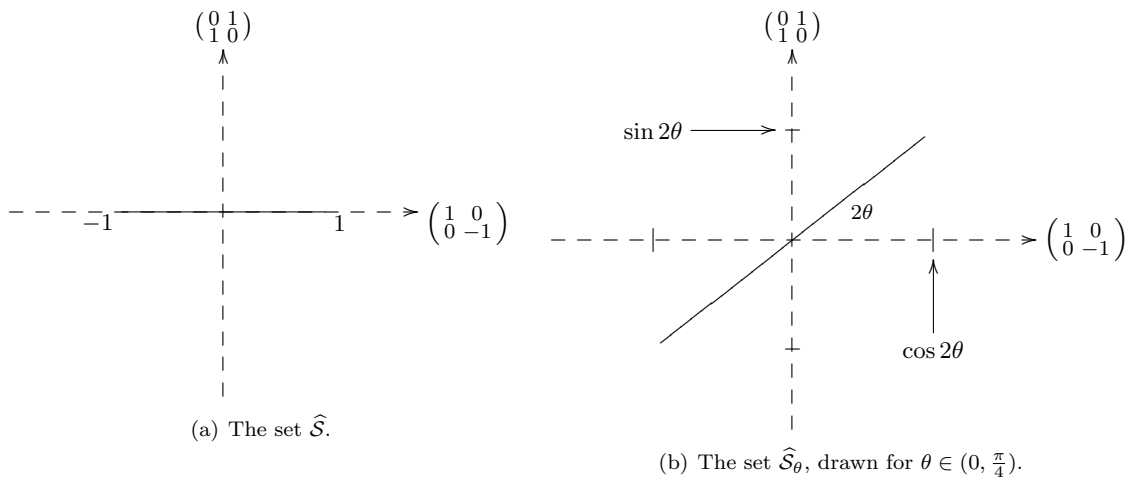


Figure 5.3: The sets \widehat{S} and \widehat{S}_θ , drawn for $\theta \in (0, \frac{\pi}{4})$.

where $\hat{\epsilon}_{2\theta}$ is shorthand for $\frac{1}{\sqrt{2}} \begin{pmatrix} \cos 2\theta & \sin 2\theta \\ \sin 2\theta & -\cos 2\theta \end{pmatrix}$. \widehat{S} and \widehat{S}_θ are illustrated in Figure 5.3.

5.2.1 Fields in a grain

The wave equation associated with \widehat{S}_θ . From (5.5), for $\epsilon \in \widehat{S}_\theta$, ϵ is constrained to be of the form

$$\epsilon(x, y) = s(x, y)\hat{\epsilon}_{2\theta} \quad |s(x, y)| \leq \sqrt{2}$$

for some $s \in L^\infty(\mathbb{R}^2, \mathbb{R})$. This with the 2-D strain compatibility equation,

$$\frac{\partial^2}{\partial y^2} \epsilon_{xx} - 2 \frac{\partial^2}{\partial x \partial y} \epsilon_{xy} + \frac{\partial^2}{\partial x^2} \epsilon_{yy} = 0 \tag{5.6}$$

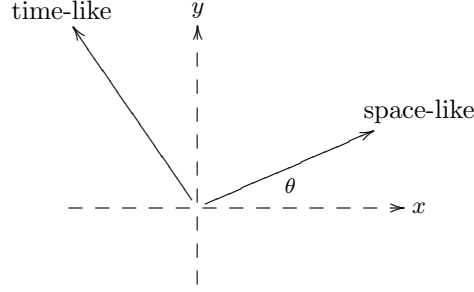


Figure 5.4: The ‘space-like’ and ‘time-like’ directions of the wave operator \square_{θ}^2 .

implies

$$\cos 2\theta \frac{\partial^2}{\partial x^2} s(x, y) + 2 \sin 2\theta \frac{\partial^2}{\partial x \partial y} s(x, y) - \cos 2\theta \frac{\partial^2}{\partial y^2} s(x, y) = 0 \quad (5.7)$$

assuming θ is constant. Since ϵ is allowed to be discontinuous, we must interpret these equations in the sense of distributions. For brevity we define the wave operator \square_{θ}^2 as

$$\square_{\theta}^2 \equiv \cos 2\theta \frac{\partial^2}{\partial x^2} + 2 \sin 2\theta \frac{\partial^2}{\partial x \partial y} - \cos 2\theta \frac{\partial^2}{\partial y^2}. \quad (5.8)$$

Notice that this is the wave operator with the ‘space-time’ coordinates oriented at an angle θ to the $x - y$ coordinates (Figure 5.4). Thus we obtain the hyperbolic partial differential equation

$$\square_{\theta}^2 s(x, y) = 0. \quad (5.9)$$

The characteristics of the wave equation. The equations of the characteristics of the above wave equation are given by [Wei95, pg.41ff]

$$\xi_{\theta}(x, y) = \cos\left(\theta + \frac{\pi}{4}\right)x + \sin\left(\theta + \frac{\pi}{4}\right)y \quad (5.10a)$$

$$\eta_{\theta}(x, y) = \cos\left(\theta - \frac{\pi}{4}\right)x + \sin\left(\theta - \frac{\pi}{4}\right)y. \quad (5.10b)$$

The characteristics ξ_{θ} and η_{θ} are inclined at angles $\theta - \frac{\pi}{4}$ and $\theta + \frac{\pi}{4}$, respectively. From (5.10),

$$d\xi_{\theta} = \cos\left(\theta + \frac{\pi}{4}\right)dx + \sin\left(\theta + \frac{\pi}{4}\right)dy = \hat{n}\left(\theta + \frac{\pi}{4}\right) \cdot d\mathbf{x} \quad (5.11a)$$

$$d\eta_{\theta} = \cos\left(\theta - \frac{\pi}{4}\right)dx + \sin\left(\theta - \frac{\pi}{4}\right)dy = \hat{n}\left(\theta - \frac{\pi}{4}\right) \cdot d\mathbf{x} \quad (5.11b)$$

where $\hat{n}(\theta)$ is shorthand for $(\cos \theta, \sin \theta)^T$. For (a region occupied by) a single crystal oriented at θ we define its *characteristics* to be $\Xi_{\theta} := \{(x, y) \mid \xi_{\theta}(x, y) : \text{constant}\}$ and $H_{\theta} := \{(x, y) \mid \eta_{\theta}(x, y) : \text{constant}\}$.

The strain field. From (5.10), in every convex domain, $s: \mathbb{R}^2 \rightarrow \mathbb{R}$ which satisfies $\square_\theta^2 s(x, y) = 0$ in a distributional sense is constrained to be of the form

$$s(x, y) = p(\xi_\theta) + q(\eta_\theta) \quad (5.12)$$

for some $p, q \in L^\infty(\mathbb{R})$. For a strain field $\epsilon(x, y) \equiv s(x, y) \hat{e}_{2\theta}$ with $\square_\theta^2 s(x, y) = 0$, we define the *strain on the characteristic* ξ_θ to be $p(\xi_\theta)\hat{e}_{2\theta}$ and the *strain on the characteristic* η_θ to be $q(\eta_\theta)\hat{e}_{2\theta}$.

The displacement gradient. Let $H := \nabla u$ be the displacement gradient. Since $\epsilon \equiv \mathbf{sym}(H)$, the constraint $\epsilon \in \widehat{S}_\theta$ is equivalent to the constraint $H \in \widehat{S}_\theta \oplus \text{Span} \left\{ \begin{pmatrix} 0 & 1 \\ -1 & 0 \end{pmatrix} \right\}$:

$$H(x, y) = s(x, y)\hat{e}_{2\theta} + \omega(x, y)\frac{1}{\sqrt{2}} \begin{pmatrix} 0 & 1 \\ -1 & 0 \end{pmatrix} \quad |s(x, y)| \leq \sqrt{2} \quad (5.13)$$

for some $s \in L^\infty(\mathbb{R}^2, \mathbb{R})$ and some $\omega: \mathbb{R}^2 \rightarrow \mathbb{R}$. This with the compatibility condition $\nabla \times H = 0$ implies

$$-\sin 2\theta \frac{\partial}{\partial x} s(x, y) + \cos 2\theta \frac{\partial}{\partial y} s(x, y) = \frac{\partial}{\partial x} w(x, y) \quad (5.14a)$$

$$\cos 2\theta \frac{\partial}{\partial x} s(x, y) + \sin 2\theta \frac{\partial}{\partial y} s(x, y) = \frac{\partial}{\partial y} w(x, y). \quad (5.14b)$$

These are a pair on non-homogeneous transport equations which can be written as

$$\nabla w(x, y) = \begin{pmatrix} -\sin 2\theta & \cos 2\theta \\ \cos 2\theta & \sin 2\theta \end{pmatrix} \nabla s(x, y). \quad (5.15)$$

This implies that

$$\square_\theta^2 w(x, y) = 0. \quad (5.16)$$

Note that $\begin{pmatrix} -\sin 2\theta & \cos 2\theta \\ \cos 2\theta & \sin 2\theta \end{pmatrix}$ is a reflection operator that leaves $\hat{n}(\theta + \frac{\pi}{4})$ invariant. From (5.11) and (5.12),

$$\nabla s(x, y) = p'(\xi_\theta) \hat{n}(\theta + \frac{\pi}{4}) + q'(\eta_\theta) \hat{n}(\theta - \frac{\pi}{4}).$$

Using this in (5.15),

$$\nabla w(x, y) = p'(\xi_\theta) \hat{n}(\theta + \frac{\pi}{4}) - q'(\eta_\theta) \hat{n}(\theta - \frac{\pi}{4})$$

and thus,

$$w(x, y) = p(\xi_\theta) - q(\eta_\theta) + \text{constant}. \quad (5.17)$$

From these we obtain

$$\begin{aligned} H(x, y) &= s(x, y)\hat{\epsilon}_{2\theta} + w(x, y)\frac{1}{\sqrt{2}} \begin{pmatrix} 0 & 1 \\ -1 & 0 \end{pmatrix} \\ &= p(\xi_\theta) \left(\hat{\epsilon}_{2\theta} + \frac{1}{\sqrt{2}} \begin{pmatrix} 0 & 1 \\ -1 & 0 \end{pmatrix} \right) + q(\eta_\theta) \left(\hat{\epsilon}_{2\theta} - \frac{1}{\sqrt{2}} \begin{pmatrix} 0 & 1 \\ -1 & 0 \end{pmatrix} \right) + c \begin{pmatrix} 0 & 1 \\ -1 & 0 \end{pmatrix} \\ &= \sqrt{2}p(\xi_\theta)\hat{n}(\theta - \frac{\pi}{4}) \otimes \hat{n}(\theta + \frac{\pi}{4}) + \sqrt{2}q(\eta_\theta)\hat{n}(\theta + \frac{\pi}{4}) \otimes \hat{n}(\theta - \frac{\pi}{4}) + c \begin{pmatrix} 0 & 1 \\ -1 & 0 \end{pmatrix}. \end{aligned} \quad (5.18)$$

Here c is a constant and we have used (5.12), (5.17) and the relations

$$\hat{\epsilon}_{2\theta} = \sqrt{2}\hat{n}(\theta - \frac{\pi}{4}) \otimes_s \hat{n}(\theta + \frac{\pi}{4}) \quad (5.19a)$$

$$\begin{pmatrix} 0 & 1 \\ -1 & 0 \end{pmatrix} = \hat{n}(\theta - \frac{\pi}{4}) \otimes \hat{n}(\theta + \frac{\pi}{4}) - \hat{n}(\theta + \frac{\pi}{4}) \otimes \hat{n}(\theta - \frac{\pi}{4}) \quad (5.19b)$$

$$\hat{\epsilon}_{2\theta} + \frac{1}{\sqrt{2}} \begin{pmatrix} 0 & 1 \\ -1 & 0 \end{pmatrix} = \sqrt{2}\hat{n}(\theta - \frac{\pi}{4}) \otimes \hat{n}(\theta + \frac{\pi}{4}) \quad (5.19c)$$

$$\hat{\epsilon}_{2\theta} - \frac{1}{\sqrt{2}} \begin{pmatrix} 0 & 1 \\ -1 & 0 \end{pmatrix} = \sqrt{2}\hat{n}(\theta + \frac{\pi}{4}) \otimes \hat{n}(\theta - \frac{\pi}{4}). \quad (5.19d)$$

In an un-oriented grain $\theta = 0$, and thus from (5.13),

$$H(x, y) = \frac{1}{\sqrt{2}} \begin{pmatrix} s(x, y) & w(x, y) \\ -w(x, y) & -s(x, y) \end{pmatrix} \quad (5.20)$$

For a strain field $\epsilon(x, y) \equiv s(x, y)\hat{\epsilon}_{2\theta}$ that satisfies $\square_\theta^2 s(x, y) = 0$, we define the *displacement gradient on the characteristic ξ_θ* to be $p(\xi_\theta) \left(\hat{\epsilon}_{2\theta} + \frac{1}{\sqrt{2}} \begin{pmatrix} 0 & 1 \\ -1 & 0 \end{pmatrix} \right) = \sqrt{2}p(\xi_\theta)\hat{n}(\theta - \frac{\pi}{4}) \otimes \hat{n}(\theta + \frac{\pi}{4})$ and the *displacement gradient on the characteristic η_θ* to be $q(\eta_\theta) \left(\hat{\epsilon}_{2\theta} - \frac{1}{\sqrt{2}} \begin{pmatrix} 0 & 1 \\ -1 & 0 \end{pmatrix} \right) = \sqrt{2}q(\eta_\theta)\hat{n}(\theta + \frac{\pi}{4}) \otimes \hat{n}(\theta - \frac{\pi}{4})$.

Remark 5.7. From (5.17), $\omega \in L^\infty(\mathbb{R}^2, \mathbb{R})$ and thus from (5.13) $H \in L^\infty(\mathbb{R}^2, M^{2 \times 2})$. Thus u is in fact in $W^{1, \infty}(\Omega, \mathbb{R}^2)$.

The displacement. From (5.18) and (5.11) the displacement $u(\mathbf{x}) = \int H(\mathbf{x})d\mathbf{x}$ in every convex subset of a grain oriented at θ is given by

$$\begin{aligned} u(x, y) &= \sqrt{2} \int p(\xi_\theta)\hat{n}_- \otimes \hat{n}_-^\perp d\mathbf{x} + \sqrt{2} \int q(\eta_\theta)\hat{n}_-^\perp \otimes \hat{n}_- d\mathbf{x} + c \int \begin{pmatrix} 0 & 1 \\ -1 & 0 \end{pmatrix} d\mathbf{x} \\ &= \sqrt{2} \int (p(\xi_\theta) + c)\hat{n}_-^\perp \cdot d\mathbf{x}\hat{n}_- + \sqrt{2} \int (q(\eta_\theta) - c)\hat{n}_- \cdot d\mathbf{x}\hat{n}_-^\perp \\ &= \left(\sqrt{2} \int p(\xi_\theta) d\xi_\theta + c\xi_\theta \right) \hat{n}(\theta - \frac{\pi}{4}) + \left(\sqrt{2} \int q(\eta_\theta) d\eta_\theta - c\eta_\theta \right) \hat{n}(\theta + \frac{\pi}{4}) + \mathbf{d} \end{aligned}$$

where $c \in \mathbb{R}$ and $\mathbf{d} \in \mathbb{R}^2$ are constants.

Characterization of dual fields with zero conjugate energy. The conjugate of \widehat{W} is [BK97, pg. 125]

$$\widehat{W}_\theta^*(\sigma) := \sup_{\epsilon \in M_{\text{sym}}^{2 \times 2}} \left\{ \epsilon \cdot \sigma - \widehat{W}_\theta(\epsilon) \right\} = \sqrt{2} |\sigma \cdot \hat{\epsilon}_{2\theta}|. \quad (5.21)$$

From (5.21), $\widehat{W}_\theta^*(\sigma) = 0$ precisely when $\sigma \cdot \hat{\epsilon}_{2\theta} = 0$. This occurs precisely when σ is of the form

$$\sigma(x, y) = \sigma_h(x, y)I + \sqrt{2}t(x, y)\hat{\epsilon}_{2\theta + \frac{\pi}{2}}.$$

Here I is shorthand for $\begin{pmatrix} 1 & 0 \\ 0 & 1 \end{pmatrix}$. This with the compatibility equation $\text{div}(\sigma) = 0$ implies

$$-\sin 2\theta \frac{\partial}{\partial x} t(x, y) + \cos 2\theta \frac{\partial}{\partial y} t(x, y) = \frac{\partial}{\partial x} \sigma_h(x, y) \quad (5.22a)$$

$$\cos 2\theta \frac{\partial}{\partial x} t(x, y) + \sin 2\theta \frac{\partial}{\partial y} t(x, y) = \frac{\partial}{\partial y} \sigma_h(x, y). \quad (5.22b)$$

These are a pair on non-homogeneous transport equations which can be written as

$$\nabla \sigma_h(x, y) = \begin{pmatrix} -\sin 2\theta & \cos 2\theta \\ \cos 2\theta & \sin 2\theta \end{pmatrix} \nabla t(x, y). \quad (5.23)$$

These imply that

$$\square_\theta^2 t(x, y) = 0, \quad (5.24a)$$

$$\square_\theta^2 \sigma_h(x, y) = 0. \quad (5.24b)$$

Compare (5.22) with (5.14); (5.23) with (5.15); and (5.24) with (5.9) and (5.16). In particular the characteristics of each of the two wave equations in (5.24) are inclined at angles $\theta - \frac{\pi}{4}$ and $\theta + \frac{\pi}{4}$.

5.2.2 Polycrystals

Note that $0 \in \overline{\mathcal{S}}$ for any polycrystal since the Taylor bound $\mathcal{T} = \{0\}$. We shall call a polycrystal ‘rigid’ if $\overline{\mathcal{S}} = \{0\}$ and ‘flexible’ otherwise. The characterization of strain fields in a grain in §5.2.1 leads to the following observation: any polycrystal in which a non-negligible set of characteristics percolate — i.e., do not intersect interfaces — is flexible. Example 5.13 presents one such polycrystal. However the flexibility of any polycrystal is limited:

Proposition 5.8. For any polycrystal, $\dim(\overline{\mathcal{S}}) \leq 1$.

Bhattacharya and Kohn [BK97, Thm. 5.3, pg.163] used a translation to prove this result for strain fields in $L^2(\Omega, M_{\text{sym}}^{2 \times 2})$. Here we use duality in the context of $L_{\text{per}}^\infty(\Omega, M_{\text{sym}}^{2 \times 2})$.

Proof. We shall prove the equivalent statement: for any polycrystal, $\dim(\bar{\mathcal{S}}) \neq 0 \Rightarrow \dim(\bar{\mathcal{S}}) = 1$. Let $0 \neq \bar{\epsilon} \in \bar{\mathcal{S}}$. Thus $\exists s, w \in L_{\text{per}}^\infty(\Omega, \mathbb{R})$ such that in a grain oriented at θ , the displacement gradient H is of the form

$$H(x, y) = \sqrt{2}s(x, y)\hat{\epsilon}_{2\theta} + w(x, y) \begin{pmatrix} 0 & 1 \\ -1 & 0 \end{pmatrix} \quad (5.13)$$

where

$$\nabla w(x, y) = \begin{pmatrix} -\sin 2\theta & \cos 2\theta \\ \cos 2\theta & \sin 2\theta \end{pmatrix} \nabla s(x, y); \quad (5.15)$$

at an interface between grains, for all (x, y) in the interface,

$$\llbracket H(x, y) \rrbracket \parallel \hat{n}^\perp(x, y) \otimes \hat{n}(x, y); \quad (5.25)$$

and

$$\sqrt{2}\langle s(x, y)\hat{\epsilon}_{2\theta(x, y)} \rangle = \bar{\epsilon}. \quad (5.26)$$

Consider the field which in each grain is given by

$$\sigma(x, y) = w(x, y)I + \sqrt{2}s(x, y)\hat{\epsilon}_{2\theta(x, y) + \frac{\pi}{2}}. \quad (5.27)$$

Note that $\sigma(x, y) \cdot \hat{\epsilon}_{2\theta(x, y)} = 0$. Observe that this is a dual field since it is divergence free: in each grain, (c.f. (5.15)),

$$\text{div}(\sigma(x, y)) = \nabla w(x, y) - \begin{pmatrix} -\sin 2\theta & \cos 2\theta \\ \cos 2\theta & \sin 2\theta \end{pmatrix} \nabla s(x, y) = 0;$$

at an interface between grains, for all (x, y) in the interface, $\llbracket \sigma(x, y) \rrbracket \hat{n}(x, y) = 0$:

$$\begin{aligned} \llbracket \sigma(x, y) \rrbracket &= \llbracket w(x, y)I + \sqrt{2}s(x, y)\hat{\epsilon}_{2\theta(x, y) + \frac{\pi}{2}} \rrbracket \\ &= \llbracket \sqrt{2}s(x, y)\hat{\epsilon}_{2\theta(x, y)} + w(x, y) \begin{pmatrix} 0 & 1 \\ -1 & 0 \end{pmatrix} \rrbracket \begin{pmatrix} 0 & 1 \\ -1 & 0 \end{pmatrix} \\ &= \llbracket H(x, y) \rrbracket \begin{pmatrix} 0 & 1 \\ -1 & 0 \end{pmatrix} \\ &= (\hat{n}^\perp(x, y) \otimes \hat{n}(x, y)) \begin{pmatrix} 0 & 1 \\ -1 & 0 \end{pmatrix} \\ &= \hat{n}^\perp(x, y) \otimes \hat{n}^\perp(x, y) \end{aligned}$$

where we have used $\hat{\epsilon}_{2\theta(x,y)+\frac{\pi}{2}} = \hat{\epsilon}_{2\theta(x,y)} \begin{pmatrix} 0 & 1 \\ -1 & 0 \end{pmatrix}$ and (5.25). Thus, using (5.26),

$$\begin{aligned} \langle \sigma(x, y) \rangle &= \langle w(x, y) \rangle I + \langle \sqrt{2}s(x, y) \hat{\epsilon}_{2\theta(x,y)+\frac{\pi}{2}} \rangle \\ &= \langle w(x, y) \rangle I + \langle \sqrt{2}s(x, y) \hat{\epsilon}_{2\theta(x,y)} \rangle \begin{pmatrix} 0 & 1 \\ -1 & 0 \end{pmatrix} \\ &= \langle w(x, y) \rangle I + \bar{\epsilon} \begin{pmatrix} 0 & 1 \\ -1 & 0 \end{pmatrix}. \end{aligned} \quad (5.28)$$

Let ϵ' be such that $\text{Tr } \epsilon' = 0$. By the dual variational principle (theorem 5.3) and (5.21),

$$\begin{aligned} \delta_{\bar{\mathcal{S}}}(\epsilon') &\geq \langle \sigma(x, y) \rangle \cdot \epsilon' - \langle |\sigma(x, y) \cdot \hat{\epsilon}_{2\theta(x,y)}| \rangle \\ &= \langle \sigma(x, y) \rangle \cdot \epsilon' \\ &= \langle w(x, y) \rangle I \cdot \epsilon' + \left(\epsilon' \begin{pmatrix} 0 & 1 \\ -1 & 0 \end{pmatrix} \right) \cdot \bar{\epsilon} \\ &= \left(\epsilon' \begin{pmatrix} 0 & 1 \\ -1 & 0 \end{pmatrix} \right) \cdot \bar{\epsilon} \\ &> 0, \end{aligned}$$

(by changing the sign of σ if necessary) except when $\epsilon' \parallel \bar{\epsilon}$. Thus

$$0 \neq \bar{\epsilon} \in \bar{\mathcal{S}} \quad \Rightarrow \quad \bar{\mathcal{S}} \subset \text{Span} \{ \bar{\epsilon} \} \quad \Rightarrow \quad \dim(\bar{\mathcal{S}}) = 1$$

□

We also present a variant of the above proof that does not use the dual variational principle:

Proof. Assume on the contrary that for a polycrystal $\dim(\bar{\mathcal{S}}) = 2$. Then, since $\bar{\mathcal{S}}$ is balanced⁷ and convex, there exists $\bar{\epsilon} \neq 0$ such that $\bar{\epsilon} \in \bar{\mathcal{S}}$ and $R_{\frac{\pi}{4}}^T \bar{\epsilon} R_{\frac{\pi}{4}} = \bar{\epsilon} \begin{pmatrix} 0 & 1 \\ -1 & 0 \end{pmatrix} \in \bar{\mathcal{S}}$. Since $\bar{\epsilon} \in \bar{\mathcal{S}}$, as in the proof above, there exist $s, w \in L_{\text{per}}^\infty(\Omega, \mathbb{R})$ such that $\sigma \in L_{\text{per}}^\infty(\Omega, M_{\text{sym}}^{2 \times 2})$ given by

$$\sigma(x, y) = w(x, y)I + \sqrt{2}s(x, y) \hat{\epsilon}_{2\theta(x,y)+\frac{\pi}{2}}. \quad (5.27)$$

and satisfying

$$\langle \sigma(x, y) \rangle = \langle w(x, y) \rangle I + \bar{\epsilon} \begin{pmatrix} 0 & 1 \\ -1 & 0 \end{pmatrix} \quad (5.28)$$

is divergence free. Since $\bar{\epsilon} \begin{pmatrix} 0 & 1 \\ -1 & 0 \end{pmatrix} \in \bar{\mathcal{S}}$, there exist $s', w' \in L_{\text{per}}^\infty(\Omega, \mathbb{R})$ such that $H \in L_{\text{per}}^\infty(\Omega, M^{2 \times 2})$ given by

$$H(x, y) = \sqrt{2}s'(x, y) \hat{\epsilon}_{2\theta(x,y)} + w'(x, y) \begin{pmatrix} 0 & 1 \\ -1 & 0 \end{pmatrix} \quad (5.29)$$

⁷ This follows from $\hat{\mathcal{S}}$ being balanced.

0	$\frac{\pi}{4}$	0	$-\frac{\pi}{4}$
$\frac{\pi}{4}$	0	$\frac{\pi}{4}$	0
0	$\frac{\pi}{4}$	0	$\frac{\pi}{4}$
$\frac{\pi}{4}$	0	$\frac{\pi}{4}$	0

Figure 5.5: A rigid checkerboard. Four periodic cells are shown.

and satisfying

$$\langle H(x, y) \rangle = \bar{\epsilon} \begin{pmatrix} 0 & 1 \\ -1 & 0 \end{pmatrix} + \langle w'(x, y) \rangle \begin{pmatrix} 0 & 1 \\ -1 & 0 \end{pmatrix} \quad (5.30)$$

is curl-free. Thus

$$\begin{aligned} \|\bar{\epsilon}\|^2 &= (\bar{\epsilon} \begin{pmatrix} 0 & 1 \\ -1 & 0 \end{pmatrix}) \cdot (\bar{\epsilon} \begin{pmatrix} 0 & 1 \\ -1 & 0 \end{pmatrix}) \\ &= \langle \sigma(x, y) \rangle \cdot \langle H(x, y) \rangle \end{aligned}$$

using (5.28) and (5.30). Since σ is divergence free and H is curl free, using the div-curl lemma this is

$$= \langle \sigma(x, y) \cdot H(x, y) \rangle$$

using (5.27) and (5.29)

$$\begin{aligned} &= \left\langle \left(w(x, y)I + \sqrt{2}s(x, y)\hat{\epsilon}_{2\theta(x, y) + \frac{\pi}{2}} \right) \cdot \left(\sqrt{2}s'(x, y)\hat{\epsilon}_{2\theta(x, y)} + w'(x, y) \begin{pmatrix} 0 & 1 \\ -1 & 0 \end{pmatrix} \right) \right\rangle \\ &= 0. \end{aligned}$$

Thus $\bar{\epsilon} = 0$, which is a contradiction. \square

Examples 5.9 and 5.10 below demonstrate optimal dual fields that are signed Radon measures supported on sets of Lebesgue measure zero.

Example 5.9 (A rigid checkerboard). Four periodic cells of a checkerboard whose grains are oriented at 0 and $\frac{\pi}{4}$ are shown in Figure 5.5. For this polycrystal $\bar{S} = \{0\}$.

Proof. Consider a measure valued field σ supported on the diagonal line shown in Figure 5.6 and taking the value $\begin{pmatrix} 1 \\ 1 \end{pmatrix} \otimes \begin{pmatrix} 1 \\ 1 \end{pmatrix} = \begin{pmatrix} 1 & 1 \\ 1 & 1 \end{pmatrix}$. Note that this field is divergence free and thus is contained in \mathcal{S}_{ad} . The average of this field is $\frac{1}{2} \begin{pmatrix} 1 & 1 \\ 1 & 1 \end{pmatrix}$. The support of the dual field lies within the grains oriented at 0. From the remark following (5.24) the conjugate energy of the dual field is zero. Thus from the dual variational principle (theorem 5.3), $\delta_{\mathcal{S}}^*(\bar{\epsilon}) \geq \langle \sigma \rangle \cdot \bar{\epsilon}$ which — changing the sign of σ if necessary — is positive except when $\bar{\epsilon} \parallel \begin{pmatrix} 1 & 0 \\ 0 & -1 \end{pmatrix}$.

Consider next a family σ_θ of measure valued fields, parameterized by $\theta \in (0, \frac{\pi}{4})$, supported on the lines shown in Figure 5.6 and taking the value

$$\left\{ \begin{array}{ll} \begin{pmatrix} 0 \\ 1 \end{pmatrix} \otimes \begin{pmatrix} 0 \\ 1 \end{pmatrix} & \text{on the vertical line} \\ & \text{(which, in a grain, is of length } 1 - \tan \theta), \\ \frac{1}{2 \sin \theta} \begin{pmatrix} \cos \theta \\ \sin \theta \end{pmatrix} \otimes \begin{pmatrix} \cos \theta \\ \sin \theta \end{pmatrix} & \text{on the lines inclined at } \theta \\ & \text{(which, in a grain, are of total length } \frac{1}{\sin \theta}), \\ \frac{1}{2 \sin \theta} \begin{pmatrix} \cos \theta \\ -\sin \theta \end{pmatrix} \otimes \begin{pmatrix} \cos \theta \\ -\sin \theta \end{pmatrix} & \text{on the lines inclined at } -\theta \\ & \text{(which, in a grain, are of total length } \frac{1}{\sin \theta}). \end{array} \right.$$

Note that the field is divergence free and thus is contained in \mathcal{S}_{ad} . The support of the dual field lies within the grains oriented at $\frac{\pi}{4}$. The average value of this field is

$$\begin{aligned} \langle \sigma_\theta \rangle &= \frac{1}{2} \left((1 - \tan \theta) \begin{pmatrix} 0 \\ 1 \end{pmatrix} \otimes \begin{pmatrix} 0 \\ 1 \end{pmatrix} + \frac{1}{2 \sin^2 \theta} \begin{pmatrix} \cos \theta \\ \sin \theta \end{pmatrix} \otimes \begin{pmatrix} \cos \theta \\ \sin \theta \end{pmatrix} + \frac{1}{2 \sin^2 \theta} \begin{pmatrix} \cos \theta \\ -\sin \theta \end{pmatrix} \otimes \begin{pmatrix} \cos \theta \\ -\sin \theta \end{pmatrix} \right) \\ &= \frac{1}{2} (1 - \tan \theta) \begin{pmatrix} 0 & 0 \\ 0 & 1 \end{pmatrix} + \frac{1}{4 \sin^2 \theta} \left(\begin{pmatrix} \cos^2 \theta & -\cos \theta \sin \theta \\ -\cos \theta \sin \theta & \sin^2 \theta \end{pmatrix} + \begin{pmatrix} \cos^2 \theta & \cos \theta \sin \theta \\ \cos \theta \sin \theta & \sin^2 \theta \end{pmatrix} \right) \\ &= \frac{1}{2} (1 - \tan \theta) \begin{pmatrix} 0 & 0 \\ 0 & 1 \end{pmatrix} + \frac{1}{2 \sin^2 \theta} \begin{pmatrix} \cos^2 \theta & 0 \\ 0 & \sin^2 \theta \end{pmatrix} \\ &= \frac{1}{2} \begin{pmatrix} \frac{1}{\tan^2 \theta} & 0 \\ 0 & 2 - \tan \theta \end{pmatrix}. \end{aligned}$$

The average conjugate energy is

$$\langle \delta_{\mathcal{S}}^*(R^T(x) \sigma_\theta R(x)) \rangle = \frac{\sqrt{2}}{4 \sin^2 \theta} |-\cos \theta \sin \theta| + \frac{\sqrt{2}}{4 \sin^2 \theta} |\cos \theta \sin \theta| = \frac{1}{\sqrt{2} \tan \theta}.$$

Note that the ratio

$$\frac{\langle \delta_{\mathcal{S}}^*(R^T(x) \sigma_\theta R(x)) \rangle}{\langle \sigma_\theta \rangle \cdot \begin{pmatrix} 1 & 0 \\ 0 & -1 \end{pmatrix}} = \frac{2\sqrt{2} \tan \theta}{\frac{1}{\tan^2 \theta} - 2 + \tan \theta} \rightarrow 0^+ \text{ as } \theta \rightarrow 0.$$

Thus for every $0 \neq \bar{\epsilon} \parallel \begin{pmatrix} 1 & 0 \\ 0 & -1 \end{pmatrix}$ with $\|\bar{\epsilon}\|$ sufficiently small, there exists θ such that $\delta_{\mathcal{S}}^*(\bar{\epsilon}) \geq \langle \sigma_\theta \rangle \cdot \bar{\epsilon} - \langle \delta_{\mathcal{S}}^*(R^T(x) \sigma_\theta R(x)) \rangle > 0$. \square

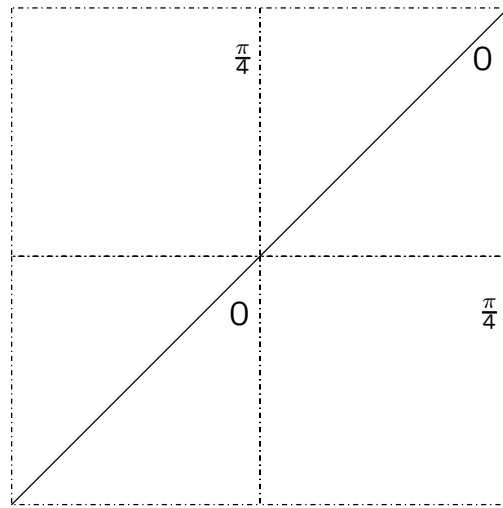


Figure 5.6: A dual field for the rigid checkerboard.

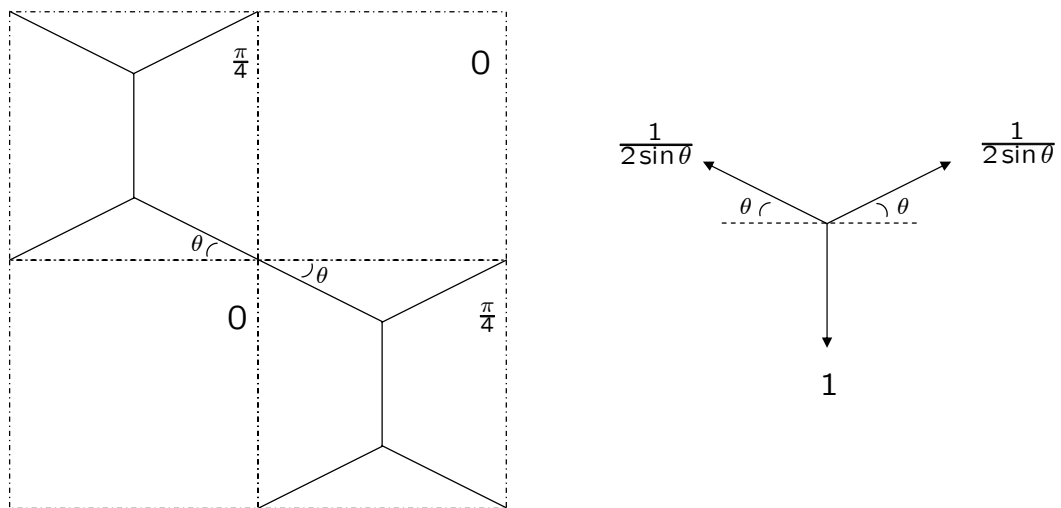


Figure 5.7: A dual field for the rigid checkerboard and a free body diagram showing force equilibrium.

ϕ	$-\phi$	ϕ	$-\phi$
$-\phi$	ϕ	$-\phi$	ϕ
ϕ	$-\phi$	ϕ	$-\phi$
$-\phi$	ϕ	$-\phi$	ϕ

Figure 5.8: A flexible checkerboard. Four periodic cells are shown.

Scalar examples presented in [BK97, §4] lead to the conjecture that a polycrystal is flexible only when strain fields ‘percolate’ through it. The following example shows that the situation is more complex in the context of elasticity by demonstrating a polycrystal that is flexible even though strain fields cannot percolate through it.

Example 5.10 (A flexible checkerboard). Four periodic cells of a checkerboard polycrystal are shown in Figure 5.8. The grains are oriented at ϕ and $-\phi$ for $\phi \in (0, \frac{\pi}{4})$. For this polycrystal $\bar{\mathcal{S}} = \{s \begin{pmatrix} 0 & 1 \\ 1 & 0 \end{pmatrix} \mid s \in \mathbb{R}, |s| \leq \tan \phi\}$.

This example also shows that the zero-set of a polycrystal could depend discontinuously on microstructure. As $\phi \rightarrow 0$ the zero-set jumps discontinuously from $\{s \begin{pmatrix} 0 & 1 \\ 1 & 0 \end{pmatrix} \mid s \in \mathbb{R}, |s| \leq \tan \phi\}$ to $\{s \begin{pmatrix} 1 & 0 \\ 0 & -1 \end{pmatrix} \mid s \in \mathbb{R}, |s| \leq 1\}$.

Proof 5.11. $\bar{\mathcal{S}} \supset \{s \begin{pmatrix} 0 & 1 \\ 1 & 0 \end{pmatrix} \mid s \in \mathbb{R}, |s| \leq \tan \phi\}$. Consider the piecewise constant displacement gradient field shown in Figure 5.9. Here

$$\hat{n}_+ = \begin{pmatrix} -\sin(\phi + \frac{\pi}{4}) \\ \cos(\phi + \frac{\pi}{4}) \end{pmatrix}, \quad \hat{n}_+^\perp = \begin{pmatrix} -\cos(\phi + \frac{\pi}{4}) \\ -\sin(\phi + \frac{\pi}{4}) \end{pmatrix},$$

$$\hat{n}_- = \begin{pmatrix} \sin(\phi + \frac{\pi}{4}) \\ \cos(\phi + \frac{\pi}{4}) \end{pmatrix}, \quad \hat{n}_-^\perp = \begin{pmatrix} -\cos(\phi + \frac{\pi}{4}) \\ \sin(\phi + \frac{\pi}{4}) \end{pmatrix}.$$

Note from (5.19) that

$$\begin{aligned} \hat{n}_- \otimes n_-^\perp - \hat{n}_-^\perp \otimes \hat{n}_- &= \begin{pmatrix} 0 & 1 \\ -1 & 0 \end{pmatrix}, \\ \hat{n}_+^\perp \otimes n_+ - \hat{n}_+ \otimes \hat{n}_+^\perp &= -\begin{pmatrix} 0 & 1 \\ -1 & 0 \end{pmatrix}, \\ \hat{n}_+ \otimes \hat{n}_+^\perp + \hat{n}_+^\perp \otimes \hat{n}_+ &= \sqrt{2}\epsilon_{2\phi}, \\ \hat{n}_- \otimes \hat{n}_-^\perp + \hat{n}_-^\perp \otimes \hat{n}_- &= -\sqrt{2}\epsilon_{-2\phi}. \end{aligned}$$

With this it is easy to see that all jump conditions are satisfied and that the (corresponding) strain

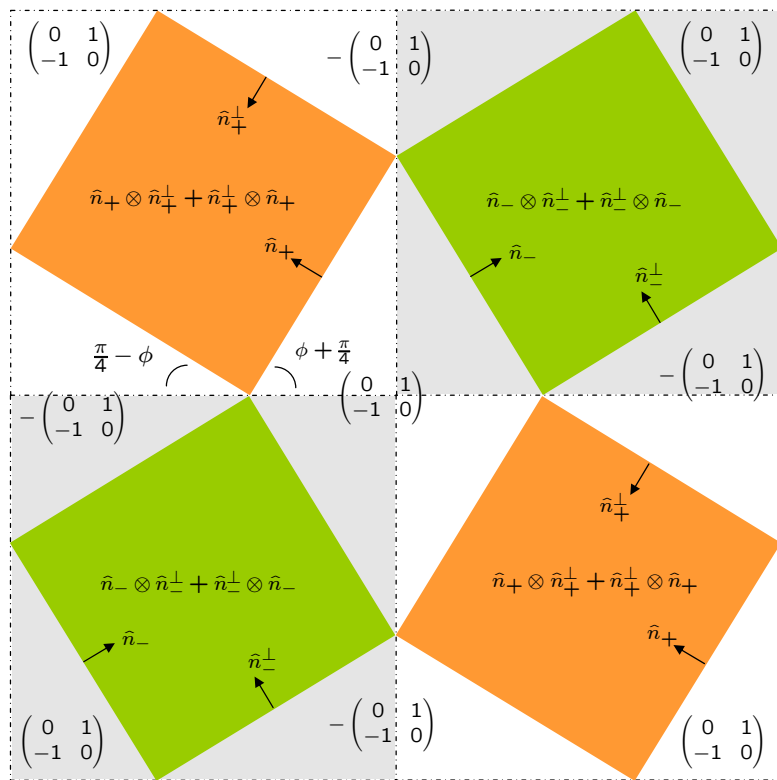


Figure 5.9: A strain field for the flexible checkerboard.

field lies within the zero set of each grain. Indeed, from (5.5) within the inner square in each grain, the strain field lies at the boundary of the zero set of that grain. Let each grain of the polycrystal be a square whose side is of length 1. A quick calculation reveals that the inner square is of area $\frac{\sec^2 \theta}{2}$. Thus the average strain in the polycrystal is

$$\frac{\sec^2 \theta}{4} (\sqrt{2}\epsilon_{2\phi} - \sqrt{2}\epsilon_{-2\phi}) = \frac{\sec^2 \theta}{4} \left(\begin{pmatrix} \cos 2\phi & \sin 2\phi \\ \sin 2\phi & -\cos 2\phi \end{pmatrix} - \begin{pmatrix} \cos 2\phi & -\sin 2\phi \\ -\sin 2\phi & \cos 2\phi \end{pmatrix} \right) = \tan \phi \begin{pmatrix} 0 & 1 \\ 1 & 0 \end{pmatrix}$$

□

Proof 5.12. $\bar{\mathcal{S}} \subset \{s \begin{pmatrix} 0 & 1 \\ 1 & 0 \end{pmatrix} \mid s \in \mathbb{R}, |s| \leq \tan \phi\}$. Since $\bar{\mathcal{S}} \supset \{s \begin{pmatrix} 0 & 1 \\ 1 & 0 \end{pmatrix} \mid s \in \mathbb{R}, |s| \leq \tan \phi\}$, from proposition 5.8, $\bar{\mathcal{S}} \subset \text{Span} \left\{ \begin{pmatrix} 0 & 1 \\ 1 & 0 \end{pmatrix} \right\}$. Consider a measure valued field σ supported on the lines shown in Figure 5.10 (see also Figure 5.11). On each line segment the value of the field is proportional to $\hat{t} \otimes \hat{t}$ where \hat{t} is tangent to the line; the magnitude of the value of the field on each line segment is marked in

Figure 5.10. Note that

$$\begin{aligned}\widehat{AB} &= \begin{pmatrix} \cos(\frac{\pi}{4}-\phi) \\ -\sin(\frac{\pi}{4}-\phi) \end{pmatrix}, & \widehat{BC} &= \begin{pmatrix} -\cos(\phi+\frac{\pi}{4}) \\ -\sin(\phi+\frac{\pi}{4}) \end{pmatrix}, & \widehat{CA} &= \begin{pmatrix} -\cos(\frac{\pi}{2}-\phi) \\ \sin(\frac{\pi}{2}-\phi) \end{pmatrix}, \\ \widehat{A'B'} &= \begin{pmatrix} -\cos(\phi+\frac{\pi}{4}) \\ \sin(\phi+\frac{\pi}{4}) \end{pmatrix}, & \widehat{B'C'} &= \begin{pmatrix} \cos(\frac{\pi}{4}-\phi) \\ \sin(\frac{\pi}{4}-\phi) \end{pmatrix}, & \widehat{C'A'} &= \begin{pmatrix} -\cos(\frac{\pi}{2}-\phi) \\ -\sin(\frac{\pi}{2}-\phi) \end{pmatrix}.\end{aligned}$$

To verify that this field is divergence free, it is sufficient to verify equilibrium at the points marked A/A' , B/B' and C/C' in Figure 5.10 (see Figure 5.12). At A/A' :

$$-\sin\phi \widehat{A'C'} + \sin(\phi + \frac{\pi}{4}) \widehat{A'B'} + \sin\phi \widehat{AC} + \cos(\phi + \frac{\pi}{4}) \widehat{AB} = 0.$$

That is,

$$\begin{aligned}-\sin\phi \begin{pmatrix} \cos(\frac{\pi}{2}-\phi) \\ \sin(\frac{\pi}{2}-\phi) \end{pmatrix} + \sin(\phi + \frac{\pi}{4}) \begin{pmatrix} -\cos(\phi+\frac{\pi}{4}) \\ \sin(\phi+\frac{\pi}{4}) \end{pmatrix} \\ + \sin\phi \begin{pmatrix} \cos(\frac{\pi}{2}-\phi) \\ -\sin(\frac{\pi}{2}-\phi) \end{pmatrix} + \cos(\phi + \frac{\pi}{4}) \begin{pmatrix} \cos(\frac{\pi}{4}-\phi) \\ -\sin(\frac{\pi}{4}-\phi) \end{pmatrix} = 0.\end{aligned}$$

At B/B' :

$$-\cos(\phi + \frac{\pi}{4}) \widehat{B'C'} + \cos(\phi + \frac{\pi}{4}) \widehat{BA} - \sin(\phi + \frac{\pi}{4}) \widehat{BC} + \sin(\phi + \frac{\pi}{4}) \widehat{B'A'} = 0.$$

That is,

$$\begin{aligned}-\cos(\phi + \frac{\pi}{4}) \begin{pmatrix} \cos(\frac{\pi}{4}-\phi) \\ \sin(\frac{\pi}{4}-\phi) \end{pmatrix} + \cos(\phi + \frac{\pi}{4}) \begin{pmatrix} -\cos(\frac{\pi}{4}-\phi) \\ \sin(\frac{\pi}{4}-\phi) \end{pmatrix} \\ - \sin(\phi + \frac{\pi}{4}) \begin{pmatrix} -\cos(\phi+\frac{\pi}{4}) \\ -\sin(\phi+\frac{\pi}{4}) \end{pmatrix} + \sin(\phi + \frac{\pi}{4}) \begin{pmatrix} \cos(\phi+\frac{\pi}{4}) \\ -\sin(\phi+\frac{\pi}{4}) \end{pmatrix} = 0.\end{aligned}$$

At C/C' :

$$-\sin(\phi + \frac{\pi}{4}) \widehat{CB} + \sin\phi \widehat{CA} - \cos(\phi + \frac{\pi}{4}) \widehat{C'B'} - \sin\phi \widehat{C'A'} = 0.$$

That is

$$\begin{aligned}-\sin(\phi + \frac{\pi}{4}) \begin{pmatrix} \cos(\phi+\frac{\pi}{4}) \\ \sin(\phi+\frac{\pi}{4}) \end{pmatrix} + \sin\phi \begin{pmatrix} -\cos(\frac{\pi}{2}-\phi) \\ \sin(\frac{\pi}{2}-\phi) \end{pmatrix} \\ - \cos(\phi + \frac{\pi}{4}) \begin{pmatrix} -\cos(\frac{\pi}{4}-\phi) \\ -\sin(\frac{\pi}{4}-\phi) \end{pmatrix} - \sin\phi \begin{pmatrix} -\cos(\frac{\pi}{2}-\phi) \\ -\sin(\frac{\pi}{2}-\phi) \end{pmatrix} = 0.\end{aligned}$$

Thus this field is contained in \mathcal{S}_{ad} . Let L be the length of a side of the inner square (shown partially

in dotted lines in Figure 5.10. Then

$$\begin{aligned}
\frac{2}{L}\langle\sigma\rangle &= \sqrt{2}\sin\phi\left(\left(\begin{array}{c}\cos(\phi+\frac{\pi}{2}) \\ \sin(\phi+\frac{\pi}{2})\end{array}\right)\otimes\left(\begin{array}{c}\cos(\phi+\frac{\pi}{2}) \\ \sin(\phi+\frac{\pi}{2})\end{array}\right)-\left(\begin{array}{c}\cos(\frac{\pi}{2}-\phi) \\ \sin(\frac{\pi}{2}-\phi)\end{array}\right)\otimes\left(\begin{array}{c}\cos(\frac{\pi}{2}-\phi) \\ \sin(\frac{\pi}{2}-\phi)\end{array}\right)\right) \\
&\quad -\sin\left(\phi+\frac{\pi}{4}\right)\left(\left(\begin{array}{c}\cos(\phi+\frac{\pi}{4}) \\ \sin(\phi+\frac{\pi}{4})\end{array}\right)\otimes\left(\begin{array}{c}\cos(\phi+\frac{\pi}{4}) \\ \sin(\phi+\frac{\pi}{4})\end{array}\right)-\left(\begin{array}{c}-\cos(\phi+\frac{\pi}{4}) \\ \sin(\phi+\frac{\pi}{4})\end{array}\right)\otimes\left(\begin{array}{c}-\cos(\phi+\frac{\pi}{4}) \\ \sin(\phi+\frac{\pi}{4})\end{array}\right)\right) \\
&\quad +\cos\left(\phi+\frac{\pi}{4}\right)\left(\left(\begin{array}{c}-\cos(\frac{\pi}{4}-\phi) \\ \sin(\frac{\pi}{4}-\phi)\end{array}\right)\otimes\left(\begin{array}{c}-\cos(\frac{\pi}{4}-\phi) \\ \sin(\frac{\pi}{4}-\phi)\end{array}\right)-\left(\begin{array}{c}\cos(\frac{\pi}{4}-\phi) \\ \sin(\frac{\pi}{4}-\phi)\end{array}\right)\otimes\left(\begin{array}{c}\cos(\frac{\pi}{4}-\phi) \\ \sin(\frac{\pi}{4}-\phi)\end{array}\right)\right) \\
&= \sqrt{2}\cos\phi\begin{pmatrix} 0 & 1 \\ 1 & 0 \end{pmatrix}
\end{aligned}$$

The average conjugate energy $\langle\delta_{\mathcal{S}}^*(R^T(x)\sigma R(x))\rangle$ is given by

$$\begin{aligned}
2\langle\delta_{\mathcal{S}}^*(R^T(x)\sigma R(x))\rangle &= (\sqrt{2}L)\sqrt{2}\left|\sin\phi\left(\begin{array}{c}\cos(\phi+\frac{\pi}{2}) \\ \sin(\phi+\frac{\pi}{2})\end{array}\right)\otimes\left(\begin{array}{c}\cos(\phi+\frac{\pi}{2}) \\ \sin(\phi+\frac{\pi}{2})\end{array}\right)\cdot\hat{\epsilon}_{2\phi}\right| \\
&\quad +(\sqrt{2}L)\sqrt{2}\left|\sin\phi\left(\begin{array}{c}\cos(\frac{\pi}{2}-\phi) \\ \sin(\frac{\pi}{2}-\phi)\end{array}\right)\otimes\left(\begin{array}{c}\cos(\frac{\pi}{2}-\phi) \\ \sin(\frac{\pi}{2}-\phi)\end{array}\right)\cdot\hat{\epsilon}_{-2\phi}\right| \\
&= 2\sqrt{2}L\sin\phi
\end{aligned}$$

Thus for any $\bar{\epsilon} = \lambda\begin{pmatrix} 0 & 1 \\ 1 & 0 \end{pmatrix}$, changing the sign of σ if necessary,

$$\langle\sigma\rangle\cdot\bar{\epsilon}-\delta_{\mathcal{S}}^*(R^T(x)\sigma R(x))\sim|\lambda|\cos\phi-\sin\phi$$

which is positive whenever $|\lambda|>\tan\phi$. □

Example 5.13 (Flexible strips). The polycrystal shown in Figure 5.13 is flexible since a non-negligible set of characteristics in the grain oriented at $\frac{\pi}{4}$ percolate. (For a grain oriented at $\frac{\pi}{4}$ the characteristics are horizontal and vertical.)

From proposition 5.8, for any polycrystal $\bar{\mathcal{S}}$ is either $\{0\}$ or a straight line segment centered at the origin. Thus

$$\bar{\epsilon}\in\bar{\mathcal{S}}\Rightarrow R_{\frac{\pi}{2}}^T\epsilon R_{\frac{\pi}{2}}=-\epsilon\in\bar{\mathcal{S}}.$$

So, as far as recoverable strains are concerned, any polycrystal has cubic symmetry. Any further symmetry would force $\bar{\mathcal{S}}$ to be $\{0\}$:

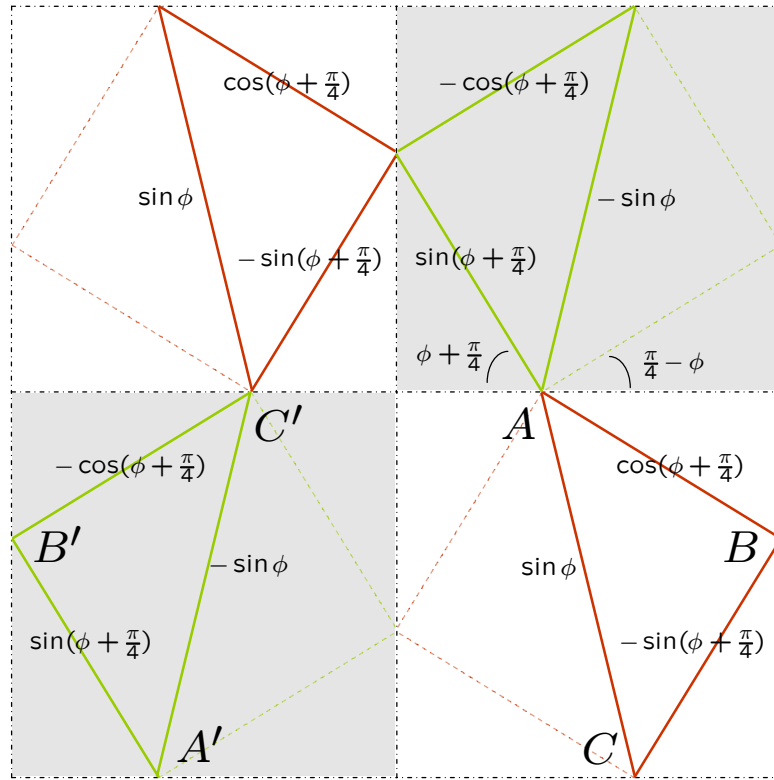


Figure 5.10: A dual field for the flexible checkerboard.

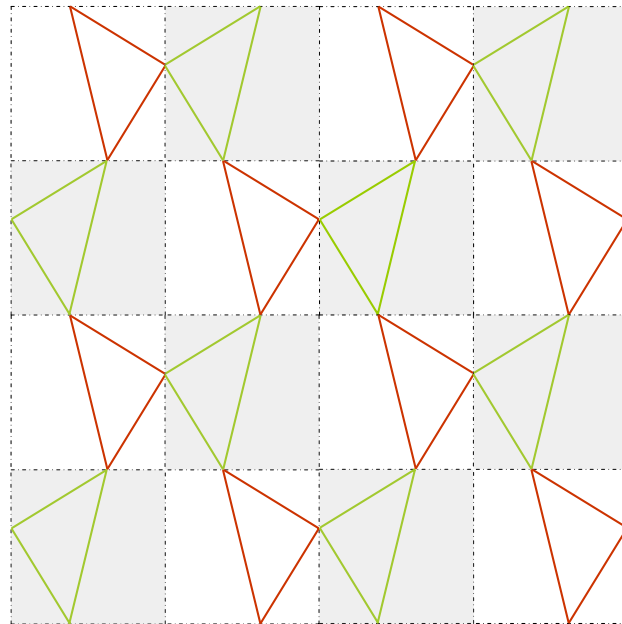


Figure 5.11: The same dual field as in Figure 5.10 with more grains shown.

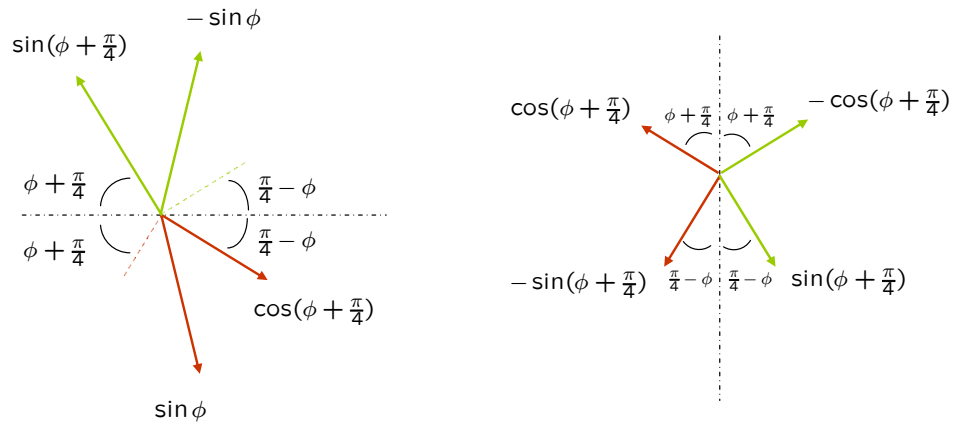
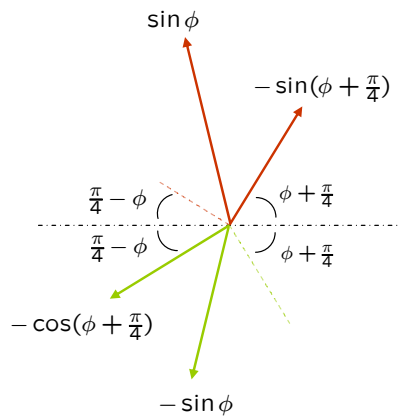
(a) Equilibrium at A/A' .(b) Equilibrium at B/B' .(c) Equilibrium at C/C' .

Figure 5.12: Free body diagrams for dual field shown in Figure 5.10.

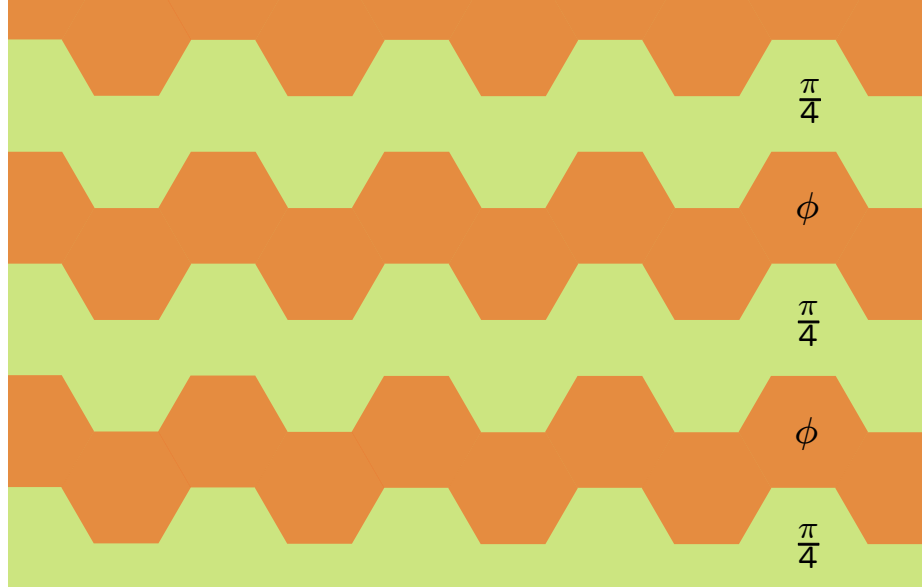


Figure 5.13: A flexible polycrystal.

Example 5.14 (Polycrystals with 120° symmetry are rigid). The polycrystals shown in Figures 5.14 and 5.15 are rigid. For the polycrystal in Figure 5.15 dual fields are easy to find and are shown in Figure 5.16.

5.3 Cubic-tetragonal materials

A material that undergoes the cubic-tetragonal transformation has a microscopic energy given by

$$W(\epsilon) = \min_{i=1,2,3} \{W_i(\epsilon)\},$$

$$W_i(\epsilon) = \frac{1}{2} \langle \alpha_i(\epsilon - \epsilon_i^T), (\epsilon - \epsilon_i^T) \rangle$$

where

$$\epsilon_1^T = \begin{pmatrix} \beta & 0 & 0 \\ 0 & \alpha & 0 \\ 0 & 0 & \alpha \end{pmatrix}, \quad \epsilon_2^T = \begin{pmatrix} \alpha & 0 & 0 \\ 0 & \beta & 0 \\ 0 & 0 & \alpha \end{pmatrix}, \quad \epsilon_3^T = \begin{pmatrix} \alpha & 0 & 0 \\ 0 & \alpha & 0 \\ 0 & 0 & \beta \end{pmatrix}.$$

The zero set of the mesoscopic energy is the convex hull of the three transformation strains [BK97, eq.(3.1), pg.116]:

$$\widehat{\mathcal{S}} = \{\epsilon \mid \epsilon_{12} = \epsilon_{13} = \epsilon_{23} = 0, \epsilon_{11} + \epsilon_{22} + \epsilon_{33} = 2\alpha + \beta, \min\{\alpha, \beta\} \leq \epsilon_{11}, \epsilon_{22}, \epsilon_{33} \leq \max\{\alpha, \beta\}\}$$

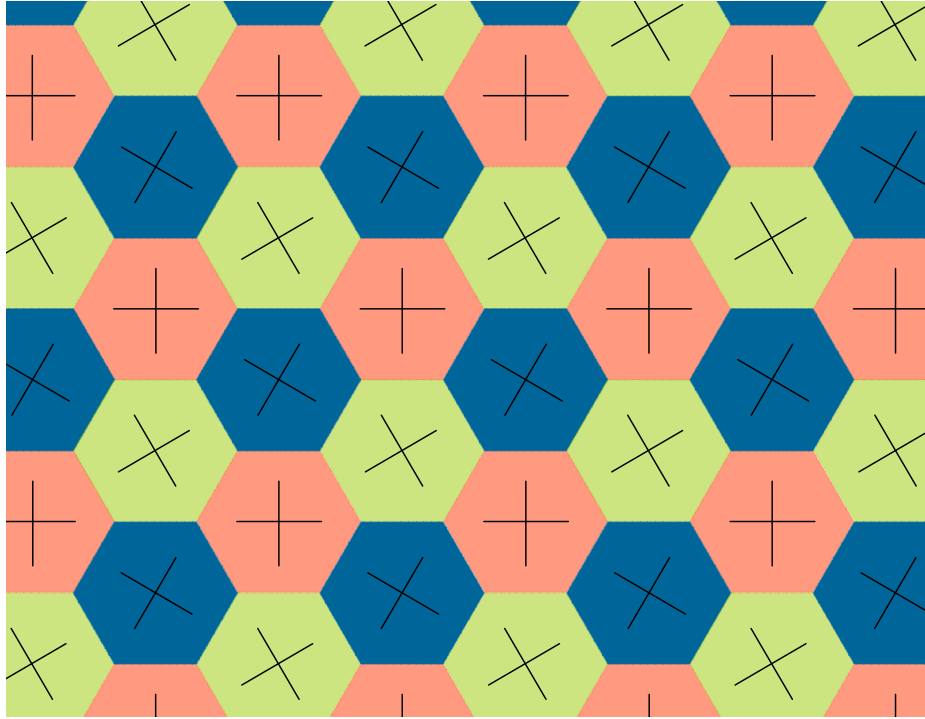


Figure 5.14: A polycrystal with 120° symmetry. The directions of the characteristics in each grain is shown.

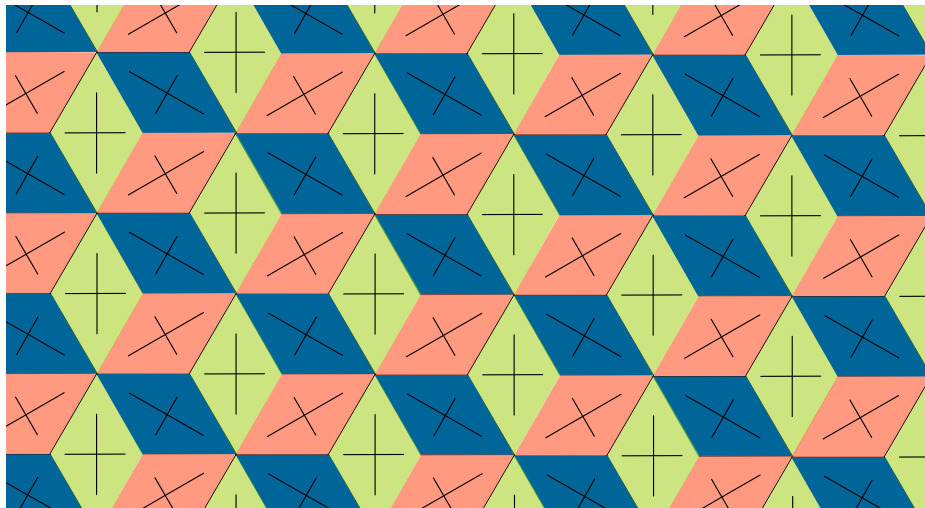


Figure 5.15: A polycrystal with 120° symmetry. The directions of the characteristics in each grain is shown.

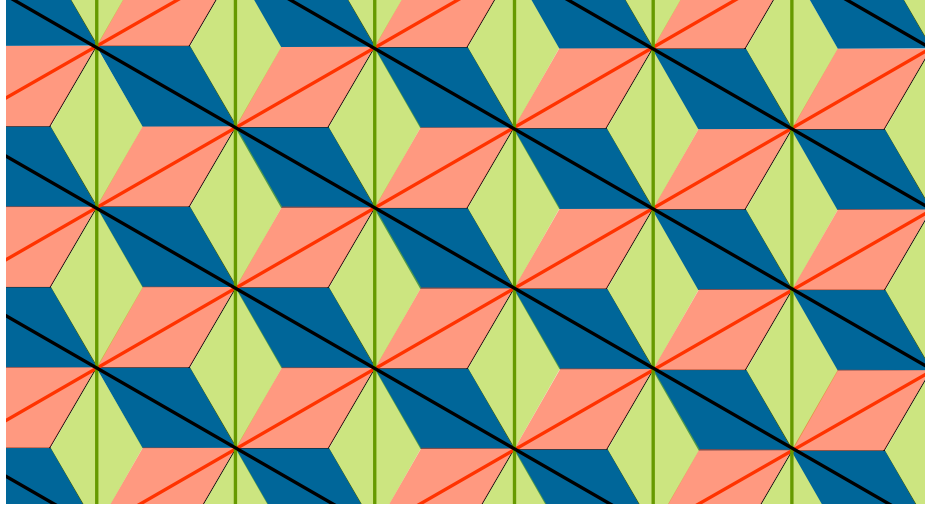


Figure 5.16: Three independent dual fields for the polycrystal shown in Figure 5.15.

The wave equation associated with $\hat{\mathcal{S}}$. The strain compatibility equation in 3-D is [Fun69, (6.3-3), pg.124] $\epsilon_{ij,kl} + \epsilon_{kl,ij} = \epsilon_{ik,jl} + \epsilon_{jl,ik}$. Since for $\epsilon \in \hat{\mathcal{S}}$, the non-diagonal components vanish, the 6 strain compatibility equations are [Fun69, (6.3-4), pg.124]

$$\frac{\partial^2}{\partial x_2 \partial x_3} \epsilon_{11} = 0, \quad (5.31a)$$

$$\frac{\partial^2}{\partial x_3 \partial x_1} \epsilon_{22} = 0, \quad (5.31b)$$

$$\frac{\partial^2}{\partial x_1 \partial x_2} \epsilon_{33} = 0, \quad (5.31c)$$

$$\frac{\partial^2}{\partial x_1^2} \epsilon_{22} + \frac{\partial^2}{\partial x_2^2} \epsilon_{11} = 0, \quad (5.31d)$$

$$\frac{\partial^2}{\partial x_2^2} \epsilon_{33} + \frac{\partial^2}{\partial x_3^2} \epsilon_{22} = 0, \quad (5.31e)$$

$$\frac{\partial^2}{\partial x_3^2} \epsilon_{11} + \frac{\partial^2}{\partial x_1^2} \epsilon_{33} = 0. \quad (5.31f)$$

Integrating the first three of these equations, for yet to be determined functions $f_1, f_2, f_3, g_1, g_2, g_3 \in L^\infty(\mathbb{R}^2, \mathbb{R})$,

$$\epsilon_{11} = f_2(x_1, x_3) + g_3(x_1, x_2),$$

$$\epsilon_{22} = f_3(x_1, x_2) + g_1(x_2, x_3),$$

$$\epsilon_{33} = f_1(x_2, x_3) + g_2(x_1, x_3).$$

Since $\epsilon_{11} + \epsilon_{22} + \epsilon_{33} = 2\alpha + \beta$ (a constant) we have

$$f_1(x_2, x_3) + g_1(x_2, x_3) + f_2(x_1, x_3) + g_2(x_1, x_3) + f_3(x_1, x_2) + g_3(x_1, x_2) = 2\alpha + \beta.$$

The first two terms are independent of x_1 ; the second two of x_2 ; and the last two of x_3 . Thus the sum of these six terms can add to an constant if and only if for constants c_1 , c_2 and c_3 ,

$$f_1(x_2, x_3) + g_1(x_2, x_3) = c_1,$$

$$f_2(x_1, x_3) + g_2(x_1, x_3) = c_2,$$

$$f_3(x_1, x_2) + g_3(x_1, x_2) = c_3.$$

Here $c_1 + c_2 + c_3 = 2\alpha + \beta$. Thus we obtain

$$\epsilon_{11} = f_2(x_1, x_3) - f_3(x_1, x_2) + c_3,$$

$$\epsilon_{22} = f_3(x_1, x_2) - f_1(x_2, x_3) + c_1,$$

$$\epsilon_{33} = f_1(x_2, x_3) - f_2(x_1, x_3) + c_2.$$

From these equations and (5.31),

$$\frac{\partial^2}{\partial x_2^2} \epsilon_{33} + \frac{\partial^2}{\partial x_3^2} \epsilon_{22} = 0 \quad \Rightarrow \quad \left(\frac{\partial^2}{\partial x_2^2} - \frac{\partial^2}{\partial x_3^2} \right) f_1(x_2, x_3) = 0,$$

$$\frac{\partial^2}{\partial x_3^2} \epsilon_{11} + \frac{\partial^2}{\partial x_1^2} \epsilon_{33} = 0 \quad \Rightarrow \quad \left(\frac{\partial^2}{\partial x_3^2} - \frac{\partial^2}{\partial x_1^2} \right) f_2(x_1, x_3) = 0,$$

$$\frac{\partial^2}{\partial x_1^2} \epsilon_{22} + \frac{\partial^2}{\partial x_2^2} \epsilon_{11} = 0 \quad \Rightarrow \quad \left(\frac{\partial^2}{\partial x_1^2} - \frac{\partial^2}{\partial x_2^2} \right) f_3(x_1, x_2) = 0.$$

The strain field. To summarize, the strain field in any un-oriented grain must be of the form

$$\epsilon_{11} = f_2(x_1, x_3) - f_3(x_1, x_2) + c_3, \tag{5.32a}$$

$$\epsilon_{22} = f_3(x_1, x_2) - f_1(x_2, x_3) + c_1, \tag{5.32b}$$

$$\epsilon_{33} = f_1(x_2, x_3) - f_2(x_1, x_3) + c_2 \tag{5.32c}$$

where $f_1, f_2, f_3 \in L^\infty(\mathbb{R}^2, \mathbb{R})$ satisfy

$$\left(\frac{\partial^2}{\partial x_2^2} - \frac{\partial^2}{\partial x_3^2} \right) f_1(x_2, x_3) = 0, \quad (5.33a)$$

$$\left(\frac{\partial^2}{\partial x_3^2} - \frac{\partial^2}{\partial x_1^2} \right) f_2(x_1, x_3) = 0, \quad (5.33b)$$

$$\left(\frac{\partial^2}{\partial x_1^2} - \frac{\partial^2}{\partial x_2^2} \right) f_3(x_1, x_2) = 0. \quad (5.33c)$$

As in §5.2 (c.f. (5.10)), associated with the three wave operators in (5.33) are three pairs of characteristic planes:

$$\Xi^{(1)} := \{(x_2, x_3) \mid \xi^{(1)} : \text{constant}\},$$

$$H^{(1)} := \{(x_2, x_3) \mid \eta^{(1)} : \text{constant}\};$$

$$\Xi^{(2)} := \{(x_3, x_1) \mid \xi^{(2)} : \text{constant}\},$$

$$H^{(2)} := \{(x_3, x_1) \mid \eta^{(2)} : \text{constant}\};$$

$$\Xi^{(3)} := \{(x_1, x_2) \mid \xi^{(3)} : \text{constant}\},$$

$$H^{(3)} := \{(x_1, x_2) \mid \eta^{(3)} : \text{constant}\}.$$

The displacement gradient. For $\epsilon \in \widehat{\mathcal{S}}$ the corresponding displacement gradient has the form

$$H = \begin{pmatrix} \epsilon_{11} & w_{12} & -w_{31} \\ -w_{12} & \epsilon_{22} & w_{23} \\ w_{31} & -w_{23} & \epsilon_{33} \end{pmatrix}.$$

Since H is a gradient, each of its rows is curl free. For the first row:

$$\frac{\partial}{\partial x_2} w_{31} + \frac{\partial}{\partial x_3} w_{12} = 0, \quad (5.34a)$$

$$\frac{\partial}{\partial x_3} \epsilon_{11} + \frac{\partial}{\partial x_1} w_{31} = 0, \quad (5.34b)$$

$$\frac{\partial}{\partial x_1} w_{12} - \frac{\partial}{\partial x_2} \epsilon_{11} = 0. \quad (5.34c)$$

For the second row:

$$\frac{\partial}{\partial x_2} w_{23} - \frac{\partial}{\partial x_3} \epsilon_{22} = 0, \quad (5.34d)$$

$$\frac{\partial}{\partial x_3} w_{12} + \frac{\partial}{\partial x_1} w_{23} = 0, \quad (5.34e)$$

$$\frac{\partial}{\partial x_1} \epsilon_{22} + \frac{\partial}{\partial x_2} w_{12} = 0. \quad (5.34f)$$

For the third row:

$$\frac{\partial}{\partial x_2} \epsilon_{33} + \frac{\partial}{\partial x_3} w_{23} = 0, \quad (5.34g)$$

$$\frac{\partial}{\partial x_3} w_{31} - \frac{\partial}{\partial x_1} \epsilon_{33} = 0, \quad (5.34h)$$

$$\frac{\partial}{\partial x_1} w_{23} + \frac{\partial}{\partial x_2} w_{31} = 0. \quad (5.34i)$$

Six of these equations involve ϵ . These with the first three equations of (5.31) give

$$\begin{aligned} \frac{\partial^2}{\partial x_1 \partial x_2} w_{31} &= -\frac{\partial^2}{\partial x_2 \partial x_3} \epsilon_{11} = 0, \\ \frac{\partial^2}{\partial x_3 \partial x_1} w_{12} &= \frac{\partial^2}{\partial x_2 \partial x_3} \epsilon_{11} = 0, \\ \frac{\partial^2}{\partial x_1 \partial x_2} w_{23} &= \frac{\partial^2}{\partial x_3 \partial x_1} \epsilon_{22} = 0, \\ \frac{\partial^2}{\partial x_2 \partial x_3} w_{12} &= -\frac{\partial^2}{\partial x_1 \partial x_3} \epsilon_{11} = 0, \\ \frac{\partial^2}{\partial x_3 \partial x_1} w_{23} &= -\frac{\partial^2}{\partial x_1 \partial x_2} \epsilon_{33} = 0, \\ \frac{\partial^2}{\partial x_2 \partial x_3} w_{31} &= \frac{\partial^2}{\partial x_1 \partial x_2} \epsilon_{33} = 0. \end{aligned}$$

That is,

$$\begin{aligned} \frac{\partial^2}{\partial x_1 \partial x_2} w_{23} &= \frac{\partial^2}{\partial x_3 \partial x_1} w_{23} = 0, \\ \frac{\partial^2}{\partial x_2 \partial x_3} w_{31} &= \frac{\partial^2}{\partial x_1 \partial x_2} w_{31} = 0, \\ \frac{\partial^2}{\partial x_3 \partial x_1} w_{12} &= \frac{\partial^2}{\partial x_2 \partial x_3} w_{12} = 0. \end{aligned}$$

From the above equations, for yet to be determined functions $h_1, h_2, h_3: \mathbb{R}^2 \rightarrow \mathbb{R}$, $w_{23} = h_1(x_2, x_3)$, $w_{31} = h_2(x_1, x_3)$ and $w_{12} = h_3(x_1, x_2)$. This with (5.32) and the six equations of (5.34) that involve

ϵ gives

$$\begin{aligned} \frac{\partial}{\partial x_2} f_1(x_2, x_3) + \frac{\partial}{\partial x_3} h_1(x_2, x_3) &= 0, \\ \frac{\partial}{\partial x_3} f_1(x_2, x_3) + \frac{\partial}{\partial x_2} h_1(x_2, x_3) &= 0, \\ \frac{\partial}{\partial x_3} f_2(x_3, x_1) + \frac{\partial}{\partial x_1} h_2(x_3, x_1) &= 0, \\ \frac{\partial}{\partial x_1} f_2(x_3, x_1) + \frac{\partial}{\partial x_3} h_2(x_3, x_1) &= 0, \\ \frac{\partial}{\partial x_1} f_3(x_1, x_2) + \frac{\partial}{\partial x_2} h_3(x_1, x_2) &= 0, \\ \frac{\partial}{\partial x_2} f_3(x_1, x_2) + \frac{\partial}{\partial x_1} h_3(x_1, x_2) &= 0 \end{aligned}$$

(the three equations of (5.34) that involve only ws are trivially satisfied). Thus we obtain three pairs of non-homogeneous transport equations for h_1 , h_2 and h_3 :

$$\begin{aligned} \nabla_{23} h_1 &= - \begin{pmatrix} 0 & 1 \\ 1 & 0 \end{pmatrix} \nabla_{23} f_1 \\ \nabla_{31} h_2 &= - \begin{pmatrix} 0 & 1 \\ 1 & 0 \end{pmatrix} \nabla_{31} f_2 \\ \nabla_{12} h_3 &= - \begin{pmatrix} 0 & 1 \\ 1 & 0 \end{pmatrix} \nabla_{12} f_3 \end{aligned}$$

where ∇_{ij} is shorthand for $\begin{pmatrix} \frac{\partial}{\partial x_i} \\ \frac{\partial}{\partial x_j} \end{pmatrix}$. This implies that $h_1, h_2, h_3 \in L^\infty(\mathbb{R}^2, \mathbb{R})$. Thus $H \in L^\infty(\mathbb{R}^3, M^{3 \times 3})$ and $u \in W^{1, \infty}(\mathbb{R}^3, \mathbb{R}^3)$. To summarize, the displacement gradient H in any un-oriented grain is of the form

$$H(x) = H^{(1)}(x_2, x_3) + H^{(2)}(x_3, x_1) + H^{(3)}(x_1, x_2) \quad (5.35a)$$

where

$$H^{(1)} = \begin{pmatrix} 0 & 0 & 0 \\ 0 & -f_1(x_2, x_3) & h_1(x_2, x_3) \\ 0 & -h_1(x_2, x_3) & f_1(x_2, x_3) \end{pmatrix}, \quad (5.35b)$$

$$H^{(2)} = \begin{pmatrix} f_2(x_1, x_3) & 0 & -h_2(x_1, x_3) \\ 0 & 0 & 0 \\ h_2(x_1, x_3) & 0 & -f_2(x_1, x_3) \end{pmatrix}, \quad (5.35c)$$

$$H^{(3)} = \begin{pmatrix} -f_3(x_1, x_2) & h_3(x_1, x_2) & 0 \\ -h_3(x_1, x_2) & f_3(x_1, x_2) & 0 \\ 0 & 0 & 0 \end{pmatrix}; \quad (5.35d)$$

$f_1, f_2, f_3 \in L^\infty(\mathbb{R}^2, \mathbb{R})$ satisfy

$$\left(\frac{\partial^2}{\partial x_2^2} - \frac{\partial^2}{\partial x_3^2} \right) f_1(x_2, x_3) = 0,$$

$$\left(\frac{\partial^2}{\partial x_3^2} - \frac{\partial^2}{\partial x_1^2} \right) f_2(x_1, x_3) = 0,$$

$$\left(\frac{\partial^2}{\partial x_1^2} - \frac{\partial^2}{\partial x_2^2} \right) f_3(x_1, x_2) = 0;$$

and $h_1, h_2, h_3 \in L^\infty(\mathbb{R}^2, \mathbb{R})$ satisfy

$$\nabla_{23} h_1 = - \begin{pmatrix} 0 & 1 \\ 1 & 0 \end{pmatrix} \nabla_{23} f_1, \tag{5.36a}$$

$$\nabla_{31} h_2 = - \begin{pmatrix} 0 & 1 \\ 1 & 0 \end{pmatrix} \nabla_{31} f_2, \tag{5.36b}$$

$$\nabla_{12} h_3 = - \begin{pmatrix} 0 & 1 \\ 1 & 0 \end{pmatrix} \nabla_{12} f_3. \tag{5.36c}$$

Comparing (5.35) to (5.20); (5.33) to (5.7) (with $\theta = 0$); and (5.36) to (5.15) (with $\theta = 0$), notice that each of $H^{(1)}$, $H^{(2)}$ and $H^{(3)}$ is essentially identical in form to the displacement gradient for the material considered in §5.2.

Chapter 6

Conclusions

In Chapters 3 and 4 we studied the relaxation of a two-well energy (possibly under fixed volume fractions) and discussed the applications of these results to the study of Nickel super-alloys used in turbine blades and other high temperature applications. The results we prove here, especially insights into extremal microstructures, provide a benchmark to evaluate computations of microstructure evolution.

From a mathematical standpoint, the methods we use follow closely those that have been used before. However, we find a surprising extension to three dimensions when the moduli are isotropic. The method also provides a lower bound when the moduli are anisotropic; however it is not yet clear if this bound is optimal. Similarly, the extension of such methods to more than two wells remains open.

In Chapter 5 we discussed some model problems that provide insight into the nature of stress and strains fields in polycrystals made of shape-memory alloys. The dual of the problem studied here concerns rigid-perfectly plastic materials. In this setting, if the single crystal of a material has a deficient number of slip systems, an important question is whether a polycrystal of this material is macroscopically rigid-perfectly plastic or simply rigid. It was recently formulated in a setting dual to ours [KL98]. Our results also have a direct implication to these problems.

Both the shape-memory and the plasticity problem have been studied extensively recently using examples [BK97, KL98, BKK99, Gol01, Gol03, GK03]. However, all of this literature has been confined to two-dimensional scalar problems. We considered two-dimensional elasticity and noted that there are nontrivial differences.

Bibliography

- [ACLM88] M. Avellaneda, Andrej V. Cherkaev, K. A. Lurie, and Graeme W. Milton, *On the effective conductivity of polycrystals and a three-dimensional phase interchange inequality*, *Journal of Applied Physics* **63** (1988), 4989–5003. (Cited on page [28](#).)
- [AF84] E. Acerbi and N. Fusco, *Semicontinuity problems in the calculus of variations*, *Archive for Rational Mechanics and Analysis* **86** (1984), 125–145. (Cited on pages [19](#), [20](#) and [23](#).)
- [AJK02] A. Artemev, Y. M. Jin, and A. G. Khachaturyan, *Three-dimensional phase field model and simulation of cubic-tetragonal martensitic transformation in polycrystals*, *Philosophical Magazine A* **82** (2002), 1249–1270. (Cited on page [89](#).)
- [AK93a] Gregoire Allaire and Robert V. Kohn, *Explicit optimal bounds on the elastic energy of a two-phase composite in two space dimensions*, *Quarterly of Applied Mathematics* **12** (1993), no. 4, 643–674. (Cited on pages [22](#) and [45](#).)
- [AK93b] ———, *Optimal bounds on the effective behavior of a mixture of two well-ordered elastic materials*, *Quarterly of Applied Mathematics* **12** (1993), no. 4, 643–674. (Cited on page [22](#).)
- [AK94] ———, *Optimal lower bounds on the elastic energy of a composite made from two non-well-ordered isotropic materials*, *Quarterly of Applied Mathematics* **52** (1994), no. 2, 311–333. (Cited on page [22](#).)
- [ALS03] R. Ahluwalia, T. Lookman, and A. Saxena, *Elastic deformation of polycrystals*, *Physical Review Letters* **91** (2003), no. 5. (Cited on page [89](#).)
- [Arl90] G. Arlt, *Twinning in ferroelectric and ferroelastic ceramics stress relief*, *Journal of Materials Science* **25** (1990), 2655–2666. (Cited on page [11](#).)
- [ATV01] Norio Akaiwa, K. Thornton, and Peter W. Voorhees, *Large-scale simulations of microstructural evolution in elastically stressed solids*, *Journal of Computational Physics* **173** (2001), 61–86. (Cited on page [5](#).)

- [Bha93] Kaushik Bhattacharya, *Comparison of the geometrically nonlinear and linear theories of martensitic transformation*, Continuum Mechanics and Thermodynamics **5** (1993), 205–242. (Cited on page 16.)
- [Bha03] ———, *Microstructure of martensite: Why it forms and how it gives rise to the shape-memory effect?*, Oxford Series on Materials Modelling 2, Oxford University Press, 2003. (Cited on pages 2, 7, 10, 18, 19, 20, 22 and 45.)
- [Bir46] G. Birkhoff, *Tres observaciones sobre el algebra lineal*, Univ. Nac. Tucumán Rev. Ser. A **5** (1946), 147–151. (Cited on page 71.)
- [BJ87] John M. Ball and Richard D. James, *Fine phase mixtures as minimizers of energy*, Archive for Rational Mechanics and Analysis **100** (1987), no. 1, 13–52. (Cited on pages 16 and 19.)
- [BJ92] ———, *Proposed experimental tests of a theory of fine microstructure*, Philosophical Transactions of the Royal Society of London. Series A **338** (1992), 389–450. (Cited on page 16.)
- [BK96] Kaushik Bhattacharya and Robert V. Kohn, *Symmetry, texture and the recoverable strains of shape-memory polycrystals*, Acta Materialia **44** (1996), no. 2, 529–542. (Cited on page 25.)
- [BK97] ———, *Elastic energy minimization and the recoverable strains of polycrystalline shape-memory materials*, Archive for Rational Mechanics and Analysis **139** (1997), 99–180. (Cited on pages 10, 21, 24, 25, 27, 96, 101, 107, 113 and 121.)
- [BKK99] Kaushik Bhattacharya, Robert V. Kohn, and S. Kozlov, *Some examples of nonlinear homogenization involving nearly degenerate energies*, Proceedings of the Royal Society of London. Series A - Mathematical Physical and Engineering Sciences **455** (1999), 567–583. (Cited on page 121.)
- [BL96] J. G. Boyd and D. C. Lagoudas, *A thermodynamical constitutive model for shape memory materials I. The monolithic shape memory alloy*, International Journal of Plasticity **12** (1996), 805–842. (Cited on page 89.)
- [BL99a] Z. H. Bo and D. C. Lagoudas, *Thermomechanical modeling of polycrystalline SMAs under cyclic loading I. Theoretical derivations*, International Journal of Engineering Science **37** (1999), 1089–1140. (Cited on page 89.)
- [BL99b] ———, *Thermomechanical modeling of polycrystalline SMAs under cyclic loading II. Material characterization and experimental results for a stable transformation cy-*

- cle*, International Journal of Engineering Science **37** (1999), 1141–1173. (Cited on page 89.)
- [BL99c] ———, *Thermomechanical modeling of polycrystalline SMAs under cyclic loading III. Evolution of plastic strains and two-way shape memory effect*, International Journal of Engineering Science **37** (1999), 1175–1203. (Cited on page 89.)
- [BL99d] ———, *Thermomechanical modeling of polycrystalline SMAs under cyclic loading IV. Modeling of minor hysteresis loops*, International Journal of Engineering Science **37** (1999), 1205–1249. (Cited on page 89.)
- [BS04] Kaushik Bhattacharya and P. Suquet, *A model problem for recoverable strains in polycrystals (draft)*. (Cited on page 96.)
- [CA97] J. H. Cho and A. J. Ardell, *Coarsening of Ni_3Si precipitates in binary Ni-Si alloys at intermediate to large volume fractions*, Acta Materialia **45** (1997), no. 4, 1393–1400. (Cited on pages 2, 3, 5, 45, 53 and 54.)
- [CA98] ———, *Coarsening of Ni_3Si precipitates at volume fractions from 0.03 to 0.30*, Acta Materialia **46** (1998), no. 16, 5907–5916. (Cited on page 2.)
- [CA01] Luciano Carbone and Riccardo De Arcangelis, *Unbounded functionals in the calculus of variations: Representation, relaxation and homogenization*, Monographs and Surveys in Pure and Applied Mathematics 125, Chapman and Hall / CRC, 2001. (Cited on page 92.)
- [CG92] Andrej V. Cherkaev and L. V. Gibiansky, *The exact coupled bounds for effective tensors of electrical and magnetic properties of two-component two-dimensional composites*, Proceedings of the Royal Society of Edinburgh. Section A, Mathematical and Physical Sciences **122** (1992), no. 1-2, 93–125. (Cited on page 28.)
- [Che00] Andrej V. Cherkaev, *Variational methods for structural optimization*, Applied Mathematical Sciences 140, Springer, 2000. (Cited on pages 28, 36 and 51.)
- [Che02] L. Q. Chen, *Phase-field models for microstructure evolution*, Annual Review of Materials Research **32** (2002), 113–140. (Cited on page 5.)
- [Chr02] John Wyrill Christian, *The theory of transformations in metals and alloys*, 3 ed., Pergamon Press, 2002. (Cited on page 2.)
- [CK88] M. Chipot and D. Kinderlehrer, *Equilibrium configurations of crystals*, Archive for Rational Mechanics and Analysis **103** (1988), 237–277. (Cited on page 19.)

- [Dac82] Bernard Dacorogna, *Quasiconvexity and relaxation of nonconvex problems in the calculus of variations*, Journal of Functional Analysis **31** (1982), 102–118. (Cited on page 20.)
- [Dac89] ———, *Direct methods in the calculus of variations*, Applied Mathematical Sciences 78, Springer-Verlag, 1989. (Cited on pages 19, 20 and 29.)
- [Dem85a] Françoise Demengel, *Déplacements à déformations bornées et champs de contrainte mesures [Displacements with bounded deformations and measure stress fields]*, Annali della Scuola Normale Superiore di Pisa. Classe di Scienze. Serie IV **12** (1985), no. 2, 243–318. (Cited on pages 92 and 95.)
- [Dem85b] ———, *Relaxation et existence pour le problème des matériaux à blocage [Relaxation and existence for the problem of locking materials]*, RAIRO Modélisation Mathématique et Analyse Numérique **19** (1985), no. 3, 351–395. (Cited on page 92.)
- [Dem89] ———, *Compactness theorems for spaces of functions with bounded derivatives and applications to limit analysis problems in plasticity*, Archive for Rational Mechanics and Analysis **105** (1989), no. 2, 123–161. (Cited on page 96.)
- [DM93] G. Dal Maso, *An introduction to Γ -convergence*, Birkhäuser, 1993. (Cited on pages 19, 23 and 24.)
- [DS86] Françoise Demengel and Pierre Suquet, *On locking materials*, Acta Applicandae Mathematicae **6** (1986), 185–211. (Cited on page 92.)
- [EH90] S. Eucken and J. Hirsch, *The effect of textures on shape memory behaviour*, Materials Science Forum **56–58** (1990), 487–492. (Cited on page 25.)
- [EMT⁺81] K. Enami, V. V. Martynov, T. Tomie, L. G. Khandros, and S. Nenno, *Deformation behavior of Ni-Al $L1_0$ (3R) martensite*, Trans. Jap. Inst. Metals **22** (1981), 357–366. (Cited on page 25.)
- [Eri84] J. L. Ericksen, *The cauchy and born hypothesis for crystals*, Phase transformations and material instabilities in solids (M. E. Gurtin, ed.), Academic Press, 1984, pp. 61–78. (Cited on page 16.)
- [Esh61] J. D. Eshelby, *Elastic inclusions and inhomogenities*, Progress in solid mechanics (I. N. Sneddon and R. Hill, eds.), 1961, pp. 87–140. (Cited on page 16.)
- [ET76] I. Ekeland and Roger Temam, *Convex analysis and variational problems*, North-Holland, 1976. (Cited on pages 43 and 93.)

- [Fal89] F. Falk, *Pseudoelastic stress-strain curves of polycrystalline shape memory alloys calculated from single crystal data*, International Journal of Engineering Science **27** (1989), 277–284. (Cited on page 89.)
- [Fir91] Nikan B. Firoozye, *Optimal use of the translation method and relaxations of variational problems*, Communications on Pure and Applied Mathematics **44** (1991), 643–678. (Cited on page 28.)
- [FM86] G. A. Francfort and S. Müller, *Homogenization and optimal bounds in linear elasticity*, Archive for Rational Mechanics and Analysis **94** (1986), no. 4, 307–334. (Cited on page 36.)
- [Fon91] I. Fonseca, *The Wulff theorem revisited*, Proceedings of the Royal Society of London. Series A - Mathematical Physical and Engineering Sciences **432** (1991), 125–145. (Cited on page 5.)
- [Fun69] Y. C. Fung, *A first course in continuum mechanics*, Prentice Hall, 1969. (Cited on page 115.)
- [GC84] L. V. Gibiansky and Andrej V. Cherkaev, *Design of composite plates of extremal rigidity*, Tech. Report 914, Ioffe Physico-technical Institute, Academy of Sciences, USSR, Leningrad, USSR, 1984, English translation in [GC97a]. (Cited on pages 28 and 126.)
- [GC87] ———, *Microstructures of composites of extremal rigidity and exact bounds on the associated energy density*, Tech. Report 1115, Ioffe Physico-technical Institute, Academy of Sciences, USSR, Leningrad, USSR, 1987, English translation in [GC97b]. (Cited on pages 28 and 126.)
- [GC97a] ———, *Design of composite plates of extremal rigidity*, Topics in the mathematical modelling of composite materials (Andrej V. Cherkaev and Robert V. Kohn, eds.), Progress in nonlinear differential equations and their applications 31, Birkhäuser, 1997, English translation of [GC84], pp. 95–137. (Cited on page 126.)
- [GC97b] ———, *Microstructures of composites of extremal rigidity and exact bounds on the associated energy density*, Topics in the mathematical modelling of composite materials (Andrej V. Cherkaev and Robert V. Kohn, eds.), Progress in nonlinear differential equations and their applications 31, Birkhäuser, 1997, English translation of [GC87], pp. 273–317. (Cited on page 126.)

- [GK95a] Yury Grabovsky and Robert V. Kohn, *Anisotropy of the Vigdergauz microstructure*, Transactions of the ASME E Journal of Applied Mechanics **62** (1995), no. 4, 1063–1065. (Cited on page [42](#).)
- [GK95b] ———, *Microstructures minimizing the energy of a two-phase elastic composite in two space dimensions. I. The confocal ellipse construction*, Journal of the Mechanics and Physics of Solids **43** (1995), no. 6, 933–947. (Cited on page [42](#).)
- [GK95c] ———, *Microstructures minimizing the energy of a two-phase elastic composite in two space dimensions. II. The Vigdergauz microstructure*, Journal of the Mechanics and Physics of Solids **43** (1995), no. 6, 949–972. (Cited on page [42](#).)
- [GK03] Adriana Garroni and Robert V. Kohn, *Some three-dimensional problems related to dielectric breakdown and polycrystal plasticity*, Proceedings of the Royal Society of London. Series A - Mathematical Physical and Engineering Sciences **459** (2003), 2613–2625. (Cited on page [121](#).)
- [GMH02] S. Govindjee, A. Mielke, and G. J. Hall, *The free energy of mixing for n -variant martensitic phase transformations using quasi-convex analysis*, Journal of the Mechanics and Physics of Solids **50** (2002), no. 9, 1897–1922, See [[GMH03](#)] for corrected version. (Cited on pages [22](#) and [127](#).)
- [GMH03] ———, *The free energy of mixing for n -variant martensitic phase transformations using quasi-convex analysis*, Journal of the Mechanics and Physics of Solids **51** (2003), no. 4, I–XXVI, Corrected version of [[GMH02](#)]. (Cited on page [127](#).)
- [Gol01] Guillermo H. Goldsztein, *Rigid perfectly plastic two-dimensional polycrystals*, Proceedings of the Royal Society of London. Series A - Mathematical Physical and Engineering Sciences **457** (2001), 2789–2798. (Cited on page [121](#).)
- [Gol03] ———, *Two-dimensional rigid polycrystals whose grains have one ductile direction*, Proceedings of the Royal Society of London. Series A - Mathematical Physical and Engineering Sciences **459** (2003), 1949–1968. (Cited on page [121](#).)
- [GP83] K. Golden and G. C. Papanicolaou, *Bounds for effective parameters of heterogeneous media by analytic continuation*, Communications in Mathematical Physics **90** (1983), 473–491. (Cited on page [24](#).)
- [Gra96] Yury Grabovsky, *Bounds and extremal microstructures for two-component composites: A unified treatment based on the translation method*, Proceedings of the Royal Society of London. Series A - Mathematical Physical and Engineering Sciences **452** (1996), 919–944. (Cited on pages [22](#) and [42](#).)

- [HC01] S. Y. Hu and L. Q. Chen, *A phase-field model for evolving microstructures with strong elastic inhomogeneity*, *Acta Materialia* **49** (2001), no. 11, 1879–1890. (Cited on page 5.)
- [JC84] W. C. Johnson and J. W. Cahn, *Elastically induced shape bifurcations of inclusions*, *Acta Metallurgica* **32** (1984), no. 11, 1925–1933. (Cited on page 5.)
- [JKO94] V. V. Jikov, S. M. Kozlov, and O. A. Oleinik, *Homogenization of differential operators and integral functionals*, Springer, 1994. (Cited on pages 23 and 24.)
- [JLL97] H. J. Jou, P. H. Leo, and J. S. Lowengrub, *Microstructural evolution in inhomogeneous elastic media*, *Journal of Computational Physics* **131** (1997), no. 1, 109–148. (Cited on page 5.)
- [JV87] W. C. Johnson and Peter W. Voorhees, *Elastic interaction and stability of misfitting cuboidal inhomogeneities*, *Journal of Applied Physics* **61** (1987), no. 4, 1610–1619. (Cited on page 5.)
- [Kat03] Daniel J. Katz, 2003, (Private Communication). (Cited on page 72.)
- [Kha83] A. G. Khachaturyan, *Theory of structural transformations in solids*, John Wiley and Sons, 1983. (Cited on pages 5, 16 and 37.)
- [KK90] S. Kajiwara and T. Kikuchi, *Shape memory effect and related transformation behavior in Fe Ni C alloys*, *Acta Metallurgica et Materialia* **38** (1990), 847–855. (Cited on page 25.)
- [KL98] Robert V. Kohn and Thomas D. Little, *Some model problems of polycrystal plasticity with deficient basic crystals*, *SIAM Journal on Applied Mathematics* **59** (1998), no. 1, 172–197. (Cited on page 121.)
- [Koh90] Robert V. Kohn, *The relationship between linear and nonlinear variational models of coherent phase transitions*, *Proceedings of the 7th Army Conference on Applied Mathematics and Computing* (F. Dressel, ed.), 1990, p. 184. (Cited on page 16.)
- [Koh91] ———, *The relaxation of a double-well energy*, *Continuum Mechanics and Thermodynamics* **3** (1991), 193–236. (Cited on pages 16, 22, 34, 37 and 77.)
- [KP91] D. Kinderlehrer and P. Pedregal, *Characterizations of gradient young measures*, *Archive for Rational Mechanics and Analysis* **115** (1991), 329–365. (Cited on page 19.)
- [KS82] Robert V. Kohn and G. Strang, *Structural design, optimization, homogenization and relaxation of variational problems*, *Macroscopic Properties of Disordered Media*

- (G. Papanicolaou R. Burridge and S. Childress, eds.), Lecture Notes in Physics 154, Springer-Verlag, 1982. (Cited on page 28.)
- [KS83] ———, *Explicit relaxation of a variational problem in optimal design*, Bulletin of the American Mathematical Society **9** (1983), 211–214. (Cited on pages 28 and 96.)
- [KS86a] ———, *Optimal design and relaxation of variational problems I*, Communications on Pure and Applied Mathematics **39** (1986), 1–25. (Cited on page 28.)
- [KS86b] ———, *Optimal design and relaxation of variational problems II*, Communications on Pure and Applied Mathematics **39** (1986), 139–182. (Cited on page 28.)
- [KS86c] ———, *Optimal design and relaxation of variational problems III*, Communications on Pure and Applied Mathematics **39** (1986), 353–357. (Cited on page 28.)
- [KSM88] A. G. Khachaturyan, S. V. Semenovskaya, and J. W. Morris, *Theoretical analysis of strain-induced shape changes in cubic precipitates during coarsening*, Acta Metallurgica **36** (1988), no. 6, 1563–1572. (Cited on page 5.)
- [KV87] Robert V. Kohn and Michael Vogelius, *Relaxation of a variational method for impedance computed tomography*, Communications on Pure and Applied Mathematics **60** (1987), 745–777. (Cited on page 20.)
- [KW92] Y. D. Kim and C. M. Wayman, *Shape recovery and phase transformation behavior in Ni Al alloys*, Metallurgical Transactions **23A** (1992), 2981–2986. (Cited on page 25.)
- [LC81] K. A. Lurie and Andrej V. Cherkaev, *G-closure of some particular sets of admissible material characteristics for the problem of bending of thin elastic plates*, Tech. Report 214, DCAMM, Technical University of Denmark, 1981, Published later as [LC84b]. (Cited on pages 28 and 130.)
- [LC82a] ———, *Exact estimates of conductivity of composites formed by two isotropically conducting media taken in prescribed proportion*, Tech. Report 783, Ioffe Physico-technical Institute, Academy of Sciences, USSR, Leningrad, USSR, 1982, English translation in [LC84a]. (Cited on pages 28 and 130.)
- [LC82b] ———, *Exact estimates of the conductivity of a binary mixture of isotropic materials*, Tech. Report 894, Ioffe Physico-technical Institute, Academy of Sciences, USSR, Leningrad, USSR, 1982, Published later in English as [LC86b]. (Cited on pages 28 and 130.)
- [LC84a] ———, *Exact estimates of conductivity of composites formed by two isotropically conducting media taken in prescribed proportion*, Proceedings of the Royal Society of

Edinburgh. Section A, Mathematical and Physical Sciences **99** (1984), no. 1-2, 71–87, English translation of [LC82a]. (Cited on page 129.)

- [LC84b] ———, *G-closure of some particular sets of admissible material characteristics for the problem of bending of thin elastic plates*, Journal of Optimization Theory and Applications **42** (1984), no. 2, 305–316, Published earlier as [LC81]. (Cited on page 129.)
- [LC86a] ———, *Effective characteristics of composite materials and the optimal design of structural elements*, Uspekhi Mekhaniki [Advances in Mechanics] **9** (1986), 3–81, Published later in English as [LC97b]. (Cited on pages 28 and 130.)
- [LC86b] ———, *Exact estimates of the conductivity of a binary mixture of isotropic materials*, Proceedings of the Royal Society of Edinburgh. Section A, Mathematical and Physical Sciences **104** (1986), no. 1-2, 21–38, Published earlier in Russian as [LC82b]. (Cited on page 129.)
- [LC97a] D. Y. Li and L. Q. Chen, *Computer simulation of morphological evolution and rafting of γ' particles in Ni-based superalloys under applied stresses*, Scripta Materialia **37** (1997), no. 9, 1271–1277. (Cited on page 5.)
- [LC97b] K. A. Lurie and Andrej V. Cherkaev, *Effective characteristics of composite materials and the optimal design of structural elements*, Topics in the mathematical modelling of composite materials (Andrej V. Cherkaev and Robert V. Kohn, eds.), Progress in nonlinear differential equations and their applications 31, Birkhäuser, 1997, English translation of [LC86a], pp. 175–258. (Cited on page 130.)
- [LC98a] D. Y. Li and L. Q. Chen, *Computer simulation of stress-oriented nucleation and growth of θ' precipitates in Al-Cu alloys*, Acta Materialia **46** (1998), no. 8, 2573–2585. (Cited on page 5.)
- [LC98b] ———, *Shape evolution and splitting of coherent particles under applied stresses*, Acta Materialia **47** (1998), no. 1, 247–257. (Cited on page 5.)
- [LLJ98] P. H. Leo, J. S. Lowengrub, and H. J. Jou, *A diffuse interface model for microstructural evolution in elastically stressed solids*, Acta Materialia **46** (1998), no. 6, 2113–2130. (Cited on page 5.)
- [LLN00] P. H. Leo, J. S. Lowengrub, and Q. Nie, *Microstructural evolution in orthotropic elastic media*, Journal Of Computational Physics **157** (2000), no. 1, 44–88. (Cited on page 5.)

- [LLN01] ———, *On an elastically induced splitting instability*, *Acta Materialia* **49** (2001), no. 14, 2761–2772. (Cited on page 5.)
- [LLN⁺03] X. F. Li, J. Lowengrub, Q. Nie, V. Cristini, and P. Leo, *Microstructure evolution in three-dimensional inhomogeneous elastic media*, *Metallurgical and Materials Transactions A-Physical Metallurgy and Materials Science* **34A** (2003), no. 7, 1421–1431. (Cited on page 5.)
- [LTT⁺00] A.H.Y. Lue, Y. Tomota, M. Taya, K. Inoue, and T. Mori, *Micro-mechanic modeling of the stress-strain curves of a TiNiCu shape memory alloy*, *Materials Science and Engineering A - Structural Materials Properties Microstructure and Processing* **285** (2000), 326–337. (Cited on page 89.)
- [Lu93] Jiangbo Lu, *Extremal microstructures for two isotropic phases with distinct stress-free strains in two space dimensions*, Ph.D. thesis, New York University, 1993. (Cited on pages 22 and 42.)
- [LV02a] A. C. Lund and Peter W. Voorhees, *Effects of elastic stress on coarsening in the Ni-Al system*, *Acta Materialia* **50** (2002), 2085–2098. (Cited on page 5.)
- [LV02b] ———, *Effects of elastic stress on microstructural development: The three-dimensional microstructure of a $\gamma - \gamma'$ alloy*, *Acta Materialia* **50** (2002), 2585–2598. (Cited on page 5.)
- [LV03] ———, *A quantitative assessment of the three-dimensional microstructure of a $\gamma - \gamma'$ alloy*, *Philosophical Magazine* **83** (2003), no. 14, 1719–1733. (Cited on page 5.)
- [LVB⁺02] C. LExcellent, A. Vivet, C. Bouvet, S. Calloch, and P. Blanc, *Experimental and numerical determinations of the initial surface of phase transformation under biaxial loading in some polycrystalline shape-memory alloys*, *Journal of the Mechanics and Physics of Solids* **50** (2002), 2717–2753. (Cited on page 89.)
- [LW98] Z.K. Lu and G.J. Weng, *A self-consistent model for the stress-strain behavior of shape-memory alloy polycrystals*, *Acta Materialia* **46** (1998), 5423–5433. (Cited on page 89.)
- [Mar78] P. Marcellini, *Periodic solutions and homogenization of nonlinear variational problems*, *Annali di Matematica Pura ed Applicata* **117** (1978), 139–152. (Cited on pages 23 and 24.)
- [MI79] Albert W. Marshall and Olkin Ingram, *Inequalities: Theory of majorization and its applications*, *Mathematics in Science and Engineering* 143, Academic Press, 1979. (Cited on page 71.)

- [Mil90a] Graeme W. Milton, *A brief review of the translation method for bounding effective elastic tensors of composites*, Continuum Models and Discrete Systems (G. A. Maugin, ed.), Longman Scientific and Technical, 1990, pp. 60–74. (Cited on page 28.)
- [Mil90b] ———, *On characterizing the set of possible effective tensors of composites: The variational method and the translation method*, Communications on Pure and Applied Mathematics **43** (1990), no. 1, 63–125. (Cited on page 28.)
- [Mil01] ———, *The theory of composites*, Cambridge Monographs on Applied and Computational Mathematics 6, Cambridge University Press, 2001. (Cited on pages 20, 28, 36, 51 and 79.)
- [MNK⁺00] S. Miyazaki, V. H. No, K. Kitamura, A. Khantachawana, and H. Hosoda, *Texture of Ti-Ni rolled thin plates and sputter-deposited thin films*, International Journal of Plasticity **16** (2000), 1135–1154. (Cited on page 89.)
- [MNM79] Toru Miyazaki, Kozo Nakamura, and Hirotarō Mori, *Experimental and theoretical investigations on morphological changes of γ' precipitates in Ni-Al single crystals during uniaxial stress-annealing*, Journal of Materials Science **14** (1979), 1827–1837. (Cited on pages 3 and 4.)
- [MT85] F. Murat and L. Tartar, *Calcul des variations et homogénéisation [Calculus of variations and homogenization]*, Collection de la Direction des Études et Recherches d'Électricité de France **57** (1985), 319–369, Homogenization methods: Theory and applications in physics (Bréau-sans-Nappe, 1983). English translation in [MT97]. (Cited on pages 28 and 132.)
- [MT97] ———, *Calculus of variations and homogenization*, Topics in the mathematical modelling of composite materials (Andrej V. Cherkaev and Robert V. Kohn, eds.), Progress in nonlinear differential equations and their applications 31, Birkhäuser, 1997, English translation of [MT85], pp. 139–173. (Cited on page 132.)
- [Mur87] F. Murat, *A survey on compensated compactness*, Contributions to Modern Calculus of Variations (L. Cesari, ed.), Longman Scientific and Technical, 1987, pp. 145–183. (Cited on page 28.)
- [NBZACP02] C. Niclaeys, T. Ben Zineb, S. Arbab-Chirani, and E. Patoor, *Determination of the interaction energy in the martensitic state*, International Journal of Plasticity **18** (2002), 1619–1647. (Cited on page 89.)

- [Ono90a] N. Ono, *Pseudoelastic behavior in a polycrystalline Cu-Al-Ni shape memory alloy in comparison with the modified Taylor model*, Mat. Trans. Jap. Inst. Metals **31** (1990), 855–860. (Cited on page 89.)
- [Ono90b] ———, *Pseudoelastic deformation in a polycrystalline Cu-Zn-Al shape memory alloy*, Mat. Trans. Jap. Inst. Metals **31** (1990), 381–385. (Cited on page 89.)
- [OS88] N. Ono and A. Sato, *Plastic deformation governed by the stress induced martensitic transformation in polycrystals*, Mat. Trans. Jap. Inst. Metals **29** (1988), 267–273. (Cited on page 89.)
- [OSO89] N. Ono, A. Sato, and H. Ohta, *A discussion on the mechanical properties of shape memory alloys based on a polycrystal model*, Mat. Trans. Jap. Inst. Metals **30** (1989), 756–764. (Cited on page 89.)
- [OW99] Kazuhiro Otsuka and Clarence M. Wayman (eds.), *Shape memory materials*, Cambridge University Press, 1999. (Cited on page 2.)
- [PBE94] E. Patoor, M. Bensalah, A. Eberhard, and M. Berveiller, *Micromechanical aspects of shape memory behavior*, Proc. ICOMAT-92 (C. M. Wayman and J. Perkins, eds.), Monterey Inst. Adv. Studies, 1994, pp. 401–406. (Cited on page 89.)
- [PC98] R. Poduri and L. Q. Chen, *Computer simulation of morphological evolution and coarsening kinetics of δ' Al_3Li precipitates in Al-Li alloys*, Acta Materialia **46** (1998), no. 11, 3915–3928. (Cited on page 5.)
- [PEB88] E. Patoor, A. Eberhard, and M. Berveiller, *Thermomechanical behavior of shape memory alloys*, Archives of Mechanics **40** (1988), 775–794. (Cited on page 89.)
- [PEB93] ———, *Micromechanical modelling of superelasticity in shape memory alloys*, Progress in Partial Differential Equations: The Metz Surveys. 2 (M. Chipot, ed.), Pitman Research Notes in Mathematics 296, Longman Scientific, 1993, pp. 38–54. (Cited on page 89.)
- [Pip91] Allen C. Pipkin, *Elastic materials with two preferred states*, Quarterly Journal of Applied Mathematics **44** (1991), no. 1, 1–15. (Cited on pages 22, 34 and 77.)
- [Pra57] William Prager, *On ideal locking materials*, Transactions of the Society of Rheology **1** (1957), no. 1, 169–175. (Cited on page 92.)
- [Pra58] ———, *Elastic solids of limited incompressibility*, Proceedings of the 9th International Congress on Applied Mechanics, vol. 5, 1958, pp. 205–211. (Cited on page 92.)

- [Roy78] A. L. Roytburd, *Martensitic transformation as a typical phase transformation in solids*, *Solid State Physics* **33** (1978), 317–390. (Cited on pages 16 and 37.)
- [Roy93] ———, *Elastic domains and polydomain phases in solids*, *Phase Transitions* **45** (1993), 1–33. (Cited on page 16.)
- [Rud91] Walter Rudin, *Functional analysis*, 2 ed., International Series in Pure and Applied Mathematics, McGraw Hill, Inc., 1991. (Cited on page 96.)
- [RV02] Lorenz Ratke and Peter W. Voorhees, *Growth and coarsening: Ripening in material processing*, *Engineering Materials*, Springer, 2002. (Cited on pages 3 and 4.)
- [RW98] Tyrrell R. Rockafellar and Roger J-B. Wets, *Variational analysis*, Grundlehren der mathematischen Wissenschaften 317, Springer, 1998. (Cited on pages 90, 92, 93 and 95.)
- [Sab92] K. Sab, *On the homogenization and the simulation of random materials*, *European Journal of Mechanics A-Solids* **11** (1992), 585–607. (Cited on page 23.)
- [SH93a] Q. P. Sun and K. C. Hwang, *Micromechanics modelling for the constitutive behavior of polycrystalline shape memory alloys - I. Derivation of general relations*, *Journal of the Mechanics and Physics of Solids* **41** (1993), 1–17. (Cited on page 89.)
- [SH93b] ———, *Micromechanics modelling for the constitutive behavior of polycrystalline shape memory alloys - II. Study of the individual phenomena*, *Journal of the Mechanics and Physics of Solids* **41** (1993), 19–33. (Cited on page 89.)
- [SK83] G. Strang and Robert V. Kohn, *Hencky-Prandtl nets and constrained Michell trusses*, *Computer Methods in Applied Mechanics and Engineering* **36** (1983), 207–222. (Cited on page 96.)
- [SK88] ———, *Optimal design of a two-way conductor*, *Topics in Nonsmooth Mechanics* (J. Moreau et al., ed.), Birkhäuser, 1988, pp. 143–155. (Cited on page 28.)
- [SLN⁺02] P. Sittner, P. Lukas, D. Neov, M. R. Daymond, V. Novak, and G. M. Swallowe, *Stress-induced martensitic transformation in Cu-Al-Zn-Mn polycrystal investigated by two in-situ neutron diffraction techniques*, *Materials Science and Engineering A - Structural Materials Properties Microstructure and Processing* **324** (2002), 225–234. (Cited on page 89.)
- [SN00] P. Sittner and V. Novak, *Anisotropy of martensitic transformations in modeling of shape memory alloy polycrystals*, *International Journal of Plasticity* **16** (2000), 1243–1268. (Cited on page 89.)

- [SNL⁺02] P. Sittner, V. Novak, P. Lukas, D. Lugovsky, D. Neov, and M. Tovar, *Load partition in NiTi shape memory alloy polycrystals investigated by in-situ neutron diffraction and micromechanics modelling*, Materials Science Forum **404** (2002), 829–834. (Cited on page 89.)
- [SP93] S. Socrate and D. M. Parks, *Numerical determination of the elastic driving force for directional coarsening in Ni-Superalloys*, Acta Metallurgica et Materialia **41** (1993), no. 7, 2185–2209. (Cited on page 5.)
- [SPBE99] N. Siredey, E. Patoor, M. Berveiller, and A. Eberhardt, *Constitutive equations for polycrystalline thermoelastic shape memory alloys. I. Intragranular interactions and behavior of the grain*, International Journal of Solids and Structures **36** (1999), 4289–. (Cited on page 89.)
- [Str79] G. Strang, *A minimax problem in plasticity theory*, Functional analysis methods in numerical analysis: Special session, American Mathematical Society, St. Louis, Missouri, 1977 (M. Zuhair Nashed, ed.), Lecture notes in mathematics 701, Springer-Verlag, 1979, pp. 319–333. (Cited on page 96.)
- [SV96a] C. H. Su and Peter W. Voorhees, *The dynamics of precipitate evolution in elastically stressed solids - I. inverse coarsening*, Acta Materialia **44** (1996), no. 5, 1987–1999. (Cited on page 5.)
- [SV96b] ———, *The dynamics of precipitate evolution in elastically stressed solids - II. particle alignment*, Acta Materialia **44** (1996), no. 5, 2001–2016. (Cited on page 5.)
- [SW99] V. P. Smyshlyaev and J. R. Willis, *On the relaxation of a three-well energy*, Proceedings of the Royal Society of London. Series A - Mathematical Physical and Engineering Sciences **455** (1999), no. 1983, 779–814. (Cited on page 22.)
- [TA01] P. Thamburaja and L. Anand, *Polycrystalline shape-memory materials: Effect of crystallographic texture*, Journal of the Mechanics and Physics of Solids **49** (2001), 709–737. (Cited on page 89.)
- [Tar79a] L. Tartar, *Compensated compactness and applications to partial differential equations*, Nonlinear Analysis and Mechanics (R.J. Knops, ed.), Heriot-Watt Symposium, IV, Pitman Publishing, 1979, pp. 136–212. (Cited on page 28.)
- [Tar79b] ———, *Estimation de coefficients homogénéisés [Estimation of homogenized coefficients]*, Computing methods in applied sciences and engineering: Third international symposium, Versailles, France, December 5–7, 1977 (R. Glowinski and J. L. Lions,

- eds.), Springer-Verlag, 1979, English translation in [Tar97]. (Cited on pages 28, 36 and 136.)
- [Tar85] ———, *Estimation fines des coefficients homogénéisés [Fine estimations of homogenized coefficients]*, Ennio de Giorgi Colloquium: Papers Presented at a Colloquium Held at the H. Poincaré Institute in November 1983 (P. Kree, ed.), Pitman Publishing, 1985, pp. 168–187. (Cited on pages 28 and 36.)
- [Tar97] ———, *Estimation of homogenization coefficients*, Topics in the mathematical modelling of composite materials (Andrej V. Cherkaev and Robert V. Kohn, eds.), Progress in nonlinear differential equations and their applications 31, Birkhäuser, 1997, English translation of [Tar79b], pp. 9–20. (Cited on page 136.)
- [Tar00] ———, *An introduction to the homogenization method in optimal design*, Optimal shape design. Lectures given at the joint C.I.M./C.I.M.E. Summer school held at Tróia, June 1–6, 1998 (A. Cellina and A. A. Ornelas, eds.), Springer-Verlag, 2000, pp. 47–156. (Cited on page 36.)
- [Tay78] J. E. Taylor, *Crystalline variational problems*, Bulletin of the American Mathematical Society **84** (1978), no. 4, 568–588. (Cited on page 5.)
- [Tem81] Roger Temam, *An existence theorem for a variational problem of plasticity*, Nonlinear problems of analysis in geometry and mechanics (M. Atteia, D. Bancel, and I. Gumnowski, eds.), Research notes in mathematics 46, Pitman, 1981, pp. 57–70. (Cited on page 96.)
- [TSV94] M. E. Thompson, C. S. Su, and Peter W. Voorhees, *The equilibrium shape of a misfitting precipitate*, Acta Metallurgica et Materialia **42** (1994), no. 6, 2107–2122. (Cited on pages 5, 6 and 53.)
- [VC02] V. Vaithyanathan and L. Q. Chen, *Coarsening of ordered intermetallic precipitates with coherency stress*, Acta Materialia **50** (2002), no. 16, 4061–4073. (Cited on page 5.)
- [Vig94] S. B. Vigdergauz, *Two-dimensional grained composites of extreme rigidity*, Transactions of the ASME E Journal of Applied Mechanics **61** (1994), no. 2, 390–394. (Cited on page 42.)
- [VWC02] V. Vaithyanathan, C. Wolverton, and L. Q. Chen, *Multiscale modelling of precipitate microstructure evolution*, Physical Review Letters **88** (2002), no. 12. (Cited on page 5.)

- [Way64] C. M. Wayman, *Introduction to the crystallography of martensitic transformations*, Macmillan, 1964. (Cited on page 16.)
- [Way92] ———, *Shape memory and related phenomena*, Progress in Materials Science **36** (1992), 203–224. (Cited on page 16.)
- [WCK91] Y. Z. Wang, L. Q. Chen, and A. G. Khachaturyan, *Shape evolution of a precipitate during strain-induced coarsening - A computer-simulation*, Scripta Metallurgica et Materialia **25** (1991), no. 6, 1387–1392. (Cited on page 5.)
- [Wei95] H.F. Weinberger, *A first course in partial differential equations with complex variables and transform methods*, Dover Publications Inc., 1995. (Cited on page 98.)
- [WW71] M. Watanabe and C. M. Wayman, *Crystallography of the martensite transformation in Fe-Al-C alloys*, Metallurgical Transactions **2** (1971), 2229–2236. (Cited on page 16.)
- [ZCS01] Jingzhi Zhu, Long-Qing Chen, and Jie Shen, *Morphological evolution during phase separation and coarsening with strong inhomogeneous elasticity*, Modelling and Simulation in Materials Science and Engineering **9** (2001), 499–511. (Cited on page 5.)